

INVESTIGATING THE ROLE OF ADENOVIRUS E1B-55K, E4ORF3 AND E4ORF6 PROTEINS DURING INFECTION

By

Abeer Saud Al-balawi

A thesis submitted to

The University of Birmingham

For the degree of
DOCTOR OF PHILOSOPHY

Institute of Cancer and Genomic Sciences
College of Medical and Dental Sciences
The University of Birmingham

June 2020

UNIVERSITY OF
BIRMINGHAM

University of Birmingham Research Archive

e-theses repository

This unpublished thesis/dissertation is copyright of the author and/or third parties. The intellectual property rights of the author or third parties in respect of this work are as defined by The Copyright Designs and Patents Act 1988 or as modified by any successor legislation.

Any use made of information contained in this thesis/dissertation must be in accordance with that legislation and must be properly acknowledged. Further distribution or reproduction in any format is prohibited without the permission of the copyright holder.

Dedicated to My Parents

Saud Mohammed Al-balawi

&

Nahla Jamman Al-balawi

&

My Sister Areej Saud Al-balawi

Abstract

Viruses have evolved to utilise host cell factors that promote viral replication and inactivate host cell factors that inhibit viral replication. For adenovirus, early region proteins modulate the functional activity of pro-viral and anti-viral host cell proteins in order to promote viral replication. In this regard, adenovirus early region proteins, E1B-55K, E4orf3 and E4orf6 engage with the cellular Ubiquitin-Proteasome System, both independently and cooperatively to inactivate anti-viral host cell proteins. The principal aims of this thesis were to: investigate further how adenovirus E1B-55K, E4orf3 and E4orf6 proteins function in isolation to modulate host cell factors through engagement with the Ubiquitin-Proteasome System; and consider the role of the cellular chromatin remodelling complex, FACT in adenovirus infection.

In order to study their functions in isolation we have developed, and characterized, clonal U2OS cell lines that express human Ad5 and Ad12 early region proteins in a tetracycline-responsive manner. Using site-directed mutagenesis coupled with pharmacological inhibition of the proteasome and Cullin Ring Ligases we determined that Ad5 E4orf6 is subject to ubiquitylation on K95 and K171 and undergoes proteasome-dependent degradation in a Cullin Ring Ligase-dependent manner. Using quantitative mass spectrometry we also established that Ad12 E4orf6, but not Ad5 E4orf6, engages with Cullin Ring Ligases to promote the proteasome-mediated degradation of core histone proteins. In this regard, both adenovirus 5 and adenovirus 12 were shown to promote the loss of core histones during infection but the mechanisms underlying this process require further investigation. Using a combination of immunofluorescence, GFP pull-down and RNA interference allied with Western blot analyses work presented here also established that FACT complex components, SPT16 and SSRP1 associated with the RPA complex at viral replication centres during infection and that ablation

of FACT gene expression affected adenovirus early region gene product expression during infection.

In consideration of previous published work and the data presented here, this study indicates that adenovirus utilises the Ubiquitin Proteasome System at multiple levels to regulate both host cell protein and adenovirus early region protein function during infection and suggests that cellular histones limit adenovirus replication. Moreover, our data suggests that the histone chaperone protein complex, FACT has pro-viral activities during adenovirus infection. Taken together, our studies have identified potential new functions for adenovirus early region proteins and have developed useful resources for studying viral protein-host protein interactions.

Acknowledgements

All praise and glory to Almighty Allah, who gave me strength to finish this work. I am deeply indebted to **Taibah University and the Ministry of Education in Saudi Arabia** for giving me this opportunity and for supporting me financially to pursue my studies. I wish to express my full gratitude and appreciation to my supervisor **Dr. Andy Turnell**, for his supervision, encouragement and valuable suggestions over the years, as well as his constructive counsel. I truly appreciate his immense knowledge and experience and I have learned a great deal from him. Special thanks to **Dr. Phil Byrd**, for his valuable advice and productive discussions during my studies. Thanks also to lab colleagues for their cooperation and assistance, as well as all the friends I have met and known.

Undertaking this PhD journey has been a fabulous experience. Four years of hard work have developed my skills and intentions, not only as a scientist, but also in life generally, and I would not have reached this day and gained all this without my **family**, they always supported me, constantly since starting this journey. My deep and sincere gratitude and appreciation for their love, understanding and sacrifices. I will never be able to express the extent of my sincere appreciation for my **Father, Mother, Sisters and Brothers**, for their unconditional love, encouragement and emotional support during my difficult days. Deep and warm thanks to my sister **Areej**, as always being my source of strength and nourishing my enthusiasm. May Allah have mercy upon my **parents**, as they brought me up and every effort worthwhile and to them, I dedicate this thesis.

(23) And never say of anything, "Indeed, I will do that tomorrow," (24) Except [when adding], "If Allāh wills." And remember your Lord when you forget [it] and say, "Perhaps my Lord will guide me to what is nearer than this to right conduct. " Quran"

Table of Contents

Abstract	II
Acknowledgements	IV
List of Figures	X
List of Tables	XII
1.0 CHAPTER 1: Introduction	1
1.1 Human Tumour Viruses	2
1.1.1. DNA Tumour Viruses.....	2
1.1.2. Adenovirus Identification and Classification.....	5
1.1.3. Adenovirus structure and genome organization.....	7
1.1.4. Adenovirus cellular entry, chromatinization and viral DNA replication.....	10
1.1.5. Viral Replication Centres	13
1.1.5.1. The FACT Complex	14
1.2. Adenovirus Early region proteins	16
1.2.1. Adenovirus E1A proteins	17
1.2.1.1. The ubiquitin-like protein SUMO and its regulation by E1A	20
1.2.2. Adenovirus E1B proteins	21
1.2.3. Adenovirus E3 region	24
1.2.4. Adenovirus E4 region	25
1.2.4.1. Adenovirus E4orf3	26
1.2.4.2. Adenovirus E4orf6	28
1.2.5. Role of early region proteins in cellular transformation.....	32
1.2.5.1. The role of E1A and E1B in cellular transformation.....	32
1.2.5.2. The role of E4orf3 and E4orf6 in cellular transformation and the concept of hit and run transformation.....	33
1.2.5.3. The role of E1A and Ras in cellular transformation	35
1.3. The Ubiquitin-Proteasome System	36
1.3.1. Cullin–Ring Ubiquitin Ligases (CRLs).....	39
1.3.2. Regulation of the ubiquitin-proteasome system by E1B-55K and E4orf6 proteins.....	41
1.3.2.1. Utilization of Cullin Ring Ligases by E1B-55K and E4orf6 proteins during infection to promote p53 degradation.....	41
1.3.2.2. Adenovirus utilisation of CRLs to promote viral replication and inhibit DDR and other antiviral pathways.....	44
1.3.2.3. Regulation of CRLs by other viruses.....	45
1.4. The cellular DNA damage response	47
1.4.1. The ATM pathway.....	48
1.4.2. The ATR pathway	49
1.4.3. The DNA-dependent protein kinase pathway.....	49
1.4.4. Regulation of the DDR by other viruses	50
1.5. Project Aims	51
2.0 CHAPTER 2: Materials and Methods	53
2.1. Tissue Culture	54
2.1.1. Cell culture.....	54
2.1.2. Maintenance and passage of cell lines	55

2.1.3. Cryopreservation of cell lines and cell recovery.....	55
2.1.4. Adenoviruses.....	56
2.1.5. Generation of U2OS FRT TREX cell lines.....	56
2.1.6. Transfection of siRNA.....	57
2.1.7. Transient DNA transfection.....	58
2.1.8. Treatment of cells with Ultra-Violet irradiation or drugs.....	58
2.2. Protein Biochemistry	59
2.2.1. Preparation of whole cell lysates.....	59
2.2.2. Protein concentration quantification.....	59
2.2.3. SDS-Polyacrylamide Gel Electrophoresis (SDS-PAGE).....	60
2.2.4. Western blotting.....	60
2.2.5. Immunoprecipitation.....	63
2.2.6. Chromatin Isolation.....	63
2.2.7. Acid extraction of histones.....	65
2.2.8. Purification of GST Fusion Proteins.....	65
2.2.9. GST-pull downs.....	66
2.2.10. GFP-pull down.....	67
2.2.11. Coomassie staining of polyacrylamide gels.....	67
2.2.12. FASP (Filter-Aided Sample Preparation) tryptic digestion of nuclear lysates.....	68
2.2.13. Dimethyl-labelling of tryptic peptides obtained from nuclear lysates.....	68
2.2.14. Mass spectrometric analysis of tryptic peptides.....	69
2.3. Molecular and Cell Biology	70
2.3.1. Preparation of media for growth of bacteria.....	70
2.3.2. Transformation of Bacteria.....	70
2.3.3. Mini-prep and Maxi-prep plasmid DNA purification.....	71
2.3.4. Sanger DNA Sequencing.....	73
2.3.5. PCR.....	74
2.3.6. Agarose gel electrophoresis.....	75
2.3.7. DNA cloning.....	76
2.3.8. Site-directed mutagenesis.....	76
2.3.9. Immunofluorescence.....	77
2.3.10. Metaphase spreads.....	78
3.0: CHAPTER 3: Generation and characterization of TET-inducible U2OS cell lines to investigate the function of adenovirus E1B-55K, E4orf3 and E4orf6 proteins.....	79
3.1. Introduction.....	80
3.2. Results.....	83
3.2.1. Use of the Flp-In T-Rex System to generate U2OS-FRT-inducible cell lines.....	83
3.2.2. Generation of Ad5 and Ad12 E1B-55K Flp-In T-Rex U2OS-FRT-inducible cell lines.....	83
3.2.2.1. Generation and characterization of Ad5 E1B-55K and Ad12 E1B-55K Flp-In T-Rex U2OS inducible cell lines.....	85
3.2.2.2. Characterization of Ad5 and Ad12 E1B-55K cell lines: E1B-55K association with p53.....	87

3.2.2.3. Characterization of Ad5 and Ad12 E1B-55K cell lines: recruitment of p53 to aggresomes in Ad5 E1B-55K Flp-In T-Rex U2OS cell lines.....	89
3.2.2.4. Characterization of Ad5 and Ad12 E1B-55K cell lines: localization of Ad12E1B-55K to cytoplasmic flecks in Flp-In T-Rex U2OS cell lines	90
3.2.2.5. Characterization of Ad5 and Ad12 E1B-55K cell lines: effects of E1B-55K expression on the levels and post-translational modification status of cellular proteins	92
3.2.3. Generation of Ad5 and Ad12 E4orf3 Flp-In T-Rex U2OS-FRT-inducible cell lines	95
3.2.3.1. Generation and characterization of Ad5 E4orf3 and Ad12 E4orf3 Flp-In T-Rex U2OS inducible cell lines.....	96
3.2.3.2. Characterization of Ad5 and Ad12 E4orf3 cell lines: effects of E4orf3 expression on the levels of cellular E4orf3-regulated proteins.....	97
3.2.3.3. Characterization of Ad5 and Ad12 E4orf3 cell lines: E4orf3-dependent recruitment of TIF1 γ to PML-containing nuclear tracks	100
3.2.3.4. Characterization of Ad5 and Ad12 E4orf3 cell lines: E4orf3-dependent	102
recruitment of SUMO-1 and SUMO-2 to PML-containing nuclear tracks	102
3.2.3.5. Characterization of Ad5 and Ad12 E4orf3 cell lines: effects of E4orf3 expression on the levels and post-translational modification status of cellular proteins	104
3.2.4. Generation of Ad5 and Ad12 E4orf6 Flp-In T-Rex U2OS-FRT-inducible cell lines	105
3.2.4.1. Generation and characterization of Ad5 E4orf6 and Ad12 E4orf6 Flp-In T-Rex U2OS inducible cell lines.....	107
3.2.4.2. Characterization of Ad5 and Ad12 E4orf6 cell lines: cellular localization of E4orf6.....	110
3.2.4.3. Characterization of Ad5 and Ad12 E4orf6 cell lines: E4orf6 association with p53	112
3.2.3.4. Characterization of Ad5 and Ad12 E4orf6 cell lines: effects of E4orf6 expression on the levels of cellular proteins.....	113
3.3. Discussion.....	116
3.3.1. Background.....	116
3.3.2. Generation and characterization of Ad5 and Ad12 E1B-55K Flp -In T-Rex_U2OS- Inducible cell lines.....	116
3.3.3. Generation and characterization of Ad5 and Ad12 E4orf3 Flp -In T-Rex U2OS- Inducible cell lines.....	119
3.3.4. Generation and characterization of Ad5 and Ad12 E4orf6 Flp -In T-Rex U2OS- Inducible cell lines.....	121
4.0: CHAPTER 4: Investigating the molecular functions of the Ad5 and Ad12 E4orf6 proteins	123
4.1. Introduction.....	124
4.2. Results.....	125
4.2.1. Post-translational modification of the Ad5 E4orf6 protein.....	125
4.2.2. Investigating the potential O-linked glycosylation of the Ad5 E4orf6 protein	125
4.2.2.1. Analysis of the Ad5 and Ad12 E4orf6 protein sequences for O-linked glycosylation	125
4.2.2. Investigating whether Ad5 E4orf6 is modified by O-linked glycosylation	127
4.2.3. Investigating whether the Ad5 E4orf6 protein is subject to ubiquitylation	128
4.2.4. Effects of the NAE inhibitor, MLN4924 on Ad5 E4orf6 expression.....	129
4.2.5. Cellular localization of ubiquitylated Ad5 E4orf6 species	131
4.2.6. Generation and characterization of K95R and K171R Ad5 E4orf6 mutants	132
4.2.6.1. Inspection of the Ad5 E4orf6 primary sequence.....	132

4.2.6.2. Generation of Ad5 E4orf6 lysine mutants.....	134
4.2.6.3. Investigating the effects of K95R and K171R mutation on Ad5 E4orf6 ubiquitylation status.....	134
4.2.7. Targeting of the Ubiquitin-Proteasome System by Ad12 E4orf6.....	136
4.2.7.1. Identification of cellular proteins that are reduced in levels following Ad12 E4orf6 expression .	137
4.2.7.2. Effect of Ad12 E4orf6 expression upon cellular histone levels: WB analyses.....	141
4.2.7.3. Role of CRLs and the 26S proteasome in the Ad12 E4orf6-dependent modulation of cellular histone levels.....	143
4.2.7.4. Effect of Ad12 E4orf6 expression on core histone protein expression.....	144
4.2.7.5. Ad12 E4orf6 interacts with core histones <i>in vitro</i>	145
4.2.7.6. Investigating the ability of Ad12 E4orf6 complexes to ubiquitylate core histones <i>in vitro</i>	147
4.2.7.7. Investigating the effects of w.t. Ad5 and w.t. Ad12 infection upon cellular histone levels.....	148
4.2.7.8. Effects of w.t. Ad5 and w.t. Ad12 on core histone protein expression.....	149
4.2.8. Effect of Ad5 E4orf6 and Ad12 E4orf6 expression on chromosomal aberrations.....	150
4.2.8.1 Metaphase spreads for Ad5 and Ad12 E4orf6 Flp-In T-Rex U2OS cell lines.....	150
4.3. Discussion.....	153
4.3.1. Background.....	153
4.3.2. Ad5 E4orf6 is post-translationally modified by ubiquitylation.....	153
4.3.3. Identification of core histone proteins as targets for CRL-dependent degradation following Ad12 E4orf6 expression.....	156
4.3.4. Chromosomal aberrations following Ad5 and Ad12 E4orf6 expression.....	159
5.0: CHAPTER 5: Investigating the role of the FACT complex during adenovirus infection.....	160
5.1. Introduction.....	161
5.2. Results.....	162
5.2.1. The protein levels of SPT16, SSRP1, Pur β and RBM14 are not altered following adenovirus infection.....	162
5.2.2. Validation of SPT16, SSRP1, PUR β and RBM14 association with RPA1 following adenovirus infection.....	164
5.2.3. Recruitment of SPT16 to VRCs with RPA following w.t Ad5 and Ad12 infection.....	165
5.2.4. Recruitment of RBM14 to VRCs during Ad5 and Ad12 infection.....	166
5.2.5. Pur β is not recruited to VRCs during Ad5 and Ad12 infection.....	167
5.2.6. The FACT complex modulates adenovirus early region gene product expression.....	170
5.3 Discussion.....	172
5.3.1. Background.....	172
5.3.2. Investigating the role of the FACT complex during adenovirus infection.....	172
5.3.3. Investigating the role of RBM14 during adenovirus infection.....	174
6.0: CHAPTER 6: Final Discussion.....	177
6.1. Introduction.....	178
6.2. Adenovirus regulation of the ubiquitin-proteasome system.....	179
6.3. Adenovirus regulation of chromatin.....	181
6.4 Adenovirus regulation of DNA damage response pathways.....	182
7. References.....	184

List of Figures

Figure 1.1: Structural representation of the adenovirus virion and schematic representation of the adenovirus transcription map..	10
Figure 1.2: Summary of adenovirus life-cycle	13
Figure 1.3: Model of FACT action in nucleosome/hexasome assembly	15
Figure 1.4: Domain structure of FACT proteins.	16
Figure 1.5: E1A functional domains and binding proteins.	19
Figure 1.6: Mitochondrial apoptosis pathway inhibition by E1B-19K.	22
Figure 1.7: Schematic representation of E1B-55K structural features.	24
Figure 1.8: Relationship between adenovirus early region proteins and the SUMO pathway.	27
Figure 1.9: Nuclear export signals and localization signals present in Ad5 E4orf6.	29
Figure 1.10: Multiple sequence alignment of E4orf6 from several adenovirus types.	31
Figure 1.11: Diagram detailing the Ubiquitin-Proteasome System.	37
Figure 1.12: Ubiquitin and ubiquitin linkages.	38
Figure 1.13: Architecture of Cullin-RING E3 ubiquitin ligase (CRL) complexes.	39
Figure 1.14: MLN4924 as an inhibitor of Cullin-RING ubiquitin ligases (CRLs).	41
Figure 1.15: Schematic model of Cullin-RING E3 ligases.	42
Figure 1.16: Schematic representation of BC boxes and CUL boxes in Ad5 and Ad12 E4orf6.	43
Figure 1.17: Regulation of host Cullin RING ligases by different viruses.	47
Figure 1.18: Role of PI3K-related protein kinases in DDR signalling pathways.	48
Figure 3.1: Chromatograms demonstrating sequence integrity of Ad5 and A12 E1B-55K pcDNA5-FRT TO clones at 5' and 3' ends.	84
Figure 3.2: Validation of Ad5 and Ad12 E1B-55K Flp-In T-Rex U2OS cell lines.	87
Figure 3.3: Ad5 and Ad12 E1B-55K associate with p53 in Flp-In T-Rex U2OS cell lines.	88
Figure 3.4: Co-localization of p53 with Ad5 E1B-55K in cytoplasmic aggresomes in Ad5 E1B-55K Flp-In T-Rex U2OS cells.	90
Figure 3.5: Localization of Ad12 E1B-55K to cytoplasmic filamentous structures in Ad12 E1B-55K Flp-In T-Rex U2OS cells.	91
Figure 3.6: Effects of Ad5 and Ad12 E1B-55K expression upon cellular proteins levels and post-translational modification status.	94
Figure 3.7: Chromatograms demonstrating sequence integrity of Ad5 and A12 E4orf3 3XFLAG pcDNA5-FRT TO clones at the 5' and 3' ends.	96
Figure 3.8: Validation of 3X FLAG Ad5 and Ad12 E4orf3 Flp-In T-Rex U2OS cell lines.	97
Figure 3.9: Effects of Ad5 and Ad12 E4orf3 expression upon cellular proteins levels and post-translational modification status.	99
Figure 3.10: Ad5 and Ad12 E4orf3-dependent recruitment of TIF1 γ to nuclear tracks.	101
Figure 3.11: Ad5 and Ad12 E4orf3-dependent recruitment of SUMO-1 and SUMO-2 to nuclear tracks.	103
Figure 3.12: Effects of Ad5 and Ad12 E4orf3 expression upon cellular proteins levels and post-translational modification status.	105
Figure 3.13: Chromatograms demonstrating sequence integrity of Ad5 and A12 E4orf6 pcDNA5-FRT TO clones at 5' and 3' ends.	107
Figure 3.14: Validation of Ad5 and Ad12 E4orf6 Flp-In T-Rex U2OS cell lines.	109
Figure 3.15: Ad5 and Ad12 E4orf6 localize to intranuclear foci in Flp-In T-Rex U2OS cell lines.	111
Figure 3.16: HA-tagged Ad5 and Ad12 E4orf6 associate with p53 in Flp-In T-Rex U2OS cell lines.	113
Figure 3.17: Effects of Ad5 and Ad12 E4orf6 expression upon cellular proteins levels and post-translational modification status.	115
Figure 4.1: Potential O-linked glycosylation sites.	127
Figure 4.2: The OGT inhibitor, OSMI-1 does not affect the PTM status of the Ad5 E4orf6 protein.	128
Figure 4.3: Effect of the proteasome inhibitor, MG132 on the PTM status of HA-tagged Ad5 E4orf6.	129
Figure 4.4: Effect of the NAE inhibitor, MLN4924.	130
Figure 4.5: Ad5 E4orf6 ubiquitylated species exist exclusively in the cytoplasm.	132
Figure 4.6: Analysis of Ad5 E4orf6 sequence and the conservation of K ubiquitin acceptor sites between different adenovirus types.	133
Figure 4.7: Generation of K95R and K171R Ad5 E4orf6 mutants.	134

Figure 4.8: Investigating a role for K95 and K171 as ubiquitin acceptor residues in Ad5 E4orf6.....	135
Figure 4.9: Effect of Ad12 E4orf6 expression on nuclear protein levels.....	137
Figure 4.10: Effect of Ad12 E4orf6 expression on nuclear protein levels.....	139
Figure 4.11: Effect of Ad12 E4orf6 expression on nuclear protein levels.....	140
Figure 4.12: Effect of Ad12 E4orf6 expression on histone H3 and H2A protein levels.....	142
Figure 4.13: Effect of Ad5 E4orf6 expression on histone H3 and H2A protein levels.....	143
Figure 4.14: Requirement for CRLs and the 26S proteasome in the Ad12 E4orf6-dependent modulation of histone H3 and H2A protein levels.....	144
Figure 4.15: Ad12 E4orf6-dependent modulation of core histone protein levels.....	145
Figure 4.16: GST-Ad12 E4orf6 associates with histones in vitro.....	146
Figure 4.17: Histone-directed in vitro ubiquitylation assay.....	148
Figure 4.18: Effects of w.t. Ad5 and w.t. Ad12 infection on cellular histone levels.....	149
Figure 4.19: Effects of w.t. Ad5 and w.t. Ad12 infection on core histone protein levels.....	150
Figure 4.20: Effects of Ad5 E4orf6 and Ad12 E4orf6 expression on chromosomal aberrations in mitosis.....	152
Figure 5.1: The protein levels of SPT16, SSRP1, Pur β and RBM14 are not altered following Ad5 or Ad12 infection.....	163
Figure 5.2: GFP-Pulldown demonstrating FACT and RBM14 association with RPA1 in Ad5-infected cells.....	165
Figure 5.3: Co-localization of SPT16 with RPA32 to VRCs during w.t Ad5 and w.t. Ad12 infection.....	166
Figure 5.4: Recruitment of RBM14 to VRCs during w.t Ad5 and w.t. Ad12 infection.....	167
Figure 5.5: Sanger sequencing indicating the integrity of 5' and 3' the pEGFP-C3- Pur β construct.....	168
Figure 5.6: Pur β is not recruited to VRCs during w.t Ad5 or w.t. Ad12 infection.....	169
Figure 5.7: The FACT complex regulates adenovirus early region gene product expression.....	171

List of Tables

Table 1.1: DNA tumour viruses as causative agents of tumourigenesis.....	5
Table 1.2: Classification of Human Adenoviruses.....	7
Table 1.3: Description of early region gene product function.....	17
Table 2.1: siRNA Used in this study.....	58
Table 2.2: Drugs used in the current study.....	59
Table 2.3: Antibodies used for Western blotting during this project.....	62
Table 2.4: Secondary Antibodies used for WB analysis.....	62
Table 2.5: Buffers Used in Chromatin Isolation.....	64
Table 2.6: Competent bacteria used for transformation.....	71
Table 2.7: Primers used for sequencing.....	74
Table 2.8: Primers used for cloning.....	75
Table 2.9: Mutagenic primers used in this study.....	77
Table 4.1: Effect of Ad12 E4orf6 expression on nuclear protein levels.....	138
Table 4.2: Effect of Ad12 E4orf6 expression on nuclear protein levels.....	141

ABBREVIATIONS

Ad	Adenovirus
Ad5	Adenovirus type 5
Ad12	Adenovirus type 12
AdPol	Ad DNA polymerase
AFT	Activating transcription factor
AIDS	Acquired Immune Deficiency Syndrome
ALCAM	Activated leukocyte cell adhesion molecule
ALL	lymphoblastic leukaemia
APC/C	Anaphase-Promoting Complex/Cyclosome
APS	Ammonium Persulphate
ASPM	Abnormal spindle-like, microcephaly associated
A-T	Ataxia telangiectasia
ATCC	American Type Culture Collection
ATF	Activating transcription factor
ATLD	Ataxia telangiectasia-like disorder
ATM	Ataxia-Telangiectasia Mutated
ATR	ATM-Rad3-related
ATRX	ATP-dependent helicase
BAK	BCL2 antagonist killer
BAX	BCL2-associated X
BCL2	B-cell lymphoma-2
BL	Burkitt lymphoma
BLAST	Basic Local Alignment Search Tool
BP	Base Pairs
BRCA1	Breast cancer susceptibility gene 1
BRK	Baby rat kidney cells
CAND1	Cullin Associated And Neddylation Dissociated 1
CAR	Coxsackievirus and adenovirus receptor
CBP	CREB binding protein
CDC42	Cell division control protein 42
ChIP	Chromatin ImmunoPrecipitation
Chk2	Checkpoint kinase 2
CMV	Cytomegalovirus
CR	Conserved Region
CRLs	Cullin-RING ligases
CSN	COP9 Signalosome
CtBP	C-terminal binding protein
CTD	C-terminal domain
C-terminal	Carboxy-terminal
CtIP	CtBP-interacting protein
Cul	Cullin
DAPI	4',6-diamidino-2-phenylindole
Daxx	Death domain-associated protein
DBP	DNA-binding protein
dCMP	Deoxycytidine Monophosphate
DCN1	DCN1-Like Protein 1
DD	Dimerization Domain
DDR	DNA damage response
DMEM	Dulbecco Modified Eagle Medium
DMSO	Dimethyl-sulphoxide
DNA	Deoxyribonucleic acid
DNA-PK	DNA-dependent protein kinase
dNTP	Deoxyribonucleotide triphosphate
Dox	Doxycycline
ds	Double-Stranded
DSBs	DNA double strand breaks

DTT	Dithiothrietol
DUB	De-ubiquitylating
DYRK1A	Dual-Specificity Tyrosine-Regulated Kinase 1A
E3	Early region 3
E4	Early region 4
E1A	Early region 1A
E2A	Early region 2A
E1B	Early region 1B
E2B	Early region 2B
E1B-AP5	E1B55K-associated protein 5
EBER2	EBV-encoded RNA 2
E2F	transcription factors
EBV	Epstein-Barr virus
EDTA	Ethylene Diamine Tetra Acetic Acid
E4orf3	Early region 4 open reading frame 3
E4orf6	Early region 4 open reading frame 6
EPHA2	Ephrin type-A receptor 2
FACT	Facilitates Chromatin Transactions
FCS	Foetal calf serum
γ TuRC	Gamma-tubulin ring complex
GST	Glutathione S-transferase
H2A	Histone 2A family member
H2B	Histone 2B family member
H3	Histone 3
H4	Histone 4
H2AX	H2A histone family member X
H3K9me3	H3 at lysine residue 9
HBV	Hepatitis B virus
HCl	Hydrogen chloride,
HCV	Hepatitis C virus
HEK	Human embryonic kidney cells
HERs	Human Embryo Retinoblasts
HepB	Hepatitis B
HHV-8	Human herpes virus 8
HIV-1	Human Immunodeficiency Viruses
HMG	High Mobility Group Domain
HPLC	High-Performance Liquid Chromatography
HPV	Human papillomavirus
HRP	Horseradish Peroxidase
HSV-1	Herpes simplex virus-1
HTLV-1	Human T-cell lymphotropic virus 1
HU	Hydroxyurea
IDD	Intrinsically Disordered Domain
IF	Immunofluorescence
IgG	Immunoglobulin G
IP	Immunprecipitaion
IPTG	Isopropyl β -D-1-thiogalactopyranoside
ITR	Inverted terminal repeats
IRS1	Insulin receptor substrate 1
K	Lysine
KCl	Potassium chloride
KDa	Kilo-Dalton
KSHV	Kaposi's sarcoma-associated herpesvirus
LANA	latency-associated nuclear antigen
LAR	Leukocyte common antigen-related
LB	Luria Broth
LMP2	Lysosomal Associated Membrane Protein-2
L4P	Late-promoter
Lys	Lysine
MD	Middle – domain

MDC1	Mediator of DNA damage checkpoint protein 1
MCV	Merkel cell polyoma virus
MED23	Mediator Complex Subunit 23
MG132	Carbobenzoxyl-L-leucyl-L-leucyl-L-leucine
MHC	Major histocompatibility complex
MoRFs	Molecular recognition features
mRNA	Messenger ribonucleic acids
MRN	Mre11-Rad50-NBS1
Mre11	Meiotic recombination 11
MSH6	DNA mismatch repair protein 6
MTOC	Microtubule-organizing Center
NaCl	Sodium chloride
NCBI	National Center for Biotechnology Information
NES	Nuclear Export Signal
NF1	Nuclear factor 1
NHEJ	Non-homologous end joining
NLS	Nuclear localization signal
NRS	Nuclear retention signal
NTD	N-terminal domain
NTR	N-terminal region
OSMI-1	OGT Small Molecule Inhibitor
PBS	Phosphate-Buffered Saline
PCR	Polymerase Chain Reaction
p.f.u	Plaque forming unit
PI3K	Phosphoinositide 3-kinase
PMSF	Phenylmethylsulfonyl Fluoride
PML	Promyelocytic Leukemia
polyA	Polyadenylation Signal
RPE1	Retinal Pigment Epithelium
pRB	Retinoblastoma protein
PTM	Post Translational Modification
PTPRF	Receptor type protein tyrosine phosphatase F
RBM14	RNA-binding protein 14
RBX1	RING-box Protein 1
RNP	Ribonucleoprotein
RPA1	Replication Protein A 1
RSV	Rous sarcoma virus
SAE1	SUMO-activating enzyme
SCM	SUMO Conjugating Motif
SDM	Site-directed mutagenesis
SDS-PAGE	Sodium Dodecyl Sulphate
Ser	Serine
SILAC	Stable Isotope Labeling by/with Amino acids
siRNA	Small-Interfering RNA
Smac	Structural Maintenance of Chromosomes
SMARCAL1	SWI/SNF-related matrix-associated actin-dependent regulator of
SP1	Chromatin Subfamily A-like Protein 1
SPT16	Specificity Protein 1
SRS	Suppressor of Ty 16
SSRP1	Substrate Recognition Subunit
STUbl	Structure Specific Recognition Protein 1
SUMO	SUMO-targeted ubiquitin ligase
SV40	Simian Virus 40
TEAB	Tetraethylammonium bromide
TEB	Triton Extraction Buffer
TBST	Tris-buffered saline
TFIID	Transcription Factor IID
Thr	Threonine
Tim	Timeless
Tim-2	Timeout

Tipin	Timeless-interacting protein
TIF1 β	Transcriptional intermediary factor1 β
TIF1 γ	Transcriptional intermediary factor1 γ
TNF	Tumor Necrosis Factor
TOPBP1	Topoisomerase (DNA) II binding protein 1
TOP2B	Topoisomerase 2-beta
TP	Terminal Protein
TRAIL	TNF-Related Apoptosis Inducing Ligand
TRIM	Tripartite motif
TRRAP	Transformation/transcription domain-associated protein
UPS	Ubiquitin Proteasome System
U2OS	Osteosarcoma Epithelial Cells
Ub	Ubiquitin
Ubc13	Ubiquitin-conjugating enzyme 13
USP1	Ubiquitin-Specific Protease 1
VHL	Von Hippel-Lindau
VRCs	Viral Replication Centres
WB	Western blot
WHO	World Health Organization
w.t.	Wild Type
XRCC4	X-ray repair cross-complementing protein 4

CHAPTER 1



Introduction

1.1 Human Tumour Viruses

The most recent data from the World Health Organization (WHO) suggests that upto 20% of all human cancers are attributable to infection, such that 2.1 million new cases of cancer in 2012 were due to infection (WHO, 2012). Infection-induced cancers have been shown to be particularly common in poor and developing countries where pathogens such as human papilloma virus (HPV) and hepatitis B and C viruses and *Helicobacter pylori* bacteria are prevalent (Plummer, et al. 2016). Human tumour viruses possess either DNA or RNA genomes and, as such, are accordingly classified as either DNA viruses and RNA viruses. Given that the main focus of this thesis is adenovirus, a small DNA tumour virus that is implicated in cellular transformation and tumourigenesis, particularly in animal models, we will now consider a brief history of DNA viruses and their role in the pathogenesis of tumourigenesis before we consider adenovirus in more detail.

1.1.1. DNA Tumour Viruses

To date studies with *Adenoviridae*, *Herpesviridae*, *Hepadnaviridae*, *Papillomaviridae* and *Polyomaviridae* have shown the capability of these DNA viruses to promote tumourigenesis in humans or other animals (**Table 1.1**; Javier and Butel, 2008). The role of human papilloma virus (HPV) in human cancer is now very well established. Early studies by Guisepe Ciuffo in the first decade of the 20th century determined that the aetiology of warts was due to a transmissible agent, as a cell-free preparation from the wart could promote this proliferative, non-malignant disease in an uninfected individual ; this transmissible agent was subsequently identified as a distinct HPV type (reviewed by Bergonzini, et al. 2010). Subsequent to the studies by Ciuffo, a genuine mammalian papilloma tumour virus was identified, the Shope virus (named after the person who discovered it, Richard Edwin Shope), that infected the cutaneous epithelium of rabbits and induced a wart-like disease of the skin (Shope and Hurst, 1933). It was only in the 1970's when work from Harald zur Hausen established that HPV strains 11, 16 and 18 were the causative agents of cervical cancer; HPV infection is responsible

for almost all cases of human cervical cancer cases and is also responsible for other anogenital malignancies and head and neck cancers (Zur Hausen, 1976; Zur Hausen, 2009).

It was not until 1962, however, that the first report of a human DNA tumour virus was published (Trentin, et al. 1962). John Trentin determined that human adenovirus 12 (Ad12), but not other adenovirus types, would induce sarcomas in the mediastinum, the chest wall and diaphragm when injected intrapulmonary into new-born hamsters. Further studies by Trentin and others determined that the ability of the Ad12, and not other human Ads to induce tumorigenesis was not only due to the expression of viral oncogenes (discussed below) but due to the virus's ability to evade the immune system (reviewed by Gallimore and Turnell, 2001). Despite these early findings, adenovirus infection is not thought to play a significant role in human tumourigenesis, although studies from Thomas Lion's group have determined that Ad groups B and D are found in a high proportion of different types of paediatric brain tumours, including glioblastomas, oligodendrogliomas and ependymomas (Kosulin, et al. 2007). Moreover, studies from Linda Gooding and David Ornelles have determined that persistent Ad infection of lymphoid tissue with group C viruses, correlates positively with children who later develop acute lymphoblastic leukaemia (ALL ; Gustafsson, et al. 2007). These studies taken alone suggest that adenovirus might also play a role in human tumourigenesis but clearly more work needs to be performed to establish a definitive role for human adenovirus types as causative agents of human cancer. Given the early findings by Trentin, however, adenovirus has become a very popular model to study the molecular basis of cellular transformation and oncogenesis and the cellular pathways that regulate these processes. A more detailed consideration of the role of adenovirus gene products in cellular transformation and oncogenicity is presented in section 1.2.5. In addition to adenovirus and HPV a number of DNA tumour viruses have been identified that play a role in human cancer (**Table 1.1**).

Neoplastic transformation of cells by DNA viruses, such as adenovirus, is a cumulative process that can occur long after the initial infection and requires other genetic changes in the cells where the cancer occurs that are independent of infection. Viral infection often results in the inactivation of cellular tumour suppressors, the inhibition of apoptosis, and cellular immortalization that aids tumourigenesis (Hanahan and Weinberg, 2000). Viral tumourigenesis is also often accompanied integration of the viral DNA into the cellular genome where the permanent expression of early viral oncogenes, or activation of cellular oncogenes deregulates cellular gene expression and signal transduction pathways that promote cell growth and inhibit cellular apoptosis. In this regard, a number of DNA tumour viruses target key cellular tumour suppressors such as p53 and the retinoblastoma gene product, pRB which are also often de-regulated in cancers that are not caused by infection (Hanahan and Weinberg, 2000). Given the ability of viruses to de-regulate host cell signalling pathways, it is no surprise that researchers have utilized other tumour viruses, in addition to adenovirus, as experimental models to investigate the critical molecular events that occur during tumourigenesis (Berk, 2005). In this regard, the last 50 years of studying DNA tumour viruses has been extremely important towards understanding the molecular events that cause cancer and important cellular processes, such as cell cycle regulation, transcription and DNA replication (Javier and Butel, 2008).

Before we consider the role of adenovirus gene products in cellular transformation and oncogenesis in more detail we will consider the classification and structure of adenoviruses and the role individual early region proteins play during infection and how they modulate host cell protein function.

Table 1.1: DNA tumour viruses as causative agents of tumourigenesis

Virus Family	Virus and Disease
Adenoviridae	Adenoviruses (Ad): Tumours in rodents- potential role in human paediatric brain tumours and leukaemias.
Papillomaviridae	Human papillomavirus (HPV): Cervical Carcinoma, anogenital, head and neck and skin cancers.
Hepadnaviridae	Hepatitis B Virus (HBV): Hepatocellular Carcinoma
Herpesviridae	Epstein-Barr Virus (EBV): Burkitt's lymphoma, Nasopharyngeal carcinoma.
Herpesviridae	Kaposi's sarcoma human virus (KSHV): Kaposi's sarcoma
Polyomaviridae	Merkel cell virus (MCV): Merkel Cell carcinoma
Polyomaviridae	Polyoma virus of the rhesus macaque (SV40): Tumours in rodents but not in natural host; potential role in human brain and bone cancers.

1.1.2. Adenovirus Identification and Classification

Adenoviruses belong to the *adenoviridae* family and are non-enveloped icosahedral DNA tumour viruses. They possess a linear double-stranded (ds) DNA genome and undergo a lytic cycle of replication. Adenoviruses were discovered in 1953 at the National Institutes of Health (Bethesda, Maryland) by researchers when they were trying to characterize viral agents isolated from the adenoid and tonsil tissue grown in cell culture; hence they were named adenoviruses “adeno” comes from the Greek word for gland (Rowe, et al. 1953). At the same time and in independent studies Hillman and Werner were investigating a flu-like virus in army recruits, whereby they isolated adenovirus from tracheal cells (Hillman and Werner, 1954). Since their discovery, this family of viruses have often been used as a model for studying different cellular processes such as viral entry and assembly, transcription and DNA replication, cell cycle control, cellular transformation and tumourigenesis and led to the seminal discovery of splicing, for which Phil Sharp and Richard Roberts received the Nobel prize (Berk and Sharp, 1977; Chow, et al. 1977).

According to the Baltimore classification the *adenoviridae* family of adenoviruses are group one ds DNA viruses, which have subsequently been divided into five different genera according to the host species they infect: *Aviadenoviridae*, *Atadenovirus*, *Mastadenoviridae*, *Siadenoviridae* and *Ichtadenovirus* (Carstens, 2010). Viruses of Ichatadenoviruses and Avianadenoviruses infect fish and birds respectively, whilst *Siadenoviruses* and *Atadenoviruses* infect a number of different hosts such as birds, ruminants, amphibians and reptiles (Davison, et al. 2003). Mastadenoviruses infect mammalian hosts, of which there are over 100 known human serotypes divided into seven species (A to G) based on their antibody neutralization properties and ability to agglutinate erythrocytes of rat, monkey and human, which broadly corresponds with their ancestral relationship, sequence homology and oncogenic potential (**Table 1.2**; Russell, 2009).

Adenovirus type 12 (Ad12) belongs to group A, which is considered to be highly oncogenic, unlike the group C viruses that includes the widely-studied adenovirus type 5 (Ad5) which has been shown to be non-oncogenic (Trentin, et al. 1962; Trentin, et al. 1968). As already discussed it is believed that adenoviruses are not major causative agents of cancer in humans; however human and rodent primary cells can be transformed by both oncogenic and non-oncogenic viruses in tissue culture (McBride and Wiener, 1964; Russell, 2009). As outlined above adenoviruses infect a broad range of species, however, their ability to cause disease is largely controlled by the effective cellular defences of the infected host. Regardless of this, it is known that roughly a third of the known human Ad types are involved in respiratory, ocular and gastrointestinal diseases detected in children and immunocompromised individuals (Echavarría, 2008). Furthermore, serious health conditions such as hepatitis, hemorrhagic cystitis, pneumonia, colitis, pancreatitis, meningoencephalitis, and disseminated disease in AIDS and other immunocompromised patients are attributed to some adenovirus types (Echavarría, 2008).

Table 1. 2: Classification of Human Adenoviruses. The adenovirus types discovered to date are classified into groups A to G and as indicated. Their oncogenicity toward rodents and transformation activity in tissue culture is also indicated (<http://hadv.wg.gmu.edu/>).

Group	Types	Oncogenicity in rodents	Transformation in vitro
A	12. 18. 31	High	Yes
A (New)	61	Unknown	Unknown
B (New)	66. 68. 76. 77. 78. 79	Unknown	Unknown
B1	3. 7. 16. 21. 50	Moderate	Yes
B2	11. 14. 34. 35. 55	Moderate	Yes
C	1. 2. 5. 6. 89.	Low or none	Yes
D	8. 9. 10. 13. 15. 17. 19. 20. 22. 30. 32. 33. 36. 39. 42. 49. 51. 53. 54.	Low or none	Yes
D (New)	56. 58. 59. 60. 62. 63. 64. 65. 67. 69. 70. 71. 72. 73. 74. 75. 80. 81. 82. 83. 84. 85. 86. 87. 88. 90. 91. 92. 93. 94. 95. 96. 97. 98. 99. 100. 101. 102. 103.	Unknown	Unknown
E	4	Low or none	Yes
F	40. 41	None-reported	Yes
G	52	None-reported	Unknown

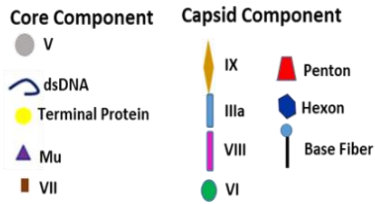
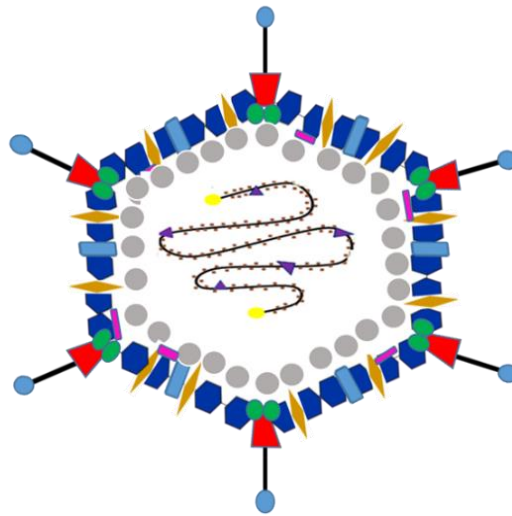
1.1.3. Adenovirus structure and genome organization

Adenovirus structure has been analysed by both electron microscopy and X-ray diffraction to a resolution of 3.5 Å which have contributed enormously to elucidating the virion's architecture. Adenoviruses are quite large viruses with a molecular weight of approximately 150 MDa and a diameter of between 70 and 100 nm. They are composed of two main parts, the outer capsid and the core. The non-enveloped capsid has an icosahedral arrangement consisting of 252 capsomeres with 240 surface facing features (homotrimeric hexons) and 12 vertices (penton bases) from which long fibres with terminal knobs extend. Together, these structures form the outer capsid (Brenner and Horne, 1959; Horne, 1959; Valentine and Pereira, 1965). Proteins such as IIIa, VI, VIII, and IX associate with the hexons and pentons, and participate to cement the virion capsid and provide structural support (**Fig. 1.1 A**; Saban, et al. 2006). The adenovirus core comprises the adenovirus genome and core proteins. Adenoviruses

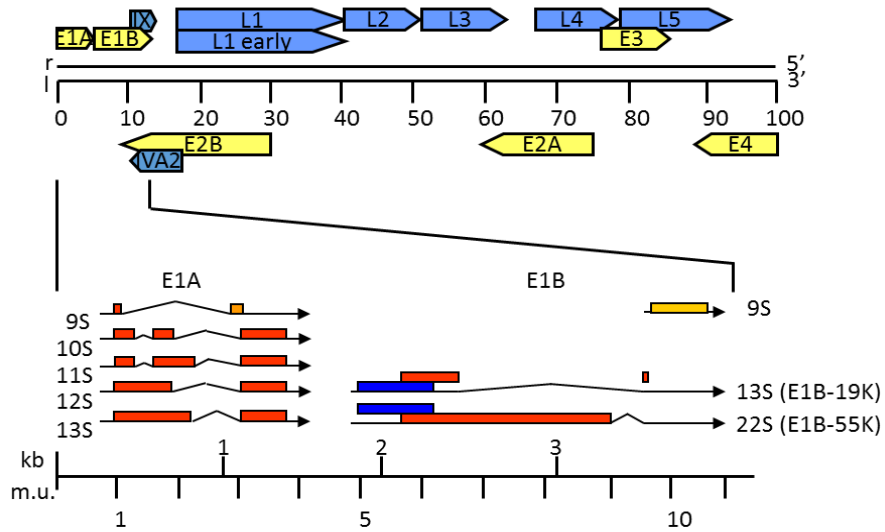
have linear, dsDNA genomes, of between 26 and 45 kb in size, which rank them as medium-sized among other DNA viruses. In this regard the Ad5 genome is 36kb in size whilst the Ad12 genome is 34kb in size (Saha, et al. 2014). Adenovirus genomes are characterized by inverted terminal repeats (ITR) about 100-140 bp in size that cap each end of the genome and are concentrated in the virion core, where they are linked to the proteins V, VII, and X, and the terminal protein (TP), which associates covalently to the 5' termini of each ITR and acts as a primer for DNA replication (**Fig. 1.1A**; Rauschhuber, 2011). The ITR possesses cis-acting elements and binding motifs for the cellular transcription factors SP1 and ATF that are required for the initiation of E1A transcription (Hatfield and Hearing, 1991).

The Ad infectious cycle can be divided in two stages, early and late, which are separated by the commencement of DNA replication (Russell, 2000). As such, the Ad genome is organized into three regions; the early region which comprises six transcription units (E1A, E1B, E2A, E2B, E3, and E4), the intermediate region consists of two transcription units (IX and IVa2), and the late region which comprises only one transcription unit which is transcribed to produce five families of late mRNAs [L1-L5] (**Fig. 1.1B**; Täuber and Dobner, 2001). A detailed transcription map showing the major E1A and E1B transcripts are also depicted in **Fig. 1.1B**, whilst the major E4 transcripts are depicted in **Fig. 1.1C**. The major late promoter (MLP) is activated upon the onset of viral DNA replication by the intermediate gene products IX and IVa2, whilst the L4 products 22K, 33K enhance MLP activation to promote the early to late switch and the synthesis of the structural proteins (Russell, 2000). Indeed, L4-22K and L4-33K stimulate late gene expression from another late-promoter (L4P) located within the L4-100K open reading frame (Morris, et al. 2010), whilst E1A, E4orf3, and IVa2 also stimulate this promoter, as does p53 (Wright and Leppard, 2013).

(A)



(B)



(C)

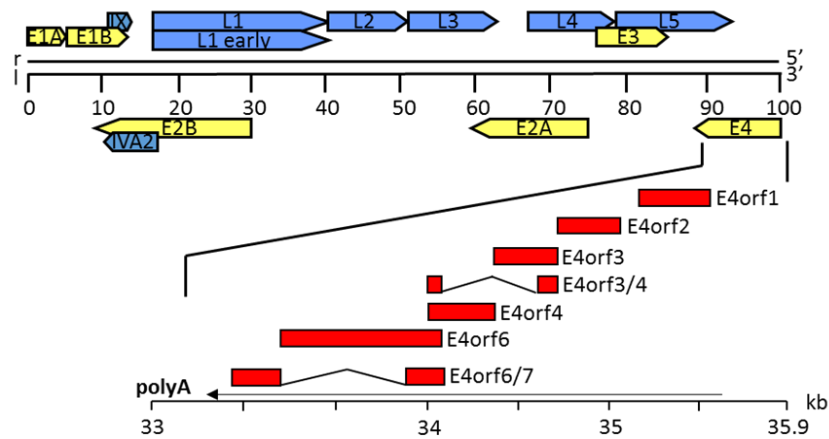


Figure 1.1: Structural representation of the adenovirus virion and schematic representation of the adenovirus transcription map. (A) This picture depicts the viral capsid and shows the linear dsDNA adenovirus genome and the core viral proteins known to associate with the genome. Illustration taken from (Waye and Sing, 2010). (B) Schematic representation of the Ad5 transcription map. The figure shows the two main transcription units from the Ad genome following viral infection: the E1A, E1B, E2A, E2B, E3 and E4 early transcription unit (highlighted in yellow), including detail of E1A and E1B transcripts produced (highlighted in red); the Late transcription unit, comprising L1 to L5 are shown in blue. (C) The E4orfs are expressed from a single mRNA with a polyadenylation signal (polyA), to produce a primary transcript of 2800 nucleotides. The mRNA spliced gene products are shown as boxes, relative to their location in the Ad5 genome and are highlighted in red.

1.1.4. Adenovirus cellular entry, chromatinization and viral DNA replication

Adenovirus entry into the host cell follows sequential steps that requires virion attachment to the host cell, entry into the host cell by receptor-mediated endocytosis, endosomal escape from the host cell machinery and entry into the cytosol and the Dyenin-mediated transport delivery of the viral genetic material to the nucleus where viral DNA replication, viral gene expression, and viral assembly take place. A schematic summary of adenovirus life cycle is depicted in (Fig. 1.2; Luisoni and Greber, 2016). Studies have revealed that viral entry is dependent upon the viral capsid components, the fibre and the penton base (Wu and Nemerow, 2004). The fibre protein facilitates cellular internalization through its ability to associate with the coxsackie virus-adenovirus receptor (CAR) - the major cellular receptor for adenovirus (Hartlerode, et al. 2015). Other cellular receptors also facilitate adenovirus binding to cells, including $\alpha v\beta 3/5$ integrins, the membrane cofactor protein, Desmoglein 2 and Sialic acid (Baker, et al. 2018).

Indeed, association of the penton base protein to surface integrins triggers viral entry by clathrin-coated mediated endocytosis (Mathias, et al. 1998). Following internalization capsid dissociation and rearrangements occur in the acidified endosome which facilitates virus particle release into the cytoplasm, whereupon hexon associates with the Dynein transport apparatus to allow for transportation of the genetic material to the nucleus through nuclear pores to initiate viral transcription programmes that ultimately results in viral DNA replication, the synthesis and assembly of new virions, DNA packaging into new virions, cell lysis and virus release (Wu and Nemerow, 2004).

Cellular DNA is packaged into the nucleosome that comprises 146bp of dsDNA wrapped around a histone octamer, comprising 2 sets each of Histone H2A-H2B and H3-H4 dimers. Incoming virus particles associate with the nuclear pore whereupon they associate with histone H1 for nuclear import, though histone H1 does not associate directly with viral DNA (Trotman, et al. 2001). It has been found that incoming adenovirus DNA is rapidly chromatinized by the cellular histone octamer in a 200bp repeat akin to normal nucleosome structure, in a manner that is independent of viral DNA replication (Daniell, et al. 1981). Chromatin Immunoprecipitation (ChIP) studies have established that the same molecule of viral DNA can be both protein VII and histone-associated suggesting that viral chromatin is distinct from cellular chromatin (Komatsu, et al. 2011). It has been determined that histone variant histone H3.3 is preferentially deposited on viral DNA by the chaperone protein HIRA, which normally coats actively transcribed DNA, whilst another histone H3.3 chaperone, Daxx is inactivated during Ad infection (Ross, et al. 2011; see section 1.2.2). It has been suggested however, that most protein VII is removed from viral DNA prior to the activation of Ad transcription programmes that can occur on viral DNA associated with cellular histones which is regulated by histone acetylases such as CBP/p300 (Komatsu, et al. 2011; see section 1.2.1). Indeed ChIP analyses have shown that acetylated histones are associated with active early region promoters.

Ad DNA replication is a very efficient process. Within 40h of DNA replication initiation approximately one million copies of viral DNA are produced and approximately 10,000 new virions per cell assembled (Hoeben and Uil, 2013). To achieve this adenovirus employs a unique protein priming mechanism for replication to begin. This process requires three viral proteins encoded by the E2 early region: the TP precursor protein (pTP), Ad DNA polymerase (Ad Pol), and the DNA-binding protein (DBP). pTP serves as a primer for viral DNA replication initiation and has the capacity to bind to both ssDNA and dsDNA. Ad pol is a member of the α -like DNA polymerases and utilises the pTP primer for replication initiation (Field, et al. 1984). Ad DBP localises at viral replication centres in the nucleus of the infected cell where it performs multiple activities during viral replication (Chang and Shenk, 1990), adenovirus utilises the cellular transcription factors nuclear factor 1 (NF1), nuclear factor 2 (NF2), and octamer-binding protein 1 (Oct1; also known as NF3) to stimulate Ad DNA replication (Nagata, et al. 1982; Pruijn, et al. 1986; Mysiak, et al. 2004; Hoeben and Uil, 2013). Multiple associations between these viral and cellular proteins coordinate the formation of the pre-initiation complex formation (Hoeben and Uil, 2013). Ad replication occurs at viral replication centres (VRCs) in the nucleus of the infected cell, where both pro-viral and anti-viral cellular factors accumulate to modulate viral replication.

The Ad pol mediates the formation of deoxycytidine monophosphate (dCMP)/pTP complex by catalysing the covalent association between the β -OH group of a serine residue in pTP and the α -phosphoryl group of deoxycytidine monophosphate (dCMP). This complex is important as a primer for synthesis of the nascent strand (Liu, et al. 2003). The interaction between NF1 and Ad pol, as well as Oct1 to pTP is coordinated by DBP, which is also important in enhancing their affinity for viral DNA sequences (De Jong, et al. 2003). DBP also controls the unwinding of viral duplex DNA in an ATP-dependent manner and viral DNA elongation (De Jong, et al. 1999). After replication, the viral protease cleaves pTP to produce its mature, smaller form TP

(Hoeben and Uil, 2013). TP remains covalently attached to the 5' end of the genome during replication, although the reason for this is currently unknown, although it has been suggested to be involved in: facilitating unwinding of the DNA duplex; allowing for DNA-nuclear matrix association; protecting viral DNA from exonuclease activity (Dunsworth-Browne, et al. 1980; Stillman, et al. 1981; Schaack, et al. 1990). Indeed, protection from cellular exonucleases may be one strategy how adenovirus evades the cellular DNA damage response (DDR). Other strategies employed by adenoviruses to evade cellular antiviral DDR activities will be addressed later in this chapter (see section 1.4). Newly replicated Ad viral DNA is also coated with cellular histones though is ultimately packaged into new virions by protein VII.

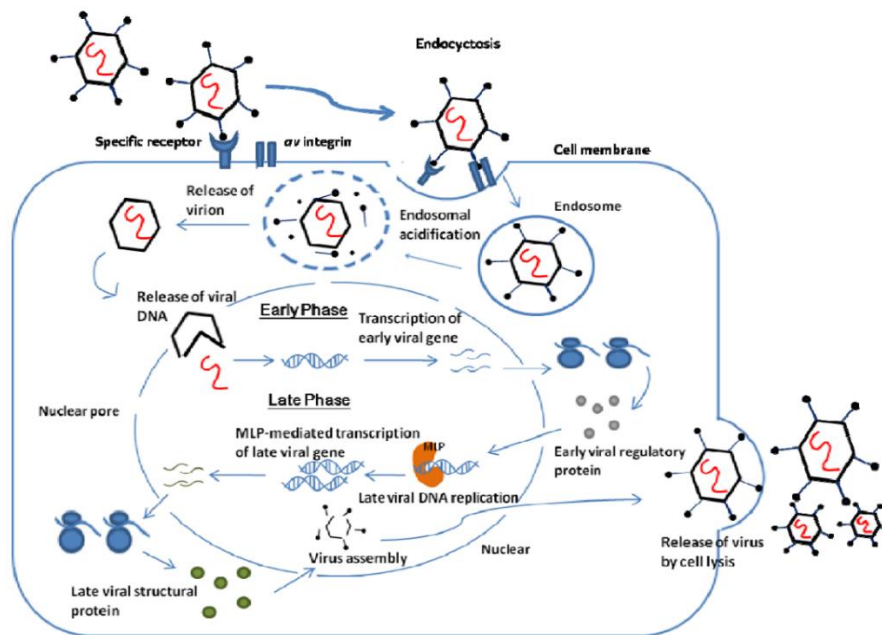


Figure 1.2: Summary of adenovirus life-cycle. Taken from (Waye and Sing, 2010).

1.1.5. Viral Replication Centres

Viral replication centres (VRCs) comprise the major regions of nascent viral transcription and post-transcriptional processing as well as viral DNA replication, viral particle assembly and packaging (Charman, et al. 2019). They serve as molecular hubs and serve to regulate host-cell interactions. As such, cellular proteins required for viral replication are actively recruited to VRCs by Ad early region proteins, particularly E1A, E1B-55K, E2A and E4orf6 (see section

1.2 for more details). Moreover, proteins that form the cellular defence to viral infection are targeted to VRCs, where they are often inactivated by interaction and sequestration by viral early proteins, or are targeted for degradation by cellular CRLs (see section 1.3.2.2.).

The Replication A protein complex is recruited to VRCs following adenovirus infection and are often considered a surrogate marker for VRCs. As cellular proteins recruited to VRCs often possess either pro-viral or anti-viral activities our laboratory attempted to identify proteins that are recruited to VRCs through interaction with the RPA complex (Qashqari, PhD thesis, University of Birmingham, 2017). By analysing proteins that associated specifically with GFP-RPA1 during both Ad5 and Ad12 infection our laboratory identified a number of cellular proteins that were potentially recruited to VRCs during infection. Of those proteins identified, the FACT chaperone complex, comprising SPT16 and SSRP1, Pur α and Pur β transcriptional regulators and the RNA-binding protein, RBM14 were all suggested to be recruited to VRCs.

1.1.5.1. The FACT Complex

The FACT (Facilitates Chromatin Transcription) chaperone complex serves to regulate the assembly/disassembly of nucleosomes that comprise chromatin, as compact chromatin creates a barrier for critical cellular processes such as transcription, replication and DNA damage responses (**Fig.1.3**). As such, the FACT complex temporarily modulates chromatin architecture so that these processes can be completed. Specifically, FACT promotes the dissociation of the histone H2A-H2B dimer from the nucleosome to allow for processes such as transcriptional regulation, but also has the capacity to mediate nucleosome reconstitution (reviewed by Belotserkovskaya, et al. 2004). As FACT is recruited to VRCs during adenovirus infection, it is likely that complex possesses either pro- or anti- viral activities during infection, though its exact role requires clarification.

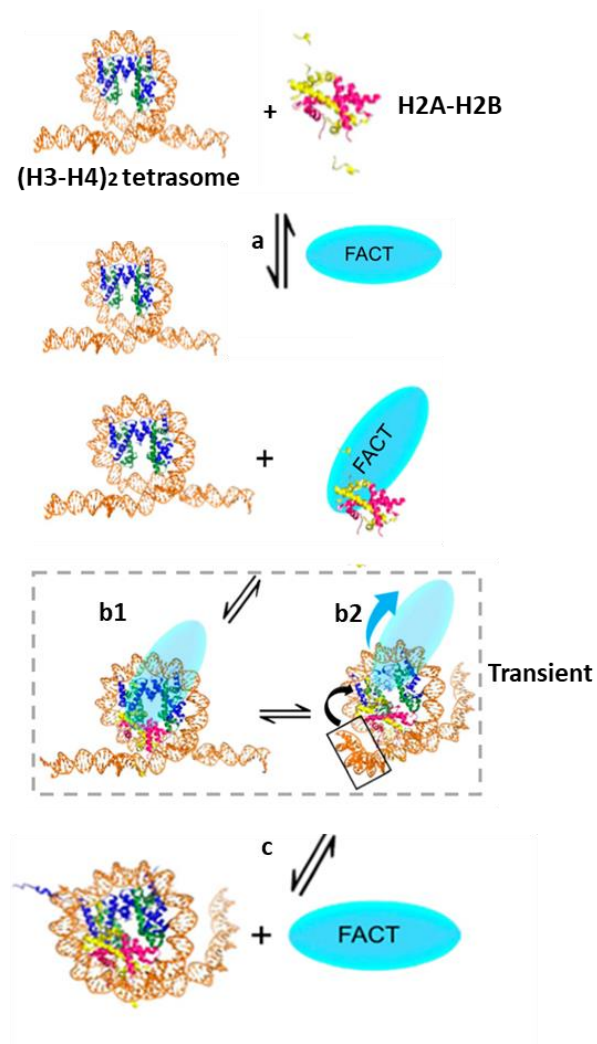


Figure 1.3: Model of FACT action in nucleosome/hexasome assembly. a: FACT associates with H2A–H2B dimer; b1: FACT chaperones H2A–H2B onto $(H3-H4)_2$ tetrasome; (B2): free DNA end competes FACT off H2A–H2B; c: hexasome is formed. Taken from: (Wang, et al. 2018).

The FACT complex is a heterodimer of two proteins: Structure-Specific Recognition Protein1 (SSRP1) and Suppressor of Ty (SPT16; **Fig. 1.4**; Winkler and Luger, 2011; Formosa, 2012; Garcia, et al. 2013). Both proteins have been shown to be involved in nucleosome remodelling, cell cycle regulation and the DNA damage response (Belotserkovskaya, et al. 2003; Dinant, et al. 2013). FACT has also been shown to be overexpressed in different types of cancers. Although, FACT proteins do not function directly as oncogene products they have been shown

to cooperate with other oncogenes and serve to enhance tumourigenicity; FACT is both a potential cancer biomarker and a target for cancer therapeutics. There are very few studies that have identified roles for FACT in viral replication, although FACT has reported to be involved in suppressing HIV-1 transcription and enhancing viral latency (Huang, et al. 2015).

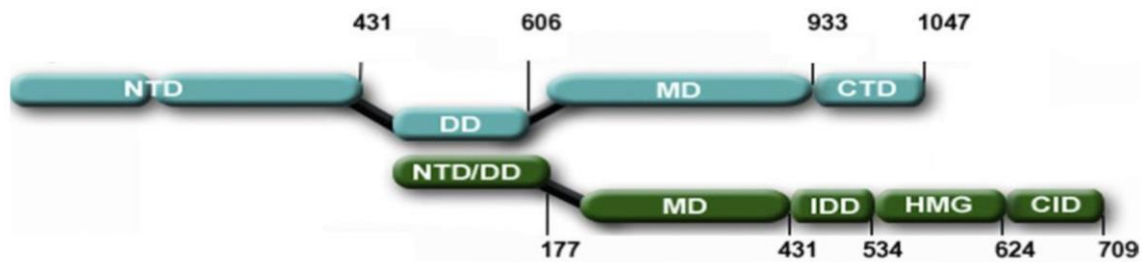


Figure 1.4: Domain structure of FACT proteins. The FACT heterodimeric is composed of Spt16 (cyan) and SSRP1 (dark green) subunits. SPT16 protein for all eukaryotic has multiple domains: N-terminal domain (NTD), Middle - domain (MD), dimerization domain (DD) and C-terminal domain (CTD). SSRP1 has the following domains N-terminal domain (NTD), dimerization domain (DD) Middle - domain (MD), intrinsically disordered domain (IDD), high mobility group domain (HMG) and C-terminal domain (CTD). Taken from: (Winkler and Luger, 2011).

1.2. Adenovirus Early region proteins

This section will consider mainly the function of the early region proteins, 12S and 13S E1A, E1B-19K and E1B-55K, as well as the E4orf's that arise from differential splicing of the E1A, E1B and E4 transcription units, respectively (**Fig. 1.1B** and **C**). Specific attention will be given to the E1B-55K, E4orf3 and E4orf6 proteins that are the major focus of this thesis. As such the roles of these proteins both during infection, and in cooperation with E1A during cellular transformation will be considered. For convenience a table highlighting the major biological functions of the early region proteins is shown below.

Table 1. 3: Description of early region gene product function. The Table indicates functions of E1A, E1B, E2, E3 and E4 proteins.

Early region protein	Biological functions
<p>12S E1A 13S E1A</p>	<p>Transcription, transformation, induction of S-phase entry early region gene transactivation</p>
<p>E1B-19K E1B-55K</p>	<p>Inhibits apoptosis, oncogenic transformation, host cell shut-off, inhibits apoptosis, oncogenic transformation</p>
<p>E2A</p>	<p>DNA-binding protein; viral replication centres function and integrity</p>
<p>E2B</p>	<p>DNA polymerase</p>
<p>E3 proteins</p>	<p>Immune modulation</p>
<p>E4 open reading frames</p>	<p>Transcriptional regulation, mRNA transport, DNA replication, host cell shut off, oncogenic transformation</p>

1.2.1. Adenovirus E1A proteins

Adenovirus early region 1A (Ad E1A) is located within the first 11.2% of the Ad genome on the left side and is transcribed from the top strand. Its molecular weight is found to vary from 35 to 48 kDa, which is dependent upon the E1A species expressed and also post-translational modification-PTM (Gallimore and Turnell, 2001). Although E1A is not a DNA-binding protein, E1A functions primarily as a transcriptional regulator that promotes cell cycle progression and viral replication, and has the capacity to induce oncogenic transformation due its association with various proteins through distinct conserved region (CR) domains in the E1A protein, or a less well conserved N-terminal region (NTR; Subramanian, et al. 2013). By binding to and radically changing the activity of many cellular proteins, AdE1A promotes a productive adenovirus infection and, in certain circumstances, Ad-induced transformation (Gallimore and Turnell, 2001). In this regard E1A possesses the ability to transform both

primary human and rodent cells in cooperation with Ad E1B, or activated *ras* (Byrd, et al. 1982; Ruley, 1983). Indeed, in the absence of cooperating oncogenes E1A induces p53-dependent apoptosis (Lowe, et al. 1993).

Ad E1A is the first protein to be expressed following adenovirus infection and is expressed as two major mRNA products, 12S and 13S, which give rise to proteins of 243 and 289 amino acids, respectively for Ad2 and Ad5 and 235 and 266 amino acids for Ad12 (Boulanger and Blair, 1991). Both isoforms possess three highly conserved regions CR1, CR2, and CR4 with the larger 13S gene product possessing an additional domain, CR3 (**Fig. 1.5**; Avvakumov, et al. 2002; Avvakumov, et al. 2004). 13S E1A is generally regarded as a transcriptional activator whereas the 12S E1A gene product is regarded as a transcriptional repressor. Three other splice variants, 9S, 10S and 11S E1A gene products are also produced during the late stages of infection. Their function is not well understood, although the 9S E1A gene product does retain some functions of the larger 12S and 13S gene products (Miller, et al. 2012).

The CR3 region of Ad E1A is a transcriptional activator and drives the expression of the other early region genes. As such it associates with the cellular transcriptional machinery and viral early promoters through protein-protein interactions. CR3 can also modulate cellular transcription programmes through interaction with cellular promoters. The CR3 transactivation domain is composed of two regions, a zinc finger region (residues 147-177, in Ad5 E1A) that associates with a number of transcriptional regulators and a carboxyl region (residues 183-188, in Ad5 E1A) that targets E1A to promoters (Webster and Ricciardi, 1991). The CR3 zinc finger region associates with TBP, the MED23 component of the Mediator complex as well as 19S, 20S and 26S proteasomes, and histone acetylases, CBP/p300 and P/CAF to stimulate transcription (Berk, 2005; Rasti, et al. 2006). One of E1A's primary functions is to re-programme cellular gene expression in order to induce S-phase in the infected cell and to create an environment permissive for viral DNA replication. As such, E1A function is dependent

upon short motif/molecular recognition features (MoRFs) that direct E1As interaction with numerous cellular proteins (**Fig. 1.5**). For instance, it has been established that the NTR, CR1 and CR2 domains of E1A are required to induce S-phase entry. CR1 and CR2 of E1A bind to the tumour suppressor protein, pRB, and related proteins p107 and p130, to activate E2F-dependent transcription, whilst the NTR and CR1 bind independently to CBP/p300 to modulate cellular histone acetylation (Egan, et al. 1988; Whyte, et al. 1988; Howe, et al. 1990; Eckner, et al. 1994). It has been established that E1A can, during infection, redistribute CBP/p300 to specific genomic loci to modulate histone H3 K18 acetylation; E1A interaction with p300/CBP enhances the acetylation of pRB at K873/K874 which associates with repressive chromatin-modifying enzymes to repress transcription of genes that would otherwise inhibit viral replication (Ferrari, et al. 2008; Horwitz, et al. 2008; Ferrari, et al. 2014). The roles of these E1A-binding proteins in cellular transformation will be considered later (see section 1.2.5.1).

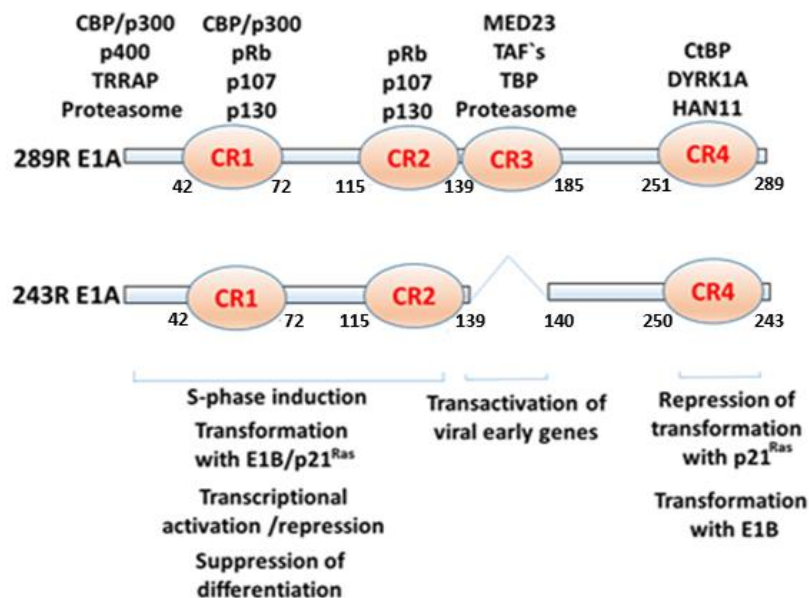


Figure 1.5: E1A functional domains and binding proteins. The conserved regions (CR) of the 12S and 13S E1A are shown as orange circles. Key E1A binding proteins are listed as are the biological functions of specific E1A domains. Adapted from: (Berk, 2005).

1.2.1.1. The ubiquitin-like protein SUMO and its regulation by E1A

SUMO is a small ubiquitin-like modifier that covalently attaches to lysine residues of target substrates to regulate enzymic activity, protein stability, protein-protein interactions and cellular localization that affects multiple biological activities including transcription, cell cycle and the DDR (Wilkinson and Henley, 2010). In mammalian cells there are five SUMO genes, SUMO-1 to SUMO-5; SUMO-1, SUMO-2, and SUMO-3, are the most extensively studied SUMO species. SUMO-2 shares 97% amino acid similarity with SUMO-3 (often known as SUMO-2/3) and 50% homology with SUMO-1. SUMO is an 11 kDa protein that exists as inactive precursor and so requires first to be cleaved by a SENP (SUMO-specific protease) at its C-terminus, which allows SUMO to be covalently attached through its C-terminal glycine residue to a catalytic cysteine in the heterodimeric E1 SUMO-activating enzyme SAE1/SAE2 in an ATP-dependent manner. SUMO is then transferred to a catalytic cysteine residue in the E2 SUMO-conjugating enzyme, Ubc9 before being conjugated to a lysine residue in target substrate in the absence or presence of a SUMO E3 ligase.

It was established in 1996 through a yeast two-hybrid screen that the CR2 region of E1A interacted with Ubc9 (see **Fig. 1.8 A**; Hateboer, et al. 1996). Given its association with CR2 it was postulated that E1A interaction with Ubc9 was important for the cellular functions of E1A. It was later established that an E1A MoRF comprising the sequence EVIDLT in CR2 bound to the NTR of Ubc9, the same region of Ubc9 that binds to SUMO in a non-covalent manner. It was therefore postulated that E1A affected Ubc9-mediated polySUMOylation of substrate proteins. It was established however that E1A expression did not affect global polySUMOylation and that E1A interaction with Ubc9 was not required for E1A-mediated transformation. Despite this the E1A-Ubc9 interaction was shown to modulate promyelocytic leukemia body reorganization by E1A and pseudohyphal growth in yeast (Yousef, et al. 2010). Studies from another laboratory indicated that E1A expression inhibited pRB SUMOylation at

K720, a modification that was suggested to modulate pRB-mediated repression of E2F-dependent transcription (Ledl, et al. 2005). To date, pRb is the only known protein whose SUMOylation is regulated by E1A. In consideration of the activities of the E1B-55K (section 1.2.2) and E4orf3 (section 1.2.4.1) gene products, adenovirus modulates the SUMO pathway at multiple levels during infection.

1.2.2. Adenovirus E1B proteins

The adenovirus early region 1B (E1B) gene is differentially spliced to give five gene products for Ad2/5: E1B-84R, E1B-93R, E1B-156R (E1B-19K), E1B-176R and E1B-496R (E1B-55K) that all participate in promoting viral DNA replication and, moreover, participate in promoting cellular transformation. E1B-55K and E1B-19K are the most widely studied E1B gene products that serve to inhibit the pro-apoptotic effects of p53 during both infection and cellular transformation (Berk, 2005; Sieber and Dobner, 2007). The function of the other E1B polypeptides is not known.

E1B-19K is a homologue of the cellular anti-apoptotic protein, BCL-2 and binds to the pro-apoptotic proteins, BAX and BAK to prevent the assembly of BAK/BAX oligomers that would otherwise promote mitochondrial outer membrane permeabilization and activation of the intrinsic pathway of apoptosis (Sundararajan, et al. 2001; White, 2001). Indeed, BAK and BAX are nuclear-encoded proteins that in response to pro-apoptotic signals permeabilize the mitochondrial outer membrane that leads to the release of cytochrome c and Smac/DIABOLO and the activation of caspase-9 and caspase-3 (White, 2001; Cuconati, et al. 2003), E1B-19K inhibits this pathway (Cory, et al. 2003; **Fig. 1.6**).

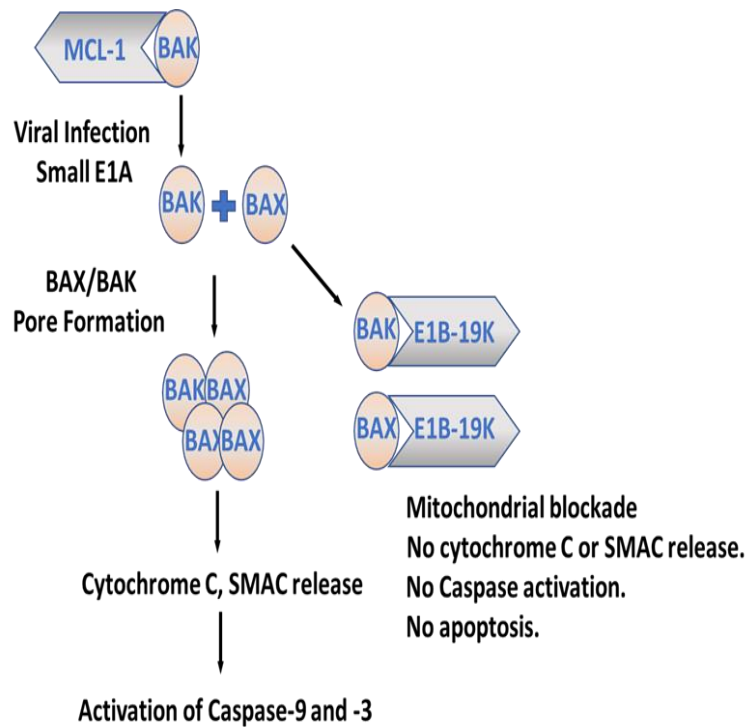


Figure 1.6: Mitochondrial apoptosis pathway inhibition by E1B-19K. Adenovirus infection leads to the E1A-induced proteasomal degradation of BAK-binding protein, MCL-1. This serves to release BAK that would otherwise associate with BAX to stimulate apoptosis. E1B-19K expression inhibits this pro-apoptotic pathway by sequestering BAX and BAK and preventing mitochondrial outer membrane permeabilization (Berk, 2005).

E1B-55K protein expression is fundamental for a productive adenoviral infection and oncogenic transformation and plays a role host-cell shut-off, viral mRNA export and the inhibition of p53 (Hidalgo, et al. 2019). The Ad5 E1B-55K polypeptide encompass a highly conserved cysteine and histidine C2H2 zinc finger around amino acids 350-370 and a conserved hydrophobic core between amino acids 215-345 that encodes a ribonucleoprotein (RNP) motif implicated in the non-sequence-specific interaction with RNA *in vitro* and with viral RNA *in vivo* (Tejera, et al. 2019). Other recognized conserved sequences in E1B-55K include a nuclear export signal (NES), a nuclear localization signal (NLS), and a number of C-terminal amino acids that are modified by PTM, particularly phosphorylation at serine 490, 491 and threonine 495 though the significance of these modifications is not known (Hidalgo, et al. 2019; **Fig. 1.7**).

Ad5 E1B-55K inhibits p53-dependent apoptosis during infection and transformation. It binds directly to p53 and inhibits the activation of pro-apoptotic p53-dependent transcription programmes (Sarnow, et al. 1984; Yew and Berk, 1992). E1B-55K and p53 associate in cytoplasmic compartments known as aggresomes (Zantema, et al. 1985; Yew and Berk, 1992). It has been reported that E1B-55K is SUMOylated at lysine 104 (**Fig. 1.7**; Endter, et al. 2001). The SUMOylation consensus motif sequence V/IKRE (ψ -K-x-E), has been shown to be conserved within many E1B-55K proteins, but not Ad12 E1B-55K. Moreover, it has been shown that Ad5 E1B-55K, but not Ad12 E1B-55K, is a SUMO E3-ligase that can undergo auto-SUMOylation. In this regard SUMO 1, 2 and 3 can covalently attach to E1B-55K lysine 104 at its consensus SUMOylation motif (Endter, et al. 2001; Wimmer, et al. 2013). It also possesses the ability to SUMOylate p53, which serves to inhibit p53 activity (**Fig. 1.8 B**; Muller and Dobner, 2008). E1B-55K SUMOylation is also important in the regulation of E1B-55K nuclear export and the degradation of the cellular antiviral protein, Daxx (Wimmer, et al. 2013).

E1B-55K cooperates during infection with other early region proteins, E4orf3 and E4orf6 to regulate processes such as host cell shut-off and, in the absence of infection, cellular transformation (Nevels, et al. 1997; Nevels, et al. 1999; Nevels, et al. 2001). For instance, it cooperates with E4orf6 to target many antiviral factors, such as p53, for ubiquitin-mediated proteolysis (Querido, et al. 2001). In this regard, E1B-55K serves predominantly as a substrate adaptor (Blanchette, et al. 2004), whereas the E4orf6 protein recruits a cellular E3 ubiquitin ligase to E1B-55K to promote the polyubiquitylation of the E1B-55K-associated substrate (Schreiner, et al. 2012). A growing numbers of target proteins including components of the MRN complex, Rad50 (Harada, et al. 2002), and meiotic recombination 11 (Mre11), DNA ligase IV (Baker, et al. 2007), p53 (Querido, et al. 2001) the Bloom helicase (Orazio, et al. 2011) and ATRX (Schreiner, et al. 2013) are all substrates for the Ad ubiquitin ligase (see section 1.3.1. for more details).

The intracellular distribution pattern of E1B-55K in Ad-infected cells varies during the viral replication cycle and in Ad-transformed cells. Early during infection, E1B-55K localizes diffusely in the nucleus and in perinuclear spots in transformed 293 cells (Liu, et al. 2005). The nuclear accumulation of E1B-55K is linked to the expression of E4orf3 protein and its reorganization of PML-nuclear bodies (PML-NB; Leppard and Everett, 1999); alternatively E1B-55K can associate with the nuclear matrix, independently of E4orf3 (Lethbridge, et al. 2003). Later during infection, E1B-55K localizes to the periphery of virus replication centres with E4orf6 (Ornelles and Shenk, 1991), where the SUMOylation of E1B-55K has been reported to play a role in its nuclear localization (Kinds Müller, et al. 2007). Indeed, E1B-55K is a substrate for the E4orf3 SUMO E3-ligase; SUMOylation of E1B-55K recruits E1B-55K to nuclear inclusion bodies (Sohn and Hearing, 2019).

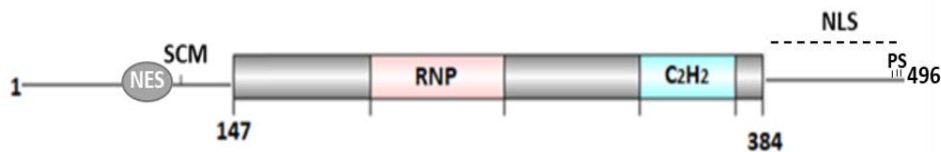


Figure 1.7: Schematic representation of E1B-55K structural features. The domain architecture of E1B-55K is shown, including an N-terminal NES region and SUMO Conjugating Motif (SCM) at Lysine 104. Also shown is the central region (residues 147–384), which possesses a ribonucleoprotein (RNP) motif and a C2H2 zinc finger. Also shown is the C-terminal NLS and region that is subject to phosphorylation (Serine 490, Serine 491, and Threonine 495; Hidalgo, et al. 2019).

1.2.3. Adenovirus E3 region

The E3 region is involved in host immune evasion and promoting viral virulence and persistence. The E3 region is not a major consideration of this thesis and will only be considered briefly here. AdE3 proteins E3-6.7K, E3-14.7K and E3-10.4K/14.5K (also known as the receptor internalization and degradation protein complex (RID α /RID β)) all protect Ad-infected cells from cytolysis by ligands, such as TNF, Fas and TRAIL that activate the TNF receptor family of proteins (Gooding, et al. 1991). Indeed, the RID complex promotes the

internalization and degradation of the TRAIL receptor 1 to block Fas and TRAIL-dependent cytolysis, whilst AdE3-6.7K cooperates with RID to target TRAIL receptor 2 for degradation (Benedict, et al. 2001; Lichtenstein, et al. 2004). The Ad2/5E3-19K protein also plays a role in immune evasion through its ability to bind to the heavy chain of the class I major histocompatibility complex (MHC1; Pääbo, et al. 1983). The consequence of this is to retain MHC1 molecules in the endoplasmic reticulum so that CD8+ lymphocytes do not target Ad5-infected cells for clearance (Cox, et al. 1990).

1.2.4. Adenovirus E4 region

The E4 transcription unit generates a primary transcript of 2800 nucleotides that is transcribed from the bottom strand on the right hand side of the Ad genome (Täuber and Dobner, 2001). Alternative splicing of this transcript generates approximately 18 different mRNAs which encode for seven orfs: orf1, orf2, orf3, orf3/4, orf4, orf6 and orf6/7 (**Fig. 1.1C**; Täuber and Dobner, 2001; Thomas, et al. 2001). E4 proteins exert their biological activities through interaction with host cell proteins that function in cell growth and cell survival processes. As such E4 proteins regulate viral DNA replication, viral mRNA transport, host cell shut-off of protein synthesis, transcriptional control and modulation of antiviral pathways, including the DDR (Halbert, et al. 1985; Weiden and Ginsberg, 1994; Täuber and Dobner, 2001). Given that proteins of the E4 region often cooperate functionally it is perhaps not surprising that the deletion of entire E4 region significantly hinders viral DNA replication, accumulation of late viral proteins and the shut-off of host protein synthesis, whilst the individual deletion of E4orfs has a more modest affect upon these activities (Halbert, et al. 1985; Falgout and Ketner, 1987). E4orf1 and E4orf2 have ill-defined functions during the late phase of viral infection, though E4orf1 from Ad9 is highly oncogenic and enhances mammary tumours formation in rats (Thomas, et al. 2001). E4orf4 is not important for efficient viral infection. In fact, it has a negative effect upon viral replication, particularly on the E1A-dependent transactivation of E2

and E4 viral promoters (Kleinberger, 2015). It is known however to interact with protein phosphatase 2A regulatory B-subunits to induce p53-independent apoptosis and as such is a potential cancer therapeutic agent (Kleinberger and Shenk, 1993). E4orf4 has also been shown to inhibit Ataxia-Telangectasia Mutated (ATM) and ATM and Rad3-related (ATR) activities in response to viral infection or treatment with DNA damaging drugs (Brestovitsky, et al, 2016). E4orf4 also associates with DNA-PK to modulate its activity during infection (Nebenzahl-Sharon, et al. 2019). Not a lot is known about the E4ORF6/7 protein, though it is known to activate E2F-dependent transcription (Kleinberger, 2015).

This region of viral genome also encodes two other proteins, E4orf3 and E4orf6, which together with E1B-55K cooperate to perform many functions during infection such as to inhibit Ad viral genome concatenation, although they also function individually during infection (Dobner and Kzhyshkowska, 2001). E4orf3 and E4orf6 proteins also participate in Ad-mediated 'hit and run' mediated transformation (Nevels, et al. 1999; Nevels, et al. 2001). The properties of E4orf3 and E4orf6 will be addressed in more detail below.

1.2.4.1. Adenovirus E4orf3

E4orf3 is an 11kDa, 116 amino acid protein that serves primarily to inactivate the host cell antiviral response to infection. As such, it reorganizes PML nuclear bodies into nuclear track-like structures (Doucas, et al. 1996), where it also sequesters the TIF1 tumour suppressor proteins TRIM24 (TIF1 α) and TRIM33 (TIF1 γ) and the MRE11/RAD50/NBS1 (MRN) DNA repair complex. It also targets TIF1 γ , at least, for proteasomal-mediated degradation (Yondola and Hearing, 2007; Forrester, et al. 2012). Immunofluorescent microscopy studies have revealed that E4orf3 forms a network of track-like structures throughout the nucleus of the infected cell where they physically separate cellular chromatin from viral replication centres (Doucas, et al. 1996). It has been determined by crystallography that the E4orf3 protein exists as a dimer that self-assembles to give extensive linear and branched oligomeric chains that

form a polymeric structure, which forms multivalent binding sites that increase avidity for partner proteins (Ou, et al. 2012). E4orf3 has also been shown to function epigenetically, and silence p53 transactivation by inducing Histone H3K9me3 heterochromatin formation at p53 target promoters (Soria, et al. 2010).

More recent studies have determined that E4orf3 is a SUMO E3-ligase that drives the SUMO2/3 polySUMOylation and SUMO-targeted ubiquitin ligase (STUbL)-mediated proteasomal degradation of TFII-I and TIF1 γ (Fig. 1.8 C; Sohn, et al. 2015; Bridges, et al. 2016). As such, targets for E4orf3-directed SUMOylation are recognised by STUbLs that subsequently target them for ubiquitin-mediated degradation. It also possesses the ability to promote the SUMOylation and reorganization to nuclear tracks of MRN components, MRE11 and NBS-1 (Sohn and Hearing, 2012). As described earlier it also serves to SUMOylate E1B-55K and promote its retention in the nucleus (Sohn and Hearing, 2019).

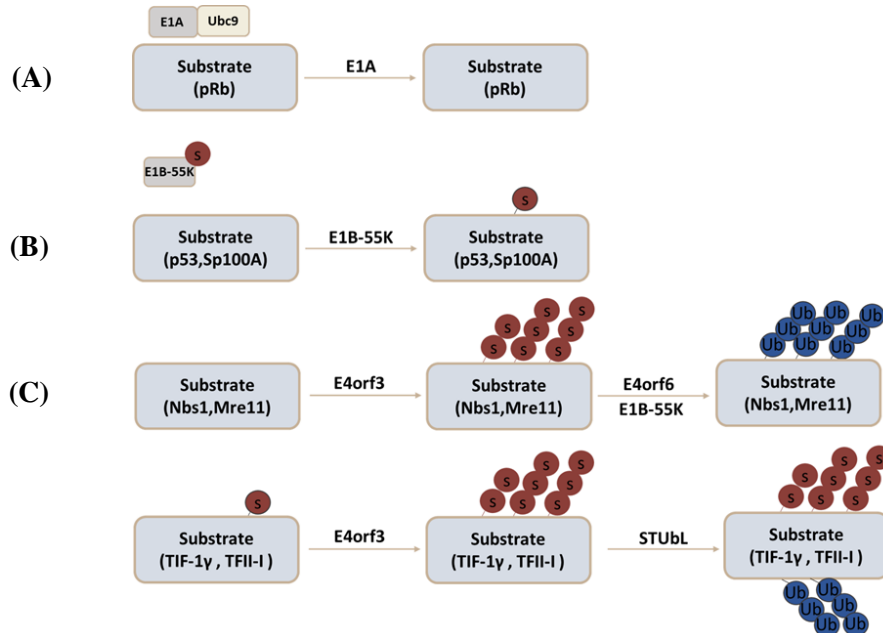


Figure 1.8: Relationship between adenovirus early region proteins and the SUMO pathway. (A) E1A inhibits the SUMOylation of pRb by binding to SUMO E2 enzyme Ubc9. (B) E1B-55K is SUMOylated and serves as an E3 ligase for p53 and Sp100A. (C) E4orf3 is also a SUMO ligase and regulates the SUMOylation of Nbs, Mre11, TIF1 γ and TFII-I. Adapted from: (Sohn and Hearing, 2016). S = SUMO moiety; Ub = ubiquitin moiety. STUbL = SUMO-targeted ubiquitin ligase.

1.2.4.2. Adenovirus E4orf6

The 34kDa product of the adenovirus early region 4 (E4) open reading frame 6, E4orf6, is a multifunctional protein that regulates viral late gene expression, viral mRNA export, p53 function and the host DDR pathway. In this regard it interacts with multiple viral and host cell proteins in both infected and transformed cells. Indeed, E4orf6 physically associates with E1B-55K and that this complex has the capacity to shuttle between the nucleus and cytoplasm (Dobbelstein, et al. 1997), such that E4orf6 is responsible for E1B-55K localization during infection and, in cooperation with E1B-55K, the export of viral mRNA from the nucleus to the cytoplasm (Dobbelstein, et al. 1997). E4orf6 also cooperates with E1B-55K to drive the ubiquitin-mediated degradation of cellular substrates for degradation during infection. This will be discussed in detail in section 1.3.2. Mutagenesis studies have revealed that E4orf6 possesses a putative nuclear localization signal (NLS) within the NTR, and an amphipathic arginine rich α -helical nuclear retention signal (NRS), within the CTR. The N-terminal NLS is important in re-directing E1B-55K to the nucleus during infection (**Fig. 1.9A**; Goodrum, et al. 1996; Orlando and Ornelles, 1999) whilst E1B-55K association with E4orf6 has been shown to mask the NRS and allow for the nuclear export of both proteins (**Fig. 1.9A**; Dobbelstein, et al. 1997). E4orf6 also possesses a functional nuclear export site (NES), similar to rev and rex retroviral proteins, which play a role in nuclear-cytoplasmic shuttling of the E1B-55K-E4orf6 complex (Dobbelstein, et al. 1997; Dobbelstein, et al. 1997), which is important in promoting viral replication (Weigel and Dobbelstein, 2000).

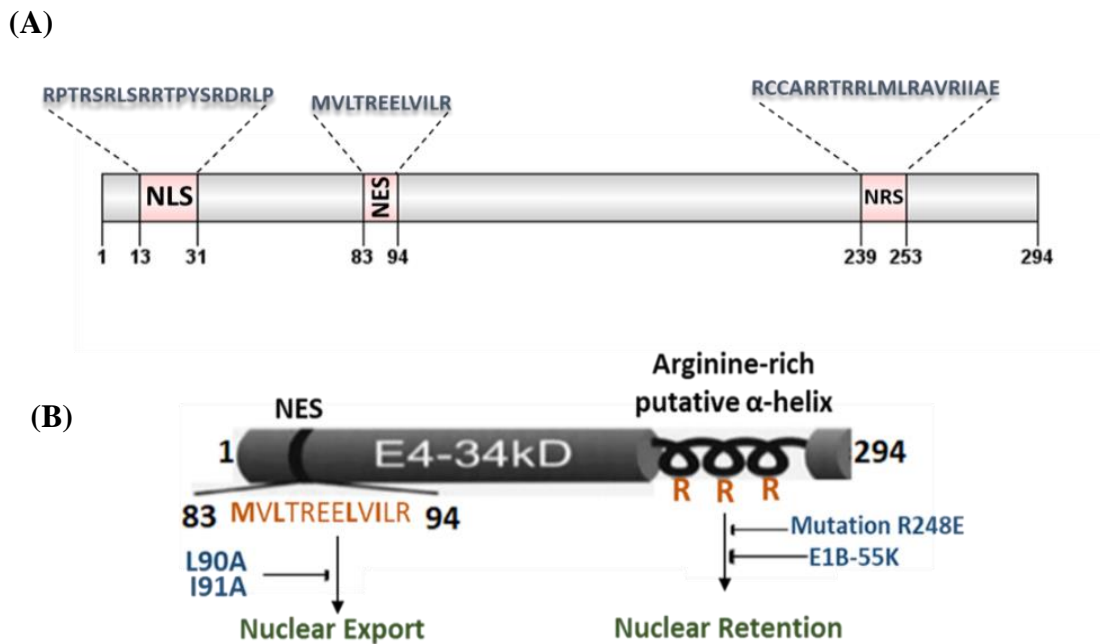


Figure 1.9: Nuclear export signals and localization signals present in Ad5 E4orf6. (A) Schematic model of the 294 residue wild -type Ad5 E4orf6 protein, indicating the position and the putative amino acids sequences for nuclear localization (NLS), nuclear export signal (NES) and nuclear retention (NRS). (B) An NES motif sequence MVLTREELVILR (amino acids 83-94), is important in directing nuclear-cytoplasmic shuttling of the E1B-55K-E4orf6 complex. Mutation from L90A or I91A impairs nuclear-cytoplasmic shuttling. The Arginine-rich NRS promotes nuclear retention, unless mutated from R248E or inhibited by E1B-55K association Adapted from: (Dobbelstein, et al. 1997).

Analysis of the E4orf6 amino acid sequence from multiple Ad types has revealed several conserved cysteine and histidine residues (**Fig. 1.10**). Zinc binding assays indicate Ad5 E4orf6 is a zinc-binding protein, though the role of the cysteine and histidine residues in zinc binding has not been established (Boyer and Ketner, 2000). Mutagenesis studies have revealed however that mutation of a number of these cysteine and histidine residues abolishes the ability of Ad5

E4orf6 to associate with E1B-55K association and re-localize E1B-55K to the nucleus, and associate with p53 and promote p53 degradation (Boyer and Ketner, 2000).

In addition to the well-established role of E1B-55K in inhibiting p53 activity, Ad5 E4orf6 is also known to inhibit p53 transcriptional activity independently of E1B-55K following infection with mutant viruses that lack E1B-55K, and in Ad E4orf6-transfected cells (Dobner, et al. 1996). As stated earlier functional p53 would be detrimental to Ad replication, unless otherwise inactivated by early region proteins (Debbas and White, 1993; Lowe and Ruley, 1993). Ad5 E4orf6 has been shown to bind specifically to the CTR of p53 between amino acids 318 to 360 and antagonize p53-mediated transcriptional activity (Dobner, et al. 1996). This region of the p53 protein is known to be required for p53 tetramerisation and DNA-binding, however Ad5 E4orf6 was shown not affect p53 oligomerisation or p53 binding to DNA. Instead, E4orf6 was shown to inhibit the ability of the transcription factor (TFIID) component, TAFII31 to associate with the N-terminal transactivation domain of p53 (Dobner, et al. 1996). It has been suggested that Ad5 E4orf6 association with the CTR of p53 might induce a conformational change in p53 that alters the function of the NTR. Consistent with this view previous studies have suggested that CTR modifications of p53 do affect p53 DNA-binding activity (Hupp, et al. 1992).

1.2.5. Role of early region proteins in cellular transformation

1.2.5.1. The role of E1A and E1B in cellular transformation

As stated in section 1.1.1. John Trentin and colleagues determined, over 50 years ago, that Ad12 was oncogenic in new born rodents. Further work demonstrated that the E1 region from a number of different Ad types could transform primary human embryonic retinoblast (HER) cells, and baby rat kidney (BRK) cells and rat embryo fibroblasts to give immortal transformed cell lines that resembled the neoplastic state. These studies made an immense contribution towards our understanding of the molecular processes that underlie adenovirus-induced oncogenic transformation (Endter and Dobner, 2004). As described earlier, E1A is a transcription regulator that promotes cell-cycle progression into S-phase, but that in the absence of cooperating oncogenes promotes cellular apoptosis.

The ability of E1A to drive oncogenic transformation is dependent upon its ability to bind pRB and CBP/p300 as mutants unable to bind these proteins (e.g. LXCXE and RG2 mutants, respectively) are transformation defective (Egan, et al. 1988; Jelsma, et al. 1989; Rasti, et al. 2005). The NTR of E1A also associates with chromatin remodellers, TRRAP and p400, to promote E1A-induced cellular transformation (Deleu, et al. 2001; Fuchs, et al. 2001). CR4, at the C-terminal region of E1A, interacts with the C-terminal binding protein (CtBP) transcriptional repressor, HAN11 proteins and the dual-specificity tyrosine-regulated kinase 1A (DYRK1A) in order to modulate cellular transformation (Schaeper, et al. 1995; Turnell, et al. 2000).

Initially, it was shown that transformation of mammalian cells could be induced by introducing to the cells, DNA fragments that contained the Ad5 E1 region (Gallimore, et al. 1974; Graham, et al. 1974). Indeed, it was subsequently reported that complete cellular transformation of rodent cells required both E1B transcription units, E1B-55K and E1B-19K in addition to E1A (Gallimore, et al. 1985). Other studies with BRK cells also determined that transformation

required the entire Ad E1 region, suggesting the importance of both E1B-19K and E1B-55K (Bernards, et al. 1986). Likewise, the transformation of HER cells only occurred with an entire Ad E1 region (Whittaker, et al. 1984; Gallimore, et al. 1986). The role of the E1B proteins in cellular transformation is mainly ascribed to their ability to inhibit p53 activity and prevent cellular apoptosis (Debbas and White, 1993). E1B-19K disrupts both p53- dependent and independent apoptotic pathways by possessing bcl-2 activities (White, 1996), whilst E1B-55K inhibits p53 directly through association (Sarnow, et al. 1982) and is able to inhibit p53 activities in BRK cells expressing E1A (Yew, et al. 1994; Sabbatini, et al. 1995).

1.2.5.2. The role of E4orf3 and E4orf6 in cellular transformation and the concept of hit and run transformation

In addition to the known roles of E1A and E1B oncogenes in the cellular transformation of primary cells in culture, the roles of the E4 proteins, E4orf3 and E4orf6 in Ad-mediated cellular transformation have also been investigated in detail (Bernards, et al. 1984; Zalmanzon, 1987). The first indication that proteins from the E4 region might participate in transformation comes from the observation of the presence of E4 gene products in virus-transformed cells (Flint, et al. 1976; Flint and Sharp, 1976). The detection of E4 products in serum from hamsters with Ad12 tumours (Brackmann, et al. 1980; Downey, et al. 1983), and ultimately, that co-expression of E1 and E4 early regions from the highly oncogenic Ad12, transformed completely rat cells in culture (Shiroki, et al. 1984).

Studies investigating the individual contribution of E4 gene products in cellular transformation has demonstrated that two of the Ad5 E4 region gene products, E4orf3 and E4orf6 have transforming and oncogenic potential (Moore, et al. 1996; Nevels, et al. 1999). Both E4 proteins promote enhanced focus formation in primary BRK cells in cooperation with either E1A alone or Ad E1 in its entirety. Indeed, transformed BRK cells, that express either E4orf6 or E4orf3 in the presence of E1A and E1B, exhibit more advanced oncogenic transformation, compared to cells expressing only E1A and E1B (Moore, et al. 1996; Nevels, et al. 1999). The

ability of E4orf6 to promote foci formation and morphological transformation is dependent upon the C-terminal cysteine-histidine rich region of the protein, whilst accelerated tumour growth in nude mice is dependent upon both the NTR and CTR of the protein (Nevels, et al. 2000). Studies with E4orf3 have indicated that its oncogenic potential does not correlate with p53 inactivation, but is rather based upon its ability to associate with E1B-55K and reorganise PML bodies and associated cellular proteins into nuclear tracks. It has been suggested that reorganisation of PML bodies during transformation might trigger cellular signalling pathways that promote dysregulated cell proliferation and neoplastic growth (Nevels, et al. 1999).

The oncogenic and potential of E4orf3 and E4orf6 is linked to their overlapping activities during lytic infection and their capability to modulate the cellular activity of proteins through cooperative interactions with E1B-55K. For instance, these two E4 proteins have been reported to interact with E1B-55K and facilitate the nuclear accumulation of E1B-55K Leppard and (Everett, 1999; Nevels, et al. 1999). Such activities are believed to increase the oncogenic activities of E1/E4orf3 or E1/E4orf6-transformed rat cells (Nevels, et al. 1999).

It is now well established that adenovirus E1A, E1B synergistically cooperate with E4 gene products to mediate the full neoplastic transformation of both primary human and rodent cells (Moore, et al. 1996; Nevels, et al. 1999; Shenk, 2001). It has been determined that E1A/E1B transformation results in cell lines that continue to express these viral gene products (Graham, et al. 1977; Hutton, et al. 2000). This is consistent with the conventional concept of viral oncogenesis which claims that viral oncogene expression persists in the transformed cells and the corresponding tumours such that the expression of viral oncogene products maintains the transformed phenotype (Weiss and Javier, 1997). There is another concept in viral oncology known as hit-and-run transformation, whereby viral oncogenes initiate cellular transformation-the hit, whilst maintenance of the transformed state is not dependent upon the expression of viral oncogenes and is accompanied by the run of viral genes, whereby other genetic changes

in the transformed cell maintain the transformed phenotype (Skinner, 1976). Interestingly, although both E4orf3 and E4orf6 can cooperate with E1A in the transformation of primary rat cells, the majority of transformed cells lacked detectable viral DNA, mRNA or protein (Nevels, et al. 2001). This is in opposition to the conventional concepts of oncogenesis induced by viruses and is consistent with the hit-and-run model of transformation. In this situation it has been suggested that E4orf3 and E4orf6 have increased mutagenic potential which introduces oncogenic mutations in cellular genes and increases genomic instability (Nevels, et al. 2001). In addition to these findings Ad5 E1A is also known to induce chromosomal aberrations (Caporossi and Bacchetti, 1990). Taken together, these studies are suggestive that adenovirus could contribute towards human oncogenesis through hit-and-run transformation, though ultimately this will be difficult to establish.

1.2.5.3. The role of E1A and Ras in cellular transformation

Apoptosis is an important biological process that protects hosts against possible malignant formation (Williams, 1991). The adenovirus E1B genes, E1B-55K and E1B-19K inhibit cellular apoptosis during adenovirus E1-mediated cellular transformation (White, 1993). Activation of the Ras oncoprotein, predominantly through point mutation at exons 12, 13 or 61, is linked to the formation of many different types of human cancers (Bos, 1988; Bos, 1989). Despite its oncogenic activity, paradoxically in primary cells, activated Ras promotes growth arrest, which is considered as a defence strategy against oncogenic transformation (Serrano, et al. 1997; Spyridopoulos, et al. 2002). Consistent with the model of multiple genetic hits being required for oncogenesis it is not surprising that transformation by Ras requires further genetic alterations such as Rb inactivation (Peeper, et al. 2001) and loss of p53 functionality (Shvarts, et al. 2002). E1A expression has been shown to render primary human fibroblasts resistant to Ras senescence and promote oncogenic transformation (Serrano, et al. 1997). Indeed, several studies have demonstrated that activated *ras* genes can like, E1B-55K and E1B-19K, promote

E1A-dependent transformation by suppressing E1A-induced apoptosis through the mechanism by which this occurs is not well understood (Jochemsen, et al. 1986; Byrd, et al. 1988; Lin, et al. 199). Interestingly, E1A/Ras transformation is inhibited by the interaction of the CR4 region of E1A with DYRK1A and HAN11 as E1A deletion mutants unable to bind DYRK1A and HAN11 enhanced E1A/*ras* transformation which is presumably modulated through E1A's known ability to bind cellular tumour suppressors pRB, CBP/p300 and p400 (Boyd, et al. 1993).

1.3. The Ubiquitin-Proteasome System

One of the most abundant PTMs in cells is ubiquitylation in which a ubiquitin polypeptide, comprising 76 amino acids, is covalently attached through its C-terminal glycine residues to a lysine residue on a target protein through a coordinated multiple enzymatic cascade (**Fig. 1.11**). This process often leads to proteasomal degradation of the substrate, hence the ubiquitin-proteasome system (UPS). Initially, ubiquitin is activated by an E1 ubiquitin activating enzyme that forms a high energy thioester bond with an active site cysteine residue. The ubiquitin is then transferred to an E2 ubiquitin conjugating enzyme, again through a high energy thioester bond with cysteine. Finally, the ubiquitin transfer to the target substrate is catalysed by an E3 ubiquitin ligase enzyme (Dye and Schulman, 2007; Kulathu and Komander, 2012; Yau and Rape, 2016; Dybas, et al. 2018).

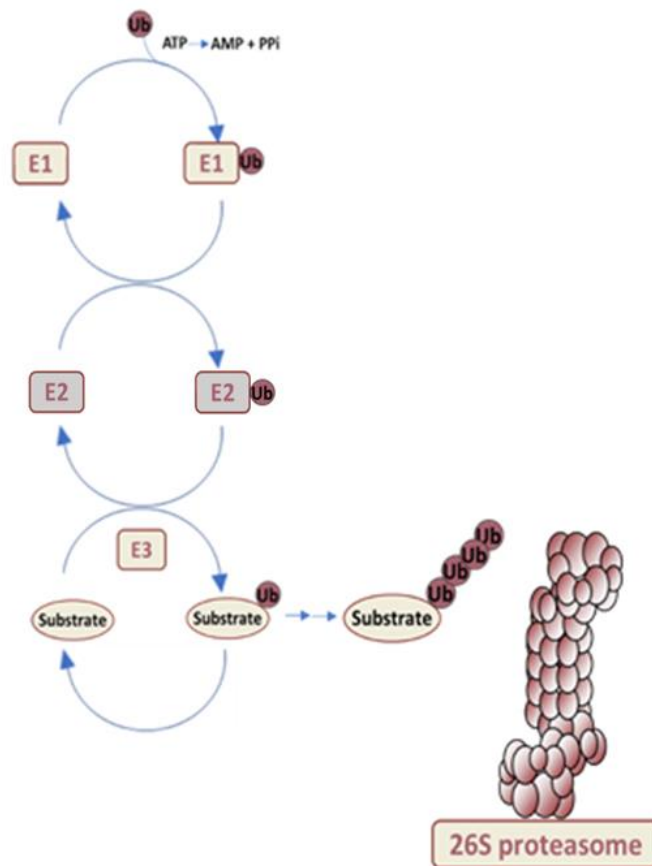


Figure 1.11: Diagram detailing the Ubiquitin-Proteasome System. Ubiquitylation of protein substrates is an ATP-dependent process that requires the action of three enzymes E1, E2, E3 (see text for details). K11 and K48 polyubiquitin linkages target substrates for proteasomal degradation. Adapted from: (Sarikas, et al. 2011).

The attachment of a ubiquitin molecule to a target lysine residue can be diverse. For instance, it could be attached on one or multiple lysine residues, to form either a mono- or multi-mono ubiquitylated protein. Repeated rounds of ubiquitylation on one lysine residue is termed polyubiquitylation. Polyubiquitin chain can be formed through the attachment of the C-terminal glycine residue to a Lys residue on another ubiquitin molecule (i.e. Lys6, Lys11, Lys27, Lys29, Lys33, Lys48 and Lys63), or through the ubiquitin amino terminal Met1 residue (**Fig 1.12**; Kulathu and Komander, 2012). Ubiquitin polymers formed using the same linkage type are known as homotypic ubiquitin conjugates, whilst heterotypic chains are formed using mixed linkages and can be branched (**Fig. 1.12**; Ikeda and Dikic, 2008). Polyubiquitylation

through Lys11 and Lys48 typically drive proteasomal degradation, whilst polyubiquitylation on other residues (e.g. Lys 63) are important in lysosomal targeting, DDR, and other non-degradative processes such as protein interactions, functionality or location, as does mono-ubiquitylation (Kulathu and Komander, 2012; Yau and Rape, 2016). As outlined above the versatility of ubiquitin rises from the distinct cellular functionality assigned to each of the linkages that comprise the ubiquitin polymers, though the cellular roles for Lys6, Lys27, Lys29 and Lys33 remain elusive (Kulathu and Komander, 2012).

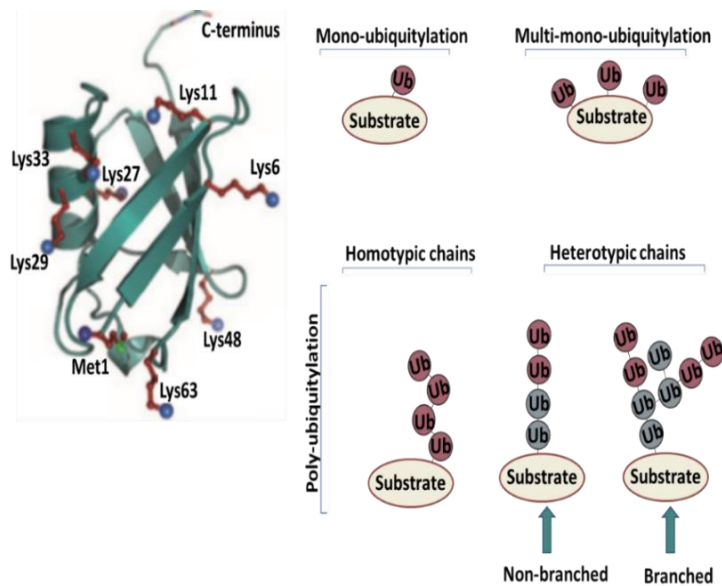


Figure 1.12: Ubiquitin and ubiquitin linkages. Multiple Lys residues present within ubiquitin that can be used to generate polyubiquitin linkages (Kulathu and Komander, 2012). Figure also shows the diversity of ubiquitylation modifications (i.e. mono-, multi-mono- or polyubiquitin chains). Ubiquitin polymers are coloured according to linkage-type. Polyubiquitin chains containing the same type of linkage are called homotypic chains, whereas, different linkages are termed heterotypic chains and can be branched or non-branched. Adapted from: (Kulathu and Komander, 2012).

1.3.1. Cullin–Ring Ubiquitin Ligases (CRLs)

Cullin–RING Ligases (CRLs) comprise the largest known class of ubiquitin ligases. CRLs are involved in diverse cellular activities including cell cycle regulation, cell signalling pathways, DDR as well as development (Petroski and Deshaies, 2005). CRLs are multicomponent complexes that comprise a Cullin, which is often curved in shape with a rigid N-terminal stalk, that serves as a scaffold to recruit other components of the ubiquitin ligase complex (Zheng, et al. 2002). The adaptor protein serves to recruit the substrate recognition subunit (SRS) to the Cullin complex, whilst the large family of SRS recruit substrates specifically to the CRL for ubiquitylation (**Fig. 1.13**). The zinc-binding (RING-H2-DOMAIN) proteins, referred to as ROC1/RBX1/HRT1 or ROC2/RBX2/HRT2 are E3 ubiquitin ligases that recruit the appropriate ubiquitin-conjugating enzyme (E2) and performs the transfer of ubiquitin to the substrate (Zheng, et al. 2002).

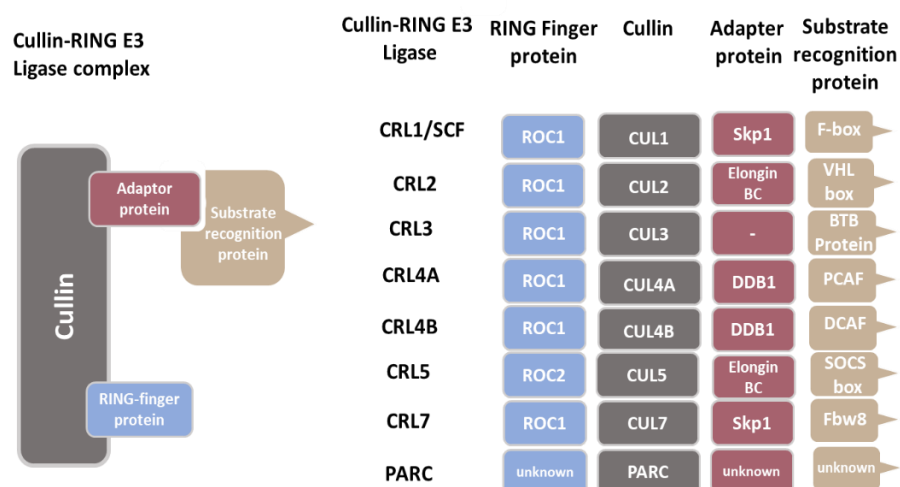


Figure 1.13: Architecture of Cullin-RING E3 ubiquitin ligase (CRL) complexes. In mammalian cells there are nine members of the Cullin family (CUL1 to CUL7, PARC and APC2). Cullin proteins in CRLs recruit a substrate-recognition subunit, through an adaptor protein, and also associate with the RING finger ligase component. (A) General CRL composition. (B) Specific composition of the CRLs assigned to Cullins 1 to 7 and PARC. Adapted from: (Sarikas, et al. 2011).

In Human cells there are seven different cullins, (CUL1, 2, 3, 4A, 4B, 5 and 7), the p53 cytoplasmic anchor protein (PARC) and the APC2 subunit of the Anaphase-Promoting Complex/Cyclosome (APC/C; Petroski and Deshaies, 2005). CRLs are activated by the covalent binding of NEDD8 to a conserved lysine near a Cullin's C-terminus and are inactivated by CAND1 (cullin-associated and neddylation-dissociated) inhibitor (Petroski and Deshaies, 2005). NEDDylation is a process of covalent attachment of a ubiquitin-like molecule NEDD8 (neuronal precursor cell-expressed developmentally down-regulated protein 8) to a lysine residue of target substrate (Kamitani, et al. 1997). This process is controlled by successive enzymatic cascade. Briefly, NEDD8 is activated by the activating enzyme (NAE) and is then transferred to the NEDD8-conjugating enzyme, UBE2M (also known as UBC12), whence it is finally transferred to a lysine residue in its target protein by a substrate specific-E3 ligase, such as RBX1/2 or DCN1 (**Fig. 1.14 A**; Walden, et al. 2003; Zhou, et al. 2018). Overall, NEDDylation of target proteins may affect their stability, localization and function. The cullin subunits of Cullin-RING ligases (CRLs) are the best-characterized targets of NEDDylation. Conjugation of NEDD8 at the C-terminus of a Cullin promotes the dissociation of the CRL negative regulator, CAND1 and activates the Cullin complex (Zhao, et al. 2014). It has been reported that the Rbx1 component of a CRL is essential in NEDDylation and any mutation within RING finger motif of Rbx1 abolishes NEDDylation *in vitro* (Kamura, et al. 1999). DeNEDDylation by COP9 Signalosome (CSN) isopeptidase activity inactivates CRL activity, whilst CAND1 association with the Cullin N-terminus blocks the NEDD8 conjugation site and the recruitment of the adapter to the Cullin (Bosu and Kipreos, 2008). It has been reported that the small molecule, MLN4924 is a potent inhibitor of the NAE, such that MLN4924 is covalently attached to NEDD8 by the NAE to form an NEDD8-MLN4924 moiety that resembles NEDD8 adenylate, which is an intermediate in the NAE reaction. The NEDD8-MLN4924 adduct is a stable entity that blocks the NAE active site and limits the activation of

Cullin-containing CRLs. MLN4924 therefore, effectively inhibits Cullin neddylation and inactivates CRLs, causing the accumulation of various CRL substrates (Fig.1.14 B; Soucy, et al. 2009; Brownell, et al. 2010).

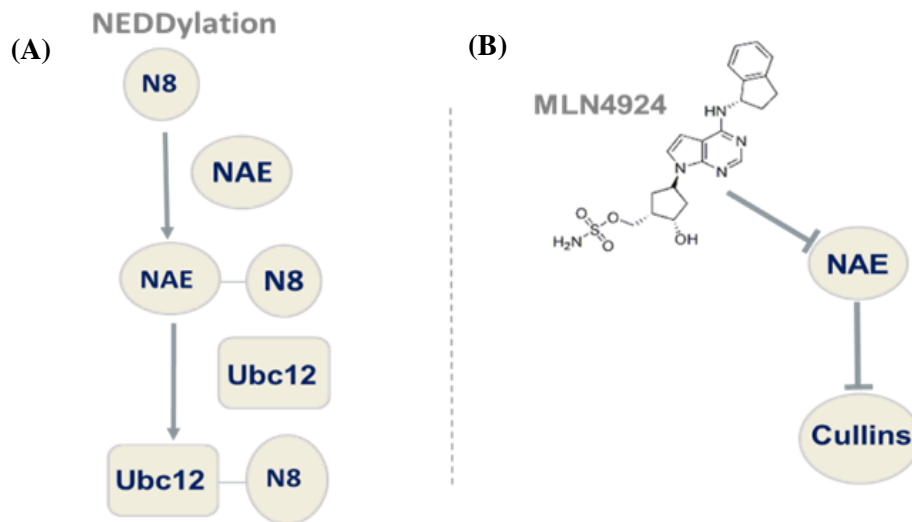


Figure 1. 14: MLN4924 as an inhibitor of Cullin-RING ubiquitin ligases (CRLs). (A) Role of NAE and Ubc12 in the activation of NEDD8 (N8). (B) Role of MLN4924 as a potent and selective inhibitor of NAE and CRLs.

1.3.2. Regulation of the ubiquitin-proteasome system by E1B-55K and E4orf6 proteins

In order to promote a productive infection viruses such as adenovirus exploit the cellular ubiquitylation machinery. Viruses have been shown to manipulate the ubiquitylation of specific target proteins by: encoding viral E3 ligases; integration into cellular ubiquitin ligase complexes to modulate E3 activity and specificity; manipulation of existing cellular E3 ligase enzymic activity to modulate E3 activity and specificity (Dybas, et al. 2018).

1.3.2.1. Utilization of Cullin Ring Ligases by E1B-55K and E4orf6 proteins during infection to promote p53 degradation

The p53 tumour suppressor protein was initially identified over 40 years ago as an SV40 large T antigen-binding protein (DeLeo, et al. 1979; Kress, et al. 1979; Lane and Crawford, 1979; Linzer and Levine, 1979). Since that time, it has been appreciated that p53 can induce cell cycle arrest, cellular senescence or apoptosis in response to cellular stresses such as ionizing

radiation, U.V. radiation or viral infection (Vogelstein, et al. 2000; Surget, et al. 2014). As such p53 acts as a potent antiviral and adenoviruses, like other viruses, have evolved to inhibit p53 during infection. Early studies determined that E1B-55K and E4orf6 independently associated with p53 in Ad-transformed cells to inhibit its transcriptional activity and affect its cellular localization, whilst in Ad-infected cells it was established that E1B-55K and E4orf6 cooperated to reduce p53 levels by reducing the protein half-life (Steegenga, et al. 1998; Cathomen and Weitzman, 2000). Phil Branton's lab then reported that the ability of E1B-55K and E4orf6 to reduce the protein levels of p53 was due to E1B-55K and E4orf6's ability to engage with cellular CRLs to target p53 for proteasomal degradation (Querido, et al. 2001). It was established that E1B-55K acted as the receptor for p53, whilst E4orf6 recruited CRL5, containing Cullin 5, to E1B-55K-p53 complexes to promote its polyubiquitylation and degradation by the proteasome (**Fig. 1.15**; Querido, et al. 2001).

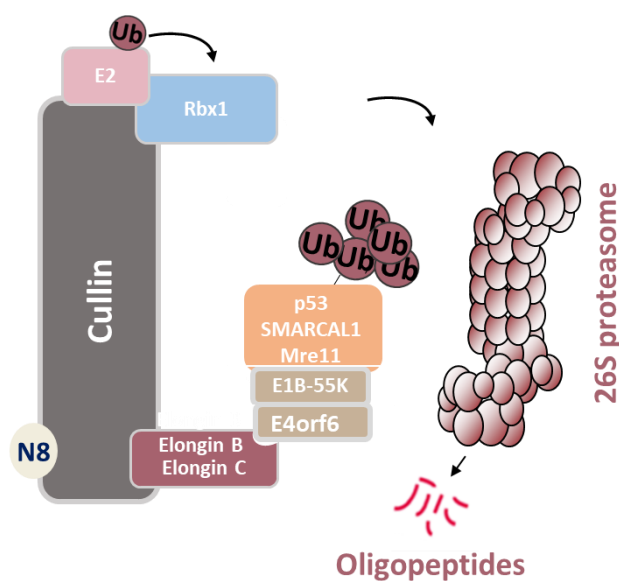


Figure 1.15: Schematic model of Cullin-RING E3 ligases and their utilization by E1B-55K and E4orf6 to target the degradation of cellular proteins such as p53 that possess anti-viral activity.

CRLs are major targets for E1B-55K and E4orf6 (Querido, et al. 2001; Harada, et al. 2002). Indeed, mass spectrometric studies with Ad5-infected cells identified all components of CRLs including the Cullin 5 and Elongin B and C proteins, and the Rbx1 ubiquitin ligase as E4orf6-interacting proteins (Querido, et al. 2001; Harada, et al. 2002). It was later established that Ad5 E4orf6 possessed three BC boxes which enabled the assembly of the cellular proteins Cul5, Elongins B and C, and RBX1 with E4orf6 prior to its association with E1B-55K, which functions as the major substrate recognition protein (Blanchette, et al. 2004; Cheng, et al. 2007). E4orf6 was shown to be crucial in the formation of ligase complex, as an E4orf6 BC-box mutant that prevents the formation of this complex was unable to promote p53 degradation (Blanchette, et al. 2008). Our laboratory then reported that Ad12 used a similar mechanism to promote the degradation of p53 in Ad12-infected cells, but in this instance used CRL2, rather than CRL5 (Blackford, et al. 2010). Further work by the Branton lab determined that E1B-55K and E4orf6 from all Ad groups associated with CRLs, such that most Ads utilize CRL5, whilst Ad groups A, F, and G utilize CRL2 (Blackford, et al. 2010; Cheng, et al. 2011). Ad5 E4orf6 possesses a Cul5 box and Ad12 E4orf6, a Cul2 box which determines CRL specificity (**Fig 1.16**; Gilson, et al. 2016).

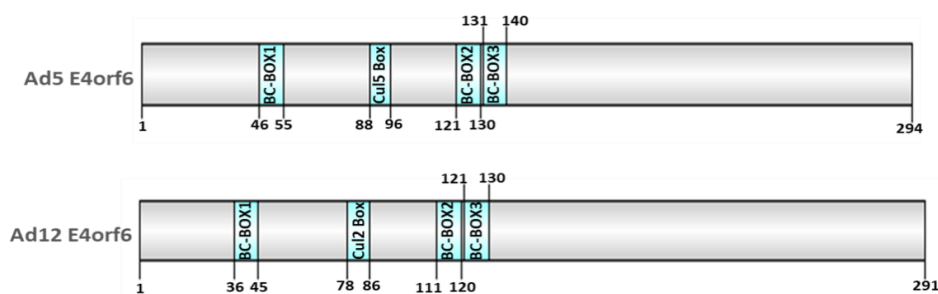


Figure 1.16: Schematic representation of BC boxes and CUL boxes in Ad5 and Ad12 E4orf6. The relative positions of the Elongin B and C –interaction motifs (BC boxes) and Cullin 2 and Cullin 5 –interaction motifs are illustrated. Adapted from: (Täuber and Dobner, 2001).

1.3.2.2. Adenovirus utilisation of CRLs to promote viral replication and inhibit DDR and other antiviral pathways

It has become apparent that, in addition to p53, E4orf6 and E1B-55K cooperate during infection to target a growing number of cellular proteins for degradation by CRL E3 ubiquitin ligases. A number of the proteins targeted for degradation by adenovirus function in the DDR pathway (see section 1.4 for a brief description of the DDR). The reason for this becomes apparent when it is considered that the Ad consists of linear dsDNA that would be seen by the host cell as a double-strand break, whilst replicated Ad DNA exists as ssDNA intermediates which would be seen by the host cell as erroneous cellular DNA replication. For instance, it has been determined that Mre11 is targeted for degradation during infection, whereby adenovirus prevents viral genome concatenation (i.e. the end-to-end joining of Ad genomes resulting in circular dsDNA) that, otherwise occurs following infection of cells with E4-deleted viruses where Mre11 expression persists; Mre11 degradation effectively inhibits the ATM-mediated repair of double-stranded DNA breaks in Ad-infected cells (Stracker, et al. 2002). Similarly, adenovirus promotes the E1B-55K/E4orf6 degradation of DNA ligase IV in order to inhibit DNA-PK-dependent non-homologous end-joining (NHEJ) and viral genome concatenation (Baker, et al. 2007). In this regard, E4orf6 also associates with DNA-PK independently and inhibits DNA PK-dependent V(D)J-recombination, in order to prevent viral genome concatenation (Boyer, et al. 1999).

Adenovirus 12 is also known to inhibit the ATR pathway, selectively through its ability to promote the degradation of ATR activator protein, TOPBP1, in a CRL2 dependent mechanism that requires Ad12 E4orf6, but not Ad12 E1B-55K, such that Ad12 E4orf6 acts as both the substrate adaptor as well as to recruit CRL2 to the substrate (Blackford, et al. 2010). Moreover, this study was the first to demonstrate that Cullin-2 is NEDDylated (i.e. activated) in response to Ad12 infection, and that Cullin-5 is NEDDylated in response to Ad5 infection. More recently, it has been established that both Ad5 and Ad12 E1B-55K/E4orf6 engage with cellular

CRLs to target the ATR substrate, SMARCAL1 for degradation in order to modulate cellular DNA replication (Nazeer, et al. 2019).

As indicated earlier E1B-55K and E4orf6 cooperate to promote viral mRNA export to the cytoplasm during infection. Mutational studies have determined the importance of both the nuclear export signal (NES) within E4orf6 in this process and E1B-55K/E4orf6 ability to associate with cellular CRLs, though the cellular substrate that is targeted for degradation in order to enhance viral mRNA transport to the cytoplasm has yet to be identified (Weigel and Dobbstein, 2000). Consistent with this view the expression of a dominant-negative Cullin 5 protein abolishes the ability of E1B-55K/E4orf6 to promote the nuclear export of viral mRNAs (Woo and Berk, 2007).

Other studies have identified other cellular proteins that are targeted for degradation during infection that might help facilitate viral release and spread. It was determined that integrin $\alpha 3$ was degraded by CRL5 in an E1B-55K and E4orf6 dependent manner during Ad5 infection (Dallaire, et al. 2009), whilst ALCAM, EPHA2, PTPRF proteins that also function in cellular adhesion were substrates for CRL and E1B-55K/E4orf6 (and E1B-55K/E4orf3) dependent degradation in Ad5-infected cells (Fu, et al. 2017). Finally Ad5 E1B-55K, like Ad12 E4orf6, has been shown to engage with CRLs independently and target the Daxx (death-domain-associated protein), for degradation during Ad5 infection (Schreiner, et al. 2010). Taken together, these studies highlight the importance of Ad modulation of cellular CRLs during infection to promote viral replication.

1.3.2.3. Regulation of CRLs by other viruses

Upto 20% of all ubiquitylated cellular proteins are attributed to CRL activity (Soucy, et al. 2009). Modulation of CRL activity is widely exploited by a number of DNA and RNA viruses to alter the host cell environment in order to allow for efficient virus replication (**Fig. 1.17**; Barry and Früh, 2006). For instance, human papillomavirus (HPV), a causative agent of several

mucosal cancers including cervical cancer, targets CRL2 through its transforming protein, E7 which through its association with Elongin C recruits the pRB protein for CRL2-dependent degradation. E7-mediated pRB degradation allows for the activation of E2F-dependent transcription and cell cycle progression past the restriction point (**Fig. 1.17 C**; Huh, et al. 2007).

KSHV is the aetiological agent of Kaposi's sarcoma. The KSHV latency-associated nuclear antigen (LANA) protein, like Ad5 E4orf6, possesses an Elongin B/C box and a Cullin 5 box, whereby it recruits CRL5 to promote the ubiquitin-mediated degradation of p53 and the VHL tumour suppressor proteins (Cai, et al. 2006). Moreover, it has been determined that the NEDDylation inhibitor MLN4924 reactivates KSHV lytic gene expression and as such, identifies CRLs as novel KSHV therapeutic targets (Hughes, et al. 2015). The HIV-1 virion infectivity factor, Vif, similarly associates with CRL5 and Elongin's B and C to promote the degradation of APOBEC3G during infection to protect HIV-1 DNA from G to A hypermutation (Kobayashi, et al. 2005). SV40 on the other hand interacts with CRL7 to inhibit its E3 ligase activity towards IRS1 (insulin receptor substrate 1) which allows for the activation of IRS1 promitogenic signalling pathways (Hartmann, et al. 2014).

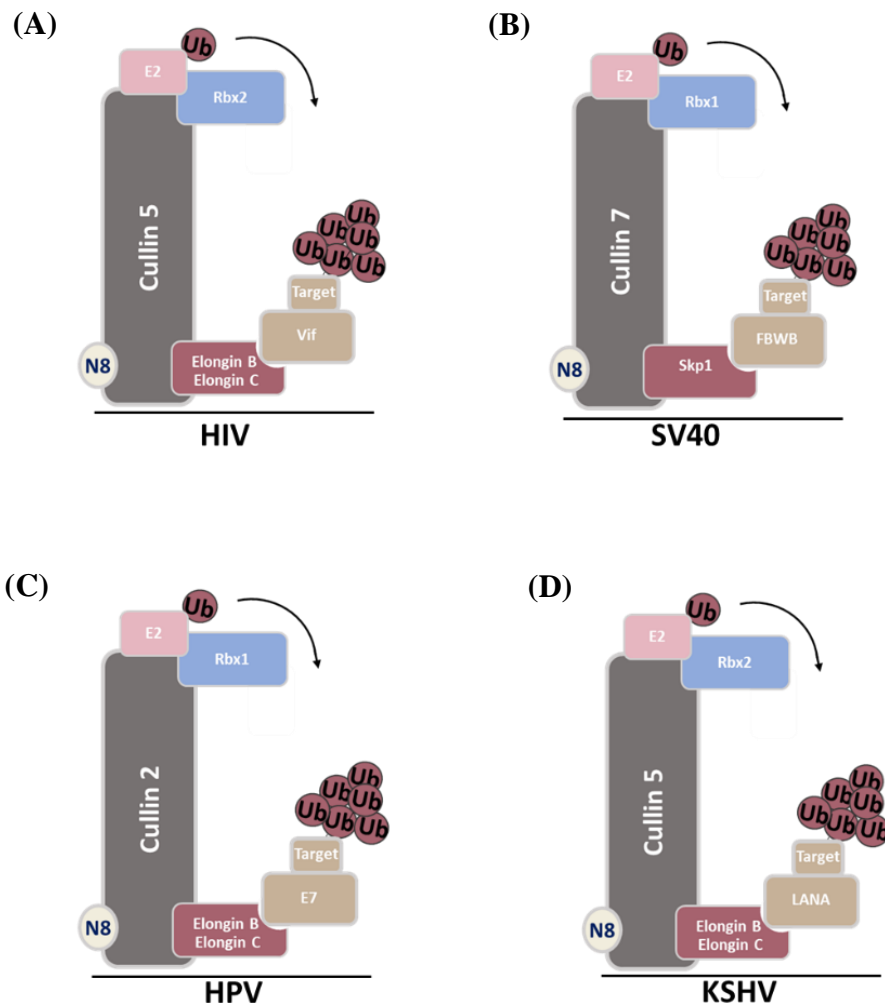


Figure 1.17: Regulation of host Cullin RING ligases by different viruses. (A) CRL complex assembled by the HIV-1 Vif protein (B) CRL complex assembled by the SV40 LT protein. (C) CRL complex assembled by the HPV E7 protein (D) CRL complex assembled by the KSHV LANA protein. Adapted from: (Barry and Früh, 2006).

1.4. The cellular DNA damage response

The DDR is a surveillance mechanism that ensures genomic stability in the presence of genotoxic agents such as ionizing radiation and virus infection and ensures the proper transmission of genetic information from generation to generation (Ciccia and Elledge, 2010; Turnell and Grand, 2012; Maréchal and Zou, 2013; Yoshiyama, et al. 2013). The DDR is orchestrated by three phosphoinositide 3-kinase (PI3K)-related protein kinases ATM and DNA-PK, and ATR which respond to double-strand, and single-strand breaks, respectively (Turnell and Grand, 2012; Maréchal and Zou, 2013). At the molecular level, the DDR response

requires different cellular factors: DNA damage sensors/mediators, signal transducers and effectors that serve to detect and correct damaged DNA, whilst modulating cell cycle progression; in situations where the extent of DNA damage is too great apoptosis is induced (**Fig. 1.18**). Given the relationship between adenovirus and DDR pathways (section 1.3.2.2) it is worthwhile to give a brief overview of cellular DDR pathways.

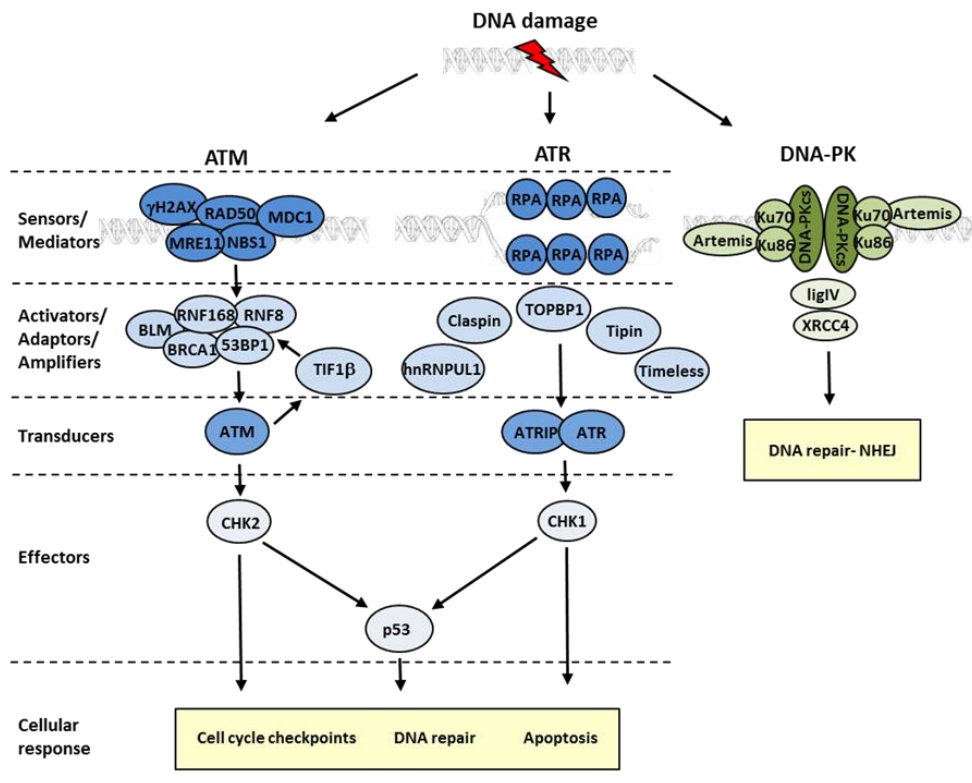


Figure 1.18: Role of PI3K-related protein kinases in DDR signalling pathways. See text for details. Taken from: (Turnell and Grand, 2012).

1.4.1. The ATM pathway

ATM is the gene that when inactivated gives rise to the autosomal recessive syndrome, Ataxia-Telangiectesia (A-T), which is characterized by defects in cerebellar degeneration, immunodeficiency and cancer susceptibility. In undamaged cells, ATM exists as an inactive dimer, but in response to DNA damage ATM becomes auto-phosphorylated on S1981 leading to its activation, its association with MDC1 and recruitment to the DNA double-strand break sites (So, et al. 2009). Recruitment of the MRN (Mre11- Rad50-NBS1) complex enhances

ATM activation. Collectively, ATM mediated phosphorylation of Chk2, p53, H2AX, TIF1 β /KAP1, BRCA1, 53BP1 and NBS1 at the DNA double-strand break ensures that cell cycle checkpoints are activated and DNA double-strand breaks are repaired by homologous recombination (Sancar, et al. 2004; Turnell and Grand, 2012). As discussed earlier adenovirus inhibits the ATM pathway by promoting the targeted degradation of Mre11 (section 1.3.2.2).

1.4.2. The ATR pathway

ATR is an essential gene in proliferating cells; hypomorphic mutations in ATR gives rise to the human autosomal recessive disorder, Seckel syndrome, which is characterised by microcephaly and mental, and growth, retardation (Sancar, et al. 2004; Byun, et al. 2005). ATR acts to correct ssDNA damage often as the result of DNA replication errors. In response to DNA damage ATR and its partner protein, ATR-interacting protein (ATRIP), are recruited to DNA damage sites via the replication protein A (RPA) complex which coats ssDNA (Zou, et al. 2003). ATR is activated by TopBP1 which results in the activation of the CHK1 kinase, through ATR-dependent phosphorylation on serine residues 317 and 345 which allows for checkpoint activation (Liu, et al. 2000; Zhao and Piwnica-Worms, 2001). ATR-dependent regulation of proteins such as SMARCAL1 allows for the replication re-start after fork collapse (Cortez, 2015). As detailed earlier, adenovirus inhibits ATR signalling during infection by promoting the degradation of TopBP1 and SMARCAL1 (see section 1.3.2.2.).

1.4.3. The DNA-dependent protein kinase pathway

The DNA-activated protein kinase (DNA-PK) is a nuclear serine/threonine protein kinase that is involved in modulating NHEJ. It is composed of catalytic subunit (DNA-PKcs / 470KDa) and two additional regulatory subunits Ku70 and Ku86 (Smith, et al. 1999). Following DNA damage Ku associates with the broken DNA end and recruits DNA-PKcs (Cary, et al. 1997; Gell and Jackson, 1999). DNA-PKcs in turn tether the DNA ends and bridge them together to allow for their re-ligation. DNA-PK then stimulates the recruitment and activation of DNA

ligase IV - XRCC4 complexes that are required for the re-joining step (**Fig. 1.18**; Hsu, et al. 2002). As detailed earlier, adenovirus inhibits DNA-PK signalling during infection by promoting the degradation of DNA ligase IV (see section 1.3.2.2.).

1.4.4. Regulation of the DDR by other viruses

It is apparent that a number of viruses, including the DNA tumour viruses discussed earlier (section 1.1.1.) all modulate DDR pathways during infection to promote viral replication (Pancholi, et al. 2017). Some viruses negatively regulate DDR pathways, while others utilize or exploit DDR pathways, and some viruses can selectively utilize or repress DDR pathways for viral growth and/or oncogenesis (Pancholi, et al. 2017). Like adenovirus, most other viruses often engage with the UPS to regulate DDR pathways (Dybas, et al. 2018). For instance HPV negatively regulates the DDR effector protein, p53 through E6 association with the E3-ubiquitin ligase, E6-AP. Interestingly however, HPV utilises the DDR machinery directly. E7 associates with, and activates, ATM in order to promote the phosphorylation of Chk2, BRCA1 and Nbs1 to stimulate viral genome replication (Moody and Laimins, 2009). It has been proposed that the rapid replication of the 8Kb HPV genome creates aberrant DNA structures that need to be resolved by the DDR machinery which requires its activation (Bristol, et al. 2017). Moreover, HPV replication proteins E1 and E2 localize at sites of viral DNA replication with phosphorylated, activated forms of ATM, H2AX and p53, as well as with viral genomes and the MRN component NBS1 (Nishiyama, et al. 2011). These data suggest that the ATM pathway is crucial in facilitating HPV genome replication. HPV16 E2 also interacts with the ATR activator TopBP1 at centrosomes during mitosis, suggesting that DDR pathways also be utilized by HPV to modulate genome segregation during mitosis (Donaldson, et al, 2007). Given these few examples, it is clear that an understanding of the relationship between viruses and DDR pathways is important in understanding how viruses subvert host cell pathways in order to promote viral replication and transformation.

1.5. Project Aims

In recent years it has become increasingly clear that viruses such as adenovirus promote viral replication and cellular transformation through their ability to modulate host cell PTMs and cell signalling pathways. As such, adenoviruses have evolved complex mechanisms to regulate and exploit these cellular pathways to maximise viral production. Indeed, E1B-55K, E4orf3 and E4orf6 early region proteins cooperate functionally to regulate host cell UPS and SUMO pathways in order to promote viral replication and cellular transformation. It is becoming more apparent however that these proteins also function separately during cellular infection and cellular transformation. It is also not clear how many functions of E1B-55K, E4orf3 and E4orf6 are conserved between different Ad types given that Ad12 E4orf6 can promote TopBP1 degradation, whilst Ad5 E4orf6 cannot.

Given these observations the aims of my project were to:

- Generate and characterize Tet-On inducible cell lines that express Ad5 and Ad12 E1B-55K, E4orf3 and E4orf6 proteins in isolation.
- Investigate the function of both Ad5 and Ad12 E4orf3 proteins in the SUMO pathway in an attempt to identify new cellular proteins that are substrates for E4orf3-targeted SUMOylation.
- Investigate the post-translational modification status of Ad5 E4orf6
- Investigate the function of both Ad5 and Ad12 E4orf6 proteins in the UPS in an attempt to identify new cellular proteins that are substrates for E4orf6-targeted ubiquitylation

Given that E1B-55K, E4orf3 and E4orf6 accumulate at VRCs and nuclear tracks here is also considerable interest in the relationship between the UPS and SUMO pathways and these virally-induced structures. Indeed, our laboratory had determined that the FACT complex

which functions as a chromatin regulator was recruited to VRCs during Ad infection. Another aim of my project was therefore to:

- Determine the role of the FACT complex during adenovirus infection.

The results of these studies are presented in this thesis.

CHAPTER 2



Materials and Methods

2.1. Tissue Culture

2.1.1. Cell culture

A derivative of the human osteosarcoma U2OS cell line has been used throughout this study. The U2OS- FRT-TREX cell line expresses the TET repressor and contains a single Flp recombination site to allow for the integration of an exogenous gene that is under the control of the CMV immediate early promoter (Life Technologies). This cell line was used to generate cells that expressed Ad5 or Ad12 E1B-55K, E4orf3, and E4orf6 in a TET-dependent manner (see 2.1.5). Human A549 small cell lung carcinoma cells (CCL-185) and U2OS osteosarcoma cells (HTB-96), which both possess normal, wild-type [w.t.] p53 alleles (Lehman, et al. 1991; Landers, et al. 1997) were obtained from the American Type Culture Collection (ATCC) and typically used for adenovirus infection. As p53 is the main target for adenovirus during infection it was important to use cells whose p53 status was known. Ad5 E1-transformed human embryonic kidney (HEK) 293 cells and Ad12 E1-transformed human embryo retinoblast (HER) 3 cells were used to propagate adenovirus 5 and adenovirus 12, respectively. GFP-U2OS and GFP-RPA1-U2OS cells, derived from human U2OS osteosarcoma cells and engineered to express GFP-tagged proteins, were provided by Dr. Andrew Blackford (The University of Oxford; Galanty, et al. 2012). All cell lines used were adherent, epithelial in nature and permissive for adenovirus infection. Cells were grown in HEPES-buffered Dulbecco Modified Eagle Medium (DMEM; Sigma-Aldrich) enriched with 8% (v/v) foetal calf serum (FCS; Sigma-Aldrich) and 2mM L-glutamine (Sigma-Aldrich). The growth medium for U2OS-FRT-TREX cell lines was supplemented with 200µg/ml Hygromycin (Gibco) whilst the medium for GFP-U2OS cells was supplemented with 500µg/ml G418 (Gibco). All tissue culture reagents were bought pre-sterilized and stored at 4°C. Prior to use reagents were warmed to 37°C in a water bath.

2.1.2. Maintenance and passage of cell lines

Cell lines were grown in monolayer and passaged by removing the existing medium from the cells followed by washing with pre-warmed phosphate-buffered saline (PBS; Oxoid). Cells were then detached from the plate by the addition of 1ml of trypsin (Tryple E; Life Technologies) and the incubation of cells for approximately 5 min at 37°C in a humidified atmosphere containing 5% (v/v) CO₂ (CO₂ AIR Jacketed incubators by NUAIRE AUTOFLOW). A Nikon Eclipse TS 100 Microscope was used to confirm the detachment of cells from the plastic. Growth medium containing FCS was then added to the cells to inactivate the trypsin. Cells were then pelleted by centrifugation at 1500 rpm for 5 min. The pellet was resuspended in fresh medium then re-plated at the required density, using a haemocytometer to measure cell number, and incubated in the CO₂ incubator until required. All techniques were performed under sterile conditions using a Mars Safety Class 2 hood (SCANLAF).

2.1.3. Cryopreservation of cell lines and cell recovery

To store cell-lines for a long time, cells were trypsinized and resuspended in HEPES-buffered Dulbecco Modified Eagle Medium containing 8% (v/v) FCS, 2mM L-glutamine and 10% (v/v) dimethyl-sulphoxide (DMSO HybriMax; Sigma-Aldrich) at a density of 5 x10⁶ cells/ml. Cells were cooled to -80°C at a controlled rate of 1°C/min in isopropanol using a Mr Frosty then transferred to the liquid nitrogen tanks for storage at -180°C. When cells were recovered from liquid nitrogen, they were thawed rapidly in water bath at 37°C. The cells were immediately pelleted by transferring to a tube containing 10 ml of fresh culture medium then centrifuged at 1500 rpm for 5 min. After that the cells were washed once more with fresh medium then re-plated and incubated at 37 °C in a 5% (v/v) humidified CO₂ incubator.

2.1.4. Adenoviruses

Human, Ad5 (VR-5) and Ad12 (Huie; VR-863) types were from the ATCC. Ad5 was propagated on Ad5 E1-transformed HEK293 cells, whilst Ad12 was propagated on Ad12 E1-transformed E1 HER3 cells. The FLAG-tagged E4orf3 Ad12 virus was made in collaboration with Thomas Dobner's laboratory (HPI, Hamburg, Germany). This virus is a mutant Ad12 virus that expresses FLAG-tagged E4orf3 that retains normal expression of other viral gene products. Stock titres of Ad5 and Ad12 viruses were determined by plaque assay on Ad5 E1-transformed HER911 and Ad12 E1-transformed HER3 cells, as appropriate. All adenovirus-transformed cells were grown in DMEM-HEPES containing 8% (v/v) FCS. For infection, subconfluent monolayers of A549 or U2OS cells were washed twice with 5 ml of pre-warmed serum-free, HEPES-buffered DMEM containing 2mM L-glutamine. Cells were then infected with the virus at a multiplicity of infection (m.o.i.) of 10 plaque forming units (p.f.u)/cell, unless otherwise stated, and then incubated in an incubator with a humidified atmosphere containing 5% CO₂. Dishes were agitated every 10 min for 2 h at 37°C to ensure that cells were covered with medium. After infection the medium containing the virus was replaced with HEPES-buffered DMEM containing 8% (v/v) FCS and 2mM L-glutamine until required.

2.1.5. Generation of U2OS FRT TREX cell lines

Prior to transfection the FRT-U2OS TREX cells were grown to 90% confluence on a 10cm dish. For transfection, 1.5µg of the pcDNA5-FRT plasmid containing the adenovirus gene of interest was mixed with 13.5µg of the pOG44 plasmid, which expresses the Flp recombinase required for exogenous gene integration, in 200µl reduced-serum containing medium (Opti-MEM, Life Technologies) in a sterile Eppendorf. Secondly, 15µl of the Lipofectamine 2000 transfection reagent was added to a separate Eppendorf containing 200µl Opti-MEM medium. After 5 min incubation, the transfection reagent was mixed with the pcDNA5-FRT/pOG44 mixture and incubated for an additional 45 min at room temperature to produce Lipofectamine-

plasmid complexes. The cells were then washed with 5ml Opti-MEM and incubated in 5ml of Opti-MEM. The DNA: Lipofectamine transfection complex was then added to the cells in a dropwise manner, after which cells were incubated in CO₂ incubator at 37°C for 6 h. Following incubation the plate's media was changed and fresh DMEM supplemented with 8% (v/v) FCS and 2mM glutamine was added. Two days post-transfection cells were split 1 in 4 onto 10cm dishes. 72 h post-transfection cells were incubated with media containing 200µg/ml Hygromycin B (Life Technologies) for selection of positive cell clones that had integrated the adenovirus gene of interest. Cells were fed every three days until individual colonies could be isolated under a light microscope at low magnification. Selected cells were isolated and expanded after which time they were incubated with 0.1µg/ml Doxycycline (Duchefa Farma) to assess expression of the particular adenovirus gene product.

2.1.6. Transfection of siRNA

In order to knockdown endogenous SSRP1 and SPT16 genes small-interfering RNA (siRNA) oligonucleotides (silencer select and validated siRNA) were purchased from Life Technologies/Ambion (**Table 2.1**). Four h prior to transfection, A549 were plated at a confluency of 30%-40% (5×10^5 cells per 6cm dish). For transfection the appropriate siRNA was incubated in 200µl of Opti-MEM medium, whilst 10µl of transfection reagent, RNAiMax (Life Technologies) was incubated in a separate tube with 200µl of Opti-MEM. After 5 min the siRNA and the RNAiMax solutions were mixed and incubated at room temperature for 30 min to produce RNAiMax-siRNA complexes. Cells were then washed twice with Opti-MEM and incubated in 2.5ml of Opti-MEM. The RNAiMax-siRNA complexes were then added to the cells (siRNA final concentration, 30nM) and incubated at 37°C in humidified atmosphere containing 5% CO₂, for 6 h. After incubation the transfection mix was removed, and the cells were incubated in fresh medium at 37°C in 5% (v/v) CO₂. 48 h post-RNAi treatment adenovirus infection was performed.

Table 2.1: siRNAs used in this study.

Target	siRNA Sequence	Supplier
Control (si Luciferase)	5'- CGUACGCGGAAUACUUCGAdTdT -3'	Ambion
SPT16	5'- GGUUUGGGAUGGGAAUUGAdTdT -3'	Ambion
SSRP1	5'- GGACUAAAACUGCUUACAAAdTdT -3'	Ambion

2.1.7. Transient DNA transfection

Target cells were grown to approximately 90% confluence on 6 cm dishes. The transfection mixture was prepared by adding 4 µg of plasmid DNA to 200µl of Opti-MEM and incubating for 5 min at room temperature. Similarly, 10µl of Lipofectamine 2000 was added to 200µl of Opti-MEM and left for 5 min. After this incubation time the plasmid DNA mixture and the transfection reagent were combined and mixed gently and incubated for 30 min at room temperature. Cells were then washed twice with Opti-MEM then incubated in 2.5ml of Opti-MEM to which the plasmid DNA-Lipofectamine mix was added in a drop-wise manner. After 6 h incubation at 37°C in 5% (v/v) CO₂ the existing media was replaced with fresh DMEM supplemented with 8% (v/v) FCS and 2mM glutamine. Cells were then incubated at 37°C, before being harvested at the appropriate times.

2.1.8 Treatment of cells with Ultra-Violet irradiation or drugs

Prior to ultra-violet (UV) irradiation, the existing medium was removed and stored in a sterile tube. Cells were then either mock-irradiated or irradiated at a dose of 25 J/m² from a 254 nm UV light source, after which the culture medium was replaced. Where indicated, target cells were treated with a specific drug (**Table 2.2**). MLN-4924 is a cell-permeable NEDD8-Activating Enzyme inhibitor used to inhibit Cullin Ring Ligase activation *in vivo* (Soucy, et al. 2009). Salinosporamide A is a non-competitive, cell-permeable inhibitor of the 26S proteasome (Feling, et al. 2003). Lactacystin is also a non-competitive, cell-permeable inhibitor of the 26S proteasome (Fenteany, et al. 1995). MG132 is a competitive, cell permeable inhibitor of the

26S proteasome (Sesta, et al. 2020). Hydroxyurea induces DNA replication stress by inhibiting ribonucleoside diphosphate reductase and depleting the cellular pool of dNTPs (Koç, et al. 2004).

Table2.2: Drugs used in the current study.

Drug	Working concentration	Supplier
MLN-4924	3 μ M	Cayman
Salinosporamide A (Marizomib)	1 μ M	Sigma-Aldrich
Lactacystin	1 μ M	Tocris
MG132 (N-carbobenzoxy-L-leuciny-L-leuciny-L-leucinal)	10 μ M	Sigma-Aldrich
Hydroxyurea (HU)	1mM	ACROS

2.2. Protein Biochemistry

2.2.1. Preparation of whole cell lysates

The existing medium was removed from the cells which were then washed twice with ice-cold PBS and then incubated with lysis buffer containing 9M urea, 50mM Tris-HCl (pH 7.4), and 0.15M β -mercaptoethanol (UTB) at room temperature for 5 min. Then cells were detached using a cell scraper and transferred into a 1.5ml Eppendorf. Cell lysates were then sonicated for 20 sec (setting 4), using a Misonix microsin ultrasonic cell disruptor, to cleave DNA. Insoluble cell debris was precipitated by centrifugation at 15,000 rpm for 20 min at 4°C in a chilled centrifuge (Eppendorf) and then either stored at -80 °C prior to use or prepared for protein quantification.

2.2.2. Protein concentration quantification

The Bradford assay was used to determine the protein concentration of lysates (Bio-Rad). Bovine serum albumin (BSA) was used to generate a standard curve from 0-30 μ g/ml. Typically, 4 μ l of whole cell lysate or known amounts of BSA were incubated with 1ml of

Bradford reagent (diluted 1 in 4 with dH₂O). The absorbance of the solution at a wavelength of 595nm was determined using a Cecil CE9200 spectrophotometer. Protein concentrations were calculated from the BSA standard curve.

2.2.3. SDS-Polyacrylamide Gel Electrophoresis (SDS-PAGE)

Typically, 50 µg protein samples were separated based on their relative molecular weight by SDS-PAGE. They were first incubated with an equal volume of sample buffer (6M Urea, 33.3mM Tris pH 7.4, 3.33% (w/v) Sodium Dodecyl Sulphate (SDS) and 0.1% (w/v) Bromophenol Blue) and boiled at 95°C for 5 min prior to their separation by SDS-PAGE using 8% (w/v) or 10% (w/v) polyacrylamide gels (made from a 40% (w/v) acrylamide/Bis-acrylamide (37.5:1) stock solution [Severn Biotech]), containing 0.1M Tris, 0.1M Bicine, 0.1% (w/v) SDS, 0.3% (v/v) TEMED and 0.06% (w/v) ammonium persulphate. Gels were run in the presence of running buffer (0.1M Tris, 0.1M Bicine and 0.1% (w/v) SDS) at constant amperes until the desired separation had been achieved.

2.2.4. Western blotting

After SDS-PAGE proteins were transferred onto Bio-Trace nitrocellulose membranes (PALL). According to the proteins being analysed membranes were cut to size and soaked in transfer buffer (24mM Tris, 193mM Glycine, 20% (v/v) methanol), The gel was then laid upon the top of pre-wetted nitrocellulose membrane and then sandwiched between two pieces of Whatman 3MM blotting filter paper pre-soaked in transfer buffer and two blotting sponges, before being closed in a plastic cassette and placed into a Transfer tank filled with transfer buffer. Electrophoretic transfer was performed at 280 mA for 6 h, or 180 mA overnight at room temperature such that the protein was transferred on to the nitrocellulose membrane towards the anode. Following the transfer, and in order to block non-specific protein binding, nitrocellulose-immobilized proteins were incubated in Tris-buffered saline (TBST; 20mM

Tris-HCl pH 7.5, 150mM NaCl, 0.1% (v/v) Tween-80), containing either 5% (w/v) dried milk powder (Melford laboratories), or 2.5 % (w/v) BSA (Melford Laboratories) for 45 min depending on the antibody to be used. Membranes were then washed in TBST buffer then incubated with the appropriate primary antibody (**Table 2.3**), diluted in TBST-milk or TBST-BSA overnight at 4°C with agitation on a rocker. The following day, the membranes were washed with TBST buffer for 15 min prior to incubation with the appropriate Horseradish Peroxidase (HRP) -conjugated secondary antibody (Dako) diluted in TBST-milk or TBST-BSA for 3 h at room temperature (**Table 2.4**). Following incubation with the secondary antibody the membrane was washed three times in TBST for 15 min per wash. To visualize the protein of interest, the membranes were covered in enhanced chemiluminescent HRP substrate (ECL, MILLIPORE) reagents for 1 min and then exposed to Blue-Sensitive X-Ray film (Wolf laboratories) in the Dark Room for the appropriate time. X-ray films were then developed using a Compact X4 developer (X-ograph Imaging System). Films were scanned and saved as TIFF files for editing with Adobe Photoshop and Figure preparation in PowerPoint. As ECL detection of proteins is at best a semi-quantitative method due to the quick ‘saturation’ of protein levels and the short linear range upon which most densitometric methods rely, for most purposes we did not measure protein levels densitometrically and relied on visual inspection of blots to recognise large changes in protein abundance. We do concede however, that this approach might not identify subtle changes in protein levels, and as such for validation of our results it would be prudent to use a LI-COR imaging system or a similar, more rigorous, quantitative ECL method for determination of protein levels. In situations where we stained proteins with coomassie we did utilise densitometric methods to quantify protein levels.

Table2.3: Antibodies used for Western blotting during this project.

Antigen	Antibody	Dilution	Blocking	Species	Supplier
Ad12 E1A	M13	1:2000	Milk	Mouse	In-house
Ad12 E1B55K	XPH9	1:3000	Milk	Mouse	In-house
Ad5 E1A	M73	1:2000	Milk	Mouse	Ed Harlow
Ad5 E1B55K	2A6	1:2000	Milk	Mouse	Arnold Levine
Ad5 E4orf3	6A11	1:100	Milk	Mouse	Thomas Dobner
Ad5 E4orf6	RSA1	1:200	Milk	Mouse	Thomas Dobner
Ad5 E2A	B-8	1:200	Milk	Mouse	Thomas Dobner
EPHA2	EPHA2	1:2000	Milk	Mouse	Abcam
β -actin	AC-74	1:50000	Milk	Mouse	Sigma-Aldrich
p53	DO-1	1:20	Milk	Mouse	David Lane
p53	FL-393	1:2000	Milk	Rabbit	Santa Cruz
PURB	PURB	1:1000	Milk	Rabbit	Proteintech
SMARCAL1	H-124	1:10000	BSA	Mouse	Santa Cruz
SPT16	H-300	1:2000	Milk	Rabbit	Santa Cruz
SSRP1	D-7	1:2000	BSA	Mouse	Santa Cruz
TOPBP1	611875	1:2000	Milk	Mouse	BD Biosciences
TopII α	G-9	1:2000	Milk	Mouse	Santa Cruz
TopII β	A-12	1:2000	Milk	Mouse	Santa Cruz
Flag-tag	Anti-Flag M2	1:3000	Milk	Mouse	Sigma
TIF1 γ	197	1:3000	Milk	Rabbit	In-house
HA-tag	12CAS	1:2000	Milk	Mouse	Sigma-Aldrich
pRB	RB1	1:500	Milk	Mouse	Fitzgerald Industries
RPA32	Ab-2	1:2000	Milk	Mouse	Calbiochem
RBM14	69	1:10.000	BSA	Rabbit	Sigma-Aldrich
Ku -70	E-5	1:2000	Milk	Mouse	Santa Cruz
Ku-86	B-1	1:2000	Milk	Mouse	Santa Cruz
Histone H3	Ab1791	1:50000	Milk	Rabbit	Abcam
Histone H2A	Ab18255	1:3000	Milk	Rabbit	Abcam
GST	Ab-1	1:2000	Milk	Rabbit	Oncogene
GFP	B-2	1:2000	Milk	Mouse	Santa Cruz
Ubiquitin	anti-Ubiquitin	1:2000	Milk	Rabbit	Cell Signalling
Timeless	anti-Tim	1:2000	Milk	Rabbit	(Yoshizawa-Sugata and Masai 2007)
LAR	7/LAR	1:2000	Milk	Mouse	BD Biosciences

Table2.4: Secondary Antibodies used for WB analysis.

Antibody	Dilution	Supplier
Polyclonal Goat anti-mouse immunoglobulins/HRP	1:3000	Dako/Agilent (P0447)
Polyclonal Goat anti-rabbit immunoglobulins/HRP	1:3000	Dako/Agilent (P0448)
Goat anti-Rat IgG – H+L HRP Conjugated	1:3000	Bethyl, A110-10 SP
Protein G	1:1000	BIO-RAD

2.2.5. Immunoprecipitation

Cells for immunoprecipitation (IP) were washed twice with ice-cold PBS then solubilized in 1 ml NETN buffer (1% (v/v) Nonidet P-40, 1mM Ethylene Diamine Tetra Acetic Acid (EDTA), 50mM Tris–HCl (pH 7.5) and 150mM sodium chloride containing 25mM sodium fluoride and 25mM β -glycerophosphate). Cell lysates were prepared using a Wheaton dounce homogenizer and tight pestle; cells were homogenized twice on ice, with 10 strokes each time. Homogenised cells were then centrifuged at 16000 rpm for 30 min at 4°C. The supernatant was removed from cell debris and lipid layer using a Terumo® Agani™ needle (25G x 1”) and transferred to a fresh Eppendorf. Protein concentrations were determined by Bradford assay (section 2.2.2) and equal amounts of protein were used for each immunoprecipitation reaction. Typically 5 μ g of immunoprecipitating antibody or normal IgG control antibody was added to the supernatant and incubated overnight at 4°C with rotation. Immune complexes were then isolated from the mixture using 20 μ l packed of Protein G-Sepharose beads (Sigma-Aldrich) by incubation for an additional 3 h at 4 °C by rotation. Immunoprecipitated complexes were then washed five times in cold NETN buffer containing 250mM NaCl. After the last wash a needle (25G x 1”) was used to remove all of the buffer. Finally, beads were resuspended in SDS-PAGE sample buffer, boiled for 5 min at 95°C and separated by SDS-PAGE using 50 μ g of whole cell lysates as indicators of protein input (section 2.2.3).

2.2.6. Chromatin Isolation

This procedure was performed as described (Wysocka, et al. 2001). Typically, existing media was discarded and cells washed twice with ice-cold PBS. Cells were then scraped in ice-cold PBS and precipitated by centrifuged at 1000 x g for 2 min at 4°C. Cell pellets were then incubated in buffer A for 8 min on ice (**Table 2.5**), after which pellets were subjected to centrifugation (1300 x g, 4°C, 5 min). The resulting supernatant was collected and centrifuged at 20,000 x g, 4°C, for 30 min to isolate the soluble, cytoplasmic fraction. The resulting pellet was washed with Buffer A and incubated for 30 min in Buffer B (**Table 2.5**) to lyse the nuclear

membrane. The nuclear lysate was then centrifuged at 1700 x g, 4°C for 15 min to isolate the Nucleoplasm Fraction (supernatant) and the Chromatin Fraction (pellet). Then to elute chromatin-binding proteins, the chromatin fraction (pellet) was washed with a 0.5M salt solution (**Table 2.5**) and centrifuged at 1700 x g, 4°C for 15 min to obtain the chromatin-binding proteins (supernatant), whilst the pellet was resuspended in solubilisation buffer (**Table 2.5**) followed by sonication for 20 sec (setting 4), and centrifugation at 1700 x g, 4°C for 20 min to collect the Chromatin Fraction (supernatant).

Table 2.5: Buffers Used in Chromatin Isolation

Buffer	Component	Final Concentration
Buffer A	HEPES (pH 7.9)	10 mM
	KCl	10 mM
	MgCl ₂	1.5 mM
	Sucrose	0.34 M
	Glycerol	10% (v/v)
	DTT	1 mM
	Triton X-100	0.1% (v/v)
Buffer B	EDTA	3 mM
	EGTA	0.2 mM
	DTT	1 mM
Lysis Buffer (UTB)	Urea	9 M
	Tris-HCl (pH 7.4)	50 mM
	β-mercaptoethanol	0.15 M
NaCl salt solution	NaCl	0.5M

2.2.7. Acid extraction of histones

Cells were washed twice with warmed PBS then detached from the tissue culture plate by applying 1 ml of trypsin (Tryple E; Life Technologies). Following incubation for 5 min at 37°C in a humidified atmosphere containing 5% (v/v) CO₂, medium containing 8% (v/v) FCS was added to the cells to inactivate the trypsin. The cells were then pelleted by centrifugation at 1500 rpm for 5 min. The cell pellet containing approximately 1x10⁷ cells/ml was then resuspended in 1 ml of ice-cold Triton Extraction Buffer (TEB; 0.5% (v/v) Triton X-100, 1 x PBS, 2mM PMSF) and incubated on ice for 10 min, after which the lysate was centrifuged at 2000 rpm for 5 min at 4°C. The resulting cell pellet was resuspended in half of the original volume of TEB and re-centrifuged at 2000 rpm for 5 min at 4°C. The cell pellet was then resuspended in 0.4M HCl (25µl per 1x10⁶ cells), then incubated on ice for a minimum of 3 h. The supernatant which contained the core histone proteins was collected by centrifugation at 2000 rpm for 10 min at 4°C. Isolated histones were separated by SDS-PAGE then stained with Coomassie Blue.

2.2.8. Purification of GST Fusion Proteins

Full-length Ad12 and Ad5 E4orf6 were cloned into pGEX 4T-1 (GE healthcare) which contains an N-terminal Glutathione-S-Transferase (GST) tag and verified by DNA sequencing (section 2.3.4). Ad5/12 E4orf6-pGEX 4T-1 constructs were then used to transform BL21 Codon plus (RIPL) competent cells (Agilent) and plated onto LB-agar plates containing 100µg/ml ampicillin (section 2.3.1) for selection. Individually isolated bacterial colonies were grown in 20ml LB, supplemented with 100ug/ml ampicillin and incubated in the orbital shaker at 220 rpm overnight at 37°C. The following day, the cultures were transferred to 500ml LB supplemented with 100ug/ml ampicillin and incubated in the orbital shaker at 250 rpm at 37°C for approximately 3 h as the optical density at 600nm was approx. 0.5-0.6. The temperature of the orbital shaker was then reduced to 30°C, 200rpm for 30 min. After that, GST fusion-protein

expression was induced by the addition of 0.5mM IPTG (Isopropyl- β -D-thio-galactoside; Sigma-Aldrich) and incubated for an additional 3 h at 30°C, 200rpm. The cell pellet was then centrifuged at 5000 rpm for 10 min 4°C and the supernatant discarded. The pellet was lysed and resuspended in 28ml of GST lysis buffer (1.0% Triton X-100, 1 x PBS, 1mM EDTA (pH=8.0)). The bacterial lysate was then sonicated on ice (5Khz output) for 1 min, three times with 1 min break in between each cycle, and centrifuged for 15 min at 16,000rpm at 4°C (twice). The supernatant was then collected and incubated with 1ml of packed glutathione agarose beads (Sigma-Aldrich), resuspended in GST lysis buffer overnight at 4°C, by rotation at 12rpm. The beads were then centrifuged at 3000rpm for 2 min and washed with 50ml of GST lysis buffer twice and twice with 50ml of GST wash buffer (1 x PBS, 1mM EDTA (pH=8.0)). For elution the GST-bound beads were incubated with 2 ml of GSH elution buffer (25mM reduced glutathione in 50mM Tris, pH 8.0), and incubated at 4°C, 12rpm for 2 h. The eluted GST proteins were then dialysed using dialysis tubing with 12,000-14,000 molecular weight cut-off, using 5L dialysis buffer (25mM Tris pH 7.4, 10% (v/v) glycerol, 0.15M sodium chloride and 1mM dithiothreitol (DTT) at 4°C. The next day, the dialysis tubing was incubated in 2 changes of 2L of fresh dialysis buffer at 4°C and left throughout the day. The protein concentration was then measured by Bradford assay and stored at -80 °C until required.

2.2.9. GST-pull downs

Following the generation of GST-Ad12 E4orf6 and GST-Ad5 E4orf6, pull-down assays were performed by either: incubating 10 μ g of GST, GST-Ad12 Eorf6 or GST-Ad5 Eorf6 in the absence or presence 10 μ g of core Histones (Histone from calf thymus type II A; Sigma) in 50mM Tris pH 7.4, 0.15M NaCl at 4°C for 16 h by rotation; or by incubating 10 μ g of GST, GST-Ad12 Eorf6 or GST-Ad5 Eorf6 in the presence of 2mg of RPE-1 lysate prepared in NETN at 4°C for 16 h by rotation. Twenty μ l glutathione beads were then added to the GST-histone mixture and incubated for 3h at 4°C by rotation. GST proteins and any associated histones

were then eluted from the glutathione beads by the addition of 30µl of 25mM glutathione in 50mM Tris pH 8.0 and incubated on ice for 1h with agitation every 5 min. The supernatant was then collected and SDS sample buffer were added and heated for 5min at 95°C. Eluted proteins were then subjected to SDS-PAGE (see section 2.2.3), transferred to nitrocellulose and stained with ponceau-S (0.1% ponceau-S in 3% (w/v) trichloroacetic acid) and washed extensively with dH₂O to visualise precipitated proteins, particularly from the GST-pull down using purified histones. GST-pull downs from RPE-1 lysates were then subjected to WB analyses for Histones H2A and H3, as well as GST.

2.2.10. GFP-pull down

GFP-U2OS and GFP-RPA1-U2OS cells were grown on 10 cm dishes. Cells were washed twice with cold PBS, solubilised with 1 ml NETN and homogenized using a Wheaton dounce homogenizer using a tight pestle, twice on ice, with 10 strokes each time. Homogenised cells were then centrifuged at 16000 rpm for 30 min at 4°C and protein concentrations determined by Bradford assay. 20 µl GFP-sepharose beads (GFP Trap- ChromoTek) were added to each sample and incubated for 3 h at 4°C with rotation. GFP Trap beads were washed five times in cold NETN containing 250 mM NaCl. The beads were then resuspended in SDS sample buffer, boiled for 5 min at 95°C and separated by SDS-PAGE (section 2.2.3).

2.2.11. Coomassie staining of polyacrylamide gels

Polyacrylamide gels were stained at room temperature overnight in colloidal coomassie solution (0.08% (v/v) Coomassie Brilliant Blue G250 (Fisher Scientific), 1.6% (v/v) orthophosphoric acid (Fisher Scientific), 8% (w/v) Ammonium Sulphate (Sigma-Aldrich) and 20% (v/v) Methanol. Gels were then extensively destained in dH₂O to visualise protein bands.

2.2.12. FASP (Filter-Aided Sample Preparation) tryptic digestion of nuclear lysates

Cells were trypsinized and pelleted at 1,000g, 4°C for 5 min. Cells were then washed with cold PBS (x2) and pelleted. The pellets were then resuspended in 5ml of ice-cold hypotonic buffer (10mM HEPES pH 7.9, 10mM KCl, 1.5mM MgCl₂, 0.5mM DTT) and allowed to swell on ice for 5 min. To disrupt the plasma membrane and obtain intact, pure nuclei, cells were subjected to Dounce homogenization using 20 strokes with a tight pestle on ice. Intact nuclei were visualised using an inverted phase-contrast microscope (Nikon eclipse TS100) and pelleted at 1,000g, 4°C for 5min. Nuclei were washed twice more in hypotonic buffer and collected by centrifugation. Nuclei were then solubilised in 9M Urea and 100mM Tetraethylammonium bromide (TEAB; Sigma), then normalized by protein concentration. Cysteine residues were then reduced following incubation with 50mM DTT (in 10% (v/v) acetonitrile and 100mM TEAB) for 1h at 55°C and then carboxymethylated following the incubation with 100mM iodoacetamide, 10% (v/v) acetonitrile and 100mM TEAB, for 30 min in the dark. Denatured lysates were then filtered through a 0.5ml Amicon 92 Ultra 10 kDa centrifugal filter (Millipore), washed five times with 100mM TEAB and subjected to digestion with Sequence-Grade Modified Trypsin (Promega) in 100mM TEAB at 37°C for 16 h. The peptides were then centrifuged and the filtrate collected. The filter was then washed twice with 100mM TEAB to obtain tryptic peptides.

2.2.13. Dimethyl-labelling of tryptic peptides obtained from nuclear lysates

To measure quantitatively the effect of Ad12 E4orf6 expression on the cellular proteome nuclear lysates from Ad12 E4orf6 U2OS cells (+/- 0.1µg/ml Dox) were isolated 24h post-treatment. Tryptic peptides were then isolated by FASP as described above (section 2.2.12). Following their isolation tryptic peptides from the nuclear lysates of U2OS cells that were induced to express Ad12E4orf6 were incubated with 1/10th volume 10.73% (w/v) heavy formaldehyde ([²H]-CH₂O; Isotec) and those from non-induced cells were incubated with

1/10th volume 10.73% (w/v) light formaldehyde (CH₂O; Sigma), both for 1 min with constant mixing. The sample was then centrifuged, and 1/10th volume 1.5M sodium cyanoborohydride was added for 30sec with constant mixing, followed by centrifugation and incubation for 1h on a shaker at 600rpm. To quench the reaction 1/10th volume 10.73% (w/v) sodium hydroxide and 1/10th volume Formic acid were added. Equimolar heavy and light peptides were then mixed and purified through a 2.1×150 mm Acclaim Mixed-Mode WAX-1 C18 reverse-phase/anion exchange chromatography column (using a Dionex HPLC (high performance liquid chromatography) system, Camberley, UK) into 20 fractions using a gradient of 0–40% B over 40 min (A: 20mM ammonium formate pH 6.5, 3% (v/v) acetonitrile, B: 2mM ammonium formate pH 3.0, 80% (v/v) acetonitrile) at a flow rate of 250µl/min. Isolated fractions were dried by vacuum centrifugation until required for mass spectrometry.

2.2.14. Mass spectrometric analysis of tryptic peptides

Dried tryptic peptide mixtures isolated above that had been labelled with both heavy and light formaldehyde were resuspended in 20µl 1% (v/v) acetonitrile/1% (v/v) formic acid, of which 10µl was analysed by LC-MS/MS using a 90 min 0–40% acetonitrile gradient in 0.1% formic acid (75 µm × 50 cm C18 Pepmap column, Dionex) and an Impact TOF mass spectrometer (Bruker Daltonics, Bremen, Germany). Peptides were identified using MASCOT 2.3 to search SWISSPROT (human and randomised version thereof). Mass tolerances for parent and fragment ions were 20 p.p.m. and 0.05 Da, respectively and the minimum peptide Mowse score was 20. Modifications considered were carboxymethylation (fixed) and methionine oxidation (+/-). Quantitation of LC-MS ms/ms data from identified peptides was performed using WARP-LC (Bruker) and ProteinScape 2.1 (Bruker Daltonics), whereupon the ratios of Heavy to Light peptides were calculated to give a quantitative readout of the effect of Ad12 E4orf6 expression on the absolute levels of nuclear proteins from U2OS cells. Protein identifications were filtered using both a 1% false discovery threshold and a requirement for two or more

peptides. All MS and HPLC solutions were made up in HPLC (High-Performance Liquid Chromatography)-grade H₂O (Chromanorm, VWR).

2.3. Molecular and Cell Biology

2.3.1. Preparation of media for growth of bacteria

Luria broth (LB) was made with 1.0% (w/v) Bacto-tryptone (Difco), 0.5% (w/v) Bacto-yeast extract (Difco) and 1.0% (w/v) sodium chloride (pH 7.2) in de-ionized water. LB-agar was made by the addition of Bacto-agar (Difco) to LB to a final concentration of 1.5% (w/v). LB and LB-agar were then sterilized by autoclaving at 121°C and 15 psi for 30 min. Prior to use, LB-agar was melted then incubated at about 50°C before the appropriate antibiotic was added to the solution and the medium was poured onto sterile petri dishes. Finally, LB-agar plates were left to cool and set inside a fume hood prior to storage at 4°C.

2.3.2. Transformation of Bacteria

Introduction of exogenous genetic plasmid material to competent bacteria is known as transformation. Plasmid DNA containing the gene of interest was introduced to competent bacteria typically for isolation of appropriate clones, clone amplification and purification of plasmid DNA (section 2.3.3), or protein expression (section 2.2.9). Prior to transformation, competent bacteria were allowed to thaw on ice after taking them from -80°C storage (**Table 2.6**). After thawing was complete, 100ng of plasmid DNA was mixed with 20µl of bacteria and incubated on ice for 30 min to allow for plasmid DNA to associate with the bacterial cell membrane. Following this incubation plasmid/bacteria mixtures are heat-shocked at 42°C for 1 min to allow plasmid DNA to enter the bacteria, after which mixtures are placed back on ice for 5 min. Transformed bacteria were then incubated in 400 µl of SOC outgrowth medium (NEB) for 1h in an orbital shaker at 37°C and 200rpm. Bacterial cultures were then spread with a disposable hockey spreader onto LB agar plates in the presence of 100µg/ml ampicillin, or 50µg/ml of kanamycin, according to the antibiotic resistance gene in the plasmid. Plates

were then dried, inverted and incubated at 37°C for 16h to allow for antibiotic-resistant clones to grow. Individual colonies were picked and dispersed in 5ml LB broth containing antibiotic and incubated at 37°C overnight with agitation. For long term storage, 500µl of a mixture of 50% (v/v) sterile glycerol and 500 µl bacterial suspension were mixed together and frozen at -80°C.

Table 2.6: Competent bacteria used for transformation.

Bacteria	Supplier
<i>DH5α subcloning efficiency</i>	Life Technologies
<i>Max Efficiency Stab2</i>	Invitrogen
<i>BL21-CodonPlus (DE3)-RIPL</i>	Stratagene
<i>NEB Stable (C30401) High Efficiency</i>	NEB

2.3.3. Mini-prep and Maxi-prep plasmid DNA purification

Plasmid DNA was purified using a technique based on the alkaline-SDS lysis method which was first developed and described by Birnboim and Doly in 1979. The lysis solution utilized contains SDS, which disrupts the bacterial cell membrane and denatures the majority of the cellular proteins. It also contains sodium hydroxide which breaks the hydrogen bonds between the DNA bases to generate single-stranded plasmid and genomic DNA. Neutralising the alkalinity of the mixture by the addition of potassium acetate selectively renatures the small plasmid DNA to its double-stranded soluble form. However, the large genomic DNA and other lysed proteins on treatment, is precipitated as insoluble clots which are separated from the plasmid DNA solution by centrifugation. We have used this method for both small-scale purification (miniprep) of plasmid DNA, as initial screens for positive bacterial clones, and large-scale purification (maxiprep) of plasmid DNA to purify high yield of DNA be used for downstream applications such as transfection.

For minipreps, single colonies were incubated overnight in 5ml of LB supplemented with the appropriate antibiotic, from which plasmid DNA was purified by using the GenElute™ Plasmid Miniprep Kit (Sigma-Aldrich). As stated in the kit instructions, bacterial cells were pelleted by centrifugation at 6000 rpm for 5 min then resuspended in 200µl of pre-chilled resuspension buffer. Then, 200µl of the lysis solution was added, mixed by gentle inversion and incubated for 5 min. After this time 350µl of the neutralisation solution was added to terminate the lysis reaction. The samples were then centrifuged at 13000 rpm for 10 min to separate the insoluble precipitate from the solution. The clear solution was transferred to a silica column and centrifuged again for 1 min. The flow through was discarded and 750µl of wash solution was added to remove any contaminants. The plasmid DNA was eluted by adding 50µl of nuclease-free water (Ambion), and followed by Sanger sequencing step to identify positive clones (section 2.3.4).

For large scale plasmid purification, a positive clone was incubated with 5 ml LB supplemented with the appropriate antibiotic and incubated for between 6 and 8 h in an orbital shaker shaking at 200 rpm at 37°C. The bacterial culture was transferred to a flask containing 200ml LB supplemented with antibiotic. The bacterial culture was then incubated overnight at 37 °C with shaking at 200 rpm. In line with the Plasmid Maxi kit (NucleoBond® Xtra Maxi, MACHEREY-NAGEL) instructions, the bacterial culture was pelleted by centrifugation at 5000 rpm for 10 min at 4°C and then resuspended in 12ml of resuspension buffer. The cells were then lysed in 12ml of lysis buffer which changed the colour of the solution to blue due to the presence of Lyseblue reagent. The solution was mixed gently for approximately 5 min until the blue colour was evenly distributed. Next 12 ml of neutralisation buffer was added to the samples and mixed until the blue indicator disappeared. The mixture was then transferred to a DNA-binding column that had been pre-washed with 25 ml of binding buffer and allowed to flow through by gravity. After that, 15 ml of binding buffer was added to the binding column

followed by 2 x 15ml wash buffer. The plasmid DNA was then eluted by adding 15ml elution buffer, which was precipitated by the addition of 10.5ml isopropanol and pelleted by centrifugation at 15.000 rpm at 4°C for 30 min. The supernatant was then decanted carefully, and the pellet washed twice with 70% (v/v) ethanol to remove salts. The DNA samples were then air-dried by leaving them with lid open in the hood for 10 min then, depending on the size of the pellet, resuspended in 50-400µl of nuclease-free water and left for 10 min to rehydrate. To assess the plasmid quantity and purity, the concentration was determined by the NanoDrop and the 260nm/280nm absorbance ratios measured had to be within the acceptable range to allow the use of samples in future applications. Typically, purified DNA had a 260/280 ratio of approximately 1.8.

2.3.4. Sanger DNA Sequencing

The sequence reaction was performed in a total volume of 20µl using 200ng of plasmid DNA template, 10ng/µl of sequencing primer (**Table 2.7**), 1µl Big Dye™ terminator V3.1 (Thermo Fisher), 4µl of 5 x sequencing buffer and 9µl of nuclease-free water. The sequencing reaction was performed by PCR using the following conditions: 96°C for 10 sec, 50°C for 5 sec, and 60°C for 4 min, for 25 thermal-cycles. After PCR the plasmid DNA was precipitated upon the addition of 80µl of a mixture of 63.5µl 100% (v/v) ethanol, 3µl 3M sodium acetate and 14µl nuclease-free water. The solutions were incubated at room temperature for 30 min and DNA pelleted by centrifugation at 13000 rpm for 20 min. The supernatant was removed and the DNA pellet washed with 2 x 100µl 70% (v/v) ethanol. After a final centrifugation step for (13000 rpm for 15 min) the supernatant was discarded and the pellet was air dried at 90°C for 1 minute. The samples were resuspended in 11 µl Hi-Di, heated for 5 min at 95°C, quickly quenched on ice, and briefly centrifuged before loading for analysis by a 3500xl Genetic Analyzer (Applied Biosystems) for sequencing. The sequence results were uploaded into Chromas and were analysed utilizing the NCBI BLAST program obtained online at <http://www.ncbi.nlm.nih.org>

Table 2.7: Primers used for sequencing.

Gene	Forward Primer sequence
Ad12 E1B55K Seq1	5'AACTGTATATTGGCAGGAGTTGCAG-3'
Ad12 E1B55K Seq2	5'- AATACCTGTTCTTGTCTTGCATGGT-3'
Ad12 E1B55K Seq3	5'- ATAACATGTTTATGCGCTGTACCAT-3'
Ad5 E1B55K Seq1	5'-GGCTACAGAGGAGGCTAGGAATCTC-3'
Ad5 E1B55K Seq2	5'-CCTGGCCAATACCAACCTTATCCT-3'
Ad5 E1B55K Seq3	5'-TGCTGACCTGCTCGGACGGCAACT-3'
pcDNA5 Seq Forward	5'-CGCAAATGGGCGGTAGGCGTG-3'
pcDNA Seq Reverse	5'-TAGAAGGCACAGTCGAGG-3'
pGEX Forward	5'-GGGCTGGCAAGCCACGTTTGGTG-3'
pGEX Reverse	5'-CCGGGAGCTGCATGTGTCAGAGG-3'

2.3.5. PCR

PCR was performed in a total volume of 50µl with 10µl of 5x reaction buffer, 500nM of forward and reverse primers (**Table 2.8**; restriction sites shown in red), 10-50ng of DNA template, 200µM dNTP mix, 1 Unit of HotStart Q5 Polymerase (New England BioLabs), made up to 50µl by the addition of nuclease-free water. PCR was performed using a 2720 Thermal cycler PCR machine (Applied Biosystems) using the following protocol: 98°C -30 sec, 24-35 cycles at 98°C for 10 sec, 50-72°C for 30 sec, 72°C for 30 sec per kb; final extension at 72°C for 2 min. The DNA products obtained were separated by agarose gel electrophoresis and purified using a Qiagen gel extraction kit (section 2.3.6).

Table 2.8: Primers used for cloning.

Gene	Forward Primer sequence	Reverse Primer sequence
Ad12 E1B55K	5'-TTGCAGGGATCCATGGAGCGA GAAATCCCACCTGAG-3'	5'-TTGCACTCGAGTCAGTTGTCGTCTCA TCACTTGA-3'
Ad5 E1B55K	5'-AGGTTGGATCCATGGAG CGAAGAAAACCATCTGAG-3'	5'-AGGTTCTCGAGTCAATCTGTATCT TCATCGCTAGA-3'
Ad12 E4orf6 HA	5'-TGATTGCAGGATCCATGCAG CGCGACAGACGGTATCGC-3'	5'-TGAACTCGAGTCAAGCGTAGTCTGGGACGTAT GGG TAGTGTCCATCAGCCGCCAAGG-3'
Ad5 E4orf6 HA	5'-GGTTGGATCCATGACTAC GTCCGGCGTTCCATTT-3'	5'-TGACTCGAGTCAAGCGTAGTCTGGGACGTCG TATGGGTACATGGGGTAGAGTCATAATC-3'
FLAG Ad12 E4orf3	5'-TGACGGTACCATGAAGTACTGC CTGCGGATGGC-3'	5'-TATGGCTCGAGTTAATCAAGACGGTCAGCAAG GAT-3'
FLAG Ad5 E4orf3	5'ATGACGGTACCATGATTCGCTGC TTGAGGCTGAA-3'	5'-AACCTCGAGTTATTCCAAAAGATTATCCA AAA-3'

2.3.6. Agarose gel electrophoresis

Gel electrophoresis was performed using 0.8% (w/v) agarose (electrostatic grade, Life science) dissolved in 60ml of Tris-Borate-EDTA buffer (TBE; 100mM Tris, 100mM boric acid, 2mM EDTA pH 8.3). 1µl of 10mg/ml ethidium bromide (Sigma-Aldrich), or 1.5µl of SyberSafe (Life Technologies) was added prior to pouring to visualise DNA. PCR products were mixed 6 x loading buffer (30% v/v glycerol, 0.25% w/v bromophenol blue and 0.25% w/v xylene cyanol FF) before being loaded onto the gel. A 1kb ladder (Life Technologies) was used to monitor DNA size. Gels were run at a constant voltage of 60V in 1 x TBE for the required time. When SyberSafe was used the DNA bands were visualized when exposed to blue light (Safe Imager-Invitrogen) and then extracted by the Qiagen QIAquick gel extraction kit (Qiagen). As such, the gel was solubilised in 600µl of QG buffer at 55°C for 10 min, after which, 200µl of isopropanol was added to the solution. After mixing the solution was transferred to a QIAquick column and centrifuged for 1min at 13000 rpm. The flow through was discarded and the column was washed with 500µl of QG buffer followed by another round of centrifugation as detailed above. The column was then washed with PE buffer and dried by two rounds of

centrifugation. The DNA was eluted into a clean tube by centrifugation at 13000 rpm for 5 min with 50µl of nuclease-free water. When ethidium bromide was used to stain agarose gels DNA bands were observed under ultraviolet light (Gene Flash; Syngene Bioimaging).

2.3.7. DNA cloning

In order to subclone the gene of interest amplified by PCR into the cloning vector, both plasmid DNA and the gene of interest were digested by incubating them with the appropriate restriction enzymes (NEB) according to the manufacturer's instructions. Digested DNA was then purified by electrophoresis as described above (section 2.3.6). After extraction and purification of DNA, plasmid DNA and insert DNA were ligated at molar ratios of between 1:5 and 1:10. Ligation reactions were performed in a final volume of 30µl using 3µl 10 x ligation buffer (NEB) and 1µl T7 DNA ligase (NEB). Ligation mixtures were then incubated in the cold room in a water bath at 16°C overnight. The reaction was stopped by heating the sample at 65°C for 15 min. Ligation mixtures were then used for the transformation of competent bacteria as described in section 2.3.2 to identify positive clones by sequencing (section 2.3.4).

2.3.8. Site-directed mutagenesis

Site-directed mutagenesis (SDM) was used to introduce specific DNA mutations into the gene of interest using the Q5 Site-Directed Mutagenesis Kit (NEB). The first step of the SDM procedure was to amplify the gene by PCR to incorporate the appropriate mutation. This was achieved using the following protocol (98°C 30sec; 98°C for 10sec, 65°C for 15sec, 72 °C for 4 min- 25 thermal cycles; final extension 72°C for 2 min). Following the PCR reaction, 1µl of the PCR product was incubated in a KLD reaction mixture containing KLD reaction buffer, KLD enzyme mix (Kinase, Ligase and DpnI enzymes; NEB) and nuclease-free water, which was incubated for 5 min at room temperature. After this time the KLD mixture was then incubated the appropriate bacterial strain for transformation (section 2.3.2), mini-prep

purification (section 2.3.3) and DNA sequencing for validation (section 2.3.4). Oligonucleotides used were designed using the NEBaseChanger tool and obtained from Sigma-Aldrich (**Table 2.9**; mutated residues shown in red).

Table 2.9: Mutagenic primers used in this study.

Mutagenic Primers	Forward primers	Reverse primer
Ad5 E4orf6 KR1	5- AATCCTGAGG AGG TGTATGCACG-3	5-ACAAGCTCCTCCCGCGTT-3
Ad5 E4orf6 KR2	5- AACATGCCAA AGG GAGGTAATGTTATG-3	5- GTAATTCACCACCTCCCG -3

2.3.9. Immunofluorescence

Cells were grown on glass, 12-well multispot microscope glass slides (Hendley-Essex) at densities of 2×10^4 cells/well. Following the appropriate treatment (e.g. viral infection of A549 cells or Dox-induction of FRT-U2OS cells) slides were washed twice in warmed PBS followed by fixation for 8 min in 4% (w/v) paraformaldehyde in PBS. Cells were then permeabilized in ice-cold acetone for 10 min. Cells were then blocked in HINGS buffer (20% v/v HINGS (heat inactivated normal goat serum), 0.2% w/v BSA in PBS) for 45 min at room temperature. After a further wash in PBS, cells were incubated with the appropriate primary antibody diluted in HINGS buffer and incubated at 37°C for 2 h. After this time cells were washed twice in PBS for 15 min each before being incubated with the appropriate fluorescent secondary antibody (either α -mouse Alexa Fluor 488 or 594 and/or α -rabbit Alexa Fluor 488 or 594, Life Technologies) diluted in HINGS buffer and incubated at 37°C for 2 h. Cells were washed again three times in PBS and mounted in Vectashield mounting medium (Vector Laboratories) containing 4',6-diamidino-2-phenylindole (DAPI), and protected with 20-70 mm glass coverslips (Menzel-Gläser). Immunofluorescent staining of cells was viewed using a Nikon Y-FL epi-fluorescence microscope or a Zeiss LSM780 confocal microscope. TIFF images were

generated following data acquisition using either NIS-Elements or Zen software, and edited using Adobe Photoshop.

2.3.10. Metaphase spreads

Cells were treated with 0.2 µg/ml colcemid (Sigma) for 4 hr prior to harvesting by trypsinisation. Cells were then subjected to hypotonic shock by incubation in hypotonic solution (10.7 mM KCl, 14.3% (v/v) foetal calf serum) for 20 min at 37°C. Cells were then fixed three times in a methanol: acetic acid (3:1 (v/v)) solution. Fixed cells were dropped onto acetic acid cleaned microscope slides, stained for 15 min in Giemsa-modified (Sigma) solution (5% v/v in H₂O) and washed twice in H₂O for 5 min to remove residual stain. Metaphases were viewed under a Zeiss Axioscop light-microscope at 100x magnification and images captured using Axiovision software. The number of chromatid breaks, gaps and exchanges from at least 30 cells were recorded. Generated TIFF images were edited using Adobe Photoshop.

CHAPTER 3



Generation and characterization of TET-inducible U2OS cell lines to investigate the function of adenovirus E1B-55K, E4orf3 and E4orf6 proteins

3.1. Introduction

Adenovirus early region proteins have been studied at the molecular level since the discovery that Ad12 induces tumours in new-born hamsters and Ad2/5 and Ad12 promote the transformation of both human cells and rodent cells in tissue culture (reviewed by Gallimore and Turnell, 2001). Indeed, the generation of Ad2/5 and Ad12 mutant viruses and the use of mammalian expression plasmids has established that early region proteins are essential for both viral replication and cellular transformation. The role of the adenovirus E1A proteins are very well understood, during infection E1A serves to activate early region gene expression and promote entry into S-phase, the latter process being important in E1A's ability to promote cellular transformation (see Introduction, section 1.2.1). E1B-19K serves to inhibit premature cellular apoptosis during infection, a function which similarly facilitates cellular transformation (see Introduction, section 1.2.2). E1B-55K, E4orf3 and E4orf6 cooperate to regulate host-cell shut-off during infection by inhibiting host cell mRNA transport and translation and inactivating antiviral pathways activated in the host cell (see Introduction, sections 1.2.2, 1.2.4.1 and 1.2.4.2). One such host cell response that is activated during infection in response to the synthesis of linear dsDNA that resemble cellular DNA breaks is the DDR (see Introduction, sections 1.4.1, 1.4.2, 1.4.3, and 1.4.4). In this regard, E1B-55K, E4orf3 and E4orf6 engage with the cellular UPS to inactivate DDR pathways during infection to inhibit cell cycle checkpoint control and cellular apoptosis. As such E1B-55K-E4orf6 complexes utilize cellular CRL ubiquitin ligases during infection (Querido, et al. 2001; Harada, et al. 2002). E1B-55K also forms complexes with E4orf3 during infection, as does E4orf6 but the significance of these interactions is largely unknown. The inactivation of DDR pathways by E1B-55K, E4orf3 and E4orf6 is key in their ability to promote cellular transformation (Nevels, et al. 2001). The individual and combined functions of E1B-55K, E4orf3 and E4orf6 have been studied in both adenovirus-infected and adenovirus-transformed cells. For instance, Ad5 E1B-55K associates with p53 in cellular structures known as aggresomes and inactivates

its transcriptional activities (Zantema, et al. 1985). Ad12 E1B-55K also inhibits p53 transactivation, though it binds less avidly to p53 than Ad5 E1B-55K and does not localise to aggresomes but resides both in the nucleus and cytoplasmic flecks; Ad12 E1B-55K associates with p53 in the nucleus (Liu, et al. 2000). Moreover, Ad5 E1B-55K is a SUMO E3 ligase that can self-SUMOylate or SUMOylate p53, which is required for maximal p53 inhibition; Ad12 E1B-55K does not possess these activities (Muller and Dobner, 2008). Interestingly, mutant virus, mammalian expression plasmid, and adenovirus vector expression studies have indicated that Ad5 E1B-55K has other cellular activities that do not require E4orf3 and/or E4orf6. As such, Ad5 E1B-55K induces the degradation of the death-associated protein, Daxx by engaging with the cellular CRL5 ubiquitin-ligase (Schreiner, et al. 2010).

Similarly, adenovirus E4orf3 also possesses individual activities during infection that do not require E1B-55K and/or E4orf6. Indeed, it has been shown that Ad5 E4orf3 disrupts both ATM and ATR pathways by causing the misslocalization of DDR protein, MRE11 into PML (promyelocytic leukemia protein)-containing nuclear track-like structures in Ad5-infected cells (Araujo, et al. 2005; Vink, et al. 2015), whilst Ad12 E4orf3 lacks this ability (Carson, et al. 2009). Data from our laboratory has determined that the transcriptional repressor, TIF1 γ is recruited to nuclear tracks by both Ad5 and Ad12 E4orf3 during infection, prior to its degradation by the UPS (Forrester, et al. 2012). Later, Ad5 E4orf3 was, (like Ad5 E1B-55K) determined to be a SUMO E3 ligase, which promoted the SUMOylation of TIF1 γ and subsequent SUMO-targeted ubiquitylation and degradation of TIF1 γ (Sohn and Hearing, 2016). E4orf3 also functions independently to inhibit p53 transcriptional activity by silencing epigenetically the activation of p53 responsive promoters (Soria, et al. 2010).

Like E1B-55K, Ad5 E4orf6 blocks p53 transcriptional activity through its ability to associate directly with the C-terminal regulatory domain of p53 (Dobner, et al. 1996). Interestingly, work

from our laboratory has determined that Ad12 E4orf6, but not Ad5 E4orf6, is required to inhibit ATR activation by associating with, and stimulating the CRL2 ubiquitin ligase-dependent degradation of the ATR activator, TopBP1 during infection (Blackford, et al. 2010).

To date, the study of E1B-55K, E4orf3 and E4orf6 function has been instrumental in establishing the molecular basis of viral replication and cellular transformation. Based on the work described above and that detailed in the introduction it is clear however, that, not only do these proteins have the capacity to function independently of one another but that these proteins utilize multiple strategies to achieve the same goal e.g. the inactivation of p53 activity through direct association, mislocalization of the p53 protein or epigenetic silencing (see introduction for more detail). Moreover, it is also clear that early region protein activities are not always conserved between different adenovirus types e.g. the mislocalization of p53 to aggresomes, or the degradation of TopBP1. Most studies in this area, however, tend to focus on the function of the Ad5 E1B-55K, E4orf3 and E4orf6 proteins and not the Ad12 equivalent proteins, such that we understand much less about the function of the Ad12 E1B-55K, E4orf3 and E4orf6 proteins. Given that the focus of my thesis is to further our understanding of how Ad5, and particularly, Ad12 E1B-55K, E4orf3 and E4orf6 proteins function at the molecular level in the host cell, in isolation, we reasoned that it would be extremely valuable to make a library of TET-inducible cell lines that expressed individually either Ad5 or Ad12 E1B-55K, E4orf3 or E4orf6 proteins, that we could use to study their cellular activities in the absence of other viral proteins, or virus particles that is not achievable using mutant adenoviruses or adenovirus vectors. We reasoned that this approach would also allow us to study the function of these proteins at consistent levels in whole populations of cells that is not achievable by transient transfection. This chapter describes the generation and characterization of such TET-inducible

FRT-U2OS cell lines that express either Ad5 or Ad12 E1B-55K, E4orf3 or E4orf6 proteins, in isolation.

3.2. Results

3.2.1. Use of the Flp-In T-Rex System to generate U2OS-FRT-inducible cell lines

In order to study the function of adenovirus early region proteins in isolation and in a systematic manner we decided to use the Flp-In T-Rex system developed by Invitrogen. In this system the gene of interest is cloned into the pcDNA5/FRT/TO plasmid whose expression is under the control of a tetracycline operator. This plasmid is then transfected along with another plasmid expressing a Flp recombinase gene (pOG44) into a cell line (U2OS) that expresses a tetracycline repressor for TET-responsive expression and possesses an engineered, single recombination site in its genome to allow for the gene of interest to be inserted in the cell genome. Therefore, to understand the complex relationship between adenovirus early region proteins and cellular signalling pathways that enhance or repress viral replication we generated Flp-In T-Rex U2OS-FRT- cell lines that express either Ad5 or Ad12 E1B-55K, E4orf3 and E4orf6 oncoproteins individually.

3.2.2. Generation of Ad5 and Ad12 E1B-55K Flp-In T-Rex U2OS-FRT-inducible cell lines

To generate Ad5 and Ad12 E1B-55K Flp-In T-Rex U2OS-FRT-inducible cell lines we synthesized w.t. Ad5 and Ad12 E1B-55K genes with appropriate restriction sites by PCR (section 2.3.5) and cloned them into the pcDNA5- FRT TO vector (see section 2.1.5). After transformation of bacteria and mini-preparation of plasmid DNA we performed DNA sequencing and used Chromas and the NCBI BLAST program to validate the sequence integrity of the clones isolated (sections 2.3.2- 2.3.4). Sequencing revealed that we had successfully isolated w.t. Ad5 and Ad12 E1B-55K pcDNA5-FRT TO clones that possessed a BamHI site prior to the ATG and XhoI site after the stop codon [Fig.3.1 A, B, C, and D

respectively]. Sequencing also revealed that the entire genes were w.t. and in-frame (data not shown).

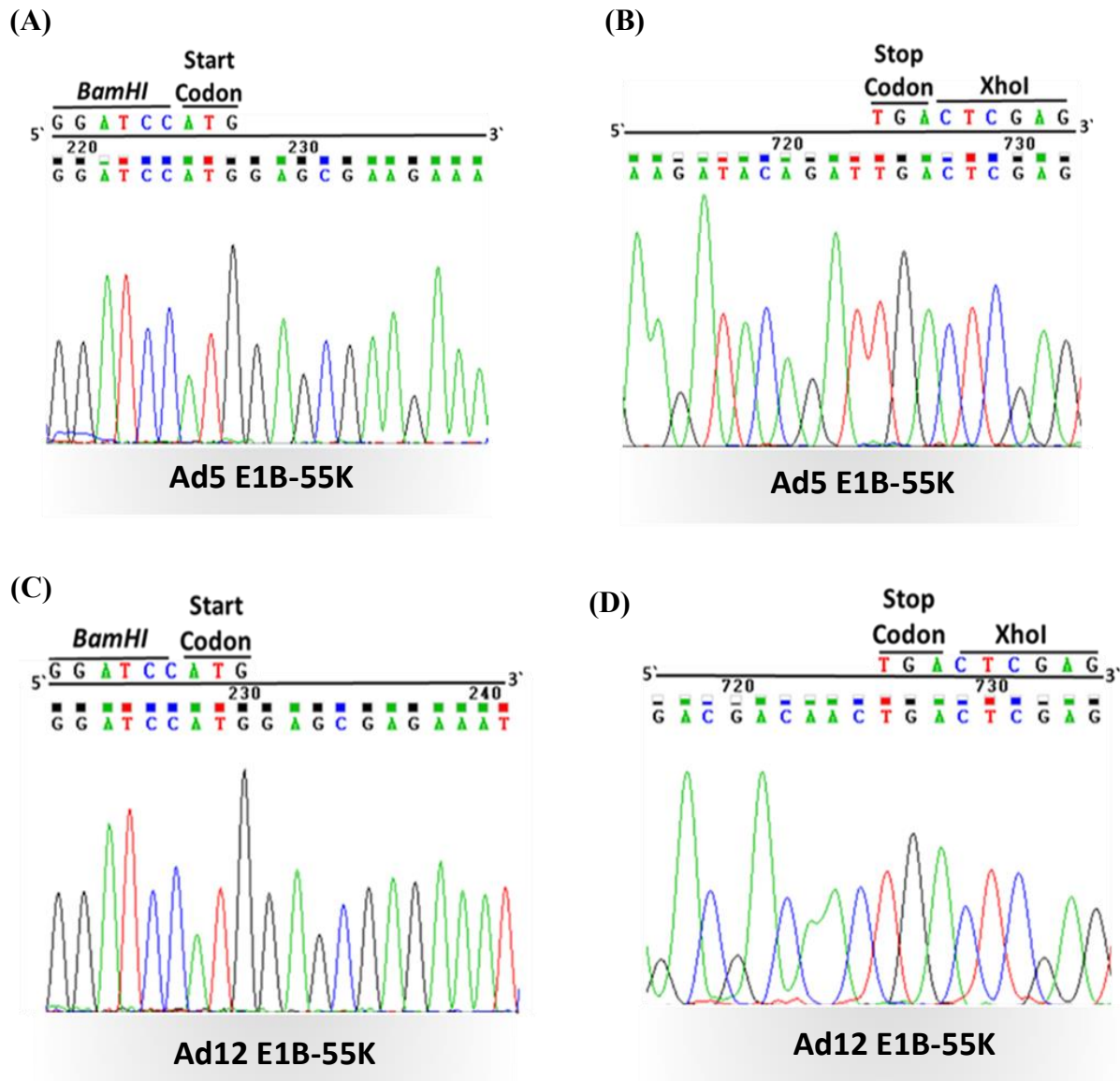


Figure 3.1: Chromatograms demonstrating sequence integrity of Ad5 and A12 E1B-55K pcDNA5-FRT TO clones at 5' and 3' ends. (A) Illustrates the 5' end of the Ad5 sequence showing the *Bam*HI cloning site and the start codon (ATG); **(B)** Illustrates the 3' end of the Ad5 sequence showing the stop codon (TGA) and the *Xho*I cloning site. **(C)** Illustrates the 5' end of the Ad12 sequence showing the *Bam*HI cloning site and the start codon (ATG); **(D)** Illustrates the 3' end of the Ad12 sequence showing the stop codon (TGA) and the *Xho*I cloning site.

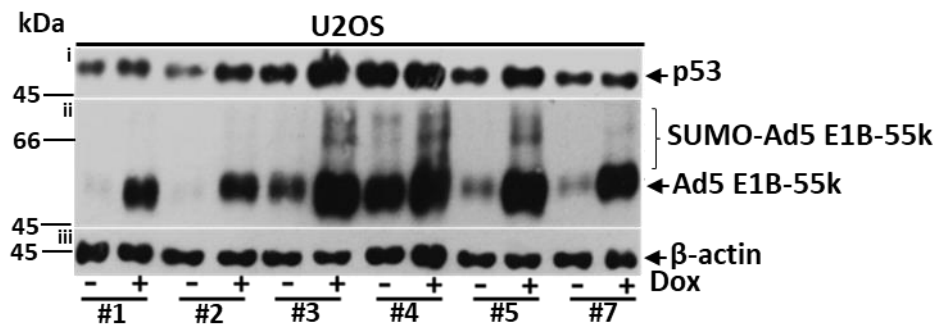
3.2.2.1. Generation and characterization of Ad5 E1B-55K and Ad12 E1B-55K Flp-In T-Rex U2OS inducible cell lines

Once we had verified the validity of our Ad5 and Ad12 E1B-55K pcDNA5-FRT TO clones, we next generated the Ad5/12 E1B-55K TET-inducible U2OS cell lines, as described [see Materials and Methods, section 2.1.5]. To test for Ad5 E1B-55K expression cells were induced to express the viral gene by the addition of Doxycycline, harvested 24 h post-induction and then subjected to SDS-PAGE and Western blot [WB] analysis. WB analysis revealed that the Ad5 E1B-55K was expressed in a Dox-dependent manner in most of the cell lines isolated but that some of the cell lines also expressed varying levels of Ad5 E1B-55K in control cells not treated with Dox [panel ii, Fig. 3.2 Ai, Aii]. Consistent with previous studies, higher molecular forms of Ad5 E1B-55K were detectable, which have previously been identified as SUMOylated Ad5 E1B-55K [panel ii, Fig. 3.2 Ai, Aii; (Endter, et al. 2001)]. It has also been reported previously that Ad5 E1B-55K expression increases p53 protein levels through the inactivation of Mdm2 and protein stabilization (Li, et al. 2011). As such that there was also an increase in the levels of p53 in response to Ad5 E1B-55K expression in most of the cell lines tested [panel i, Fig. 3.2 Ai, Aii].

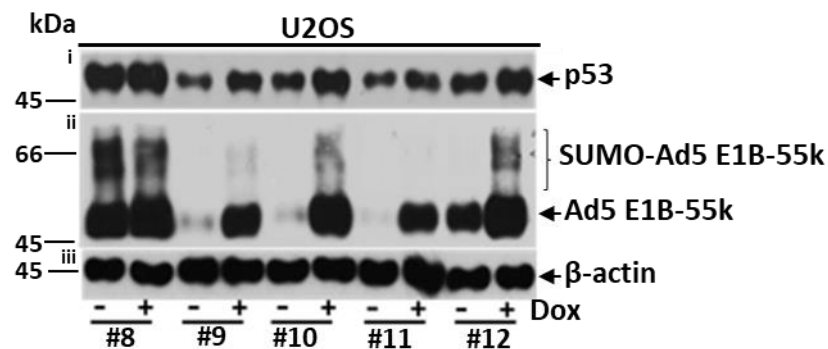
Ad12 E1B-55K cells were similarly harvested 24 h post-induction and subjected to SDS-PAGE and WB analysis, which revealed that the Ad12 E1B-55K was also expressed in a Dox-dependent manner in most of the cell lines tested [panel ii, Fig. 3.2 Bi, Bii]. Consistent with previous studies that determined that Ad12 E1B-55K was not modified by SUMOylation there were no modified forms of Ad12 E1B-55K detected by WB [panel ii, Fig. 3.2 Bi, Bii, Biii; (Endter, et al. 2001)]. Like the Ad5 E1B-55K cell lines, the induction of Ad12 E1B-55K often resulted in the expected stabilization of p53 [panel i, Fig. 3.2 Bi, Bii, Biii; (Li, et al. 2011)]. Taken together, these data indicate that we have successfully generated Flp-In T-Rex U2OS cell lines that express E1B-55K in a Dox-dependent manner. Given these results, it was important to investigate the function of E1B-55K in these cell lines in more detail to determine

whether they are a useful cell model to study E1B-55K function. To this end, we chose a few different cell lines from both Ad5 and Ad12 that showed good induction of E1B-55K in the presence of Dox, and E1B-55K induced p53 stabilization to study E1B-55K function in more detail. For simplicity, in the experiments shown results are presented from Ad5 E1B-55K cell line #10 and Ad12 E1B-55K cell line #14 although these results are representative of all cell lines used.

(Ai)



(Aii)



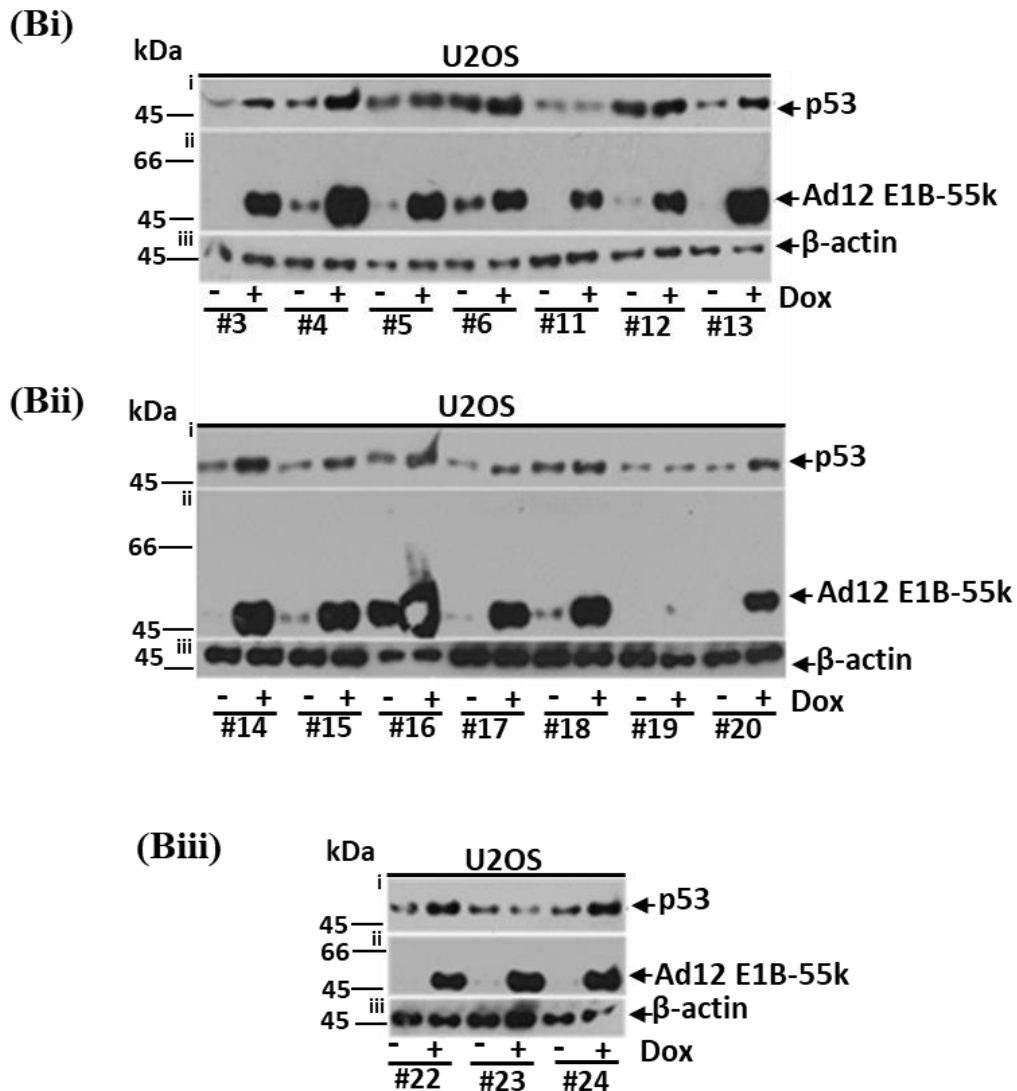


Figure 3.2: Validation of Ad5 and Ad12 E1B-55K Flp-In T-Rex U2OS cell lines. The expression of Ad5 and Ad12 E1B-55K in Flp-In T-Rex U2OS-FRT cell lines was induced with 0.1µg/ml doxycycline. 24h post-induction cells were harvested and subjected to SDS-PAGE and WB analysis with the appropriate antibodies. # represents clone number. The data shown is representative of 3 independent induction experiments.

3.2.2.2. Characterization of Ad5 and Ad12 E1B-55K cell lines: E1B-55K association with p53

It is generally accepted that both Ad5 and Ad12 E1B-55K function to repress p53 transcriptional activity, which is based on their ability to associate with p53 *in vitro* and *in vivo* (Yew, et al. 1994). Therefore, to test the functionality of Ad5 and Ad12 E1B-55K in the Flp-

In T-Rex U2OS cell lines it was deemed important to establish that Ad5/Ad12 E1B-55K interact with p53. To investigate this, co-immunoprecipitation assays were performed [section 2.2.5]. Thus, following induction of E1B-55K expression by Dox, Ad5 E1B-55K was immunoprecipitated from the corresponding Flp-In T-Rex U2OS cell lines using the 2A6 mAb [Fig. 3.3A], whilst Ad12 E1B-55K was immunoprecipitated from the corresponding Flp-In T-Rex U2OS cell lines using the XPH9 mAb [Fig. 3.3B]. Results obtained revealed that both anti-Ad5 and Ad12 E1B-55K antibodies [Fig. 3.3, Ai and Bi, respectively], co-immunoprecipitated p53 [Fig. 3.3, Aii and Bii, respectively], Consistent with previous observations Ad5 E1B-55K interacted more avidly with p53 than Ad12 E1B-55K [Fig. 3.3, Aii and Bii]. Taken together, these data demonstrate that Ad5 and Ad12 E1B-55K are functional in the Flp-In T-Rex U2OS cell lines and can be used to study E1B-55K function in isolation.

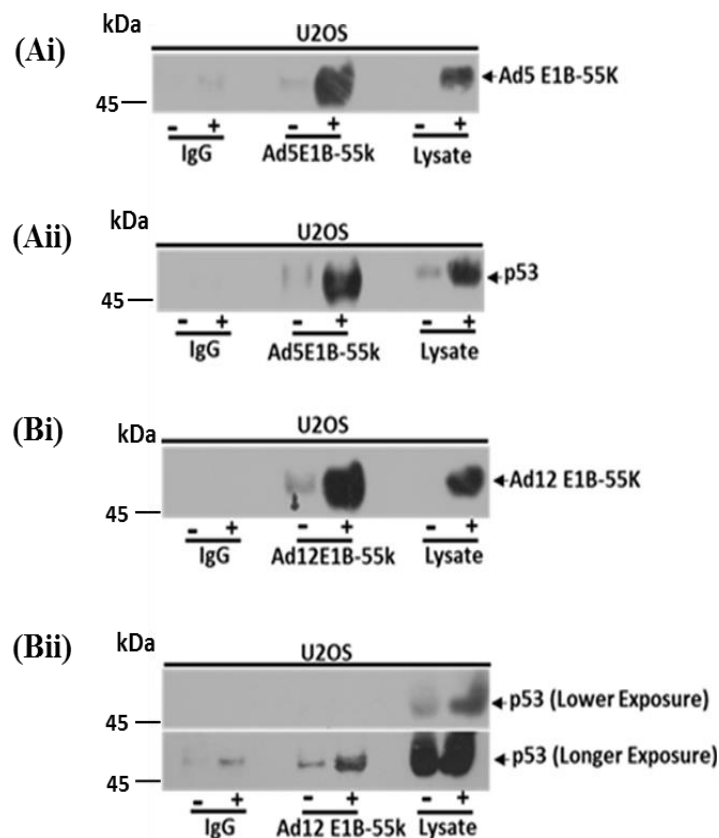


Figure 3.3: Ad5 and Ad12 E1B-55K associate with p53 in Flp-In T-Rex U2OS cell lines. Ad5 and Ad12 E1B-55K were immunoprecipitated with anti-E1B-55K mAbs from 2 mg of U2OS cell lysate, which had been collected 24 h post-treatment +/- 0.1µg/ml doxycycline (A,

Ad5 E1B-55K; B, Ad12 E1B-55K). Immunocomplexes were isolated on protein-G Sepharose, subjected to SDS-PAGE, and p53 and Ad E1B-55K detected by WB analysis using the appropriate antibodies. The data shown is representative of 2 independent experiments.

3.2.2.3. Characterization of Ad5 and Ad12 E1B-55K cell lines: recruitment of p53 to aggresomes in Ad5 E1B-55K Flp-In T-Rex U2OS cell lines

It is clear that E1B-55K is a potent repressor of p53 proapoptotic activities (Zhao, et al. 2007).

In Ad5-infected cells, E1B-55K co-operates with the E4orf6 oncoprotein to stimulate the ubiquitin-dependent degradation of p53 (Querido, et al. 2001). It has been determined that in Ad5-transformed cells however, that E1B-55K associates with p53 at p53-responsive promoters (Yew, et al. 1994), or associates with p53 in cytoplasmic aggresomal structures, which localize near the MTOC outside the nucleus, to inactivate p53 function (Zhao and Liao, 2003; Blanchette, et al. 2013). To investigate whether Ad5 E1B-55K and p53 associated at aggresomes in the Flp-In T-Rex U2OS cell lines, we assessed the localization status of p53 and Ad5 E1B-55K by indirect immunofluorescence as described [section 2.3.9]. Consistent with previous observations Ad5 E1B-55K expression localized in the cytoplasm in a diffuse manner, or localized to discrete aggresome-like structures in the cytoplasm [panel i, Fig. 3.4B]. Consistent with this localization pattern p53 was found to be localized to the cytoplasm, or localized to cytoplasmic aggresomes [panel ii, Fig. 3.4B], where they appeared to co-localize with Ad5 E1B-55K [panel iii, Fig. 3.4B].

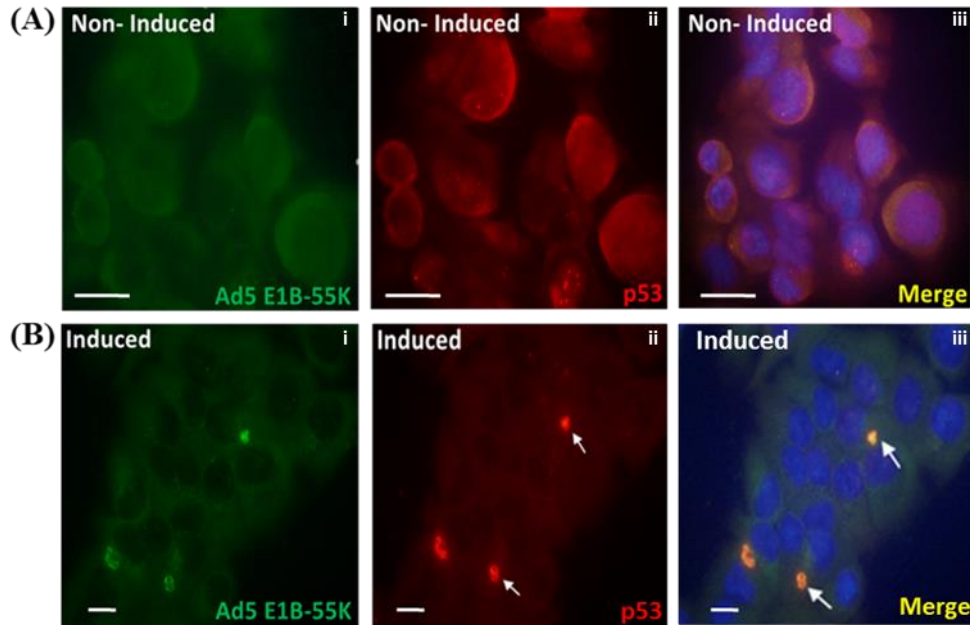


Figure 3.4: Co-localization of p53 with Ad5 E1B-55K in cytoplasmic aggresomes in Ad5 E1B-55K Flp-In T-Rex U2OS cells. Cells were plated on glass slides then fixed in 4% (w/v) paraformaldehyde and permeabilized in ice-cold acetone (Materials and Methods section 2.3.9), 24 h post +/- 0.1 $\mu\text{g/ml}$ doxycycline treatment. Cells were then incubated with an anti-Ad5 E1B-55K mAb antibody (2A6; green), an anti-p53 pAb (red) and counter-stained with anti-mouse Alexa Fluor 488 and anti-rabbit Alexa Fluor 594 secondary antibodies, respectively for both non-induced (A) and Dox-treated cells (B). Slides were then mounted in Vectashield containing DAPI. Images were visualised using a Nikon Y-FL epi-fluorescence microscope. The data shown is representative of 2 independent experiments. Upper panel scale bar = 20 μm ; lower panel scale bar = 10 μm .

3.2.2.4. Characterization of Ad5 and Ad12 E1B-55K cell lines: localization of Ad12E1B-55K to cytoplasmic flecks in Flp-In T-Rex U2OS cell lines

According to previous studies and the data presented above Ad12 E1B-55K association with p53 is weak relative to Ad5 E1B-55K (Yew and Berk, 1992); [Fig. 3.3]. It has also been reported that Ad12 E1B-55K does not co-localize with p53 at cytoplasmic aggresomes but, instead, associates and co-localizes with p53 in the nucleus (Zantema, et al. 1985), where it inhibits p53 functionality (Yew and Berk, 1992). More recently, it has reported that Ad12 E1B-55K forms cytoplasmic bodies or ‘flecks’ that are morphologically distinct from the largely spherical aggresomal structures formed by Ad5 E1B-55K. Indeed, Ad12 E1B-55K cytoplasmic bodies are elongated and filamentous in nature that are not found in a juxtannuclear locations;

p53 does not localize to Ad12 E1B-55K-containing cytoplasmic bodies (Zhao and Liao, 2003). To determine if Ad12 E1B-55K similarly forms these cytoplasmic bodies in the Flp-In T-Rex U2OS cell lines the localization status of p53 and Ad12 E1B-55K were investigated by indirect immunofluorescence [section 2.3.9]. Consistent with previous studies Ad12 E1B-55K localized in the nucleus excluded from nucleoli and was also found as elongated, filamentous structures in the cytoplasm with diffuse cytoplasmic Ad12 E1B-55K also detected [panel i, Fig. 3.5 B]. Consistent with previous reports we were unable to detect any p53 sequestration in the Ad12 E1B-55K-containing cytoplasmic bodies although there was diffuse p53 staining in the cytoplasm [panel ii, Fig. 3.5 B]. However, we did note that p53 levels were elevated particularly in the nucleus, where it co-localized with Ad12 E1B-55K, and like Ad12 E1B-55K was excluded from nucleoli [panel ii, Fig. 3.5 B]. Taken together, these data indicate that both Ad5 and Ad12 E1B-55K cells modulate p53 localization as reported previously, indicating that, as both the Ad5 and Ad12 E1B-55K Flp-In T-Rex U2OS cell lines modulate p53 as expected that they are likely to be good cell models for dissecting other functions of E1B-55K.

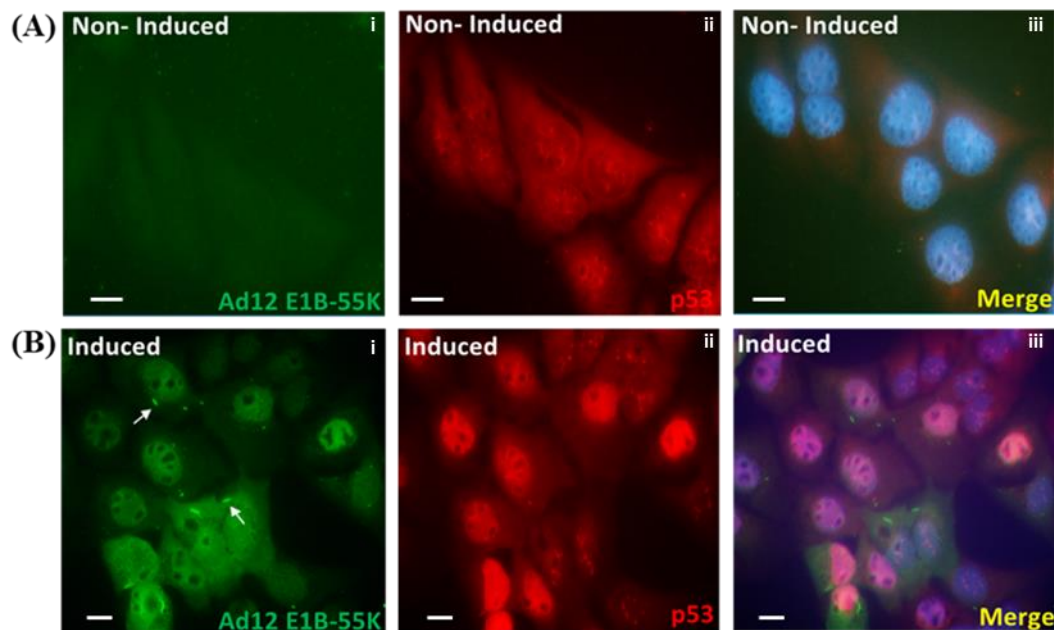


Figure 3.5: Localization of Ad12 E1B-55K to cytoplasmic filamentous structures in Ad12 E1B-55K Flp-In T-Rex U2OS cells. Cells were plated on glass slides then fixed in 4% (w/v) paraformaldehyde and permeabilized in ice-cold acetone (Materials and Methods section

2.3.9), 24 h post +/- 0.1µg/ml doxycycline treatment. Cells were then incubated with an anti-Ad12 E1B-55K mAb antibody (XPH9 mAb; green), an anti-p53 pAb (red) and counter-stained with anti-mouse Alexa Fluor 488 and anti-rabbit Alexa Fluor 594 secondary antibodies, respectively. Slides were then mounted in Vectashield containing DAPI. Images were visualised using a Nikon Y-FL epi-fluorescence microscope. The data shown is representative of 2 independent experiments. Scale bar = 10µm.

3.2.2.5. Characterization of Ad5 and Ad12 E1B-55K cell lines: effects of E1B-55K expression on the levels and post-translational modification status of cellular proteins

It is becoming increasingly clear that E1B-55K has many functions in adenovirus-infected and adenovirus-transformed cells. For instance, Ad5 E1B-55K can engage with the ubiquitin-proteasome system independently of E4orf6 and target the protein Daxx for CRL5 and proteasome-dependent degradation (Schreiner, et al. 2010). As well as being able to increase cellular levels of p53 through increased protein half-life, Ad5 E1B-55K also functions as p53-directed SUMO1 E3 ligase and also possesses the ability to self-SUMOylate (Endter, et al. 2001; Muller and Dobner, 2008; Pennella, et al. 2010). We thought therefore, it would be interesting to determine whether the expression of either Ad5 or Ad12 E1B-55K protein had the ability to promote an increase in other cellular proteins, promote the degradation of other cellular proteins or promote the SUMOylation of other cellular proteins. In this regard, we chose cellular proteins that are mostly known to be targeted by both Ad5 and Ad12 during infection and/or cellular transformation such as PTPRF/LAR and Epha2 that are targeted for proteasome-mediated degradation during infection (Fu, et al. 2017). We also chose to investigate the effects of E1B-55K expression upon the protein levels of TIF1γ, an E4orf3 and E4orf6-binding protein (Forrester, et al. 2012) and the pRB family of proteins, which are targeted by E1A (see Gallimore and Turnell, 2001).

In agreement with previous reports and analyses presented in [Fig. 3.2], we found that both Ad5 and Ad12 E1B-55K stabilized p53 levels [panel x, Fig 3.6]. Consistent with previous studies we also determined that Ad5 E1B-55K, but not Ad12 E1B-55K, promoted the,

presumably, SUMOylation of p53 [panel x, Fig 3.6]. Moreover, we also found that Ad5 E1B-55K was similarly, post-translationally modified, whereas Ad12 E1B-55K was not [panels xi and xii, Fig. 3.6]. Interestingly, although, TIF1 γ has previously been reported to be SUMOylated by E4orf3 (Sohn and Hearing, 2016), it was not modified or degraded by Ad5 E1B-55K or Ad12 E1B-55K, despite the known ability of both Ad5 and Ad12 E1B-55K to interact with TIF1 γ [panel vi, Fig. 3.6]; (Forrester, et al. 2012). Interestingly, we found that the protein tyrosine phosphatase receptor type F (PTPRF/LAR) level was reduced 48h post-induction of both Ad5 and Ad12 E1B-55K relative to non-induced cells, suggesting that E1B-55K might target PTPRF/LAR for proteasome degradation, independent of E4orf6 expression [panel i, Fig. 3.6]. Epha2 levels were somewhat reduced 48h post-induction of Ad12 E1B-55K but not following Ad5 E1B-55K induction [panel v, Fig 3.6]. It was interesting to note that Ad5/Ad12 E1B-55K expression appeared to have different effects on the pRB family of proteins such that p107 was unaffected by Ad5/Ad12 E1B-55K expression [panel viii, Fig 3.6], p130 levels were variable but largely unchanged following Ad5/Ad12 E1B-55K induction [panel vii, Fig 3.6], whereas both Ad5 and Ad12 E1B-55K expression appeared to increase pRB levels quite substantially [panel ix, Fig 3.6]. The levels of the DDR protein MSH2 also appeared to increase following Ad5 and Ad12 E1B-55K expression [panel iii, Fig 3.6], whereas its binding partner, MSH6 was unaffected [panel ii, Fig 3.6].

These experiments suggest that AdE1B-55K might affect the protein levels of a number of cellular proteins directly, and independently of other early region proteins, though no clear cellular SUMOylation substrates were identified in addition to p53. These data do indicate however that the Ad5 and Ad12 E1B-55K Flp-In T-Rex U2OS cells could be a valuable resource to study E1B-55K function.

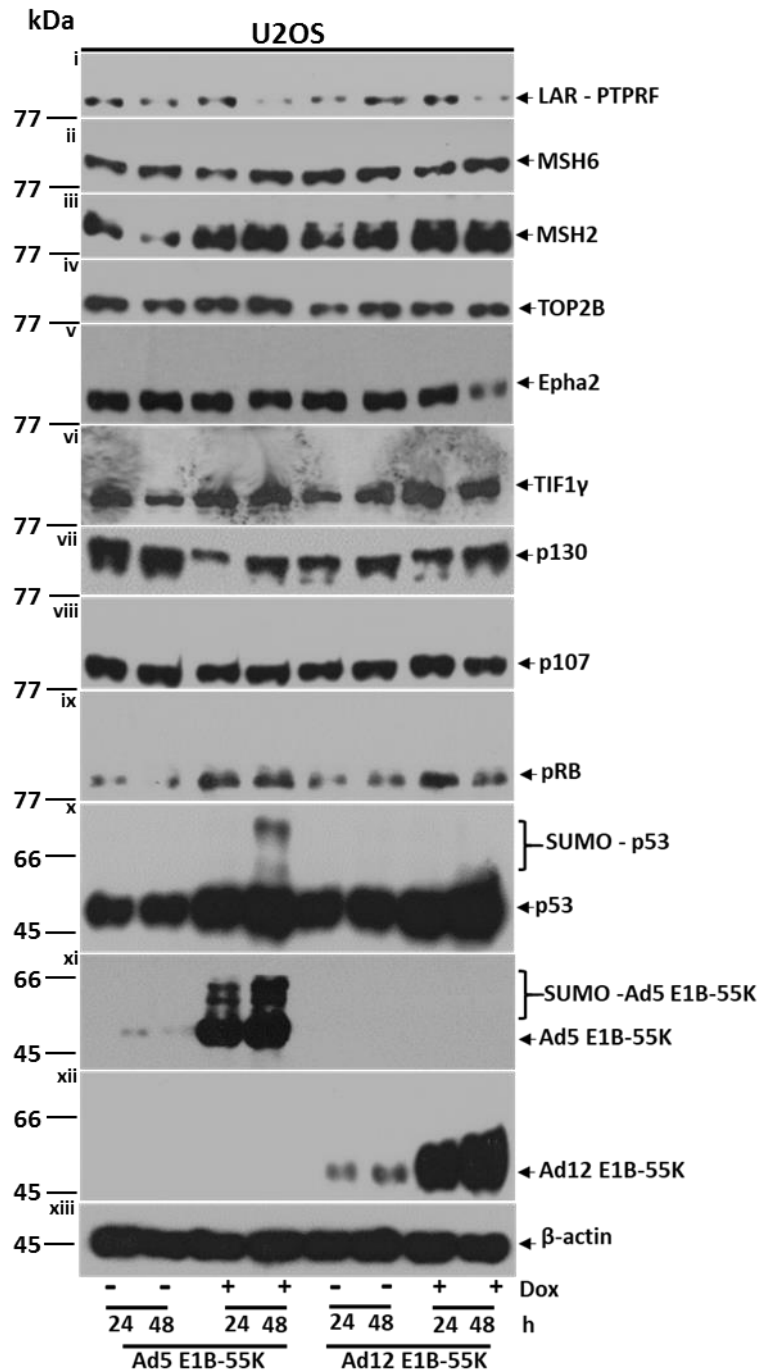
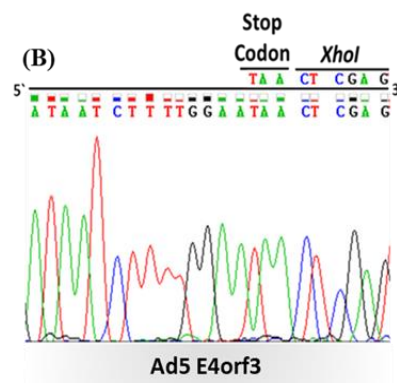
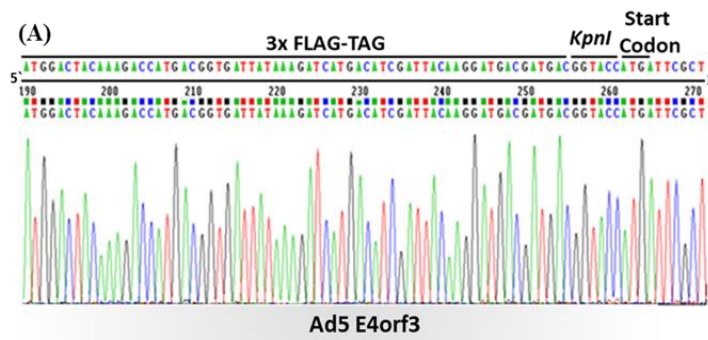


Figure 3.6: Effects of Ad5 and Ad12 E1B-55K expression upon cellular proteins levels and post-translational modification status. The expression of Ad5 and Ad12 E1B-55K in Flp-In T-Rex U2OS-FRT cell lines was induced with 0.1 μ g/ml doxycycline. 24 h and 48 h post-induction cells were harvested and subjected to SDS-PAGE and WB analysis with the appropriate antibodies. The data shown is representative of 3 independent experiments.

3.2.3. Generation of Ad5 and Ad12 E4orf3 Flp-In T-Rex U2OS-FRT-inducible cell lines

In a similar manner to that described in section 3.2.2, to generate Ad5 and Ad12 E4orf3 Flp-In T-Rex U2OS-FRT-inducible cell lines we synthesized w.t. Ad5 and Ad12 E4orf3 genes with appropriate restriction sites by PCR (section 2.3.5) and cloned them into the pcDNA5- FRT TO vector containing a 3X FLAG-tag (see section 2.1.5). After transformation of bacteria and mini-preparation of plasmid DNA we performed DNA sequencing and used Chromas and the NCBI BLAST program to validate the sequence integrity of the clones isolated (sections 2.3.2-2.3.4). We used a vector that incorporated a 3X FLAG-tag at the N-terminus of adenovirus E4orf3 to aid the detection of adenovirus E4orf3 as an Ad12 E4orf3 antibody has yet to be generated. Sequencing revealed that we had successfully isolated w.t. Ad5 and Ad12 E4orf3 3XFLAG-pcDNA5-FRT TO clones that possessed a *KpnI* site prior to the ATG and *XhoI* site after the stop codon [Fig. 3.7 A, B, C, and D respectively]. Sequencing also revealed that the Ad5 and Ad12 E4orf3 genes were w.t. and in-frame (data not shown).



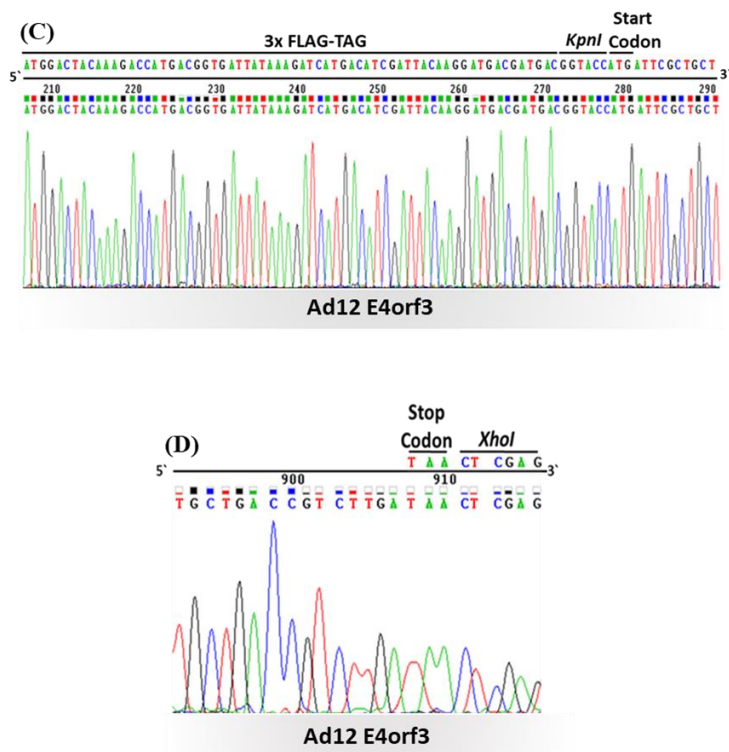


Figure 3.7: Chromatograms demonstrating sequence integrity of Ad5 and Ad12 E4orf3 3XFLAG pcDNA5-FRT TO clones at the 5` and 3` ends. (A) Illustrates the 5` end of the Ad5 sequence showing the KpnI cloning site and the start codon (ATG); (B) Illustrates the 3` end of the Ad5 sequence showing the stop codon (TAA) and the XhoI cloning site. (C) Illustrates the 5` end of the Ad12 sequence showing the KpnI cloning site and the start codon (ATG); (D) Illustrates the 3` end of the Ad12 sequence showing the stop codon (TAA) and the XhoI cloning site.

3.2.3.1. Generation and characterization of Ad5 E4orf3 and Ad12 E4orf3 Flp-In T-Rex U2OS inducible cell lines

Once we had verified the validity of our Ad5 and Ad12 3X FLAG-Ad5/12 E4orf3 pcDNA5-FRT TO clones, we next generated the Ad5 and Ad12 3X FLAG-Ad5/12 E4orf3 TET-inducible clonal U2OS cell lines, as described [see Materials and Methods, section 2.1.5]. To evaluate the expression of E4orf3 in the clonal cell lines, cell lysates were prepared 24h and 48h post-induction after which proteins were quantified, separated on SDS-PAGE and analysed by WB. Our WB analyses with an anti-FLAG mAb determined that both Ad5 and Ad12 E4orf3 cell lines expressed FLAG-tagged versions of these viral proteins in a Dox-dependent manner

in all of the Flp-In T-Rex U2OS-FRT-cell lines investigated [panel i, Fig. 3.8 A and B, respectively], although it was noted that some cell lines (e.g. Ad12 E4orf3 #6) also expressed E4orf3, albeit at lower levels, in the absence of Dox [Fig. 3.8B]. These cell lines were then used to probe the function of Ad5 and Ad12 E4orf3.

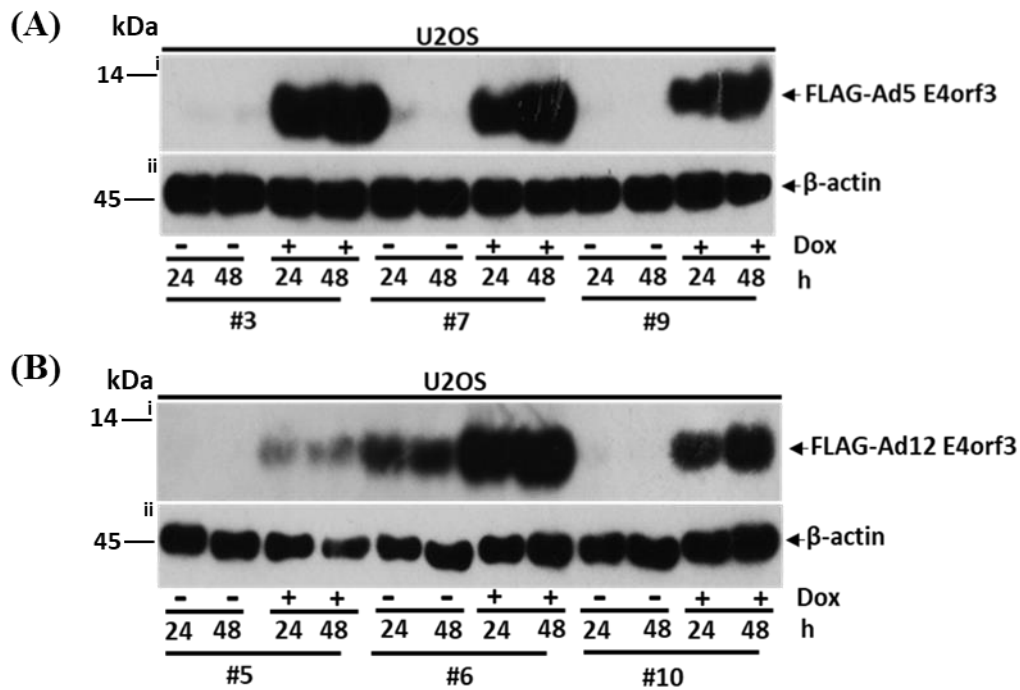


Figure 3.8: Validation of 3X FLAG Ad5 and Ad12 E4orf3 Flp-In T-Rex U2OS cell lines. The expression of FLAG-tagged Ad5 and Ad12 E4orf3 in Flp-In T-Rex U2OS-FRT cell lines was induced with 0.1µg/ml doxycycline. 24h and 48h post-induction cells were harvested and subjected to SDS-PAGE and WB analysis with the appropriate antibodies. # represents clone number. The data shown is representative of 3 independent induction experiments.

3.2.3.2. Characterization of Ad5 and Ad12 E4orf3 cell lines: effects of E4orf3 expression on the levels of cellular E4orf3-regulated proteins

Ad5 E4orf3 has reported to associate with, or regulate numerous cellular proteins including DNA-PKcs, and its regulatory proteins Ku86 and Ku70 (Boyer, et al. 1999), whilst published work from our laboratory and others has indicated that TIF1γ is subject to Ad5/Ad12 E4orf3-dependent SUMOylation and STUb1-dependent degradation (Forrester, et al. 2012; Sohn and Hearing, 2012; Sohn and Hearing, 2016). Other work from our laboratory has suggested that the cellular protein Timeless is degraded in an Ad12 E4orf3-dependent manner but is not

degraded by Ad5 E4orf3 (Patel, PhD thesis 2013, University of Birmingham), whilst work from the O'Shea laboratory has indicated that Ad5 E4orf3 is a negative regulator of p53 transcriptional activity (Soria, et al. 2010). In order to validate the functionality of Ad5 and Ad12 E4orf3 in the clonal FlpIn cell lines we performed WB analyses to examine the effects of both Ad5 and Ad12 E4orf3 expression upon the cellular levels of TIF1 γ , DNA-PK and p53 proteins which are known to be regulated by E4orf3.

Consistent with the data presented in Figure 3.8 the addition of Dox induced the expression of FLAG-tagged Ad5 E4orf3, though the levels of FLAG-tagged Ad5 E4orf3 attained in the #3 cell line were low compared with the levels of FLAG-tagged Ad5 E4orf3 achieved in #7 and #9 [panel vi, Fig. 3.9A]. Our WB data did reveal however that the induction of FLAG-tagged Ad5 E4orf3 in #7 and #9 cell lines resulted in low level post-translational modification of TIF1 γ , which is most likely to be SUMOylation or ubiquitylation [panel i, Fig. 3.9A]. Further WB analyses revealed that FLAG-tagged Ad5 E4orf3 did not affect the expression levels, nor post-translational modification status, of Timeless, p53, Ku86, or Ku70 [panels ii-v, Fig 3.9A], which is consistent with published findings, although it was not previously known whether Ku86 or Ku70 were substrates for Ad5 E4orf3-dependent SUMOylation (Boyer, et al. 1999; Soria, et al. 2010; Patel, PhD thesis 2013, University of Birmingham). The results with FLAG-tagged Ad12 E4orf3 were, however, much more encouraging as more obvious cellular effects were seen when FLAG-tagged Ad12 E4orf3 expression was induced by Dox treatment [Fig. 3.9B]. Our WB analyses revealed that TIF1 γ was post-translationally-modified, presumably by SUMOylation and ubiquitylation, and then degraded upon the induction of FLAG-tagged Ad12 E4orf3 [Panel i, Fig 3.9B]. Consistent with previous observations from the Turnell laboratory (Patel, PhD thesis, University of Birmingham, 2013), our data also demonstrated that Timeless levels were reduced 48h post-induction of FLAG-tagged Ad12 E4orf3 [Panel ii, Fig. 3.9B]. Like the Ad5 E4orf3 studies WB revealed that neither p53, Ku86 nor Ku70 levels, nor PTM

status was affected by either FLAG-tagged Ad12 E4orf3 expression [Panel iii-v Fig. 3.9B]. Taken together, these data suggest that we have generated cell lines that express FLAG-tagged Ad5 and Ad12 E4orf3 proteins in a Dox-dependent manner. These FLAG-tagged E4orf3 proteins retain the known enzymic activity of E4orf3, namely the ability to promote the PTM of TIF1 γ , suggesting that these cell lines can be used for further functional studies.

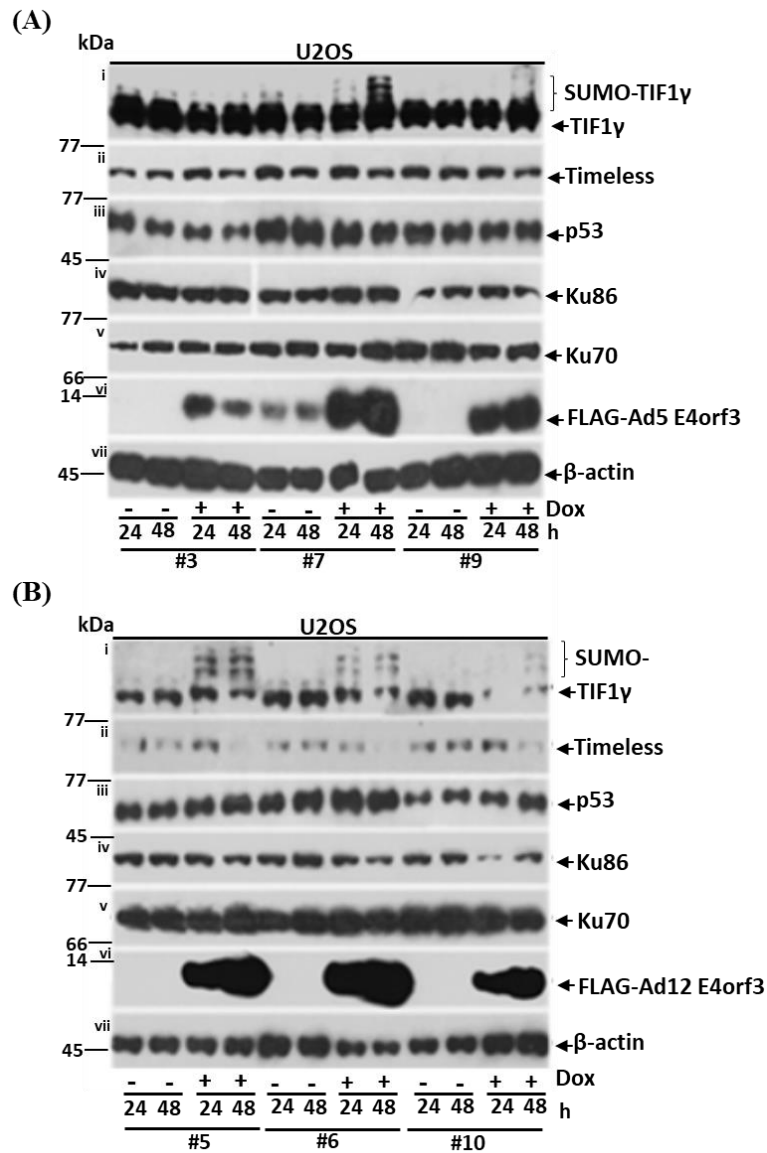


Figure 3.9: Effects of Ad5 and Ad12 E4orf3 expression upon cellular proteins levels and post-translational modification status. The expression of FLAG-tagged Ad5 and Ad12 E4orf3 in Flp-In T-Rex U2OS-FRT cell lines was induced with 0.1 μ g/ml doxycycline. Cells were harvested 24 h and 48 h post-induction and subjected to SDS-PAGE and WB analysis with the appropriate antibodies. The data shown is representative of 3 independent experiments.

3.2.3.3. Characterization of Ad5 and Ad12 E4orf3 cell lines: E4orf3-dependent recruitment of TIF1 γ to PML-containing nuclear tracks

Adenovirus promotes the spatial and dynamic reorganization of cellular structures during infection in order to facilitate viral replication and block antiviral signalling pathways. Adenovirus E4orf3 plays an important role in the reorganization of PML-containing nuclear bodies to track-like structures (Araujo, et al. 2005; Forrester, et al. 2012). Adenovirus E4orf3 also promotes the recruitment of the MRN complex, TIF1 α and TIF1 γ to nuclear tracks during infection to inhibit their antiviral functions through sequestration and then degradation (Araujo, et al. 2005; Forrester, et al. 2012). In order to evaluate further the function of the Ad5 and Ad12 E4orf3 Flp-In cell lines we investigated the ability of FLAG-tagged Ad5 and Ad12 E4orf3 to promote the recruitment of TIF1 γ to nuclear tracks by immunofluorescence [section 2.3.9.]. In non-induced cells TIF1 γ was distributed evenly throughout the nucleus and there was no obvious expression of Ad5 or Ad12 E4orf3 [Fig. 3.10 A and B]. Following induction of E4orf3 expression both Ad5 and Ad12 E4orf3 were seen as distinct nuclear foci and nuclear tracks [Fig. 3.10 A and B]. In agreement with the known functions of E4orf3, TIF1 γ was reorganized to these structures [Fig. 3.10 A and B], indicating that the E4orf3 Flp-In cell lines are a good model to identify novel cellular proteins that are recruited to nuclear tracks.

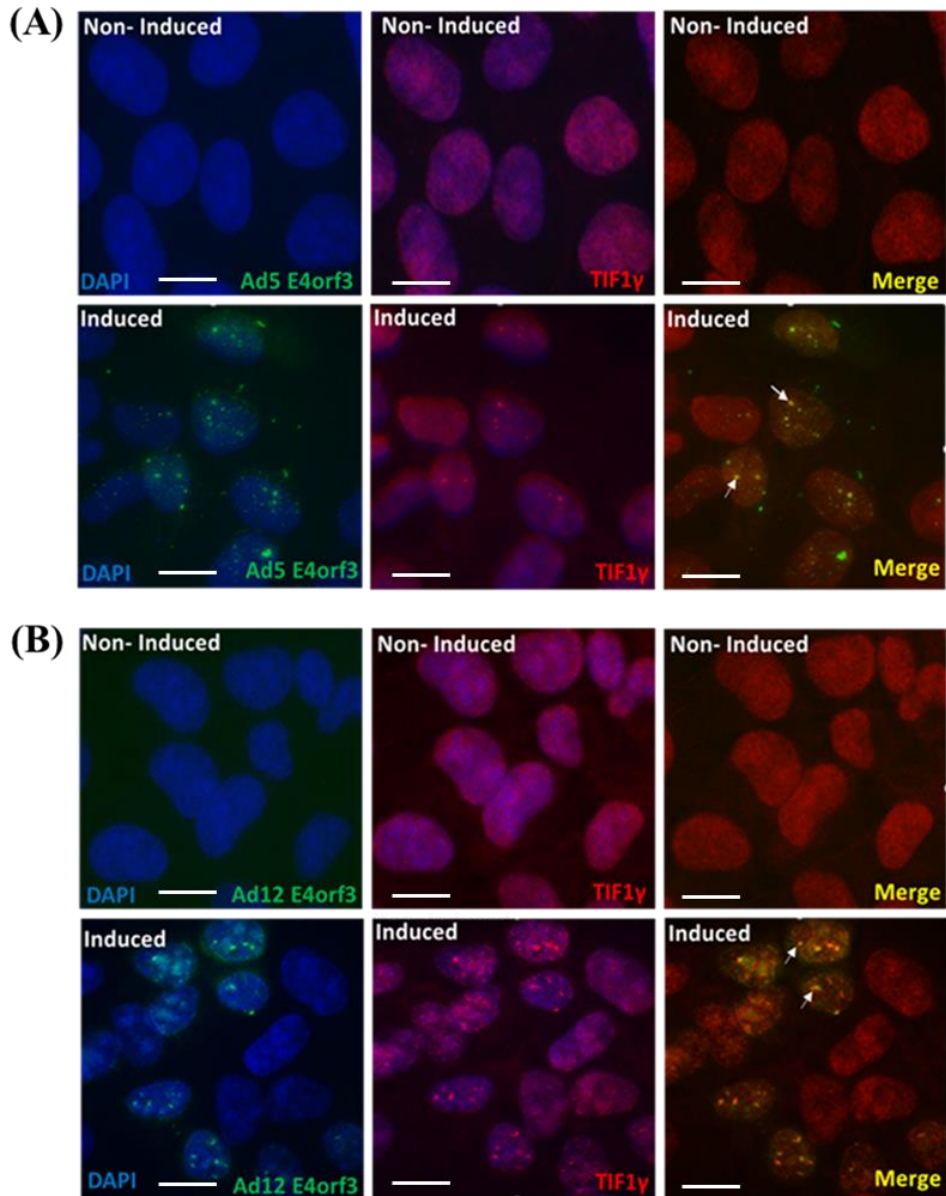


Figure 3.10: Ad5 and Ad12 E4orf3-dependent recruitment of TIF1 γ to nuclear tracks. Cells were fixed in 4% (w/v) paraformaldehyde and permeabilized in ice-cold acetone (Materials and Methods section 2.3.9), 24 h post +/- 0.1 μ g/ml doxycycline treatment. Cells were then incubated with an anti-FLAG mAb antibody (green) to stain Ad5/Ad12 E4orf3, an anti-TIF1 γ pAb (red) and counter-stained with anti-mouse Alexa Fluor 488 and anti-rabbit Alexa Fluor 594 secondary antibodies, respectively. Slides were then mounted in Vectashield containing DAPI (blue). Images were visualised using a Nikon Y-FL epi-fluorescence microscope. The data shown is representative of 3 independent experiments. Scale bar = 20 μ m.

3.2.3.4. Characterization of Ad5 and Ad12 E4orf3 cell lines: E4orf3-dependent recruitment of SUMO-1 and SUMO-2 to PML-containing nuclear tracks

The importance of SUMOylated proteins in the DDR is widely recognised, whereby the SUMO conjugation machinery localizes at DNA damage sites to control the SUMOylation of proteins that participate in DNA damage response and repair (Sarangi and Zhao, 2015). It is now established that Ad5 E4orf3, at least, is a SUMO E3-ligase and promotes the recruitment of MRN complex components to nuclear tracks and their SUMOylation (Sohn and Hearing, 2012; Sohn and Hearing, 2016). In this regard, *in vitro* SUMOylation assays revealed that Ad5 E4orf3 utilised SUMO-2 more readily than SUMO-1 in the conjugation reaction (Sohn and Hearing, 2012). To establish whether the FLAG-Ad5 and Ad12 E4orf3 Flp-In T-Rex cells are a good model to study E4orf3-dependent modulation of SUMOylation, we investigated whether SUMO-1 and/or SUMO-2 were recruited to Ad5 and Ad12 E4orf3-containing nuclear tracks [Fig. 3.11]. Immunofluorescence microscopy revealed that SUMO-1 and SUMO-2 were efficiently reorganized to nuclear tracks with Ad5 E4orf3 [Fig. 3.11A], whilst Ad12 E4orf3 appeared to preferentially re-organise SUMO-1 to nuclear tracks, but not SUMO-2 [Fig. 3.11B]. Taken together, these data indicate that the adenovirus E4orf3 Flp-In cell lines are a good model system to investigate the relationship between E4orf3 and cellular SUMOylation. Moreover, these data establish that Ad12 E4orf3 preferentially utilises SUMO-1, and not SUMO-2 [Fig. 3.11B].

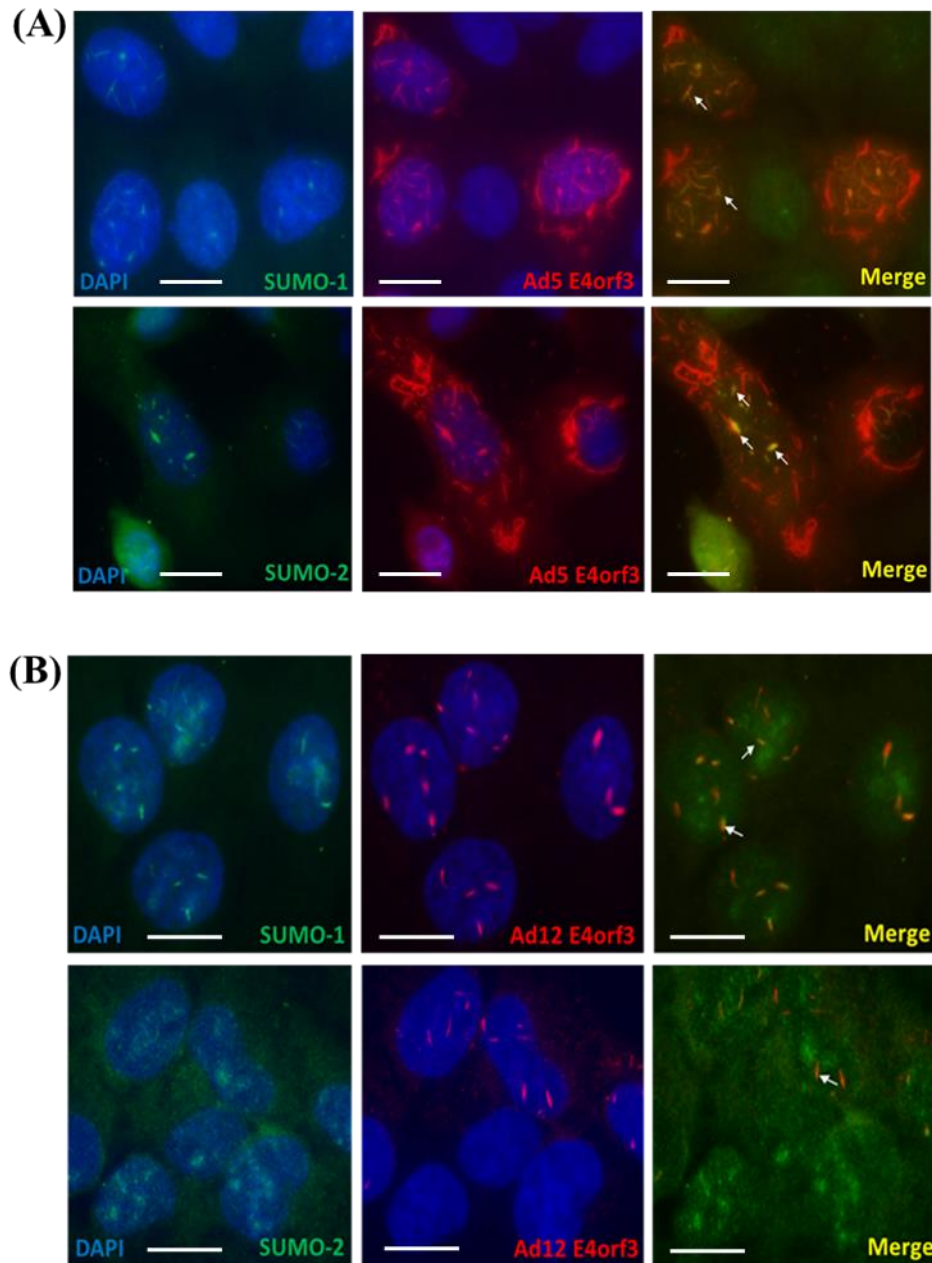
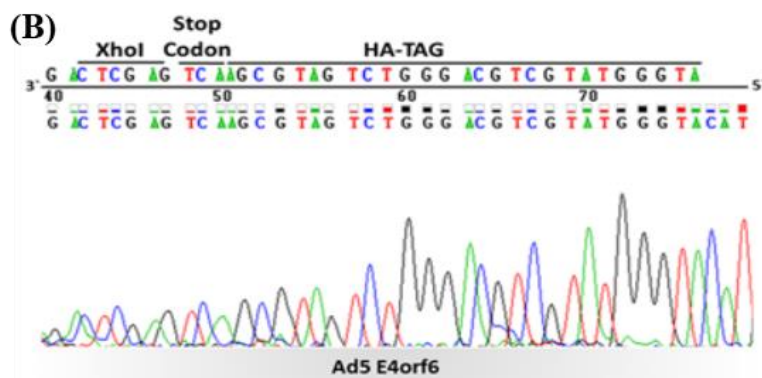
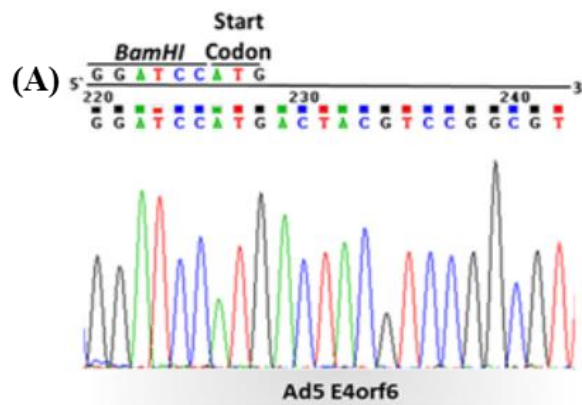


Figure 3.11: Ad5 and Ad12 E4orf3-dependent recruitment of SUMO-1 and SUMO-2 to nuclear tracks. Cells were fixed in 4% (w/v) paraformaldehyde and permeabilized in ice-cold acetone (Materials and Methods section 2.3.9), 24 h post +/- 0.1 μ g/ml doxycycline treatment. Cells were then incubated with anti-SUMO-1/SUMO-2 mAbs (green) and an anti-FLAG pAb antibody (red) to stain Ad5/Ad12 E4orf3, and counter-stained with anti-mouse Alexa Fluor 488 and anti-rabbit Alexa Fluor 594 secondary antibodies, respectively. Slides were then mounted in Vectashield containing DAPI (blue). Images were visualised using a Nikon Y-FL epi-fluorescence microscope. The data shown is representative of 2 independent experiments. Scale bar = 20 μ m.

3.2.3.5. Characterization of Ad5 and Ad12 E4orf3 cell lines: effects of E4orf3 expression on the levels and post-translational modification status of cellular proteins

Given the known ability of adenovirus E4orf3 to promote the SUMOylation of MRN components (Sohn and Hearing, 2012), and the degradation TIF1 γ (Forrester, et al. 2012) we decided to investigate by WB analyses whether adenovirus E4orf3 induced the SUMOylation and/or degradation of cellular proteins known to be targeted by adenovirus during infection as we did for E1B-55K [see section 3.2.2.5]. Our WB results revealed that, despite good expression of the FLAG-tagged Ad5 and Ad12 E4orf3 proteins [panel ix, Fig. 3.12], none of the cellular proteins investigated were altered in either their expression level, or their post-translational modification status [Fig. 3.12]. As such, the pRB tumor suppressor and its family members, p107 and p130 were not affected by E4orf3 expression [panels vi-viii, Fig. 3.12]. Similarly, no change was observed in the expression level, or the post-translational modification status of LAR-PTPRF, MSH6, MSH2, TOP2B or Epha2 in response to either Ad5 or Ad12 E4orf3 expression [panels i-v, Fig. 3.12]. Despite these findings it is likely given the effects of E4orf3 expression on TIF1 γ levels and PTM status [Fig. 3.9], that these cell lines would be useful to identify new targets for both Ad5 and Ad12 E4orf3.

pcDNA5- FRT TO vector (see section 2.1.5). After transformation of bacteria and mini-preparation of plasmid DNA we performed DNA sequencing and used Chromas and the NCBI BLAST program to validate the sequence integrity of the clones isolated (sections 2.3.2- 2.3.4). Sequencing revealed that we had successfully isolated w.t. Ad5 and Ad12 E4orf6 pcDNA5-FRT TO clones that possessed a BamHI site prior to the ATG and XhoI site after the HA-Tag and TGA stop codon [Fig.3.13 A, B, C, and D respectively]. Sequencing also revealed that the entire genes were w.t. and in-frame (data not shown).



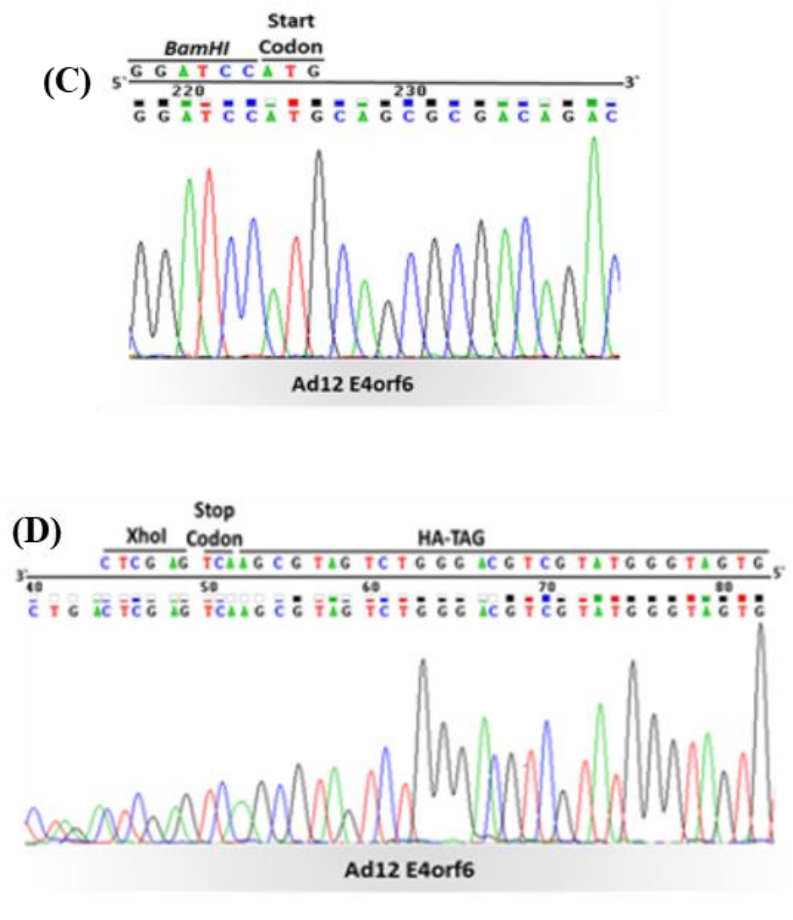


Figure 3.13: Chromatograms demonstrating sequence integrity of Ad5 and Ad12 E4orf6 pcDNA5-FRT TO clones at 5' and 3' ends. (A) Illustrates the 5' end of the Ad5 sequence showing the BamHI cloning site and the start codon (ATG); (B) Illustrates the 3' end of the Ad5 sequence showing the incorporation of the HA-tag, the TGA stop codon and the XhoI cloning site. (C) Illustrates the 5' end of the Ad12 sequence showing the BamHI cloning site and the start codon (ATG); (D) Illustrates the 3' end of the Ad12 sequence showing the the incorporation of the HA-tag, the TGA stop codon and the XhoI cloning site.

3.2.4.1. Generation and characterization of Ad5 E4orf6 and Ad12 E4orf6 Flp-In T-Rex U2OS inducible cell lines

Once we had verified the validity of our Ad5 and Ad12 HA-tagged Ad5/12 E4orf6 pcDNA5-FRT TO clones, we next generated the Ad5 and Ad12 HA-tagged-Ad5/12 E4orf6 TET-inducible clonal U2OS cell lines, as described [see Materials and Methods, section 2.1.5] and tested their expression following doxycycline treatment by WB. Our WB data indicated that we had isolated Flp-In T-Rex U2OS cell lines that expressed both Ad5 and Ad12 HA-tagged

E4orf6 [panel iii, Fig. 3.14 A and B], although the protein levels of E4orf6 were highly variable and some cells did not express any detectable HA-tagged E4orf6 [panel iii, Fig. 3.14 A and B]. Consistent with previous work from our laboratory (Blackford, et al. 2010) Ad12 E4orf6 promoted the degradation of TopBP1, whilst Ad5 E4orf6 did not [panel i, Fig. 3.14 A and B]. Reassuringly, those cell lines that did not express detectable levels of HA-tagged Ad12 E4orf6 did not promote the degradation of TopBP1 [panel iii, Fig. 3.14 B]. The expression of either Ad5 or Ad12 HA-tagged E4orf6 had a modest effect upon the levels of p53 [panel ii, Fig. 3.14], though p53 did appear to be stabilized in some of the cell lines studied [e.g. Ad5 clones 2, 4, 6, 7 and 12- panel ii, Fig. 3.14A; Ad12 clones 2, 5, 7, 11 and 12- panel ii, Fig. 3.14B]. Taken together, these data indicated that we had successfully isolated both Ad5 and Ad12 E4orf6 Flp-In T-Rex U2OS cell lines that expressed HA-tagged E4orf6 in a Dox-dependent manner.

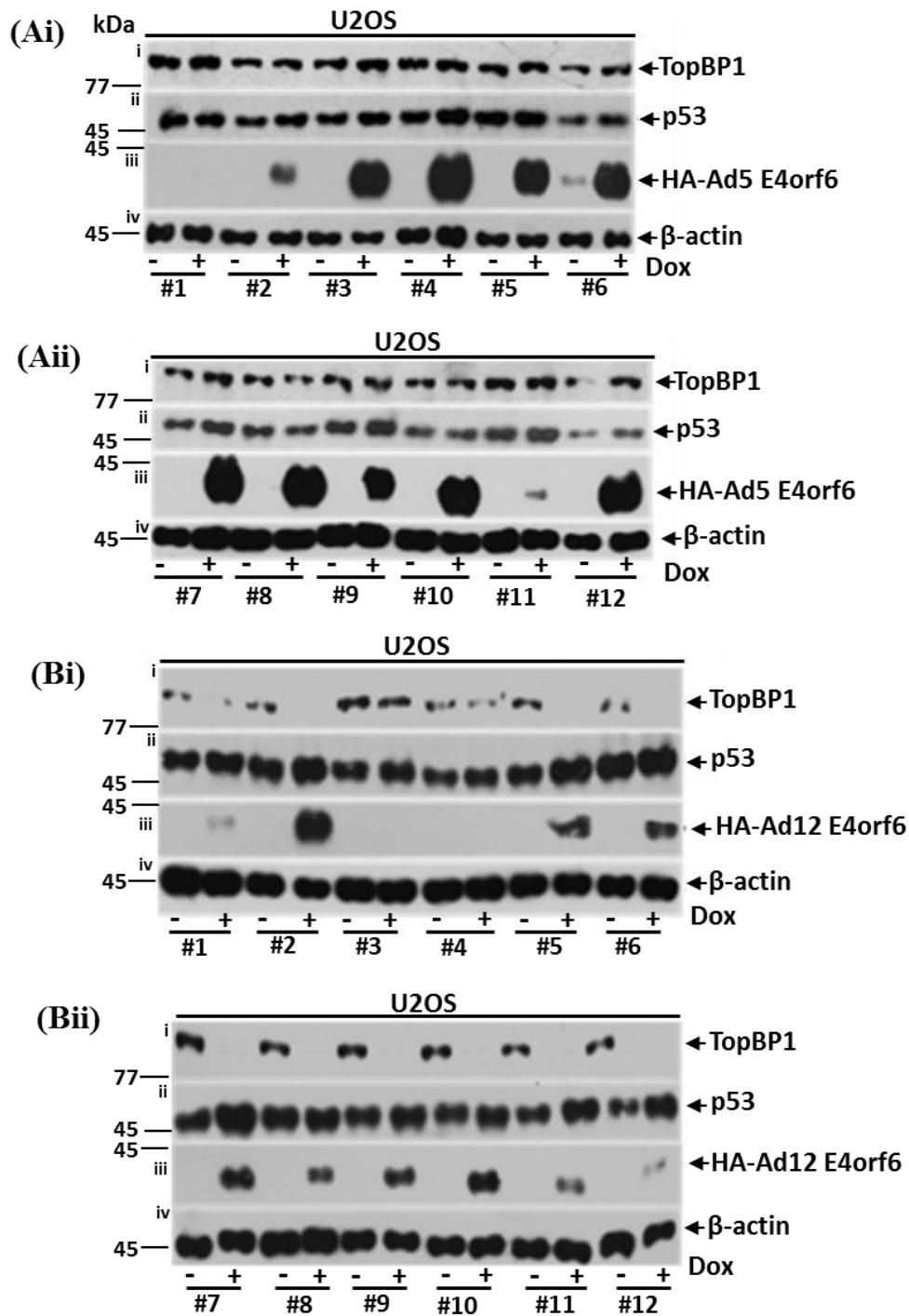


Figure 3.14: Validation of Ad5 and Ad12 E4orf6 Flp-In T-Rex U2OS cell lines. The expression of HA-tagged Ad5 and Ad12 E4orf6 in Flp-In T-Rex U2OS cell lines was induced with 0.1µg/ml doxycycline. 24h post-induction cells were harvested and subjected to SDS-PAGE and WB analysis with the appropriate antibodies. # represents clone number. The data shown is representative of 2 independent induction experiments.

3.2.4.2. Characterization of Ad5 and Ad12 E4orf6 cell lines: cellular localization of E4orf6

E4orf6 is a multifunctional protein that promotes viral DNA replication, particularly, the control of nuclear export of late viral mRNAs to the cytoplasm and the repression of cellular mRNA export from the nucleus (Halbert, et al. 1985; Bridge and Ketner, 1990). As such it not only regulates viral mRNA export, but it has been reported that E4orf6 also shuttles between the nucleus and cytoplasm in order to target E1B-55K to the nucleus (Goodrum, et al. 1996). In order to determine the cellular localization of HA-tagged E4orf6 we performed indirect immunofluorescence [Fig. 3.15 A and B]. Microscopy revealed that both Ad5 and Ad12 E4orf6 were predominantly nuclear where they formed many punctate foci, suggesting that they localized to specific sites, or structures in the nucleus [Fig. 3.15 A and B]. These data indicate the utility of these cell lines to study E4orf6 function by immunofluorescent microscopy.

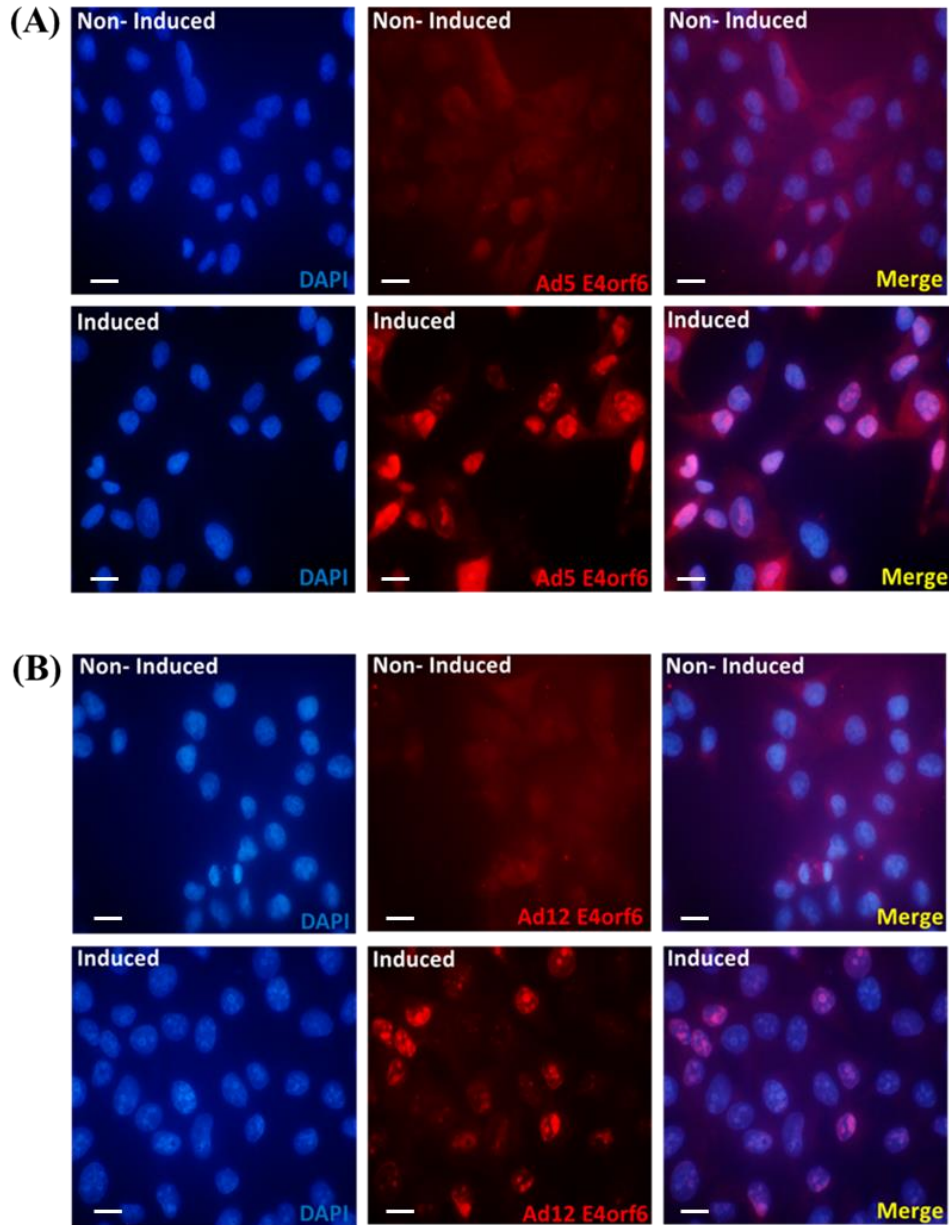


Figure 3.15: Ad5 and Ad12 E4orf6 localize to intranuclear foci in Flp-In T-Rex U2OS cell lines. Cells were fixed in 4% (w/v) paraformaldehyde and permeabilized in ice-cold acetone (Materials and Methods section 2.3.9), 24 h post +/- 0.1 μ g/ml doxycycline treatment. Cells were then incubated with an anti-HA pAb (red) and counter-stained with an anti-rabbit Alexa Fluor 594 secondary antibody. Slides were then mounted in Vectashield containing DAPI (blue). Images were visualised using a Nikon Y-FL epi-fluorescence microscope. The data shown is representative of 2 independent experiments. Scale bar = 20 μ m.

3.2.4.3. Characterization of Ad5 and Ad12 E4orf6 cell lines: E4orf6 association with p53

It is well known that the p53 tumour suppressor is stabilized following E1A expression (Lowe and Ruley, 1993), which left unchecked would be a major obstacle for adenovirus replication. However, E1B-55K and E4orf6 cooperate during infection to promote the degradation, and hence inactivation of p53 (Querido, et al. 1997). It has been shown that both E1B-55K (Sarnow, et al. 1982) and E4orf6 interact with p53 independently (Dobner, et al. 1996) to inhibit p53-mediated transcriptional activation. To determine whether HA-tagged Ad5 and Ad12 E4orf6 associate with p53 in the Ad5 and Ad12 E4orf6 in the Flp-In T-Rex U2OS cells we immunoprecipitated HA-tagged E4orf6 with an anti-HA pAb and performed WB analysis for both E4orf6 (HA) and p53 [sections 2.2.4 and 2.2.5]. WB results revealed that the immunoprecipitation was successful and that HA-tagged E4orf6 was immunoprecipitated from both Ad5 and Ad12 E4orf6 Flp-In T-Rex U2OS cells [panel Ai and Bi, Fig. 3.16], although the Ad5 E4orf6 cell line used did express some HA-tagged E4orf6 in the absence of doxycycline treatment [panel Ai, Fig. 3.16]. WB analyses of p53 revealed that both immunoprecipitation of both Ad5 and Ad12 E4orf6 resulted in the co-precipitation of p53 [panel Aii and Bii, Fig. 3.16], although it appeared that Ad12 E4orf6 associated more avidly with p53 than Ad5 E4orf6 [panel Aii and Bii, Fig. 3.16]. The small amount of co-precipitated p53 in the Ad5 E4orf6 cell line presumably reflects the leaky expression of HA-tagged Ad5 E4orf6 in these cells [panel Ai, Fig. 3.16]. These results indicate that HA-tagged E4orf6 associates with p53 in both Ad5 and Ad12 E4orf6 cell-lines, indicating that the HA-tagged E4orf6 species have retained their ability to interact with a known binding partner and could be used to study E4orf6 interactions with the host cell in more detail.

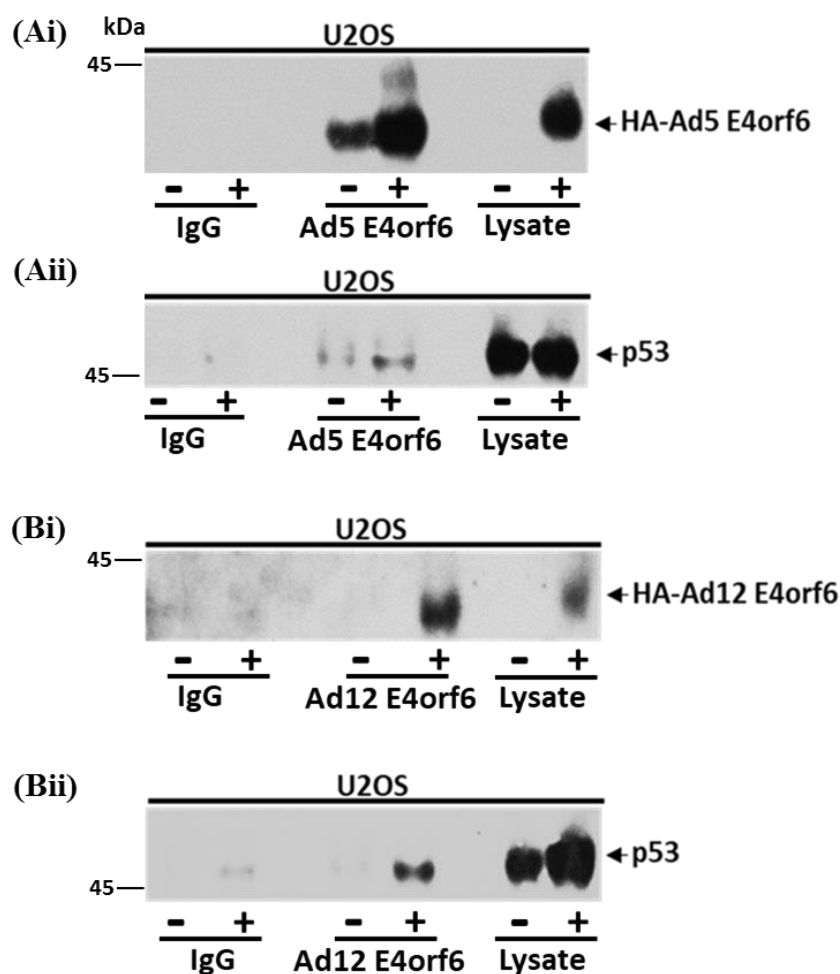


Figure 3.16: HA-tagged Ad5 and Ad12 E4orf6 associate with p53 in Flp-In T-Rex U2OS cell lines. HA-tagged Ad5 and Ad12 E4orf6 were immunoprecipitated with an anti-HA pAb from U2OS cell lysate, which had been collected 24 h post-treatment +/- 0.1µg/ml doxycycline (A, Ad5 E4orf6; B, Ad12 E4orf6). Immunocomplexes were isolated on protein-G Sepharose, subjected to SDS-PAGE, and p53 and adenovirus E4orf6 detected by WB analysis using the appropriate antibodies. The data shown is representative of 3 independent experiments.

3.2.3.4. Characterization of Ad5 and Ad12 E4orf6 cell lines: effects of E4orf6 expression on the levels of cellular proteins

Genome integrity is important for cell survival and as such, cells utilize different pathways to detect and fix DNA damage (Jackson and Bartek, 2009). As viral infection activates the host cell DDR pathway cellular proteins that participate in these pathways also inhibit viral replication (Chaurushiya and Weitzman, 2009). Previous work from our laboratory has

established that Ad12 E4orf6 inhibits the ATR pathway through its ability to target the ATR activator, TopBP1 for degradation (Blackford, et al. 2010). We therefore investigated whether adenovirus E4orf6 could target RAD51, which is involved in homologous recombination repair, and Ku86, which is involved in NHEJ repair for degradation. We also investigated whether PTPRF/LAR or Epha2, which are known to be targeted for degradation during Ad5 infection (Fu, et al. 2017) are targeted for degradation by E4orf6. In agreement with previous studies and those reported earlier (Blackford, et al. 2010), WB analyses revealed that TopBP1 was targeted for degradation by Ad12 E4orf6 but not Ad5 E4orf6 [panel i, Fig. 3.17 A and B]. The levels of RAD51, PTPRF/LAR and Ku86 were highly variable but there was no obvious positive correlation between adenovirus E4orf6 expression and the levels of these proteins [panels ii, iii, and v Fig. 3.17 A and B]. Epha2 was consistently reduced in levels following Ad5 E4orf6 expression, but not Ad12 E4orf6 expression [panel, iv Fig. 3.17 A and B]. Perhaps the most interesting finding from this study was that Ad5 E4orf6 itself appeared to be post-translationally modified as noted by the observed higher molecular weight smear on the WB for Ad5 E4orf6 [panel vi, Fig. 3.17 A]. Ad12 E4orf6 appeared however, to be only modestly post-translationally modified [panel vi, Fig. 3.17 B]. These data suggest that Ad5 E4 orf6 is post-translationally modified and that these cell lines can be used to investigate adenovirus E4orf6 function.

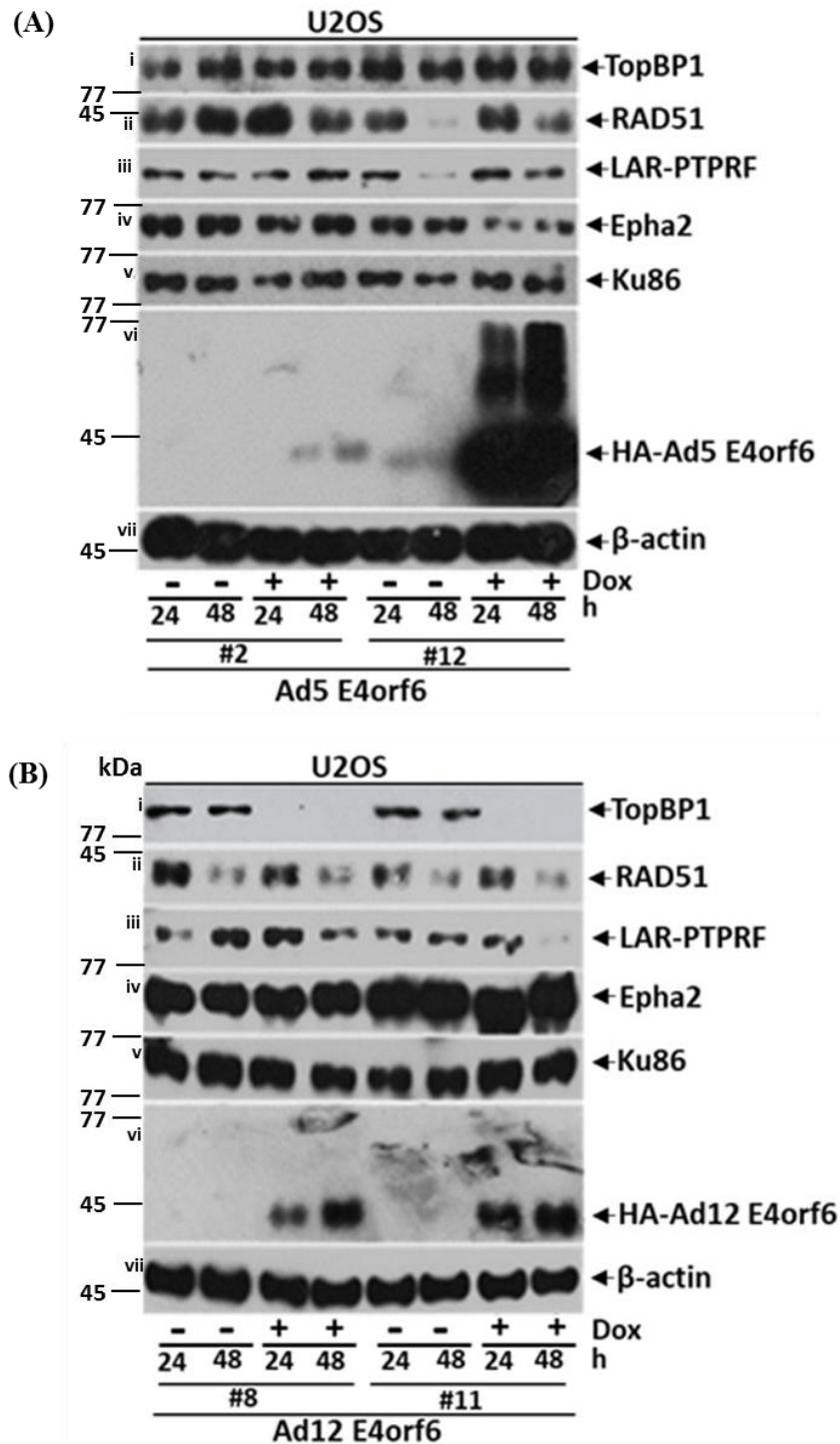


Figure 3.17: Effects of Ad5 and Ad12 E4orf6 expression upon cellular proteins levels and post-translational modification status. The expression of HA-tagged Ad5 and Ad12 E4orf6 in Flp-In T-Rex U2OS-FRT cell lines was induced with 0.1 μ g/ml Dox. 24 h and 48 h post-induction cells were harvested and subjected to SDS-PAGE and WB analysis with the appropriate antibodies. The data shown is representative of 2 independent experiments.

3.3. Discussion

3.3.1. Background

It is well established that adenovirus early region proteins E1B-55K, E4orf3 and E4orf6 cooperate during infection to promote viral replication (Weitzman, 2005). It is also appreciated that they cooperate in the transformation of primary cells (Nevels, et al. 2001). Studies with deletion viruses that fail to express one or more of these proteins has highlighted the important cooperative relationship between these proteins (Forrester, et al. 2012). Other studies however, have determined that these proteins can also function, independently both during infection (Pennella, et al. 2010; Blackford, et al. 2010) and transformation (Nevels, et al. 2001), see Introduction, sections 1.2 and 1.4). Moreover, these studies have indicated that there are subtle differences in the functions of Ad5 and Ad12 proteins. These differences have yet to be studied in detail, however. The principle aim of the study presented in this chapter was to generate cell line models that could be used to study the function of Ad5 and Ad12 E1B-55K, E4orf3 and E4orf6 in isolation, in the absence of viral infection and the presence of other viral proteins. It was hoped that these cell models would help identify new functions of these proteins and highlight similarities and differences between the two widely studied virus types, Ad5 and Ad12.

3.3.2. Generation and characterization of Ad5 and Ad12 E1B-55K Flp -In T-Rex U2OS- Inducible cell lines.

Results presented in this chapter indicate that we were able to isolate successfully, clonal cell U2OS cell lines that expressed both Ad5 and Ad12 E1B-55K in a Dox-dependent manner [Fig. 3.2 A and B]. It was noted however that there were obvious variations the levels of Ad5 and Ad12 proteins expressed following Dox treatment [Fig. 3.2 A and B]. It is not clear why this is the case. It has been suggested that these cells have one integration site, though it is possible that they possess more than one integration site, which might explain the variance in expression. Consistent with previous studies we observed that low levels of higher molecular weight forms of Ad5 E1B-55K were observed by WB [Panel ii, Fig. 3.2 Ai-Aii], which are

presumed to be SUMOylated E1B-55K (Endter, et al. 2001). The target residue for SUMOylation within Ad5 E1B-55K is K104 which lies within a ψ KxE consensus motif which is important for Ad5 E1B-55K mediated transformation (Endter, et al. 2001). It has been reported that Ad12 E1B-55K has a KxE, but however lacks the aliphatic amino acid residue, ψ , which is required for SUMO-1 conjugation (Rodriguez, et al. 2001). It has been proposed that Ad5 E1B-55K SUMOylation promotes the nuclear retention of Ad5 E1B-55K, such that mutation of the K acceptor, K104, to arginine results in the accumulation of E1B-55K in cytoplasmic aggregates (Kindsmuller, et al, 2007). Consistent with other studies, we also confirmed that Ad5 and Ad12 E1B-55K expression elicited the marked stabilization of p53 levels in most cases [Fig. 3.2]. The explanation for high protein abundance of p53 in adenovirus E1B-55K expressing cells is two-fold- the direct association between E1B-55K and p53 masks the Mdm2-binding site on p53, and adenovirus E1B-55K inhibits p53 transcription of the Mdm2 gene (Li, et al. 2011). This accumulation of p53 is not normally evident in w.t. adenovirus-infected cells, due to the concerted action of E1B-55K and E4orf6 in the degradation of p53 (Querido, et al. 2001).

Ad5 E1B-55K has also been established to function as a SUMO-ligase and promote the mono-SUMOylation of p53, its association with PML nuclear bodies and its export to the cytoplasm (Muller and Dobner, 2008; Pennella, et al. 2010). In this regard, we determined that induction of Ad5 E1B-55K, but not Ad12 E1B-55K, expression, induced the PTM of p53. Interestingly, p53 is the only known protein to be SUMOylated by Ad5 E1B-55K. It would be valuable to perform proteome-wide MS-based screens to identify other cellular proteins targeted for Ad5 E1B-55K-dependent SUMOylation. Ron Hay's group have described an antibody method to isolate SUMOylated proteins from cells that express a mutant SUMO protein that possesses a K residue before the C-terminal diG motif that conjugates to acceptor K residues on substrates (Tammsalu, et al. 2015). Upon digestion with the Lys-C proteinase a diG-K specific antibody

can be used to isolate SUMOylated proteins that can be subjected to MS identification. Adrian Whitehouse's group have developed FLAG-tagged and GFP-tagged affimers that recognize SUMO-1 and SUMO-2, specifically and could similarly be used to purify SUMOylated proteins from cell lysates for MS identification (Hughes, et al. 2017). The identification of other cellular proteins SUMOylated by E1B-55K would further our understanding of this protein and its relationship to the host cell. Interestingly, studies presented here suggested that pRB was stabilized following adenovirus E1B-55K expression, although the antibody used could not detect any obvious PTM [Fig. 3.6]. pRB, as well as p53, has been shown to be SUMOylated by a Kaposi's sarcoma -associated herpesvirus (KSHV) SUMO E3 ligase (KbZIP; Chang, et al. 2010). Given this finding it will be important to establish whether E1B-55K can SUMOylate pRB.

Our studies with the Ad5 and Ad12 E1B-55K Flp-In cells also determined that both proteins retained the capacity to interact with p53, *in vivo* [Fig. 3.3]. As such, these cell lines could be used to study the interactomes of Ad5 and Ad12 E1B-55K by IP coupled to MS. Although our laboratory has performed such studies [Forrester, PhD thesis, University of Birmingham, 2012], this was a long time ago, and the capability of the current generation of mass spectrometers are far more sensitive than previous models. We also used immunofluorescence to determine that Ad5 E1B-55K is recruited to cytoplasmic, aggresomal structures upon induction of Ad5 E1B-55K expression [Fig. 3.4]. This sequestration of p53 is known to inhibit the nuclear transcription functions of p53. Our immunofluorescence studies also revealed that Ad12 E1B-55K was mostly retained in the nucleus but also formed elongated, filamentous structure that were located at variable distances from the nucleus. This distribution of Ad12 E1B-55K has been observed previously (Gallimore, et al. 1997). Interestingly, E1B-55K from the highly oncogenic Ad12 does not translocate p53 to the aggresome [Fig. 3.5 A and B]. This is most likely due to the absence of a nuclear export signal (NES) in Ad12 E1B-55K that is

present in Ad5 E1B-55K (Liao, et al. 1999; Krätzer, et al. 2000). How and why Ad12 E1B-55K is transported into the cytoplasm is not currently known. It will be important in the future to establish, which residues are important for nuclear export and whether cellular proteins associate with Ad12 E1B-55K in the cytoplasmic filaments. In this regard, it would be interesting to see if we could purify cytoplasmic E1B-55K containing filaments and then subject them to MS characterization.

Significantly, our laboratory has already used the Ad5 and Ad12 E1B-55K cells generated here to investigate the relationship between adenovirus E1B-55K and SMARCAL1 (Nazeer, et al. 2019). These cell lines were used, specifically, to establish that both Ad5 and Ad12 E1B-55K promoted cellular DNA replication stalling and the inhibition of cellular DNA replication in order to promote viral DNA replication. We are therefore hopeful that these cells can be used in the future to perform the experiments outlined above.

3.3.3. Generation and characterization of Ad5 and Ad12 E4orf3 Flp -In T-Rex U2OS-Inducible cell lines.

During the course of this study we were also able to generate both Ad5 and Ad12 E4orf3 Flp-In T-Rex U2OS cell lines that expressed FLAG-tagged Ad5 and Ad12 E4orf3 following treatment with Dox [Fig. 3.8]. As Ad5 E4orf3 has been found to function as an E3 SUMO ligase that stimulates the SUMOylation of the Mre11 and Nbs1 DDR proteins, the TFII-I transcription factor and the TIF1 γ transcriptional repressor (Sohn and Hearing, 2016), we investigated whether Ad5 and Ad12 E4orf3 possessed the ability to induce the SUMOylation of TIF1 γ in the Ad5 and Ad12 E4orf3 Flp -In T-Rex U2OS cell lines. Interestingly, all Ad12 E4orf3 clones isolated possessed the ability to post-translationally modify TIF1 γ and promote its degradation [Fig. 3.9B]. We presume that this reflects the known ability of Ad5 E4orf3 to induce the SUMOylation of TIF1 γ and the subsequent recruitment of a STUbL to promote the ubiquitin-dependent degradation of TIF1 γ (Sohn and Hearing, 2016). Relative to Ad12 E4orf6,

Ad5 E4orf3 was not as efficient at promoting TIF1 γ SUMOylation and degradation. The reasons for these differences are not immediately apparent but might reflect inherent differences in the catalytic activities of the two proteins. Consistent with previous studies, these studies suggested that Timeless was also degraded by Ad12 E4orf3, though a role for PTM of Timeless in this process was not identified [Fig. 3.9B; Patel, PhD thesis, University of Birmingham 2013]. As for E1B-55K (section 3.3.2.) it would be valuable to use the proteome-wide screens discussed previously to identify those cellular proteins targeted for SUMOylation by Ad5 and Ad12 E4orf3. Given that adenovirus E4orf3 expression often results in the degradation of cellular proteins it would also be valuable to use these cell lines to perform SILAC (Stable Isotope Labeling by/with Amino acids in Cell culture) type experiments to identify those proteins targeted for degradation by E4orf3.

Our studies also established that both Ad5 and Ad12 E4orf3 formed nuclear tracks in E4orf3 Flp -In T-Rex U2OS cell lines in a Dox-dependent manner, and were able to recruit TIF1 γ to these structures [Fig 3.10]. It has been established previously that SUMOylation is not required for recruitment to these structures, but that SUMOylation occurs at nuclear tracks (Sohn and Hearing, 2019). Indeed, another TRIM family TIF1 α (TRIM24), has been reported to be relocalized to nuclear tracks by E4orf3 but is not SUMOylated (Sohn and Hearing, 2016). Consistent with the studies of Patrick Hearing's laboratory our study established that Ad5 E4orf3 localized with SUMO-1 and SUMO-2 at nuclear tracks [Fig 3.11A]. Interestingly however, Ad12 E4orf3 only localized with SUMO-1 at nuclear tracks, and not SUMO-2, suggesting that Ad12 E4orf3 is a SUMO-1-specific E3 ligase [Fig 3.11B]. This is not unprecedented, as Ad5 E1B-55K also functions as SUMO-1-specific E3 ligase (Pennella, et al. 2010). It would therefore be interesting to perform *in vitro* E3 SUMO-ligase reactions with Ad12 E4orf3, SUMO-1 and SUMO-2 and substrates such as TIF1 γ to establish whether this is the case.

Another known function of the Ad5 E4orf3 protein is the epigenetic silencing of p53 transcriptional activity, such that Ad5 E4orf3 expression results in histone H3 K9 trimethylation at p53-responsive promoters (Soria, et al. 2010). It would be interesting to see if Ad12 E4orf3 utilizes a similar mechanism to inhibit p53 function. Taken together, our initial studies with Ad5 and Ad12 E4orf3 have established that adenovirusE4orf3 is functional in the FlpIn cell lines generated and can be used to investigate AdE4orf3 function in more detail. Our studies have also highlighted important functional differences between Ad5 and Ad12 E4orf3 proteins that can be explored in more detail in future studies.

3.3.4. Generation and characterization of Ad5 and Ad12 E4orf6 Flp -In T-Rex U2OS-Inducible cell lines.

Work presented in this chapter indicates that we successfully generated clonal FlpIn U2OS cell lines that expressed E4orf6 in a Dox-dependent manner [Fig 3.14]. Consistent with previous studies we were able to demonstrate that Ad12 E4orf6, but not Ad5 E4orf6, promoted the degradation of TopBP1 [Fig 3.14; Blackford, et al. 2010], indicating that Ad12 HA-tagged E4orf6, is functional in this system. WB analyses indicated that Ad5E4orf6, but not Ad12 E4orf6 had undergone PTM [Fig 3.17]. PTM of Ad5 E4orf6 has not been described during infection or transfection, possibly because the levels of Ad5 E4orf6 during infection, or transfection were not as high as those observed in our inducible system. Despite this, this observation might be important in explaining Ad5 E4orf6 function and will be considered in the next chapter.

Co-IP studies confirmed that Ad5 E4orf6 interacted with p53, albeit weakly, whilst Ad12 E4orf6 associated with p53 more avidly [Fig 3.16]. This is an important finding as it has not been recognised previously that Ad12 E4orf6 interacts with p53 and suggests that Ad12 E4orf6 similarly inhibits p53 transcriptional activity. Ad5 E4orf6 has been shown to bind to p53 within its C-terminal regulatory domain and disrupt the interaction between TAFII31, a component of

transcription factor IID (TFIID) and the N-terminal activation domain of p53, which consequently blocks p53-mediated transcriptional activation (Dobner, et al. 1996). Early studies from Phillip Branton's laboratory established that Ad5 E4orf6 interacted with cellular CRL5, whilst work from our laboratory determined that Ad12 E4orf6 interacted with CRL2 (Querido, et al. 2001; Blackford, et al. 2010). The role of adenovirus E4orf6 in targeting cellular proteins for degradation by the UPS will be considered in more detail in the following chapter. Given that we have identified that Ad5 and Ad12 E4orf6 associate with p53 in the FlpIn U2OS cell lines, it would be interesting to perform IP-MS studies to identify other cellular proteins that associate with Ad5 and/or Ad12 E4orf6, *in vivo*. Such studies would be important towards a better understanding of how adenovirus E4orf6 proteins function in isolation in the cell. Immunofluorescence studies presented here demonstrated that both Ad5 and Ad12 E4orf6 were nuclear in their distribution, where they were visible as punctate foci [Fig. 3.15]. It will be important, in the future to establish whether these foci represent discrete intranuclear structures such as nucleoli, PML bodies, Cajal bodies etc, as this might give important insight into E4orf6 function.

Taken together, the work presented in this chapter has been important towards establishing a resource that we can study the function of Ad5 and Ad12 E1B-55K, E4orf3 and E4orf6 in isolation. Data presented in this chapter has highlighted important differences between Ad5 and Ad12 proteins and given some new insights into the potential function of these proteins. The following chapter will consider the role of the Ad5 and Ad12 E4orf6 proteins in more detail.

CHAPTER 4



Investigating the molecular functions of the Ad5 and Ad12 E4orf6 proteins

4.1. Introduction

According to a large number of studies the adenovirus E4orf6 protein is a highly versatile protein that can work in isolation, or cooperation with E1B-55K and/or E4orf3 to perform multiple cellular functions in order to maximise adenovirus replication (Täuber and Dobner, 2001). Adenovirus E4orf6 regulates host cell shut-off, in cooperation with E1B-55K, principally by regulating the selective transport of viral mRNAs from the nucleus to the cytoplasm as well as targeting for degradation a number of cellular proteins that possess anti-viral activities (Dobbelstein, et al. 1997). Indeed, our laboratory recently identified SMARCAL1 as a cellular substrate for CRLs targeted by adenovirus E1B-55K/E4orf6 during infection (Nazeer, et al. 2019). As such, Ad5 E4orf6 interacts specifically with Cullin 5-containing ubiquitin ligase complexes, whereas Ad12 E4orf6 interacts specifically with Cullin 2-containing ubiquitin ligase complexes to promote the ubiquitin-dependent and proteasome-mediated degradation of cellular targets (Cheng, et al. 2013).

It is generally accepted that E1B-55K functions as a substrate receptor and E4orf6 serves to recruit the CRL in this process. However, there are exceptions to this rule. For instance, Ad5 E1B-55K can promote the degradation of Daxx independently of E4orf6 (Schreiner, et al. 2010), whereas, Ad12 E4orf6, but not Ad5 E4orf6, can function independently to suppress the ATR signalling pathway by targeting its activator, TopBP1, for proteasomal degradation (Blackford, et al. 2010). These studies illustrate that adenovirus types have evolved differently, such that although homologous proteins from different types retain many of the same functions, functional differences do exist between homologous proteins, particularly for the E1B-55K and E4orf6 proteins (Forrester, et al. 2012; Blanchette, et al. 2013). As we have made Flp-In T-REx -inducible U2OS cell lines for Ad5 and Ad12 E1B-55K, E4orf3 and E4orf6 (Chapter 3), it was our intention to investigate functional differences between homologous Ad5 and Ad12 proteins. As we have previously studied differences in the functional ability of Ad5 and Ad12 E4orf6 to promote the degradation of TopBP1 for proteasomal degradation, we decided to

prioritise our studies with adenovirus E4orf6 to see if we could find other functional differences between these two proteins. These studies are presented in this Chapter.

4.2. Results

4.2.1. Post-translational modification of the Ad5 E4orf6 protein

It has long been known that adenovirus early region proteins E1A and E1B-55K exist as phosphorylated species (Tremblay, et al. 1988; Blackford and Grand, 2009), whilst more recent studies have indicated that Ad5, but not Ad12, E1B-55K functions as a SUMO E3-ligase for p53 and can also PTM, namely autoSUMOylation, or E1B-dependent SUMOylation (see Introduction, section 1.2.2; Endter, et al. 2001; Blackford and Grand, 2009). Although E4orf6 cooperates with both E1B-55K and E4orf3, it is not known whether E4orf6 possesses distinct enzymic activities or is subject to regulation through PTM. Interestingly, results presented in the last chapter suggested that Ad5 E4orf6 was subjected to PTM, whilst Ad12 E4orf6 was not [cf **Fig. 3.17 A and B**]. Given these findings we decided to identify and characterise the PTM status of Ad5 E4orf6.

4.2.2. Investigating the potential O-linked glycosylation of the Ad5 E4orf6 protein

4.2.2.1. Analysis of the Ad5 and Ad12 E4orf6 protein sequences for O-linked glycosylation

One of the well-studied PTMs is glycosylation where a sugar moiety (Glycan) is attached to proteins to modify their structure and function. Glycosylated proteins are classified into five distinct types: N-linked glycans, C-linked glycans, O-linked glycans, glypiation and phosphoglycans (Ali, et al. 2019). O-linked glycosylation-the attachment of glycans to hydroxyl groups of Ser and Thr residues in proteins passaging through the golgi to form complex branched oligosaccharide structures, have pivotal roles in different cellular processes (Karve and Cheema, 2011). Interestingly, viruses utilize the host-cell glycosylation machinery to glycosylate their surface proteins to enhance infectivity. Prominent examples include Ebola virus, HIV-1 and influenza virus (Bagdonaite and Wandall, 2018; Watanabe, et al. 2019). In

addition to these enveloped viruses, non-enveloped viruses such as adenoviruses utilize sialic acid-containing oligosaccharides as cell surface receptors (Stencel-Baerenwald, et al. 2014).

Inspection of predicted O-linked glycosylation sites in Ad5 and Ad12 E4orf6 using the NetOGlyc 4.0 - prediction software revealed major differences in the potential O-linked glycosylation of these two proteins [Fig. 4.1]. Indeed, analysis of these proteins revealed that there are ten potential O-linked glycosylation sites in Ad5 E4orf6, all located in the N-terminal region of the protein, whereas Ad12 E4orf6 was shown not to possess any potential O-linked glycosylation sites in the whole protein [Fig. 4.1]. Indeed, it was particularly striking that the N-terminal region of Ad5 E4orf6 possessed multiple Ser and Thr residues, whereas Ad12 E4orf6 did not. These analyses suggested the possibility that Ad5 E4orf6 might be modified selectively by O-linked glycosylation.

A) Ad5 E4orf6

Ad5 E4orf6	source	feature	start	end	score	comment
SEQUENCE	netOGlyc-4.0.0.13	CARBOHYD	2	2	0.734252	#POSITIVE
SEQUENCE	netOGlyc-4.0.0.13	CARBOHYD	3	3	0.821445	#POSITIVE
SEQUENCE	netOGlyc-4.0.0.13	CARBOHYD	4	4	0.823811	#POSITIVE
SEQUENCE	netOGlyc-4.0.0.13	CARBOHYD	11	11	0.856105	#POSITIVE
SEQUENCE	netOGlyc-4.0.0.13	CARBOHYD	15	15	0.898501	#POSITIVE
SEQUENCE	netOGlyc-4.0.0.13	CARBOHYD	17	17	0.764254	#POSITIVE
SEQUENCE	netOGlyc-4.0.0.13	CARBOHYD	20	20	0.870214	#POSITIVE
SEQUENCE	netOGlyc-4.0.0.13	CARBOHYD	23	23	0.91791	#POSITIVE
SEQUENCE	netOGlyc-4.0.0.13	CARBOHYD	26	26	0.879336	#POSITIVE
SEQUENCE	netOGlyc-4.0.0.13	CARBOHYD	35	35	0.490089	
SEQUENCE	netOGlyc-4.0.0.13	CARBOHYD	37	37	0.64106	#POSITIVE
SEQUENCE	netOGlyc-4.0.0.13	CARBOHYD	40	40	0.366655	
SEQUENCE	netOGlyc-4.0.0.13	CARBOHYD	53	53	0.0488223	
SEQUENCE	netOGlyc-4.0.0.13	CARBOHYD	55	55	0.0294449	

B) Ad12 E4orf6

Ad12 E4orf6	source	feature	start	end	score	comment
SEQUENCE	netOGlyc-4.0.0.13	CARBOHYD	26	26	0.0751159	
SEQUENCE	netOGlyc-4.0.0.13	CARBOHYD	29	29	0.151361	
SEQUENCE	netOGlyc-4.0.0.13	CARBOHYD	31	31	0.0268217	
SEQUENCE	netOGlyc-4.0.0.13	CARBOHYD	32	32	0.0201126	
SEQUENCE	netOGlyc-4.0.0.13	CARBOHYD	33	33	0.0693197	
SEQUENCE	netOGlyc-4.0.0.13	CARBOHYD	36	36	0.0190812	
SEQUENCE	netOGlyc-4.0.0.13	CARBOHYD	43	43	0.00475538	
SEQUENCE	netOGlyc-4.0.0.13	CARBOHYD	45	45	6.24938e-06	
SEQUENCE	netOGlyc-4.0.0.13	CARBOHYD	50	50	0.00546517	
SEQUENCE	netOGlyc-4.0.0.13	CARBOHYD	57	57	0.00375064	

Figure 4.1: Potential O-linked glycosylation sites in Ad5 E4orf6 and Ad12 E4orf6 protein. The NetOGlyc 4.0 - prediction program was used to identify potential O-linked glycosylation sites in Ad5 E4orf6 and Ad12 E4orf6 amino acids sequence. (A) Ad5 E4orf6 (B) Ad12 E4orf6. start/end relate to amino acid residue. The probability-based score of O-linked glycosylation is listed under score and the likelihood of that site being glycosylated is listed under comment.

4.2.2. Investigating whether Ad5 E4orf6 is modified by O-linked glycosylation

The first step in protein O-linked glycosylation is the transfer of GlcNAc from UDP-GlcNAc to the Ser and Thr residues of substrate proteins, which is catalysed by the O-linked N-acetylglucosamine (O-GlcNAc) transferase, OGT. An inhibitor of OGT has been developed, OSMI-1 (OGT small molecule inhibitor) which prevents the ability of OGT to catalyse the transfer of GlcNAc from UDP-GlcNAc to Ser and Thr residues such that complex glycosylation of target proteins is inhibited (Ortiz-Meoz, et al. 2015). Taking advantage of the ability of OSMI-1 to inhibit O-linked glycosylation, we investigated whether OSMI-1 could inhibit Ad5 E4orf6 PTM. WB analyses revealed however, that there was no obvious effects of

OSMI treatment upon the PTM status of the Ad5 E4orf6 protein [Fig. 4.2]. These data indicated that it was unlikely that the PTMs observed on Ad5 E4orf6 were due to O-linked glycosylation.

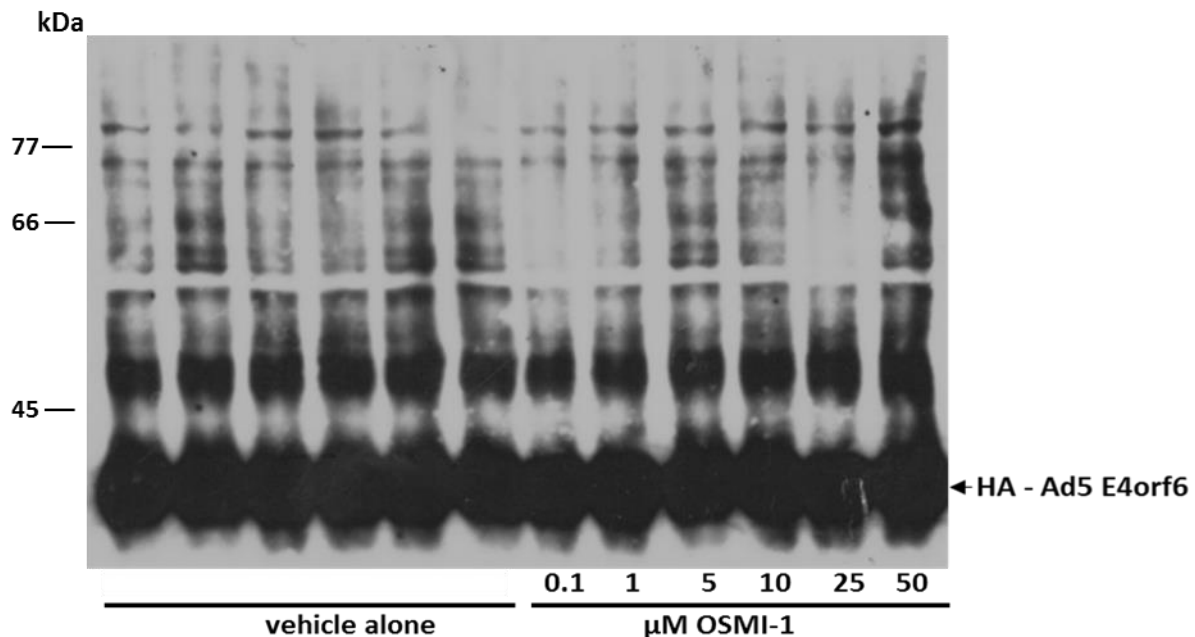


Figure 4.2: The OGT inhibitor, OSMI-1 does not affect the PTM status of the Ad5 E4orf6 protein. HA-tagged Ad5 E4orf6 expression was induced in a Flp-In T-REx U2OS-FRT cell line following treatment with 0.1 µg/ml doxycycline. Cells were simultaneously treated with different concentrations of the OGT inhibitor, OSMI-1, or equivalent amounts of DMSO vehicle. At 24 h post-treatment cells were harvested and subjected to SDS-PAGE and WB analysis with an anti-HA antibody. The data shown is representative of 3 independent experiments.

4.2.3 Investigating whether the Ad5 E4orf6 protein is subject to ubiquitylation

Given the known role of Ad5 E4orf6 in the proteasomal-mediated degradation of cellular proteins and its ability to interact with CRL5 we next investigated whether the higher molecular weight Ad5 E4orf6 species were ubiquitylated forms. In the first instance therefore, we decided to investigate whether, the peptide-aldehyde proteasome inhibitor, MG132 (carbobenzoxy-L-leucyl-L-leucyl-L-leucine), which inhibits the chymotrypsin-like peptidase activities of the 20S proteasome β 5-subunit (Goldberg, 2012), affected the cellular levels of Ad5 E4orf6. Low exposure WBs revealed that the unmodified Ad5 E4orf6 species was increased substantially in the presence of MG132 [cf lanes 3 and 4, as well as 7 and 8, Fig. 4.3]. Similarly, the higher

molecular weight forms of Ad5 E4orf6 were also increased dramatically following treatment with MG132 [cf lanes 3 and 4, as well as 7 and 8, Fig. 4.3]. These data suggest that Ad5 E4orf6 is targeted for degradation through the 26S proteasome and that the higher molecular weight forms of Ad5 E4orf6 are ubiquitylated species.

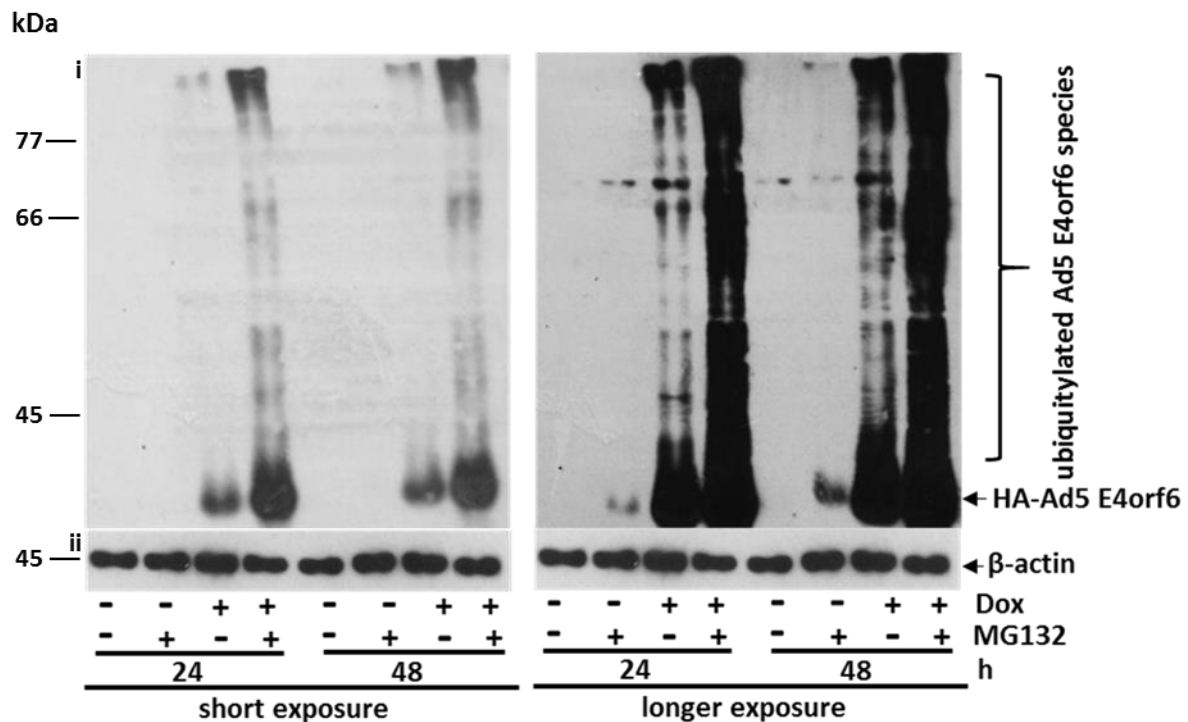


Figure 4.3: Effect of the proteasome inhibitor, MG132 on the PTM status of HA-tagged Ad5 E4orf6. Flp-In T-REx U2OS Ad5 HA-tagged-E4orf6 cells were treated +/- 0.1µg/ml doxycycline in the presence or absence of 1µM MG132. Cell lysates were harvested at 24 h and 48 h post-treatment and subject to WB analysis with anti-HA antibodies. The data shown is representative of 3 independent experiments.

4.2.4. Effects of the NAE inhibitor, MLN4924 on Ad5 E4orf6 expression

Given that the Ad5 E4orf6 protein associates with CRL5 via Elongins B and C and, potentially the Cullin itself (Querido, et al. 2001; Gilson, et al. 2014), it is possible that CRL5 itself, through direct interaction, promotes Ad5 E4orf6 ubiquitylation. MLN4924 is a small molecule inhibitor of the NEDD8-activating enzyme (NAE), which inhibits the NEDDylation and consequent activation of the CRL complex (Soucy, et al. 2009; Nawrocki, et al. 2012). Indeed, MLN treatment of Ad-infected cells is known to inhibit the Ad-mediated degradation of a

number of cellular proteins (Blackford, et al. 2010; Nazeer, et al. 2019). To investigate whether CRL5 was responsible for Ad5 E4orf6 ubiquitylation, we investigated whether MLN4924 affected Ad5 E4orf6 protein levels and/or Ad5 E4orf6 PTM status. WB analysis revealed that MLN4924 treatment increased the levels of the non-modified Ad5 E4orf6 species [first panel, Fig 4.4]. Longer exposures suggested that MLN4924 treatment also increased the overall levels of ubiquitylated Ad5 E4orf6 species but only very slightly [second panel, Fig. 4.4]. Given the increase in the overall levels of the unmodified Ad5 E4orf6 protein it is unlikely that there was an actual increase in the overall level of Ad5 E4orf6 ubiquitylation in the presence of MLN4924. These data suggest that CRL5 might also be responsible for regulating the stability of the Ad5 E4orf6 protein.

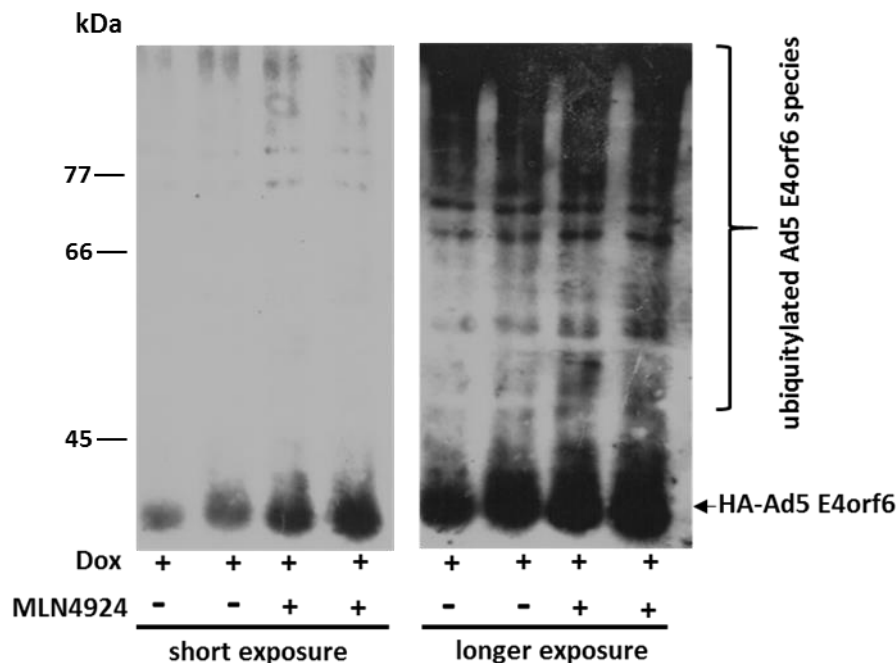


Figure 4.4: Effect of the NAE inhibitor, MLN4924 on the levels of unmodified HA-tagged Ad5 E4orf6 and the PTM status of HA-tagged Ad5 E4orf6. Flp-In T-REx U2OS Ad5 HA-tagged-E4orf6 cells were treated +/- 0.1 µg/ml doxycycline in the presence or absence of 3 µM MLN4924. Cell lysates were harvested at 24 h post-treatment and subject to WB analysis with anti-HA antibodies. The data shown is representative of 3 independent experiments.

4.2.5. Cellular localization of ubiquitylated Ad5 E4orf6 species

As discussed earlier Ad5 E4orf6 is a nucleo-cytoplasmic shuttle protein that participates in the transport of viral mRNAs from the nucleus to the cytoplasm (see section 1.2.4.2). As such, Ad5 E4orf6 exists as both nuclear and cytoplasmic species. It is also known that the 26S proteasome exists as both nuclear and cytoplasmic species (Turnell, et al. 2000). We therefore considered it important to investigate whether Ad5 E4orf6 was ubiquitylated and targeted for degradation in the nucleus or the cytoplasm. To investigate the site of Ad5 E4orf6 ubiquitylation and degradation we performed subcellular fractionation to isolate cytoplasmic, nucleoplasmic, chromatin-associated and chromatin preparations from Flp-In T-REx Ad5 HA-tagged-E4orf6 U2OS cells. WB analyses revealed that Ad5 E4orf6 was predominantly located in the cytoplasm, although it was also found in the nucleoplasm, and chromatin-associated and chromatin fractions [panel i, Fig. 4.5]. These analyses also revealed that ubiquitylated Ad5 E4orf6 species were found exclusively in the cytoplasm [panel i, Fig. 4.5], suggesting that Ad5E4orf6 is subject to CRL5-dependent ubiquitylation and 26S proteasome degradation in the cytoplasm.

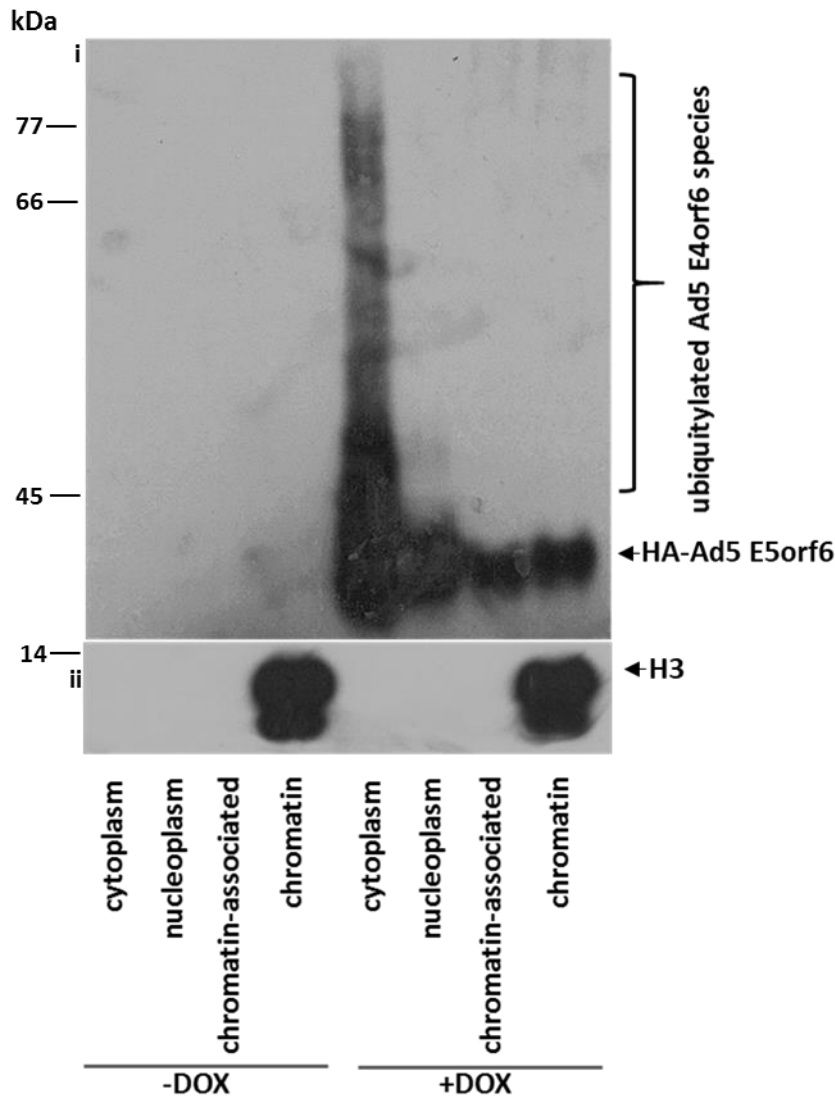


Figure 4.5: Ad5 E4orf6 ubiquitylated species exist exclusively in the cytoplasm. Flp-In T-REx Ad5 HA-tagged-E4orf6 U2OS cells were treated +/- 0.1 μ g/ml doxycycline. Cell fractionation was performed 24 h post-treatment and subject to WB analysis with anti-HA antibodies [panel i], or anti-histone H3 antibodies [panel ii]. The data shown is representative of 3 independent experiments.

4.2.6 Generation and characterization of K95R and K171R Ad5 E4orf6 mutants

4.2.6.1. Inspection of the Ad5 E4orf6 primary sequence

It is generally accepted that lysine is the canonical ubiquitin acceptor site, though non-canonical acceptor sites have also been described (e.g. N-terminal amine groups of proteins, serine and threonine hydroxyl groups, cysteine thiol groups); (McDowell, et al. 2013). In order to establish the ubiquitin acceptor sites in Ad5 E4orf6 we first inspected the Ad5 E4orf6 primary sequence and established that Ad5 E4orf6 only possesses two lysine residues in its

entire sequence, K95 and K171 [Fig. 4.6], whilst multiple alignment of adenovirus E4orf6 sequences from different adenovirus groups revealed that K95 is only weakly conserved between adenovirus types (only Ad5 and Ad12), although a number of adenovirus types did have arginine at this site but K171 was much more well conserved between adenovirus types [Fig. 4.6].

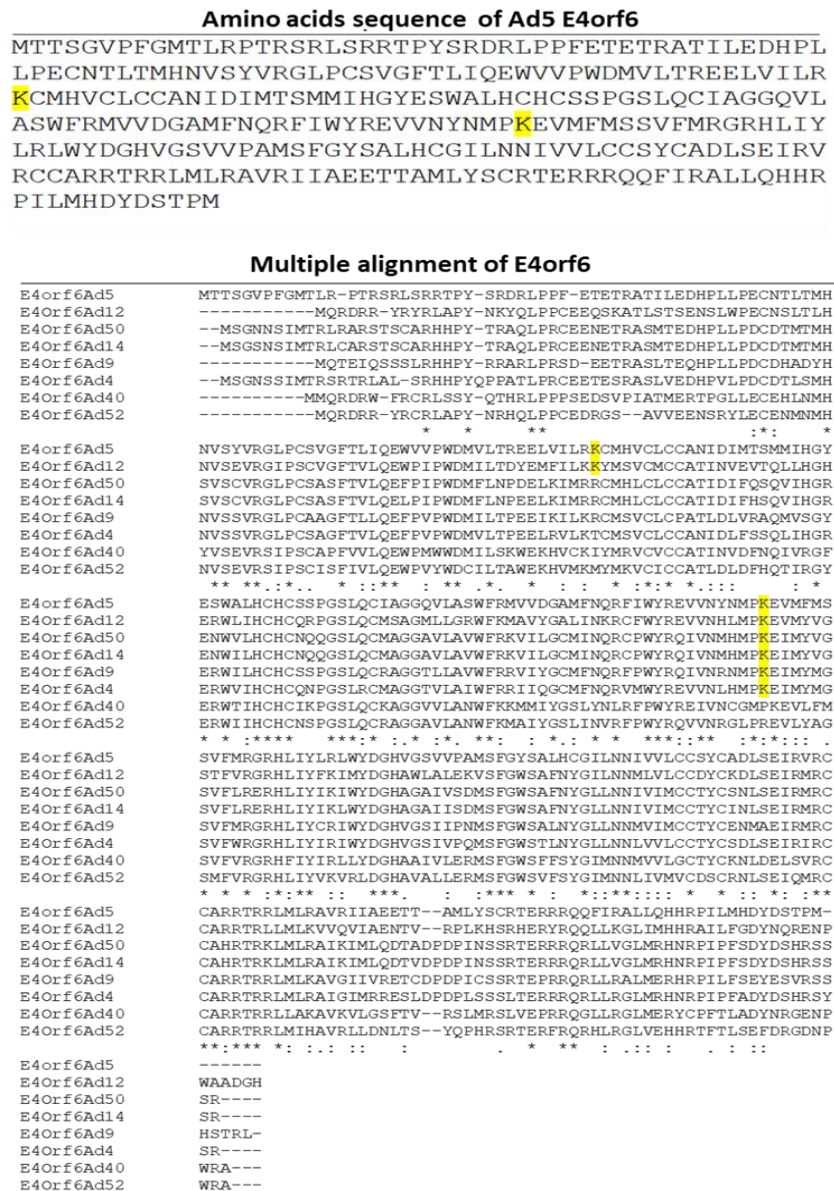


Figure 4.6: Analysis of Ad5 E4orf6 sequence and the conservation of K ubiquitin acceptor sites between different adenovirus types. Adenovirus E4orf6 species from multiple adenovirus groups were aligned using the multiple alignment program, CLUSTAL W. Potential Ad5 E4orf6 K acceptor sites are highlighted in yellow.

4.2.6.2. Generation of Ad5 E4orf6 lysine mutants

In order to establish whether K95 and/or K171 of Ad5 E4orf6 served as K acceptors for ubiquitin we decided to perform site-directed mutagenesis using the Q5 site-directed mutagenesis kit using the primers detailed using pcDNA5-FRT-Ad5 E4orf6 as a template (see Material and Methods section 2.3.8). In this regard we made replaced lysine with arginine in an attempt to conserve Ad5 E4orf6 secondary and tertiary structure. Initially, therefore we made K95R and K171R single mutants and confirmed sequence identity and mutation by Sanger sequencing of the entire gene. For clarity only the sequence where the mutation was incorporated is shown [Fig. 4.7].

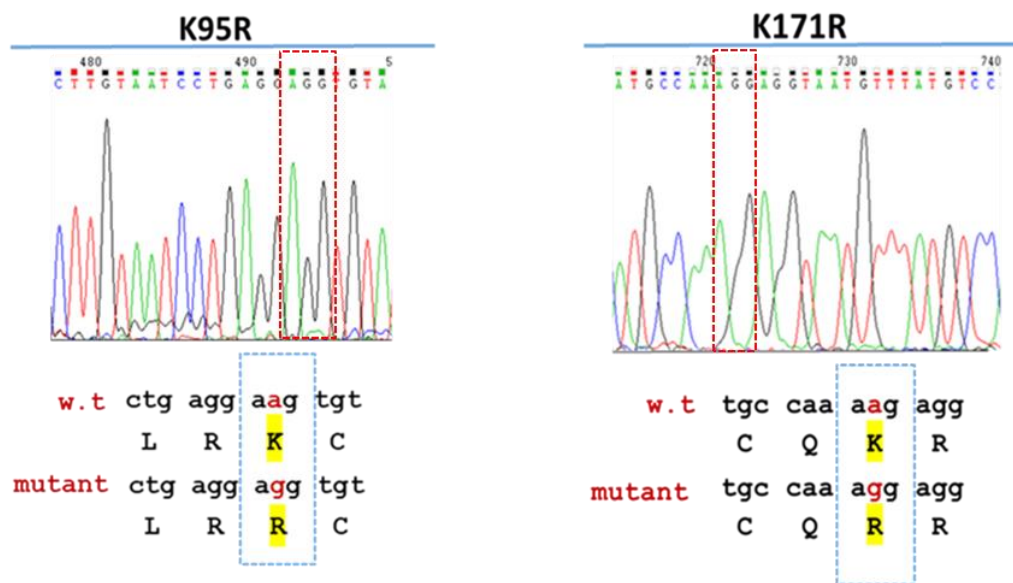


Figure 4.7: Generation of K95R and K171R Ad5 E4orf6 mutants. Chromas images of single mutants showing the K95R mutation and the K171R mutation where lysine (AAG) is mutated to arginine (AGG).

4.2.6.3. Investigating the effects of K95R and K171R mutation on Ad5 E4orf6 ubiquitylation status

To investigate the requirement for both K95 and K171 as ubiquitin acceptors we transiently transfected w.t. pcDNA5 FRT Ad5 E4orf6 and pcDNA5 FRT Ad5 E4orf6 mutants into U2OS cells that did not express a TET repressor such that the genes would be expressed in the absence

of doxycycline treatment. We took this approach as we anticipated that we would be able to get more similar expression of w.t. Ad5 E4orf6 and its mutants by transient expression rather than by generating Flp-In T-REx-inducible U2OS cell lines. Indeed, WB analyses revealed that the expression levels of unmodified HA-tagged Ad5 E4orf6 species were very similar for w.t., K95R and K171R species [Fig. 4.8]. More interestingly, it appeared that mutation of either potential K acceptor reduced the PTM of HA-tagged Ad5 E4orf6, suggestive that both of these residues were subjected to polyubiquitylation. It did appear, however that mutation of K171 was the major site for PTM, as mutation of K171 had more of a detrimental effect upon PTM than did mutation of K95 [Fig. 4.8]. Taken together these data indicate that both K95 and K171 are likely subjected to polyubiquitylation upon the expression of Ad5 E4orf6.

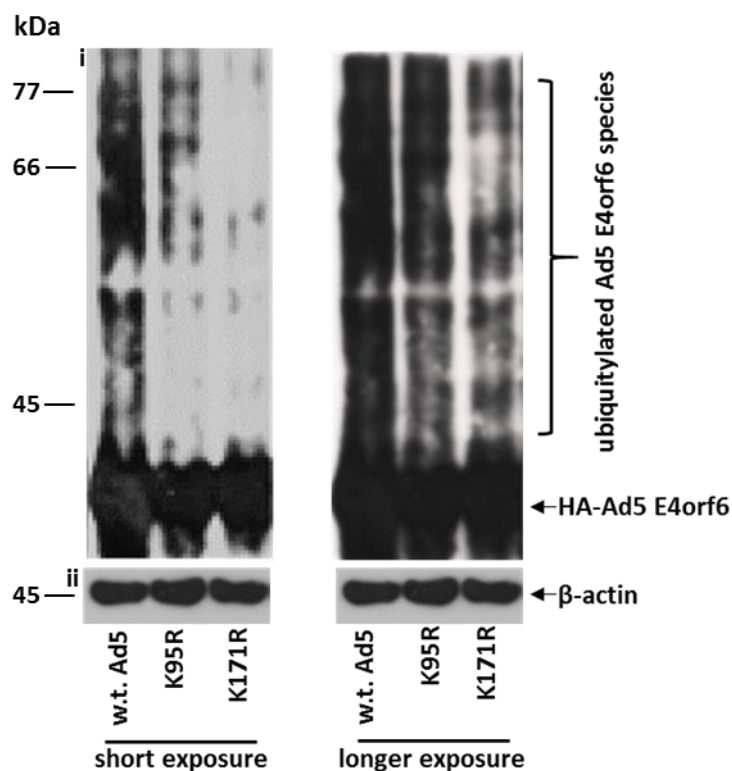


Figure 4.8: Investigating a role for K95 and K171 as ubiquitin acceptor residues in Ad5 E4orf6. U2OS cells were transfected transiently with either w.t. pcDNA5 FRT Ad5 E4orf6, pcDNA5 FRT K95R Ad5 E4orf6 or pcDNA5 FRT K171R Ad5 E4orf6 expression plasmids. Cell lysates were harvested at 24 h post-treatment and subject to WB analysis with anti-HA antibodies. The data shown is representative of 3 independent experiments.

4.2.7. Targeting of the Ubiquitin-Proteasome System by Ad12 E4orf6

Although Ad12 E4orf6 was not a major substrate for ubiquitylation we wished to investigate its function in more detail. Previous studies from our laboratory have established that Ad12 E4orf6 can promote the CRL2-dependent degradation of the ATR activator, TopBP1, independently of E1B-55K (Blackford, et al. 2010). Given this finding we wondered whether Ad12 E4orf6 could target other cellular proteins for degradation independently of E1B-55K. Indeed, this was the primary reason we made the Tet-inducible Ad12 HA-tagged-E4orf6 U2OS cells described in Chapter 3. Consistent with our earlier studies induction of Ad12 E4orf6, but not Ad5 E4orf6, promoted the degradation of TopBP1 (see Figure 3.14). To investigate whether Ad12 E4orf6 targeted other cellular proteins for degradation independently of E1B-55K we adopted a mass spectrometric approach. This approach was taken in an attempt to define, in a non-biased way, global changes in the total levels of nuclear protein levels following Ad12 E4orf6 expression. We chose to focus on nuclear proteins as most proteins targeted by adenovirus for degradation are nuclear (e.g. p53, TopBP1, Mre11, DNA-ligase IV) and to simplify the dataset. To quantify nuclear proteins +/- Ad12 E4orf6 we chose to use the dimethyl, post-trypsinization, labelling approach, where those peptides isolated from + Ad12 E4orf6 cells were labelled with 'heavy' formaldehyde ($^2\text{H-CH}_2\text{O}$), whereas those peptides isolated from - Ad12 E4orf6 cells were labelled with 'light' formaldehyde ($^1\text{H-CH}_2\text{O}$). This labelling strategy would produce peptides that would possess an N-terminal dimethyl label containing ^2H or ^1H that would produce a mass difference between identical peptide sequences of 2 mass units that could be detected by high resolution mass spectrometers. Data for each peptide pair identified from each protein would then be compared to produce a heavy:light peptide ratio, which relates to their relative abundance. This technique requires that both the heavy and the light forms of the peptide are found to provide a ratio, such that in circumstances where Ad12 E4orf6 expression induces a complete loss of a protein, these proteins will not be identified as being reduced upon Ad12 E4orf6 expression. Other issues, such as incomplete

dimethylation labelling could affect peptide quantification, though on the plus side this technique is much cheaper than similar methods such as SILAC.

4.2.7.1. Identification of cellular proteins that are reduced in levels following Ad12 E4orf6 expression

For these experiments we chose #8 of the Ad12 E4orf6 U2OS FlpIn cells which expressed Ad12 E4orf6 to high levels and also targeted TopBP1 for degradation [Fig. 3.14]. Nuclear cell lysates +/- Ad12 E4orf6 were isolated and processed for MS analysis as described (see sections 2.2.11 and 2.2.12). They were then subject to mass spectrometry using an Impact TOF mass spectrometer (Bruker Daltonics, Bremen, Germany) and analysed by WARP-LC (Bruker) and ProteinScape 2.1 (Bruker Daltonics), to obtain ratios of ‘Heavy’ to ‘Light’ peptides and a quantitative readout of the effect of Ad12 E4orf6 expression on the absolute levels of nuclear proteins from U2OS cells; data is presented as a waterfall plot for simplicity [Fig. 4.9]. In two separate experiments we identified 256 different proteins where we isolated one or more peptides to allow for the effect of Ad12 E4orf6 on cellular protein levels to be determined.

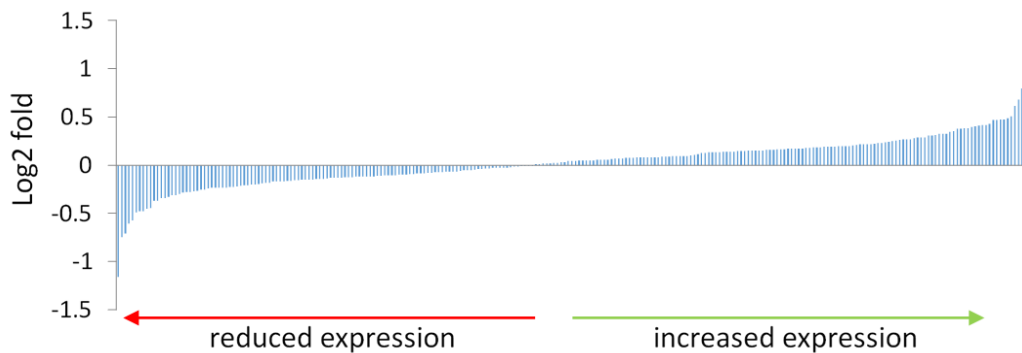


Figure 4.9: Effect of Ad12 E4orf6 expression on nuclear protein levels. Nuclear lysates from +/- Ad12 E4orf6 cells were isolated and prepared for quantitative analysis by mass spectrometry (sections 2.2.11-2.2.13). Combined data from two separate experiments is shown. The mean log₂ fold change is shown.

Accession	Protein	Peptides (1,2)	Scores (1,2)	Fold-change (1,2)	Fold-change mean
H31_HUMAN	Histone H3.1	24, 17	1034.3, 799.5	0.4, 0.49	0.44
SRP14_HUMAN	Signal recognition particle	2, 2	109.0, 111.3	0.960, 0.23	0.59
H2A2B_HUMAN	Histone H2A type 2-B	3, 3	128.4, 119.5	0.44, 0.78	0.61
H4_HUMAN	Histone H4	14, 14	674.4, 642.2	0.59, 0.72	0.65
H2A1H_HUMAN	Histone H2A type 1-H	6, 6	233.5, 231.7	0.56, 0.78	0.67
RL29_HUMAN	60S ribosomal protein L29	4, 3	180.6, 161.8	0.84, 0.57	0.70
RL35_HUMAN	60S ribosomal protein L35	2, 3	70.5, 90.8	0.71, 0.71	0.71
GNA13_HUMAN	Guanine nucleotide-binding protein subunit alpha-13	2, 3	72.5, 97.3	0.51, 0.92	0.73
RS6_HUMAN	40S ribosomal protein S6	3, 3	182.5, 169.2	0.52, 0.94	0.73
RL17_HUMAN	60S ribosomal protein L17	2, 4	65.9, 83.8	1.06, 0.4	0.77
H11_HUMAN	Histone H1.1	7, 7	468, 386	0.9, 0.72	0.81
H12_HUMAN	Histone H1.2	18, 18	1054.2, 842.1	0.78, 0.89	0.83
H2B1J_HUMAN	Histone H2B type 1-J	16, 13	867.3, 610.1	0.89, 0.97	0.93

Table 4.1: Effect of Ad12 E4orf6 expression on nuclear protein levels. Table illustrating those nuclear proteins whose levels reduced the most following the expression of Ad12 HA-tagged E4orf6. The number of peptides identified from each protein is indicated, as is the overall Mowse score, which is a statistical score for how well the experimental data matches the database sequence. The score shown for each protein is the sum of scores for individual peptides.

Close inspection of the data revealed that all of the core histone proteins (H2A, H2B, H3 and H4) which comprise the histone octamer were reduced substantially upon Ad12 E4orf6 expression, as was the histone linker protein, histone H1 [Table 4.1]. In some instances different histone isoforms were also identified as being reduced, such as histone H1.1 and H1.2 and histone H2A type 2-B and 1-H [Table 4.1]. Importantly, multiple different peptides were identified from each histone species giving a high degree of confidence that the observed reduction in the levels of these proteins is real representation of what is happening in the cell. A number of 60S and 40S ribosomal proteins were also observed as being reduced following Ad12 E4orf6 expression though typically only 3 or 4 peptides were identified and quantified from each of these proteins, and the overall confidence score was lower than those observed for the histones, though is still high enough to suspect these changes were real [Table 4.1].

Unfortunately, although we have previously shown we did not observe the known Ad12 E4orf6 target, TopBP1 in this mass spectrometric screen. This is likely due to one of two reasons. Either all of the TopBP1 was degraded in the Ad12 E4orf6 expressing cells such that no ‘heavy’ TopBP1 peptides were detected in that sample, or, alternatively that the nuclear levels of TopBP1 were not as abundant as those that were detected by mass spectrometry. An interactomic map of those proteins identified as, potentially, being targeted by Ad12 E4orf6 is shown in [Fig. 4.10].

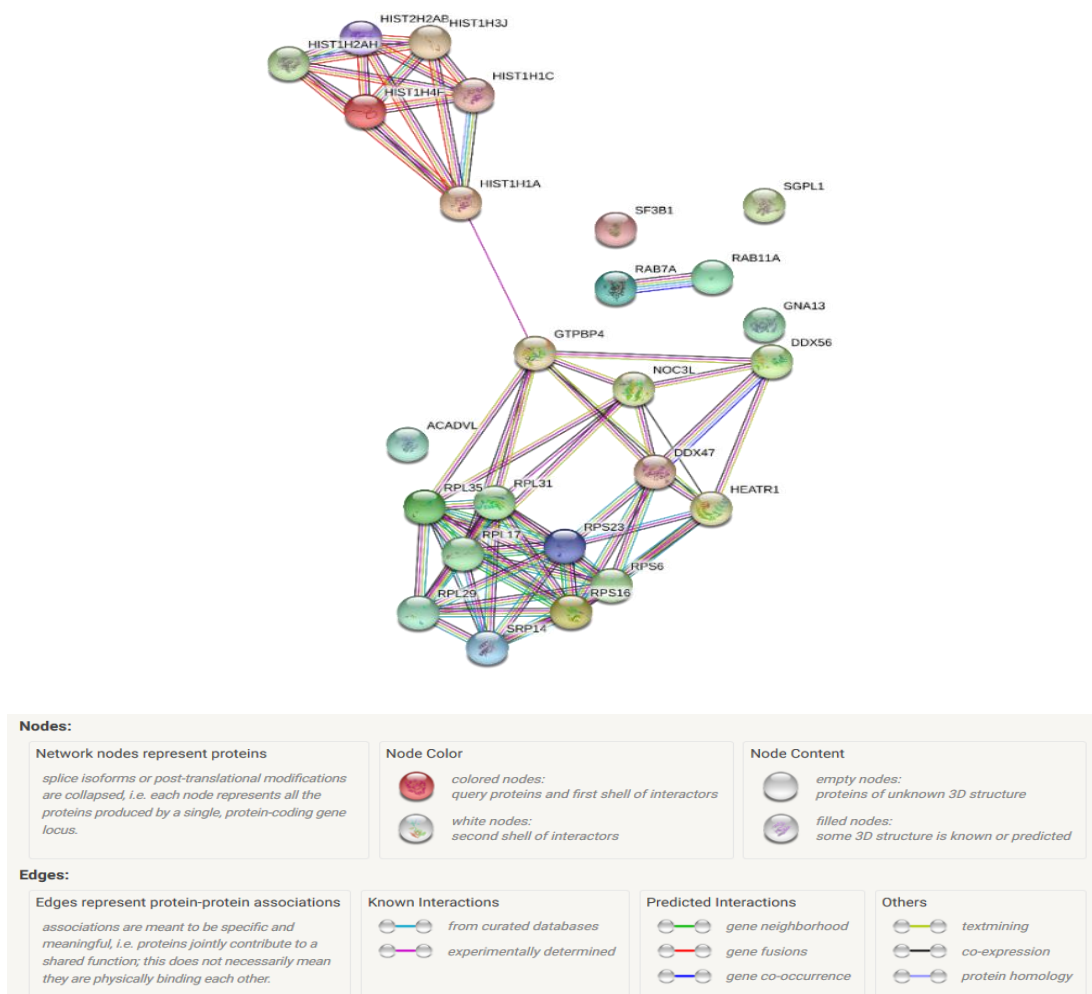


Figure 4.10: Effect of Ad12 E4orf6 expression on nuclear protein levels. Protein-Protein interaction network for those 25 proteins whose levels are reduced the most following Ad12 E4orf6 expression. The figure was generated using the Protein-Protein Interaction Networks programme, String-db (<https://string-db.org/>).

In a number of cases peptides were only detected in one or the other experiment. In total we identified 389 different proteins that were only identified in one of the two experiments. The effects of Ad12 E4orf6 expression on cellular proteins were determined and are presented as a waterfall plot below [Fig. 4.11].

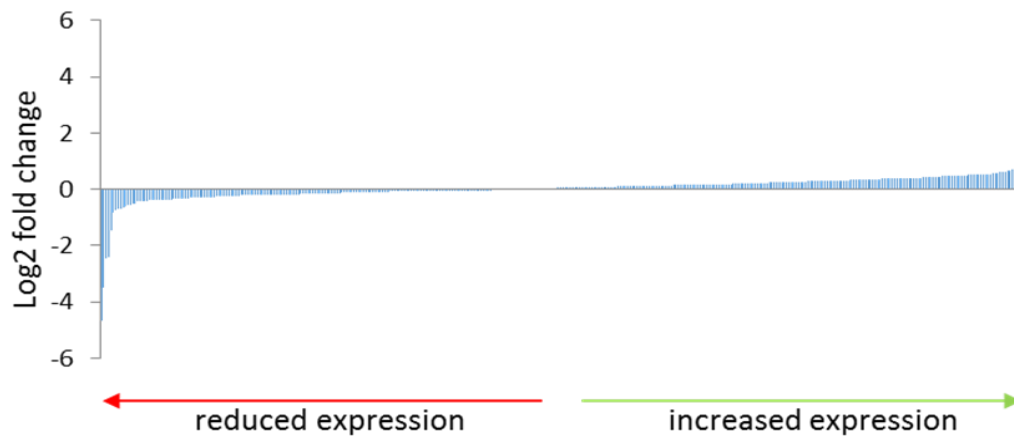


Figure 4.11: Effect of Ad12 E4orf6 expression on nuclear protein levels. Nuclear lysates from +/- Ad12 E4orf6 cells were isolated and prepared for quantitative analysis by mass spectrometry (sections 2.2.11-2.2.13). Data is combined from two experiments - proteins displayed were detected in just one of the two experiments. The log2 fold change is shown.

Inspection of the data revealed that those proteins whose levels were reduced there was, typically, only one or two peptides identified which reduces confidence in what was observed was a reflection of what happens in response to Ad12 E4orf6 expression [Table 4.2]. This is reflected in the calculated Mowse scores. A few interesting proteins were detected including the recombination-repair protein, RAD51 and the Ras-related proteins, CDC42 and RhoA. The top 10 'hits' are shown in [Table 4.2].

Accession	Protein	Peptides	Scores	Fold-change
IFI44_HUMAN	Interferon-induced protein 44	2	62.2	0.04
CXD3_HUMAN	Gap junction delta-3 protein	1	59	0.09
CDC42_HUMAN	Cell division control protein 42	2	90.4	0.18
RA51B_HUMAN	DNA repair protein RAD51 homolog 2	2	56.6	0.19
SFR12_HUMAN	Splicing factor, arginine/serine-rich 12	2	66.3	0.36
RHOA_HUMAN	Transforming protein RhoA	2	75.5	0.56
DBLOH_HUMAN	Diablo homolog, mitochondrial	2	64.2	0.6
TMC6_HUMAN	Transmembrane channel-like protein 6	1	76.6	0.61
DLDH_HUMAN	Dihydrolipoyl dehydrogenase, mitochondrial	2	106.1	0.62
RRP7A_HUMAN	Ribosomal RNA-processing protein 7 homolog A	1	64.4	0.64

Table 4.2: Effect of Ad12 E4orf6 expression on nuclear protein levels. Table illustrating those nuclear proteins which were detected in only one of the two experiments and whose levels were reduced the most following the expression of Ad12 E4orf6. The number of peptides identified from each protein is indicated, as is the overall Mowse score (see Table 4.1 for more details).

Taken together these experiments reveal that we have identified a number of cellular proteins that are down-regulated following Ad12 E4orf6 expression. In the first instance it was important to validate these findings by WB using, particular drug treatments to establish whether, or not, these changes in cellular protein levels were due to Ad12 E4orf6's ability to engage with the UPS.

4.2.7.2. Effect of Ad12 E4orf6 expression upon cellular histone levels: WB analyses

Our analyses identified two classes of nuclear proteins that appeared to be reduced following Ad12 E4orf6 expression: histones, which comprise the major protein component of the nucleosome, and ribosomal proteins that are synthesized and assembled in nucleoli before being translocated to the cytoplasm. Given that there is a large cytoplasmic component of

ribosomal proteins which our analyses did not investigate, we decided to focus our attention on the relationship between Ad12 E4orf6 expression and the levels of histones. Firstly, we decided to investigate by WB the effects of Ad12 E4orf6 expression on cellular histone levels using a number of individual Ad12 HA-tagged-E4orf6 U2OS FlpIn cell clones to establish whether the ability of Ad12 E4orf6 to reduce cellular histones was a common phenomenon. Given that we only observed between 10 and 60% reduction in nuclear histone levels by MS analyses after 24h post-induction we decided to extend the induction time to 48 h to maximize any Ad12 E4orf6 effects. WB analyses revealed that, in addition to the known Ad12 E4orf6 target TopBP1, the total cellular levels of histone H3 and histone H2A were also reduced appreciably following Ad12 HA-tagged-E4orf6 expression [Fig. 4.12]. Taken together these data validate the MS findings that histones are reduced in an Ad12 E4orf6-dependent manner

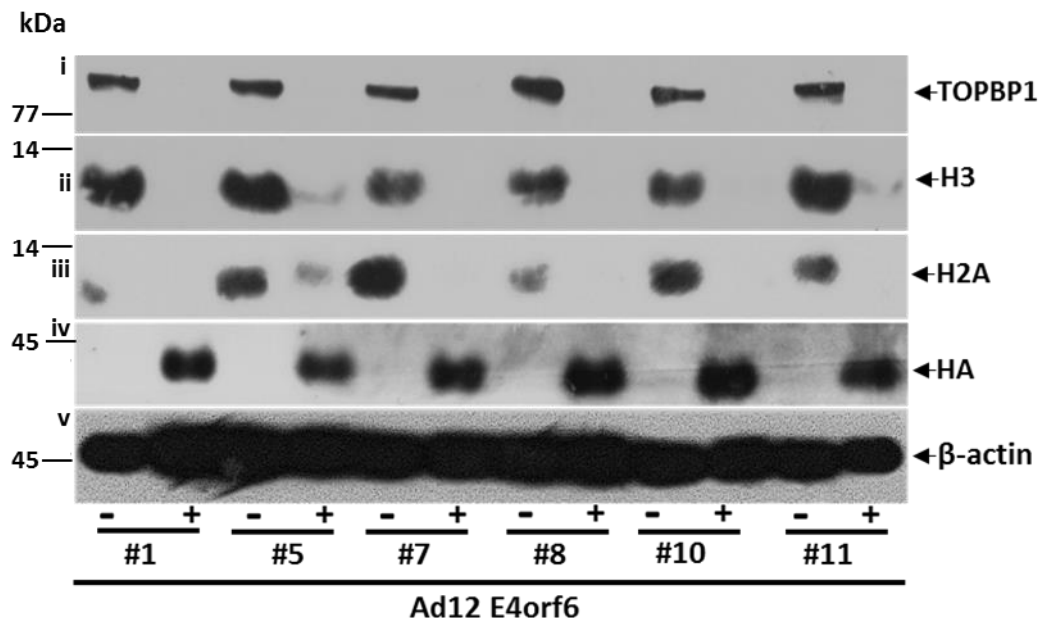


Figure 4.12: Effect of Ad12 E4orf6 expression on histone H3 and H2A protein levels. Whole cell lysates from Ad12 HA-tagged-E4orf6 U2OS FlpIn cells treated +/- 0.1 µg/ml doxycycline were harvested 48 h post-treatment and subjected to SDS-PAGE and WB analysis with the appropriate antibodies. # represents clone number. The data shown is representative of 3 independent experiments.

Given that Ad5 E4orf6 lacks the ability to promote the degradation of TopBP1 (Blackford, et al. 2010) we next investigated whether Ad5 E4orf6 could promote the cellular loss of histones. WB analyses revealed that Ad5 E4orf6 was unable to promote a reduction in the levels of TopBP1, histone H3 or histone H2A indicating that the ability of Ad12 E4orf6 to target cellular histones is not conserved in Ad5 E4orf6 [Fig. 4.13].

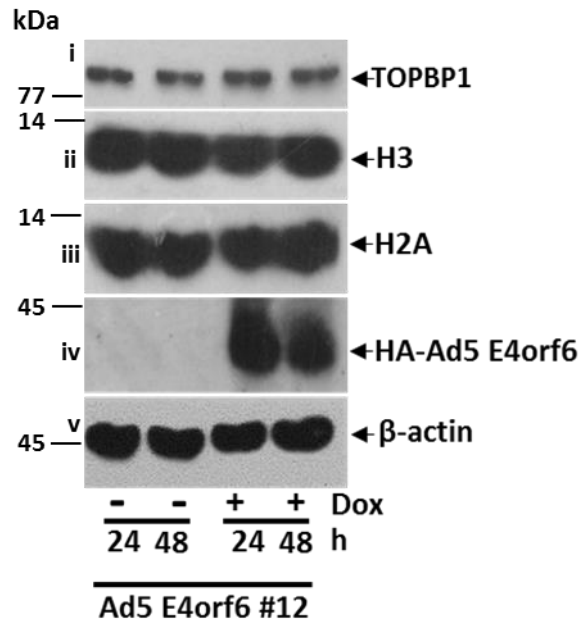


Figure 4.13: Effect of Ad5 E4orf6 expression on histone H3 and H2A protein levels. Whole cell lysates from Ad5 HA-tagged-E4orf6 U2OS FlpIn cells treated +/- 0.1 µg/ml doxycycline were harvested at 24 and 48 h post-treatment and subjected to SDS-PAGE and WB analysis with the appropriate antibodies. The data shown is representative of 3 independent experiments.

4.2.7.3. Role of CRLs and the 26S proteasome in the Ad12 E4orf6-dependent modulation of cellular histone levels

Given the role of CRLs and the 26S proteasome in the Ad-mediated degradation of cellular protein substrates (see section 1.3.2.1) we next decided to investigate whether they were similarly responsible for the Ad12 E4orf6-induced reduction in the levels of cellular histones. To do this we incubated Ad12 HA-tagged-E4orf6 U2OS cells in the absence or presence of the CRL inhibitor, MLN4924 (as described in section 4.2.4), or the irreversible 26S proteasome inhibitor, Lactacystin (Pasquini, et al. 2003). Consistent with previous work from our

laboratory induction of Ad12 E4orf6 expression promoted the CRL and 26S proteasome-mediated degradation of TopBP1 [panel i, Fig. 4.14]. Interestingly, the CRL inhibitor, MLN-4924 and the 26S proteasome inhibitor also limited the Ad12E4orf6-dependent reduction in both histone H3 and H2A protein levels which was more evident at 48 h post-treatment [panels ii and iii, respectively, Fig. 4.14]. These data suggest that Ad12 E4orf6 interacts with CRL2 in cells to target core histone proteins, H3 and H2A for 26S proteasome-dependent degradation.

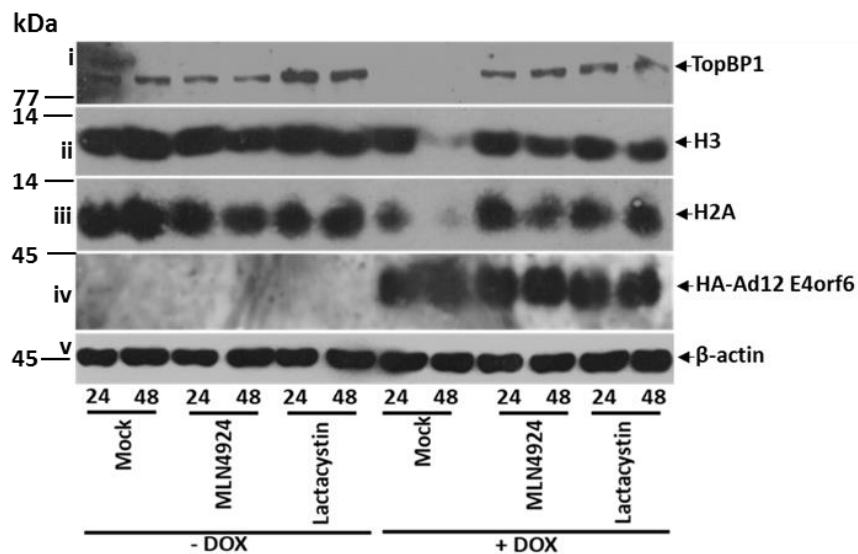


Figure 4.14: Requirement for CRLs and the 26S proteasome in the Ad12 E4orf6-dependent modulation of histone H3 and H2A protein levels. Whole cell lysates from Ad12 HA-tagged-E4orf6 U2OS FlpIn cells treated +/- 0.1µg/ml doxycycline in the absence or presence of 3µM MLN-4924 or 1 µM Lactacystin were harvested at 24 and 48 h post-treatment and subjected to SDS-PAGE and WB analysis with the appropriate antibodies. The data shown is representative of 3 independent experiments.

4.2.7.4. Effect of Ad12 E4orf6 expression on core histone protein expression

The WB analyses presented in Figures 4.12 and 4.13 indicate that Ad12 E4orf6, but not Ad5 E4orf6, expression promotes the loss of histones H2A and H3. To see if other core histones were also affected by Ad12 E4orf6 expression we decided to analyze core histone expression by SDS-PAGE following the acidic extraction of histones from Flp-In T-REx -U2OS adenovirus E4orf6 cells; acid extraction of histones is a well characterized technique for the isolation of histones (see section 2.2.7 for details). Consistent with the WB data coomassie blue

staining of SDS-PAGE gels revealed that Ad12 E4orf6 expression reduced the protein levels of all core histones, whereas Ad5 E4orf6 did not [Fig. 4.15]. Unfortunately, although the proteins were run on a 14% (w/v) acrylamide gel we could not separate H2A and H2B. These data indicate that Ad12 E4orf6, specifically modulates the protein levels of all core histones.

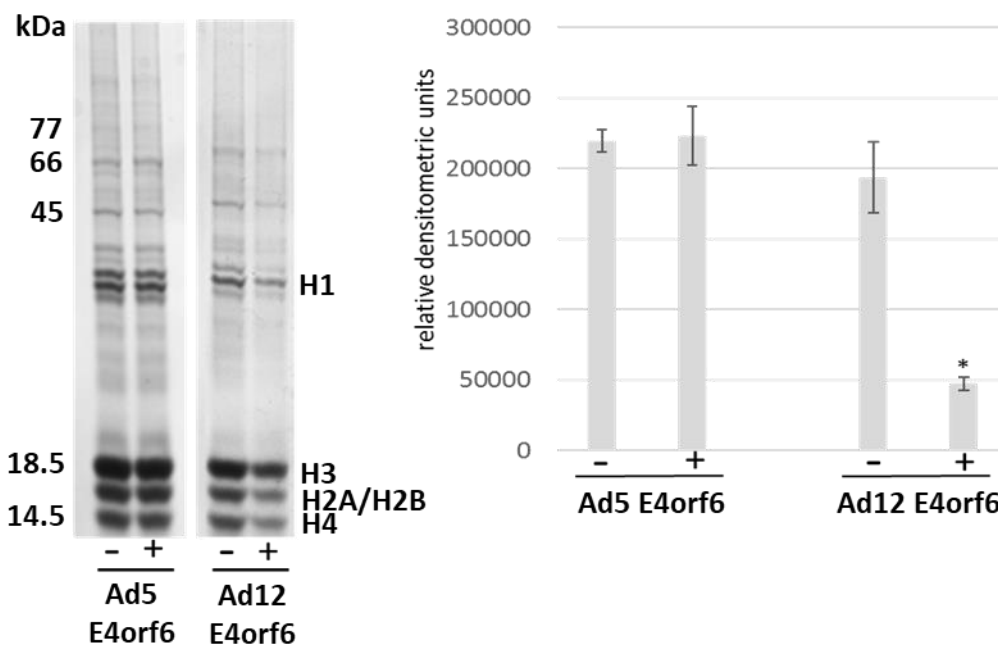


Figure 4.15: Ad12 E4orf6-dependent modulation of core histone protein levels. Ad5 and Ad12 HA-tagged-E4orf6 U2OS FlpIn cells were treated +/- 0.1µg/ml doxycycline for 24h. Histones were isolated by acid extraction (see section 2.2.7), separated by SDS-PAGE and stained with coomassie brilliant blue stain. The gel shown is representative of 3 independent experiments. The histogram represents the mean of all histone data (i.e. H3+ H2A/H2B + H4) from 3 independent experiments +/- S.D using ImageJ for densitometry. A two-tailed, paired student T-test indicated that there was no significant difference between Ad5 E4orf6 +/- doxycycline samples ($p=0.74$), whereas a two-tailed, paired student T-test indicated that there was a significant difference between Ad12 E4orf6 +/- doxycycline samples (* $p=0.009$).

4.2.7.5. Ad12 E4orf6 interacts with core histones *in vitro*

As we have shown that Ad12 E4orf6 promotes the degradation of core histones H3 and H2A [Fig. 4.12] and potentially all core components of the histone octamer [H3-H4 and H2A-H2B dimers; Fig. 4.15] and targets them for degradation in a CRL and 26S proteasome-dependent

manner we decided to investigate whether Ad12 E4orf6 could interact with core histones directly. To do this we first cloned the Ad12 E4orf6 gene into the bacterial GST expression vector, pGEX-4T-1 (using the primers listed in section 2.3.4), and then expressed and purified GST-Ad12 E4orf6 from the protease-deficient bacterial strain, BL21 as described in section 2.2.8. We then performed a GST pull-down by mixing either GST or GST-Ad12 E4orf6 with calf histones (Fraction VII; Sigma-Aldrich) that comprise all the core histones and also the linker histone, H1 (see section 2.2.9). Following SDS-PAGE and transfer to nitrocellulose filters, proteins were stained with ponceau S to visualise GST proteins and any associated histones. Protein staining revealed that GST alone did not associate with core histones but GST-Ad12 E4orf6 did [cf lanes 3 and 4, Fig. 4.16]. Staining also revealed that Ad12 E4orf6 did not associate, particularly with histone H1 [Fig 4.16]. These data indicate that AdE4orf6 has the capacity to interact directly with core histones *in vitro*.

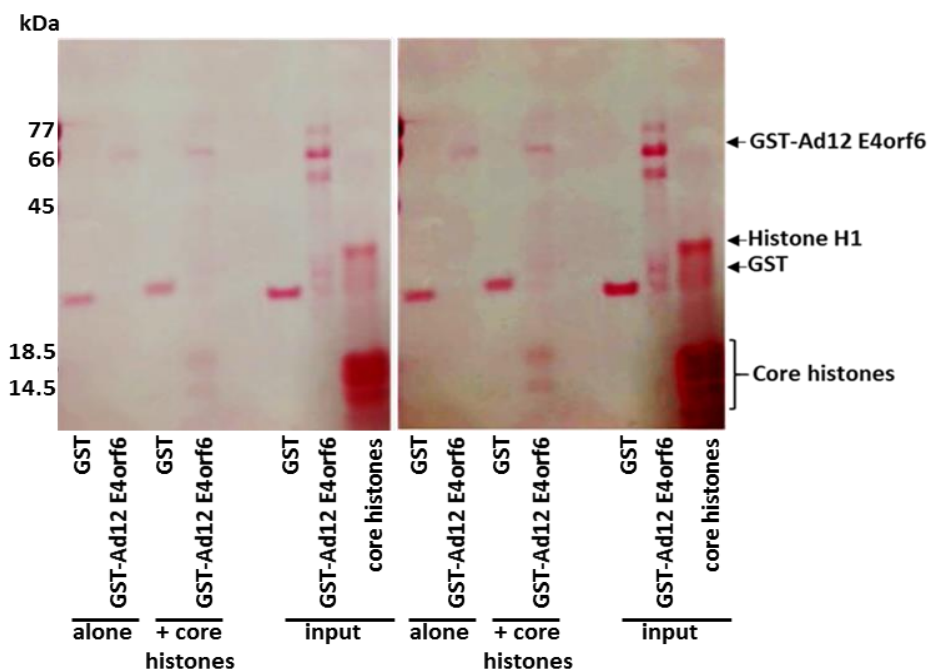


Figure 4.16: GST-Ad12 E4orf6 associates with histones *in vitro*. 5 μ g of GST and GST-Ad12 E4orf6 were incubated in the absence or presence of 5 μ g calf thymus histone fraction VII by end-to-end mixing for 2 h at 4°C. GST proteins and associated proteins were then captured upon glutathione agarose by end-to-end mixing for an additional 2 h at 4°C. Glutathione-agarose associated proteins were separated by SDS-PAGE, transferred to

nitrocellulose and stained with ponceau-S to visualise binding. The first image shows the actual staining observed. The contrast of the second image has been altered so that the difference in histone binding between GST and GST-Ad12 E4orf6 is more clearly visible. The data shown is representative of 3 independent experiments.

4.2.7.6. Investigating the ability of Ad12 E4orf6 complexes to ubiquitylate core histones *in vitro*

As Ad5 E4orf6 has previously been shown to associate with CRL5 to ubiquitylate p53 *in vitro* ubiquitylation assays (Querido, et al. 2001), we decided to adopt a similar approach to see if Ad12E4orf6 complexes immunoprecipitated from HA-Ad12 E4orf6 U2OS cells could promote the ubiquitylation of core histones *in vitro*. To do this we immunoprecipitated Ad12 E4orf6 from HA-Ad12 E4orf6 U2OS cells [section 2.2.5] and incubated immunoprecipitates with histone fraction VII (Sigma-Aldrich) in the presence of an E1-activating enzyme, the promiscuous E2-conjugating enzyme-UbcH5a, ubiquitin and an ATP regeneration mix. After the reactions had been performed they were separated upon SDS-PAGE and analysed by WB for H2A and H3 ubiquitylation. WB revealed that histone H2A was not post-translationally modified to any great extent, although a faint higher molecular weight band was observed [Fig. 4.17]. WBs revealed that histone H3 was modified but there was no obvious difference between the levels of modification between the IgG control and the anti-HA immunoprecipitates. This experiment was only performed once in duplicate and thus requires optimisation but it suggests that under the experimental conditions used Ad12 E4orf6 immunocomplexes do not possess the ability to ubiquitylate histones *in vitro*.

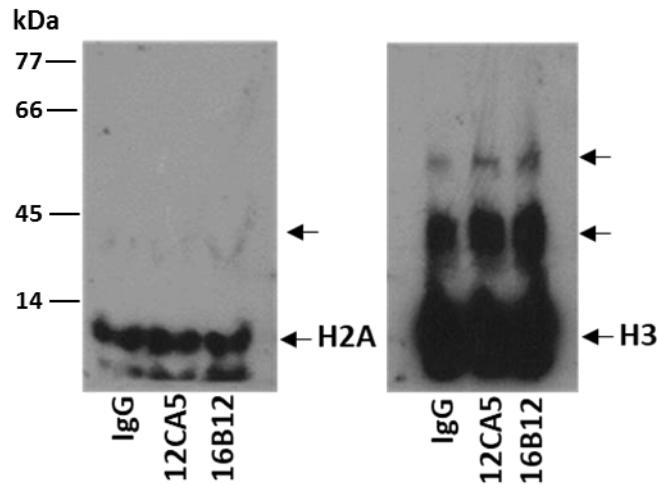


Figure 4.17: Histone-directed *in vitro* ubiquitylation assay. HA-Ad12 E4orf6 was immunoprecipitated from Flp-In T-REx Ad12 HA-tagged-E4orf6 U2OS cells with anti-HA antibodies, 12CA5 and 16B12, or a mouse IgG control onto Protein G sepharose beads. Immunoprecipitates were incubated with an E1-activating enzyme, an E2-conjugating enzyme-UbcH5a, ubiquitin and an ATP regeneration mix in the presence of 1 μ g core histones (histone fraction VII; Sigma-Aldrich) for 1 h at 37°C. Samples were then separated on SDS-PAGE and subject to WB analysis with anti-H2A and anti-H3 antibodies. Arrows indicate potential ubiquitylated versions of H2A and H3. Images taken from one experiment performed in duplicate.

4.2.7.7. Investigating the effects of w.t. Ad5 and w.t. Ad12 infection upon cellular histone levels

As we have shown that Ad12 E4orf6, in isolation, promotes the degradation of all core histones we wished to investigate whether the levels of core histones were also reduced during infection with w.t. Ad12 or w.t. Ad5. WB analyses revealed that the levels of cellular histone proteins, histone H2A and histone H3, were reduced considerably after infection with either w.t. Ad5 or w.t. Ad12 [panels i and ii, Fig. 4.18]. The Ad12 data is consistent with the Ad12 E4orf6 data presented earlier [Fig. 4.12], whilst the Ad5 data is inconsistent with the Ad5 E4orf6 data presented earlier [Fig. 4.13]. The reasons for these discrepancies will be considered in the discussion of this chapter. Consistent with previous studies both Ad5 and Ad12 promoted the degradation of p53 [panel iii, Fig. 4.18], whilst only Ad12 promoted the degradation TopBP1 [panel iv, Fig. 4.18]. Taken together these data suggest that adenoviruses from diverse groups

have the conserved ability to promote the reduction of cellular histone expression during infection.

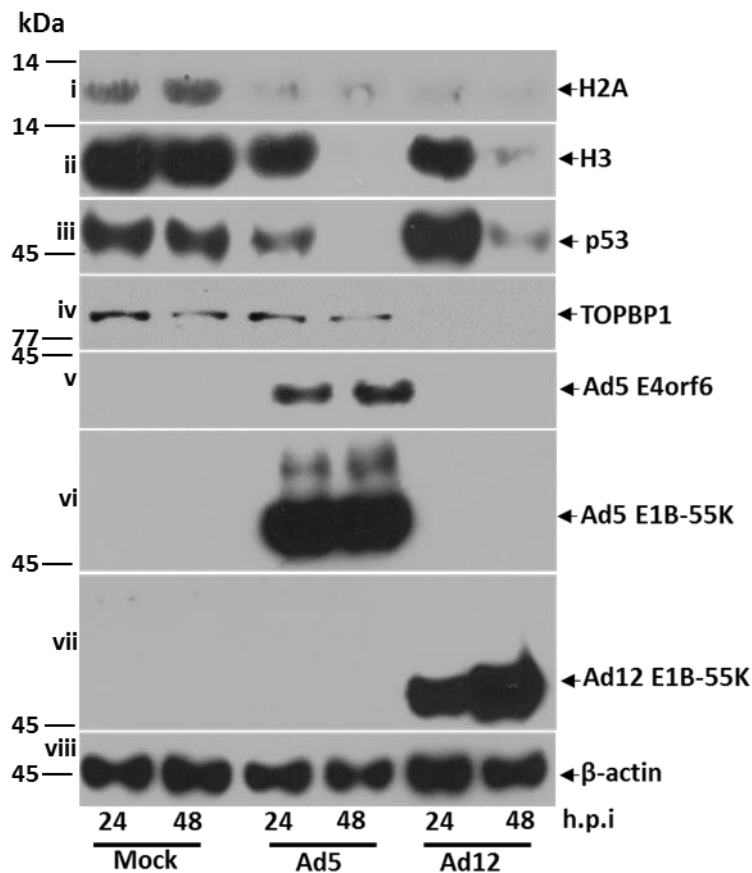


Figure 4.18: Effects of w.t. Ad5 and w.t. Ad12 infection on cellular histone levels. A549 cells were mock-infected or infected with w.t. Ad5 or Ad12 at an m.o.i of 10 p.f.u./cell. Cells were harvested and subjected to WB analysis at the indicated times post-infection using antibodies raised against the proteins indicated. β -actin was used as a loading control. Representative of 3 independent experiments.

4.2.7.8. Effects of w.t. Ad5 and w.t. Ad12 on core histone protein expression

As w.t. Ad5 infection reduced the amount of cellular histone H3 and histone H2A we next decided to investigate whether Ad5 and Ad12 similarly reduced the levels of the other core proteins. We therefore infected A549 cells with these viruses, as described above and performed acidic extraction of basic proteins after 24h post-infection. The isolated proteins were then separated by SDS-PAGE and stained with coomassie blue. Consistent with the WB studies, protein staining revealed that all core histones were reduced following both w.t. Ad5

and w.t. Ad12 infection [Fig. 4.19]. These data are consistent with those presented in [Fig. 4.18] and confirm that a reduction in cellular histone levels is a common feature of both Ad5 and Ad12 infection.

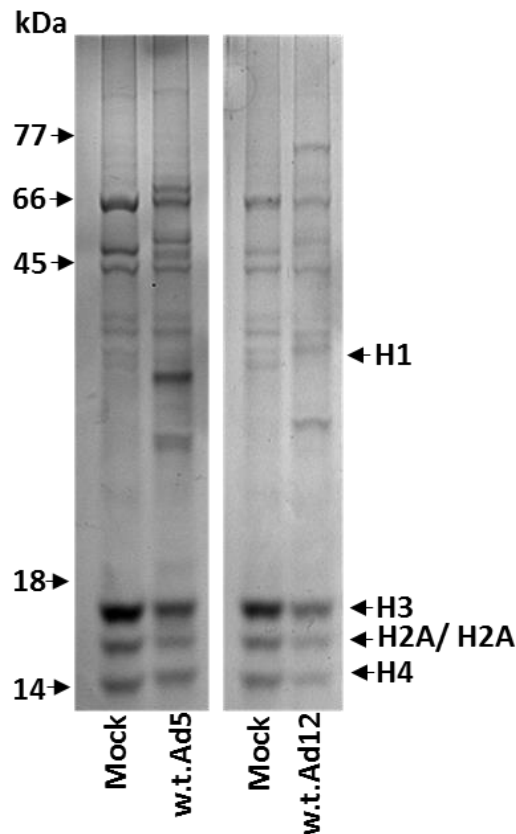


Figure 4.19: Effects of w.t. Ad5 and w.t. Ad12 infection on core histone protein levels. A549 cells were mock-infected or infected with w.t. Ad5 or Ad12 at an m.o.i of 10 p.f.u./cell. Histones were isolated 24 h post-infection by acid extraction (see section 2.2.7), separated by SDS-PAGE and stained with coomassie brilliant blue stain. The data shown is from one experiment, and representative of one other independent experiment.

4.2.8 Effect of Ad5 E4orf6 and Ad12 E4orf6 expression on chromosomal aberrations

4.2.8.1 Metaphase spreads for Ad5 and Ad12 E4orf6 Flp-In T-Rex U2OS cell lines

It is well known that in order to maintain genomic integrity host cells trigger cellular defence pathways (Blackford and Jackson, 2017; see section introduction, section 1.4), but, in mitosis, there is no DNA damage repair (Rieder and Cole, 1998), such that DNA lesions are stabilised and undergo repair in the following G1 phase (Lee, et al. 2016). However, DNA lesions are marked for repair during mitosis such that phosphorylation of histone H2AX marks sites of

DNA damage and recruits the DDR and scaffold protein, MDC1 to these sites (Giunta and Jackson, 2011). Recently, it was found that MDC1 associates with TopBP1 to tether DSBs during mitosis until repair factors are reactivated in G1 phase (Leimbacher, et al. 2019). Disruption of MDC1-TopBP1 association in mitosis is responsible for increased chromosomal aberrations during cell cycle (Leimbacher, et al. 2019). We have shown that TopBP1 is targeted for degradation following the expression of Ad12 E4orf6 but, not Ad5 E4orf6 (see section 3.2.3.4), which is consistent with published results from our laboratory (Blackford, et al. 2010). Given this relationship between Ad12 E4orf6 and TopBP1 we hypothesized that, the loss of TopBP1 following Ad12 E4orf6, but not Ad5 E4orf6, expression would increase the number of chromosomal aberrations during mitosis. To test this possibility we investigated the effects of Ad5 and Ad12 E4orf6 expression upon chromosomal aberrations in mitosis by performing metaphase-spread analyses (Materials and Methods, section 2.3.10). Metaphases were viewed using a Zeiss Axioscop light-microscope; images were captured using Axiovision software. We then quantified the number of chromosomal aberrations observed in each metaphase: i.e. chromosome and chromatid breaks and gaps were scored.

Our analyses revealed that chromosomal aberrations were observed in all experimental conditions [Fig. 4.20, A and B], however, we observed more chromosomal aberrations, particularly chromosome breaks, following the expression of Ad12 E4orf6, relative to Ad5 E4orf6, though significant increases in chromosomal aberrations were observed following the induction of both Ad5 E4orf6 and Ad12 E4orf6 [Fig. 4.20]. These results are consistent with our hypothesis that the Ad12 E4orf6-dependent degradation of TopBP1 destabilises MDC1 at chromosome and chromatid breaks and gaps, leading to higher levels of chromosomal aberrations in the presence of Ad12 E4orf6, although for completeness we do need to establish that Dox-treatment alone does not cause chromosomal damage. It is possible that Ad5 E4orf6

destabilises MDC1 via other mechanisms than TopBP1 degradation to cause chromosomal aberrations (Leimbacher, et al. 2019).

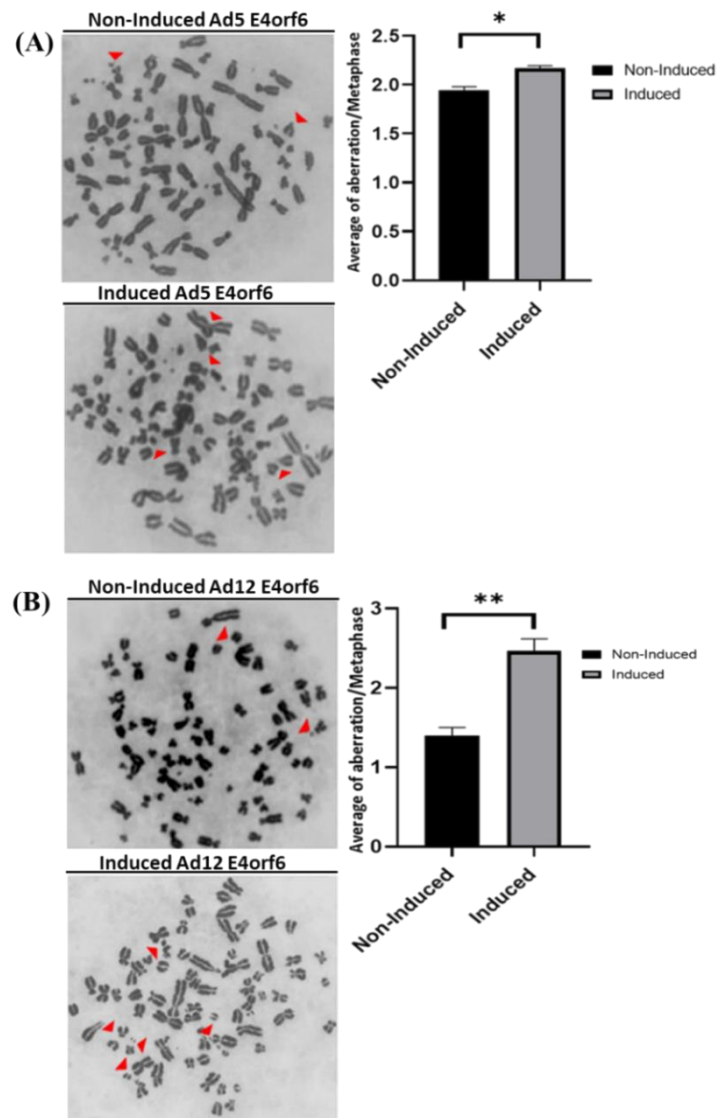


Figure 4.20: Effects of Ad5 E4orf6 and Ad12 E4orf6 expression on chromosomal aberrations in mitosis. The Ad5 and Ad12 E4orf6 Flp-In T-Rex U2OS-FRT cell lines were induced with 0.1µg/ml doxycycline. 24h post induction cells were treated with 0.2µg/ml colcemid 4 hr prior to harvesting. Metaphase spreads were then isolated as described in the Materials and Methods, section 2.3.10). 30 individual metaphases for each experimental condition were viewed under a Zeiss Axioscop light-microscope at 100x magnification and images captured using Axiovision software. The data are represented as mean +/- S.D. two-tailed, unpaired t test (n=3); *P<0.02, **P<0.003. Red triangles indicate chromosomal damage, predominantly in the form of double-strand breaks.

4.3. Discussion

4.3.1. Background

Several studies have identified a number of cellular substrates that are targeted for ubiquitin-mediated proteolysis in an E4orf6 and E1B-55K CRL-dependent manner (Stracker, et al. 2002; Baker, et al. 2007). Importantly, the E4orf6 protein from all human adenovirus types (A-G) are characterised by their ability to associate with cellular CRLs (Gilson, et al. 2016). As such, E4orf6 from different adenovirus species (mast-, at- and avi- adenoviruses) all possess conserved Elongin B and C boxes and Cul boxes that allow E4orf6 to associate with specific CRLs (Gilson, et al. 2016). Work from our laboratory has also shown that Ad12E4orf6, at least, also has the ability to recruit TopBP1 for degradation (Blackford, et al. 2010). E1B-55K and E4orf6 help adenoviruses exploit ubiquitylation during infection to shape the cellular proteome in order to enhance productive infection (Dybas, et al. 2018). The generation of Ad5 and Ad12 E4orf6 U2OS FRT-TREX cell lines (Chapter 3), has afforded us the opportunity to study E4orf6 function in isolation, particularly to investigate the role of E4orf6 in cellular degradation programmes independent of E1B-55K and the possibility that E4orf6 undergoes PTMs. These possibilities were considered in this chapter.

4.3.2. Ad5 E4orf6 is post-translationally modified by ubiquitylation

There is much evidence to indicate that adenovirus proteins are modified by different PTMs, such as phosphorylation and SUMOylation, which help promote viral replication and pathogenesis (Dybas, et al. 2018). Work presented in this chapter identified that Ad5 E4orf6 but not, Ad12 E4orf6 was post-translationally modified, which has not been described previously [Fig. 3.17]. As Ad12 E4orf6 did not undergo PTM, we inspected the E4orf6 protein sequences from Ad5 and Ad12 and determined that Ad5 had 10 potential O-glycosylation sites, whilst Ad12 E4orf6 did not have any [Fig. 4.1]. Given that some viruses exploit glycosylation (Baker, et al. 2007; Bagdonaite and Wandall, 2018; Watanabe, et al. 2019), we investigated the effect of the OGT inhibitor, OSMI-1, on Ad5 E4orf6 PTM but it did not reduce its PTM

suggesting that the PTM observed on Ad5 E4orf6 was not O-glycosylation [Fig 4.2]. We next investigated whether manipulation of the UPS affected the PTM of Ad5 E4orf6. Significantly the proteasome inhibitor, MG132, elevated the level of both unmodified Ad5 E4orf6 and the PTM forms of Ad5 E4orf6, suggesting that the PTM on Ad5 E4orf6 was likely to be ubiquitylation [cf lanes 3 and 4, as well as 7 and 8, Fig. 4.3]. Studies with the NAE inhibitor were suggestive that the ubiquitylation of Ad5 E4orf6 was dependent upon cellular CRLs [Fig. 4.4] and that Ad5 E4orf6 ubiquitylated species were found in the cytoplasm [panel i, Fig 4.5]. We next mutated K95 and K171 in isolation to ablate ubiquitin K acceptor function, which reduced appreciably Ad5 E4orf6 PTM suggesting both of these K residues were acceptor sites for ubiquitylation though K171 was the preferred site of ubiquitylation [Fig. 4.8], which interestingly is the most well conserved K residue in E4orf6 from multiple species [Fig. 4.6], suggesting that E4orf6 ubiquitylation might be conserved between species.

The engagement of E1B-55K and E4orf6 with the cellular UPS to inactivate antiviral pathways during infection is well established (e.g. Querido, et al. 2001; Harada, et al. 2002; Blanchette, et al. 2004). Although viral early proteins have been shown to undergo PTM the data presented here is the first to suggest that a viral early protein is modified by ubiquitin, although co-IP-WB studies with HA-tagged ubiquitin, or anti-ubiquitin antibodies needs to be performed to establish definitively that the PTM observed is ubiquitylation. Moreover, it will also be important to investigate whether Ad5 E4orf6 is subject to PTM during infection with w.t. Ad5 or following cellular transformation. Although Ad5 E4orf6 function during infection has been extensively studied no publication has commented specifically on Ad5 E4orf6 PTM. Careful analysis of published work suggests that Ad5 E4orf6 is subject to PTM during infection (e.g. Fig 1B, (Schmid, et al. 2011), which interestingly appears to be increased following ablation of E4orf6's nuclear export signal (Fig 1B, (Schmid, et al. 2011), though this was not mentioned in the text. In consideration of our data that indicates that ubiquitylated Ad5 E4orf6 is

cytoplasmic [Fig 4.5], the data published by Schmid and colleagues might suggest that E4orf6 is ubiquitylated in the nucleus and then transported to the cytoplasm. Cellular transformation of baby rat kidney (BRK) cells with E1A, E1B-55K and E4orf6 also suggests that Ad5 E4orf6 might undergo PTM (Fig. 2B, Nevels, et al. 2001), though again this was not discussed in the paper.

The cellular consequence of Ad5 E4orf6 ubiquitylation needs to be considered in more detail. Initially, it would be worthwhile to establish that proteasome and NAE inhibitors increase the stability of Ad5 E4orf6, by measuring their effect upon Ad5 E4orf6 protein levels over a time-course in the presence of the protein synthesis inhibitor, cycloheximide. Functionally, it could be envisaged that by engaging with CRLs, Ad5 E4orf6 effectively controls its own destruction and the activity of cellular CRLs against adenovirus targeted substrates, during infection in a temporally-coordinated manner. As such, it would be interesting to establish, using the Ad5E4orf6 KR mutants, whether Ad5 E4orf6 degradation is required for the E1B-55K/E4orf6 and CRL-dependent degradation of substrates, like p53 or Mre11, or whether enhanced stability of the KR E4orf6 mutants enhances the degradation of adenovirus substrates. As ubiquitylated Ad5 E4orf6 is found in the cytoplasm and that the E1B-55K/E4orf6-CRL is required for the transport of viral mRNA into the cytoplasm, it would also be interesting to establish, using the KR E4orf6 mutants, whether the transport of viral transcripts from the nucleus to cytoplasm is dependent on Ad5 E4orf6 ubiquitylation. This could be achieved by qPCR detection of viral transcripts in the cytoplasm using mutant KR-E4orf6 adenoviruses. Given that E4orf6 also possesses transforming capability in the presence of E1A and E1B-55K it would be also interesting to see whether ablation of Ad5 E4orf6 ubiquitylation sites by mutation also affects the ability of E4orf6 to participate in the cellular transformation of Rat embryo fibroblasts or BRKs with E1A and E1B-55K. Finally, it would be interesting to establish whether E4orf6 ubiquitylation was conserved between different adenovirus types and

if so, whether ablation of E4orf6 ubiquitylation from these adenovirus types affected its biological functions.

Although many viruses encode proteins that modulate cellular CRL activity (e.g. HPV, SV40, EBV, KSHV, HSV1, HIV-1, HepB; reviewed by (Mahon, et al. 2014) there is little published information to indicate that the viral protein is also a substrate for the CRL to which it associates. The only possible exception is HPV E7 which associates with CRL2 to promote the degradation of pRB (Huh, et al. 2007). Although the Huh paper does not investigate E7 ubiquitylation by CRL2, an earlier publication indicated that a Cullin 1 and Skp2- containing CRL could ubiquitylate E7 in an *in vitro* E3 ligase assay (Oh, et al. 2004). Experiments with proteasome inhibitors suggested that ubiquitylated E7 was transported to intranuclear bodies for proteasomal degradation (Oh, et al. 2004), though further studies have not considered whether HPV E7 association with CRL2 is responsible for regulating HPV E7 stability.

4.3.3. Identification of core histone proteins as targets for CRL-dependent degradation following Ad12 E4orf6 expression

Previous studies from our laboratory indicated that Ad12 E4orf6, in the absence of E1B-55K expression, targeted TopBP1 for degradation in a CRL2- dependent manner (Blackford, et al. 2010). Here, we used a quantitative mass spectrometric approach using ‘heavy’ and ‘light’ formaldehyde to label peptides retrieved from cell lysates +/- Ad12 E4orf6 expression, in order to identify other cellular proteins targeted for degradation by Ad12 E4orf6 (section 4.2.7). Using this approach we identified 256 different proteins from 2 independent experiments that were labelled with both ‘heavy’ and ‘light’ formaldehyde such that we could quantify the effects of Ad12 E4orf6 expression on their levels. Given that we only identified 256 cellular proteins it is perhaps not surprising that we did not identify TopBP1 in our analyses and identified, more abundant cellular proteins using this approach. Interestingly, however, we

identified core histone proteins as major targets for CRL and proteasome-mediated degradation following Ad12 E4orf6 expression [Table 4.1; Figs. 4.12-4.15].

DNA is packaged inside the nucleus of the cell in chromatin. Approximately 146 DNA base pairs wrap around an octamer of core histone proteins (2 copies each of H3-H4 and H2A-H2B dimers) to form the nucleosome, the basic unit of chromatin (Mirza, et al. 1982). The function of the core histones goes beyond simple packaging of the DNA and histone PTM by acetylation, methylation, ubiquitylation, phosphorylation etc (modulated by histone writers and erasers), through histone readers regulates cellular gene expression, DNA replication and DNA repair. Core histones also have the capacity to modulate viral gene expression and DNA replication, as either proviral or antiviral agents (Stern and Berger, 2000; Kobiyama, et al. 2010). Indeed, Ad5 E1A interacts with the histone acetyltransferases CBP/p300 to modulate H3K18 acetylation, and moreover, regulates cellular transcription programmes during infection through interaction with both CBP/p300 and pRB (Horwitz, et al. 2008). Indeed, although E1A does not interact with core histones directly it has long been known to interact with histone writers, erasers and readers during infection to modulate histone function (Turnell and Gallimore, 2001). Moreover, most, if not all, viruses similarly encode proteins that interact with cellular chromatin writers, erasers and readers to regulate cellular transcription programmes to support viral replication (Wei and Zhou, 2010).

Consistent with the ability of Ad12 E4orf6 to target core histones for degradation, we showed by GST pull-down assay that Ad12 E4orf6 interacts with core histones directly [Fig. 4.16]. These data are consistent with our earlier studies that determined that Ad12 E4orf6 also interacted with CRL2 substrate TopBP1 directly (Blackford, et al. 2010). Although many viral genomes, including adenovirus, become ‘chromatinized’ during infection and many viral proteins (e.g. adenovirus protein VII) also act as histone mimics to package viral DNA (see section 1.1.4), to date there aren’t many viruses whose proteins are known to associate directly

with core histones to modulate their activity or levels. The Dengue virus capsid protein DENVC accumulates in the nucleus, where it associates with all core histones as heterodimers in order to disrupt and inhibit normal histone function (Colpitts, et al. 2011), whilst LANA from KSHV (Barbera, et al. 2006) and IE1 from CMV (Mücke, et al. 2014) bind directly to histones to an acidic pocket on the nucleosome surface to modulate higher order chromatin organization. The EBV BKRF4 tegument protein also binds to histone H2A-H2B and H3-H4 dimers, through a different mechanism to LANA and IE1, to inhibit DDR signalling during EBV infection (Ho, et al. 2018). As such, it will be important to establish where Ad12 E4orf6 binds to core histones and whether this is modulated by histone PTM.

Work presented here indicated that although Ad5 E4orf6 could not promote the degradation of core histones directly, infection with w.t. Ad5, like w.t. Ad12, promoted the loss of cellular core histones [Figs. 4.18 and 4.19]. This might suggest that E4orf6 cooperates with E1B-55K during infection to promote histone degradation, and further studies should investigate this possibility and the role played by CRLs in this process. Work by Jane Flint over 35 years ago determined that histone gene expression was reduced following Ad2 infection of HeLa cells (Flint, et al. 1984) though the cellular protein levels of core histones were not investigated in that study, or in any study since. It is possible therefore during infection that histone levels are controlled at the level of transcription and translation. Interestingly, it has recently been shown that DNA damage promotes the proteasomal-mediated degradation of core histones by 20-40% (Hauer, et al. 2017). It might be that although adenovirus inhibits a number of DDR pathways during infection it is possible that other DDR pathways in Ad-infected cells are activated, which promote core histone loss.

The question arises why adenovirus promotes the loss of cellular core histones during infection. It is most likely that adenoviruses modulate cellular transcription programmes and DNA replication programmes through the loss of core histones. It is possible that loss of histones

leads to an open chromatin configuration that promotes gene expression. It would be extremely interesting, given our findings to characterise whether histone loss is selective at the level of gene promoters and gene regions at the genomic level and correlates with cellular gene expression levels. It is also possible that core histone loss helps the virus to inhibit cellular DNA replication which requires histone deposition on newly synthesized DNA. These studies will help establish why adenoviruses selectively promote the loss of core histones during infection.

4.3.4. Chromosomal aberrations following Ad5 and Ad12 E4orf6 expression

Here we determined that the expression of both Ad5 E4orf6 and Ad12 E4orf6 induced chromosomal aberrations, particularly chromosomal breaks [Fig. 4.20, A and B]. The Ad12 studies are in good agreement with the finding that loss of TopBP1 affects MDC1 stabilization of chromosome breaks and gaps during mitosis (Leimbacher, et al. 2019). How Ad5 E4orf6 promotes chromosomal aberrations in this circumstance is not immediately clear as it does not promote TopBP1 degradation, though it might disrupt MDC1 function via other pathways (Leimbacher, et al. 2019). These findings are consistent with very early studies that indicate that adenovirus 12 infection resulted in chromosomal aberrations (zur Hausen, 1967; McDougall, 1970; Zur Hausen, 1976). Such chromosomal disruption might be important in how adenovirus can promote chromosomal and genomic instability that leads to cellular transformation by a ‘hit and run’ mechanism (Nevels, et al. 2001), and might explain why persistent adenovirus infection of lymphocytes has been linked with childhood acute lymphoblastic leukaemia (Gustafsson, et al. 2007).

Collectively, the studies detailed in this Chapter have provided insights into the molecular functions of Ad5 and Ad12 E4orf6 proteins which have important ramifications for understanding E4orf6 function during infection, cellular transformation and oncogenesis.

CHAPTER 5



Investigating the role of the FACT complex during adenovirus infection

5.1. Introduction

Adenovirus viral replication centres are structural entities in the nucleus that coordinate viral transcription, viral DNA replication, viral particle assembly and packaging (Charman, et al. 2019). Previous work in our laboratory attempted to identify proteins that are recruited to VRCs through interaction with the RPA complex, a cellular protein complex known to be recruited to VRCs (Qashqari, PhD thesis, University of Birmingham, 2017). Of those proteins identified, the FACT chaperone complex, comprising SPT16 and SSRP1, Pur α and Pur β transcriptional regulators and the RNA-binding protein, RBM14 were all identified as cellular proteins that are recruited to VRCs during infection and are thus considered worthy of further investigation. The FACT complex has been considered in detail in the introduction (section 1.1.5.1), so here, we will consider Pur α , Pur β and RBM14.

Pur α , Pur β and Pur γ are members of the Pur protein family that are characterized by their high affinity for purine-rich elements (Lezon-Geyda, et al. 2001; Gupta, et al. 2007; Johnson, et al. 2013). Pur proteins function in diverse aspects of cell growth and differentiation by regulating both transcription, translation and the modulation of apoptosis (Gupta, et al. 2007). Pur α and Pur β have been reported to be dysregulated in acute myelogenous leukemia and brain tumours (Lezon-Geyda, et al. 2001; Johnson, et al. 2013). In addition, both Pur α and Pur β have been suggested to participate in cellular senescence (Munich, et al. 2014). Pur α has been shown to be required for human polyomavirus 2 gene expression and viral replication (Sariyer, et al. 2016). RNA binding motif protein 14 (RBM14) belongs to the family of RNA binding proteins. RBM14 is a multifunctional protein that is involved in transcription, splicing, DNA repair and genome integrity (Li, et al. 2019; Jang, et al. 2020). Influenza A virus has been shown to utilise RBM14 for its replication cycle and the NS1 protein actively reorganises RBM14 to the nucleolus for this purpose (Beyleveld, et al. 2018). The EBV non-coding RNA, EBER2 also interacts with RBM14 to modulate LMP2 oncogene expression (Lee, et al. 2016).

The aim of the work presented in this chapter was to take forward previous findings that suggested the FACT complex, Pur α , Pur β and RBM14 were recruited to VRCs during adenovirus infection. As such, we investigated whether these proteins were: recruited to VRCs during infection; targeted for degradation during infection; and/or possessed anti-viral or pro-viral activities during infection. Findings from these studies are described here.

5.2. Results

5.2.1. The protein levels of SPT16, SSRP1, Pur β and RBM14 are not altered following adenovirus infection.

Previous studies from our laboratory had indicated that in addition to SMARCAL1 (Nazeer, et al. 2019), FACT complex components-SPT16 and SSRP1, nucleotide binding proteins-Pur α and Pur β and RNA binding protein-RBM14 all associated with RPA complex component, RPA1, following GFP-RPA1 pulldown from both Ad5 and Ad12 infected GFP-RPA1 U2OS cells, but not GFP U2OS cells (Qashqari, University of Birmingham PhD thesis 2017). Given that other studies from our laboratory have indicated that SMARCAL1 was targeted in an E1B-55K/E4orf6- and cullin RING ligase-dependent manner for proteasomal degradation during both Ad5 and Ad12 infection we decided to investigate whether SPT16, SSRP1, Pur β or RBM14 were similarly targeted for degradation following adenovirus infection.

To test this possibility A549 cells were either mock-infected or infected with w.t. Ad5 or w.t. Ad12 and subjected to WB. WB analyses showed that consistent with previous observations anti-viral proteins p53 and SMARCAL1 were targeted for degradation following both Ad5 and Ad12 infection [panels i and ii, Fig. 5.1 A and B, respectively]. Interestingly, however, those proteins that had previously been shown to associate with RPA1 during infection-SSRP1, SPT16, Pur β and RBM14 were not targeted for degradation during either Ad5 or Ad12 infection [panels iii-vi, Fig. 5.1 A and B]. Furthermore, the WB data suggested that SSRP1, SPT16, Pur β and RBM14 were not subjected to PTM following adenovirus infection. Taken

together, these data indicate that SSRP1, SPT16, Pur β and RBM14 are not typical anti-viral cellular proteins that undergo degradation during infection. However, at this stage it is not possible to discern these proteins possess pro- or anti- viral activities.

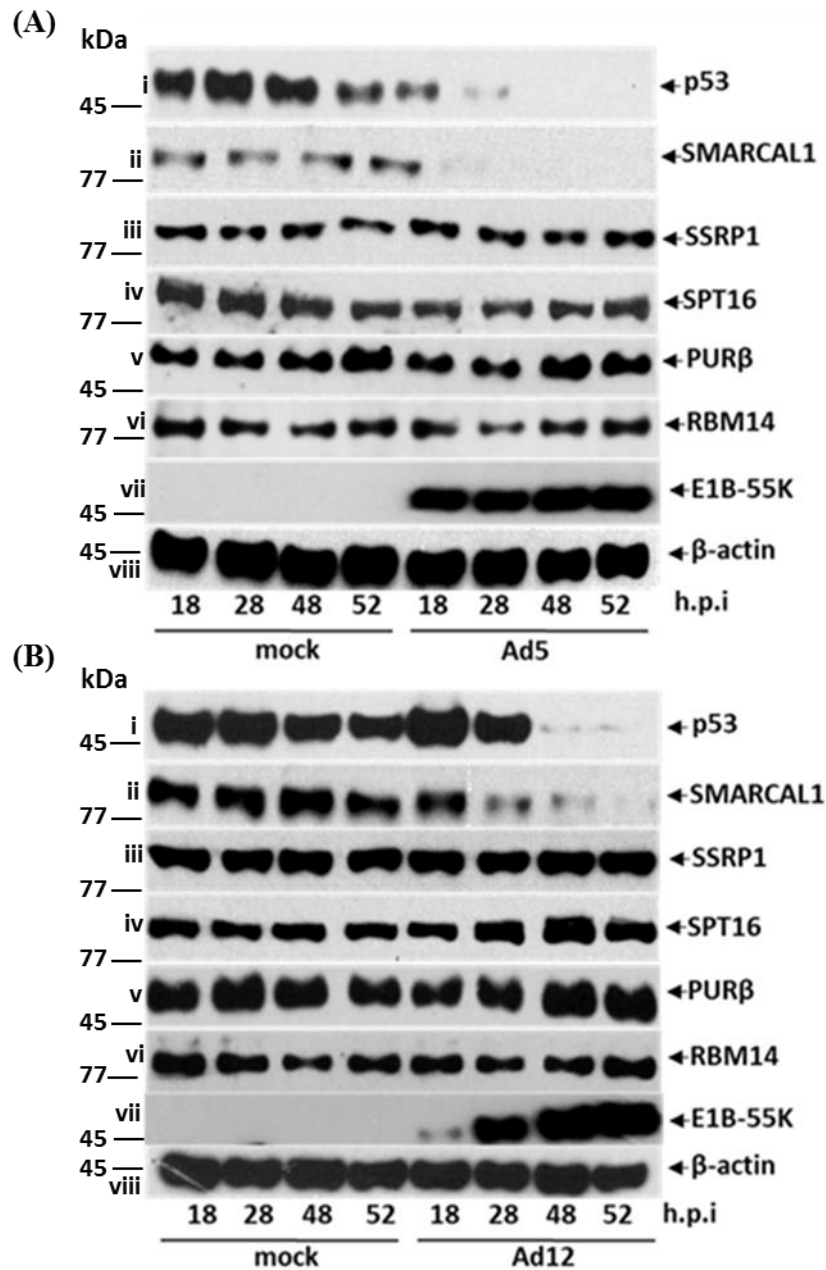


Figure 5.1: The protein levels of SPT16, SSRP1, PUR β and RBM14 are not altered following Ad5 or Ad12 infection. A549 cells were mock-infected or infected with w.t. Ad5 or w.t. Ad12 at an m.o.i of 10 p.f.u./cell. Cells were harvested at the indicated times and subjected to SDS-PAGE and WB using the appropriate antibodies. The data shown is representative of 3 independent experiments.

5.2.2. Validation of SPT16, SSRP1, PUR β and RBM14 association with RPA1 following adenovirus infection

Our laboratory previously used GFP-U2OS and GFP-RPA1 U2OS cell lines in combination with MS to identify proteins that associated with RPA1 in both uninfected cells and in cells following Ad5 or Ad12 infection (Qashqari, University of Birmingham PhD thesis 2017). As none of the candidate proteins investigated here were shown to be degraded after adenovirus infection, as would be expected for most anti-viral cellular proteins, we next decided to establish whether these proteins did, indeed, associate with RPA1 in uninfected cells or in cells following Ad5 infection. To do this, we either mock-infected or infected GFP-U2OS and GFP-RPA1 cells with w.t Ad5 and subjected cell lysates to GFP pulldown with GFP-Trap beads (Materials and Methods, section 2.2.10). Isolated proteins were then separated by SDS-PAGE and subjected to WB analysis to establish whether or not, these cellular proteins associated with RPA1.

WB analysis confirmed that GFP and GFP-RPA1 were expressed to similar levels [panel i, Fig. 5.2] and useful conclusions could be drawn about the ability of the proteins studied to bind to RPA. Consistent with our MS studies our GFP pulldown experiments revealed that, like SMARCAL1, SSRP1 and SPT16 were both recruited to RPA1 following Ad5 infection [cf panels iii and iv with panel ii, Fig. 5.2]. The RNA-binding protein, RBM14, although it did bind RPA1 specifically, its ability to associate with RPA1 was not altered by Ad5 infection [panel v, Fig. 5.2]. Interestingly however, Pur β , which had previously been shown to bind RPA1 following adenovirus infection did not bind to RPA1, either in uninfected cells or Ad5-infected cells [panel vi, Fig. 5.2]. Taken together, these data help establish that FACT components, SPT16 and SSRP1 associate with RPA1 selectively after Ad5 infection and that RBM14 also associates with RPA1, whereas Pur β does not appear to bind RPA1.

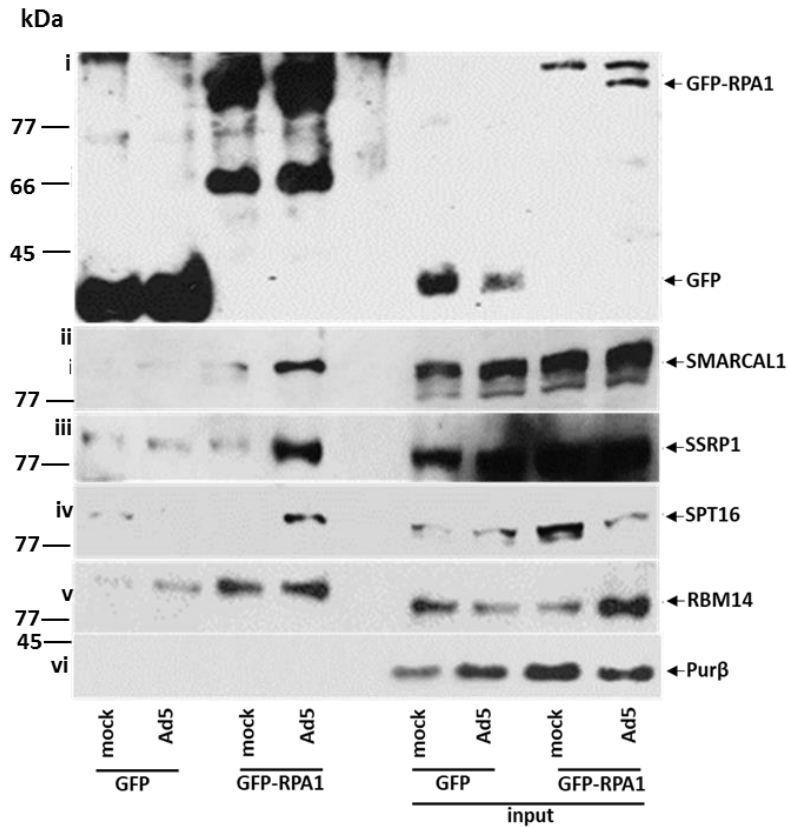


Figure 5.2: GFP-Pulldown demonstrating FACT and RBM14 association with RPA1 in Ad5-infected cells. GFP-U2OS and GFP-RPA1-U2OS cells were either mock-infected, or infected with Ad5 at an m.o.i of 10 p.f.u./cell. 24h post infection cells were harvested and subjected to GFP pulldown utilizing GFP-Trap beads (Materials and Methods, section 2.2.10). Isolated proteins were then separated by SDS-PAGE, and subjected to WB analysis. The data shown is representative of 3 independent experiments.

5.2.3. Recruitment of SPT16 to VRCs with RPA following w.t Ad5 and Ad12 infection

Previous studies from our laboratory have determined that the FACT complex component, SSRP1, associates with RPA2 at VRCs (Qashqari, University of Birmingham PhD thesis 2017). As we had not established previously whether SPT16 was also recruited to VRCs during infection we next sought to establish whether this was the case or not. We therefore co-stained the cells with an anti-rabbit SPT16 antibody and a mouse anti-RPA2 antibody and appropriate fluorophore-conjugated secondary antibodies to visualise these proteins by immunofluorescence. These studies revealed that RPA2 was pan-nuclear in mock-infected cells, whilst in Ad5 and Ad12 -infected cells it was reorganised to VRCs. Interestingly,

however, SPT16 existed as discrete intranuclear foci in both mock-infected, and Ad5 and Ad12-infected cells [Fig. 5.3]. Consistent with the GFP pull-down studies [Fig. 5.2] it appeared that RPA2 and SPT16 did not co-localize in mock-infected cells but did co-localize in both Ad5 and Ad12-infected cells [Fig. 5.3]. These data suggest that as RPA2 is a marker for VRCs that VRCs might originate at intranuclear sites occupied by SPT16.

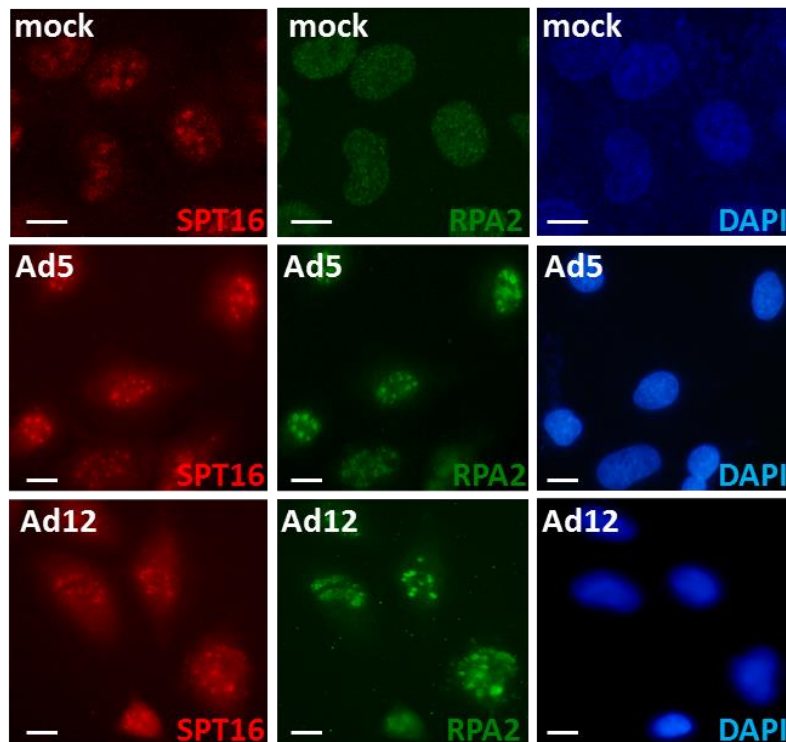


Figure 5.3: Co-localization of SPT16 with RPA32 to VRCs during w.t. Ad5 and w.t. Ad12 infection. Cells were plated on glass slides then fixed in 4% (w/v) paraformaldehyde and permeabilized in ice-cold acetone. 24 h post-infection cells were incubated with an anti-SPT16 antibody (red), an anti-RPA32 antibody (green) and counter-stained with anti-mouse Alexa Fluor 488 and anti-rabbit Alexa Fluor 594 secondary antibodies. Slides were then mounted in Vectashield containing DAPI. Images were visualised using a whole-field Nikon Y-FL epi-fluorescence microscope. The data shown is representative of 2 independent experiments. Scale bar = 20 μ m.

5.2.4. Recruitment of RBM14 to VRCs during Ad5 and Ad12 infection

We next investigated whether RBM14 was similarly recruited to VRCs or nuclear tracks during adenovirus infection. We therefore infected A549 cells with w.t. Ad5 or a recombinant Ad12 virus, where the E4orf3 gene had been replaced with HA-tagged E4orf3 to facilitate its

detection and analysed their recruitment to nuclear tracks by immunofluorescence [section 2.3.9.]. Immunofluorescent staining revealed that RBM14 was mostly cytoplasmic in mock-infected cells, whereas in both w.t. Ad5 and Ad12-infected cells it was reorganized to discrete intranuclear sites that co-localized to some extent with E4orf3, although not exclusively [Fig. 5.4]. These data suggest that RBM14 is likely recruited to both VRCs and nuclear tracks during both Ad5 and Ad12 infection.

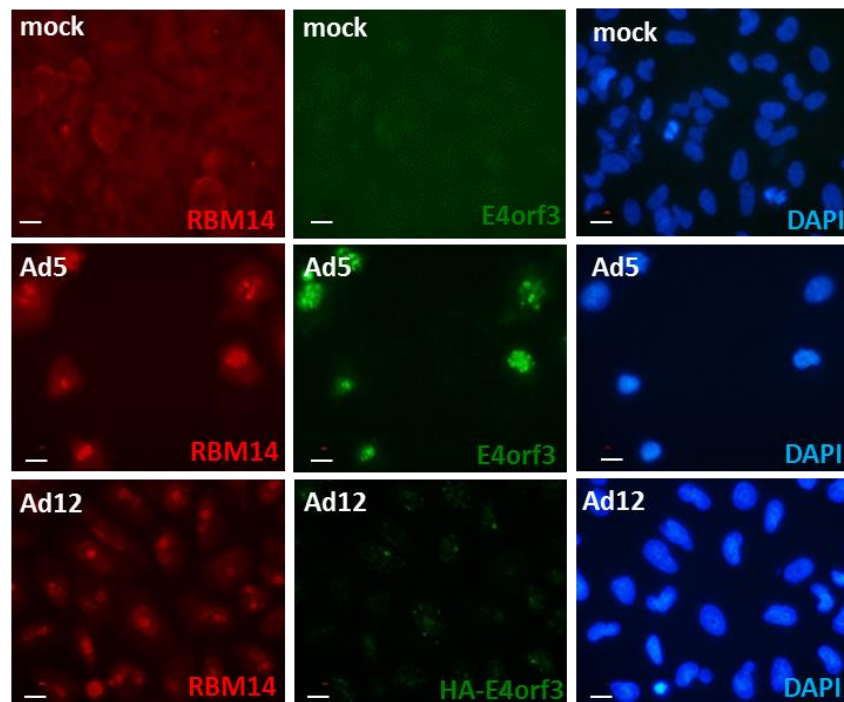


Figure 5.4: Recruitment of RBM14 to VRCs during w.t. Ad5 and w.t. Ad12 infection. Cells were plated on glass slides then fixed in 4% (w/v) paraformaldehyde and permeabilized in ice-cold acetone (see section 2.4.5). 24 h post-infection cells were incubated with an anti-RBM14 antibody (red), or an anti-Ad5E4orf3 antibody (green), or an anti-HA antibody (HA-Ad12 E4orf3, green) and counter-stained with anti-mouse Alexa Fluor 488 and anti-rabbit Alexa Fluor 594 secondary antibodies. Slides were then mounted in Vectashield containing DAPI. Images were visualised using a whole-field Nikon Y-FL epi-fluorescence microscope. The data shown is representative of 2 independent experiments. Scale bar = 10 μ m.

5.2.5. Pur β is not recruited to VRCs during Ad5 and Ad12 infection

We next wished to investigate whether Pur β was also recruited to VRCs during adenovirus infection. Unfortunately, the commercially available Pur β antibody was not suitable for

immunofluorescence studies. We therefore decided to construct a GFP-tagged Pur β construct as we knew that GFP-tagged RPA1 was recruited to VRCs successfully following adenovirus infection (Nazeer, et al. 2019). To do this we first amplified and cloned Pur β into the GFP vector, pEGFP-C3 (see Materials and Methods section 2.3.4) and validated sequence integrity by Sanger sequencing and a combination of Chromas and the NCBI BLAST program [Fig. 5.5]. Sequencing results indicated that we had successfully generated full-length w.t. GFP-Pur β plasmid [Fig. 5.5 and data not shown].

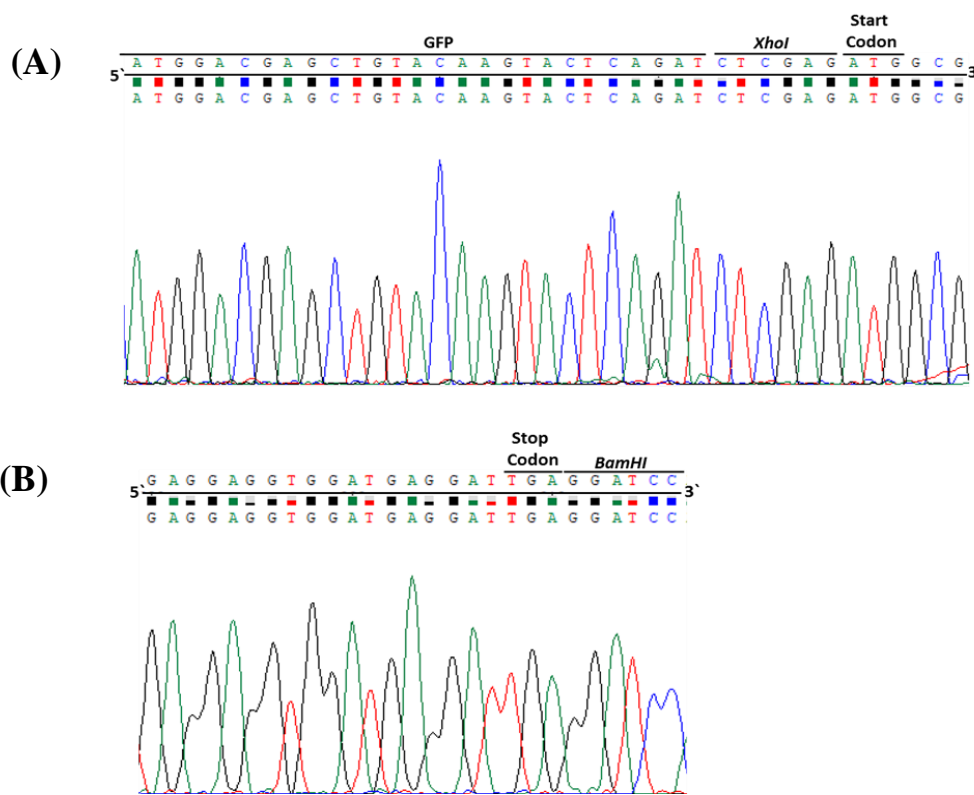


Figure 5.5: Sanger sequencing indicating the integrity of 5' and 3' the pEGFP-C3- Pur β construct. (A) Illustrates the 3' end of the GFP sequence showing the XhoI cloning site and the start codon of the Pur β gene (ATG); (B) Illustrates the 3' end of the Pur β gene sequence showing the stop codon (TGA) and the BamHI cloning site.

To generate a GFP-Pur β RPE-1 stable cell line we transfected the pEGFP-Pur β plasmid into RPE-1 cells and isolated by selection [section 2.1.7]. Following the generation of these cells we next investigated whether GFP-Pur β was recruited to VRCs during adenovirus infection.

Clonal GFP-Pur β RPE-1 cells were therefore infected with w.t. Ad5 or w.t. Ad12 and the cellular localisation of GFP-Pur β in these clonal RPE-1 cells visualized using an EVOS fluorescent digital inverted microscope [Fig. 5.6]. In mock-infected cells GFP-Pur β was almost predominantly cytoplasmic, with only a small amount of nuclear staining visible [Fig. 5.6]. The cellular localisation of GFP-Pur β remained cytoplasmic throughout the time-course of infection up to 72 h and there was no obvious accumulation of GFP-Pur β at intranuclear sites [Fig. 5.6 and data not shown]. Taken together, these data suggest Pur β is not recruited to VRCs during either Ad5 or Ad12 infection. The reasons for these apparent discrepancies will be discussed in detail later.

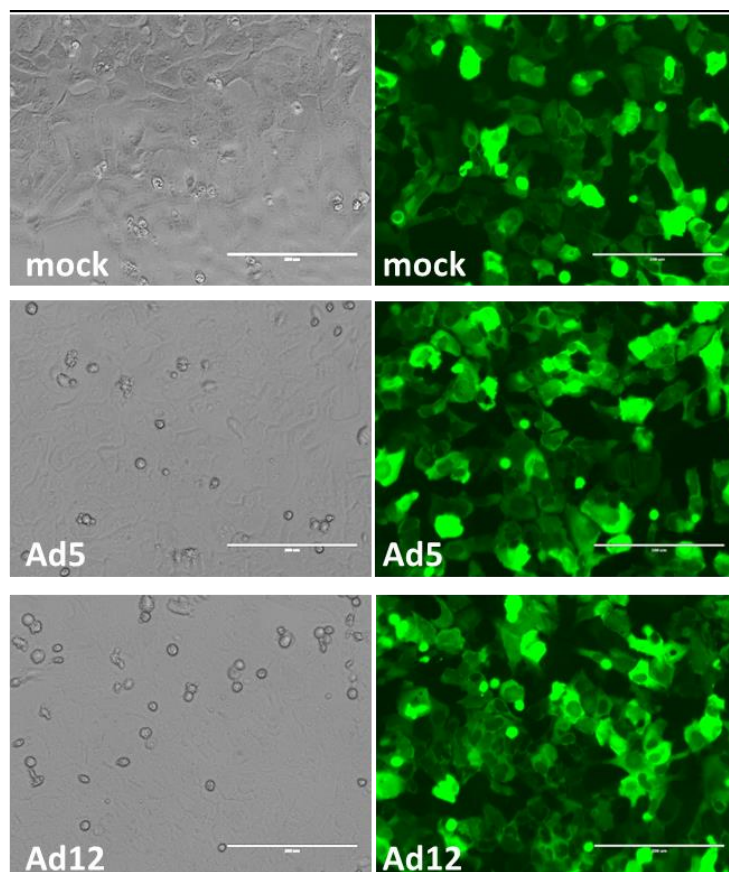


Figure 5.6: Pur β is not recruited to VRCs during w.t. Ad5 or w.t. Ad12 infection. Cells were either mock-infected, or infected with w.t. Ad5 or w.t. Ad12. 24 h post-infection cells were visualized with an EVOS fluorescent digital inverted microscope, scale bar = 200 μ m showing both cells under phase-contrast and cell GFP expression. The data shown is representative of 2 independent experiments.

5.2.6. The FACT complex modulates adenovirus early region gene product expression

Given that the FACT complex was shown to be present at VRCs in Ad-infected cells this suggests that SPT16 and SSRP1 might possess either pro-viral or anti-viral activity. As FACT possesses the ability to regulate transcription we decided to examine whether SPT16 and SSRP1 regulate adenovirus early region transcription programmes during infection. To do this we used RNA interference to knock down the expression of both SPT16 and SSRP1 in A549 cells then infected cells with either w.t. Ad5, or a w.t. Ad12 species that expresses FLAG-tagged E4orf3. Cell lysates were then subjected to SDS-PAGE and WB analyses for early region proteins. WB analyses revealed that we had successfully knocked-down the expression of both SPT16 and SSRP1 [panels v and vi, Fig. 5.7 A and B respectively]. Our results also suggested that, FACT complex knockdown affected differentially the expression of early region gene products E1B-55K, E2A and E4orf3 following both Ad5 and Ad12 infection. As such, FACT complex component knockdown reduced the expression of Ad5 E1B-55K, E2A and E4orf3, though E1A expression was not altered appreciably [panels i-iv, Fig. 5.7 A]. This was particularly evident for E2A and E4orf3 at all time-points and E1B-55K at later times of infection. The response in Ad12-infected cells was more complex: E1A and E1B-55K levels were elevated following the infection of knockdown cells, whereas E2A and E4orf3 levels were reduced [panels i-iv, Fig. 5.7 B]. Taken together, these data suggest that the FACT complex serves to regulate viral gene expression during adenovirus infection.

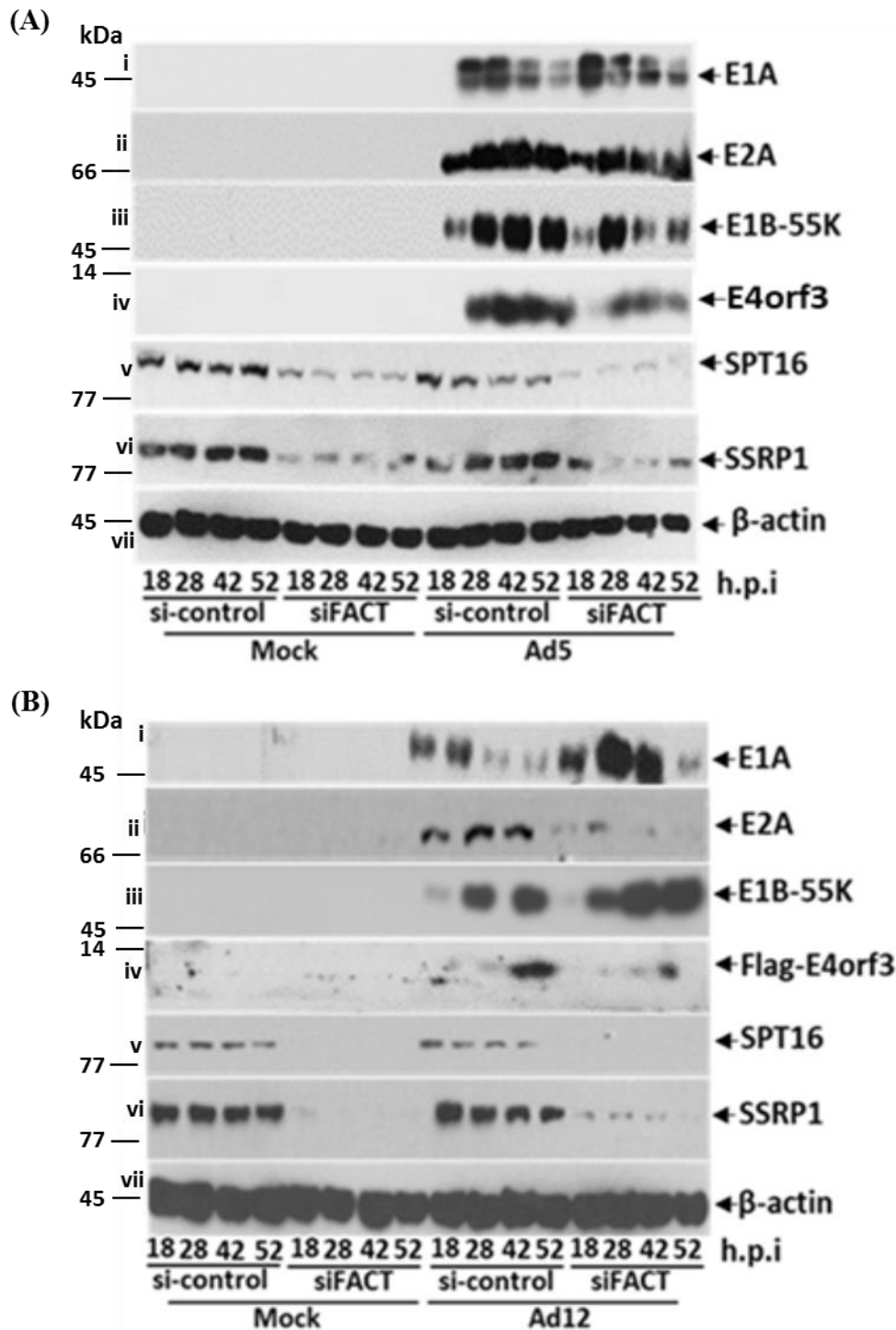


Figure 5.7: The FACT complex regulates adenovirus early region gene product expression. A549 cells were transfected with the indicated siRNAs for 48 h, before being mock-infected or infected with Ad5 (A) or Ad12 (B). Cells were harvested at the indicated times post-infection and subjected to SDS-PAGE and WB analysis using the appropriate antibodies. The data shown is representative of 3 independent experiments.

5.3 Discussion

5.3.1 Background

As outlined in section 5.1 VRCs are discrete intranuclear structures where adenovirus genome transcription and replication occurs, as well as viral particle assembly and Charman, (Herrmann, et al. 2019). Although we know that both pro-viral and anti-viral cellular proteins are recruited to VRCs during infection we do not fully appreciate the extent to which cellular proteins participate in modulating viral genome replication at these sites. As such, we previously identified cellular proteins that were recruited to the cellular RPA complex at VRCs during adenovirus infection, which identified the FACT complex, RBM14, and Pur α and Pur β (Qashqari, PhD thesis, University of Birmingham, 2017). Work detailed in this Chapter attempted to validate these findings and investigate their role in adenovirus replication. Whilst we confirmed that both the FACT complex and RBM14 were components of VRCs we could not confirm the recruitment of Pur β to VRCs.

5.3.2. Investigating the role of the FACT complex during adenovirus infection

Studies in this chapter established that FACT components, SPT16 and SSRP1 are not targeted for degradation during infection, suggesting that they do not participate in the host DDR response to viral infection [Fig. 5.1]. This is perhaps surprising as SPT16, at least, has been shown to interact with SMARCAL1 in both 293T and HeLa cells, and is therefore likely to participate in DDR signalling during cellular DNA replication (Bétous, et al. 2013). Indeed, previous studies from our laboratory have established that SMARCAL1 is targeted for degradation during infection (Nazeer, et al. 2019). The study detailed here established that both SPT16 and SSRP1 only associated with RPA, component, RPA1 during infection [Fig. 5.2] and that SPT16 co-localized with RPA component, RPA2 at VRCs during both Ad5 and Ad12 infection [Fig. 5.3]. Interestingly, it appeared that RPA2 was recruited to SPT16 during infection such that VRCs formed at FACT-containing intranuclear loci [Fig. 5.3] and suggests that the FACT complex might be important in the nascent production of VRCs. This is an

interesting and perhaps, unexpected, finding. Previous studies looking at VRC formation for DNA viruses at least, suggests that VRCs from DNA viruses that form in the cytoplasm (e.g. *Poxviridae* family) originate at, or close to microtubule-organising centres (MTOCs), whilst DNA viruses that form VRCs in the nucleus (e.g. *Adenoviridae* family) originate adjacent to PML-containing nuclear bodies (PML-NBs; (Schmid, et al. 2014). Although PML-NBs are known to be involved in transcription and DNA replication amongst other functions, the FACT complex is not known to be a component of PML-NBs (Van Damme, et al. 2010), though whether they lie adjacent to PML-NBs has not been explored. Given our finding that SPT16 is a component of VRCs, it will be important in future studies to explore whether the nuclear foci occupied by the FACT complex lie close to PML-NBs. Moreover, given that E2A/DBP is a major component of VRCs (Pombo, et al. 1994), it would be interesting to study whether FACT knockdown affects E2A/DBP localisation during infection or affects viral DNA genome replication which could be assessed by qPCR.

Although previous studies have indicated both pro-viral and anti-viral roles for the FACT complex in viral replication, there are no publications to date have reported that FACT is a component of VRCs. Our knockdown data suggests that FACT is pro-viral for both Ad5 and Ad12 and participates in viral early gene transcription [Fig. 5.7]. Other viruses similarly utilise the FACT complex to promote viral gene transcription. For instance, it has been reported that HSV-1 viral protein ICP22 binds to FACT directly, and recruits the FACT complex to the HSV-1 genome to facilitate viral gene transcription, such that an ICP22 mutant virus, is attenuated in its ability to synthesize most viral mRNAs during infection, relative to a w.t. virus (Pombo, et al. 1994). Additionally, the FACT complex is utilised by HCMV viral protein LANA to promote the transactivation of the major immediate early promoter (MIEP) to stimulate the expression of the IE genes, UL122 and UL123, such that small molecule anti-cancer curaxins, which promote FACT ‘trapping’ on chromatin inhibits IE gene expression

(O'Connor, et al. 2016). Given these findings it would be interesting to see if curaxins also inhibit adenovirus early gene expression. Interestingly, FACT has also been reported to suppress viral gene transcription. For instance, depletion of FACT by RNAi enhances HIV-transcription initiation and elongation, and promotes viral latency; FACT associates with the HIV-1 Tat transactivator to suppress transcriptional activity at LTRs (Huang, et al. 2015). The FACT complex is also required to promote latent replication of KSHV, through the association of KSHV latency protein, LANA with SSRP1, such that knockdown of FACT reduces KSHV latent replication (Hu, et al. 2009). Given the known role of the FACT complex in transcription it will be important in the future to determine by Chromatin immunoprecipitation coupled with qPCR whether SPT16 or SSRP1 associate with viral gene promoters, viral gene sequences or viral genomes during Ad5 or Ad12 infection through interaction with viral early proteins such as the 13S E1A gene product which serves to transactivate viral early genes during adenovirus infection.

5.3.3. Investigating the role of RBM14 during adenovirus infection

Experiments presented here indicate that RBM14 protein levels do not change following either Ad5 or Ad12 infection suggesting that like the FACT complex, RBM14 is not involved in the DDR response to viral infection [Fig 5.1]. Other experiments established that RBM14 had the capacity to associate with the RPA complex component, RPA1, but unlike the FACT complex RBM14 associated with RPA1 in both uninfected and Ad-infected cells [Fig. 5.2]. We also established that RBM14 is likely recruited to VRCs as it did not co-localize to any great extent with E4orf3 [Fig. 5.4] during adenovirus infection though this needs to be confirmed by co-staining with RPA2 or E2A/DBP. Like the FACT complexes a number of different viruses target RBM14 during infection. Interestingly, RBM14 has known pro-viral activities and facilitates Influenza A virus replication such that depletion of RBM14 inhibits viral mRNA production (Beyleveld, et al. 2018). In this regard, Influenza A viral protein NS1, relocates

RBM14 to nucleoli during infection through the biological requirement for this is not known (Beylevel, et al. 2018). Given these findings it would be interesting to establish whether RBM14 is recruited to nucleoli during adenovirus infection by co-staining with a nucleolar protein, such as nucleophosmin, although RBM14 was not identified by an early proteomic screen as being recruited to the nucleolus during Ad5 infection (Lam, et al. 2010; Reyes, et al. 2017). RBM14 also participates in viral gene expression programmes, such that it interacts with EBV protein, EBER2 at genomic terminal repeats to impair LMP2A transcription, such that knockdown of RBM14 enhances LMP2A transcription (Lee. et al, 2016; Salahuddin, et al. 2019). It is perhaps not surprising given the known functions of RBM14 that it also regulates viral mRNA splicing during infection. It has been found that RBM14 associates with the HIV-1 Rev protein to enhance the CRM1-dependent transport of unspliced viral transcripts to the cytoplasm, such that knockdown of RBM14 impaired Rev function (Budhiraja, et al. 2015). The RBM14 protein is characterized with RNA recognition motif (RRM), and is involved in diverse cellular process, including RNA export and stability, RNA splicing and transcription regulation (Iwasaki, et al. 2001). Given that adenovirus utilises splicing during infection to maximise its coding potential it would be interesting to see if RBM14 knockdown affected viral mRNA levels or splicing using a recently developed method of long-read direct RNA sequencing of polyadenylated adenovirus mRNA. It is interesting to note that, three viral proteins implicated in splicing, L4-33K, L4-22K, and E4-ORF4 all found in VRCs (Hidalgo and Gonzalez, 2019). As such it would be interesting to see if these adenoviral proteins associate with RBM14 during infection.

Earlier studies from our laboratory also identified the Pur family proteins, Pur α and Pur β as proteins that are potentially recruited to VRCs during adenovirus infection. We could not detect any association between Pur β and RPA however following adenovirus infection [Fig. 5.2]. We also made a cell-line that expressed GFP-Pur β constitutively but unfortunately we did not

observe any recruitment to VRCs during adenovirus infection [Fig. 5.6]. It is clear that we need to re-visit these studies but future priorities are to investigate the function of the FACT complex and RBM14 at VRCs during adenovirus infection. Indeed, the data presented in this Chapter confirm that FACT and RBM14 are recruited to VRCs during infection and suggest that FACT participates in viral early gene transcription programmes, though more work needs to be done to establish the precise roles of these proteins during adenovirus infection.

CHAPTER 6



Final Discussion

6.1. Introduction

It is now well accepted that adenovirus, like many other viruses, modulates host cell processes in order to promote viral replication. As such, adenoviruses utilise pro-viral host cellular factors that facilitate viral entry and viral transport, stimulate viral gene transcription and DNA replication, or promote viral packaging and virus exit from the cell. On the other hand adenovirus inactivates anti-viral host cell factors that limit these processes. It is well established that many anti-viral cellular factors participate in host cell DDR pathways or regulate some aspect of chromatin function. Adenovirus has therefore evolved to engage with the host cell UPS to promote the inactivation of such anti-viral host cell factors by ubiquitin-mediated proteolysis or SUMOylation (see sections 1.3 and 1.2.4.1). The viral early region proteins, E1B-55K, E4orf3 and E4orf6 function specifically during infection, either together or independently, to inactivate host cell anti-viral proteins. Consistent, with this notion, our laboratory has recently shown that E1B-55K and E4orf6 from both Ad5 and Ad12 inactivate host cell DNA replication by targeting the host cell DDR and replication protein, SMARCAL1 for proteasome-mediated degradation during infection (Nazeer, et al. 2019).

The work detailed in this thesis has been important in developing cell models to identify novel cellular anti-viral proteins targeted by Ad5 and Ad12 E1B-55K, E4orf3 and E4orf6 proteins in isolation. Consistent with previous work from our laboratory that identified TopBP1 as a target for Ad12 E4orf6 (Blackford, et al. 2010), we determined, using these cell models, that Ad12 E4orf6, but not Ad5 E4orf6, engaged independently with a CRL to promote the ubiquitin-mediated degradation of core histones. Most of the follow-on experiments for the findings described in this thesis have been described in the discussion sections of the relevant results chapters. Given the complex relationship between adenovirus and the host cell, however, I would like to discuss how we can utilise cell models and whole proteome and genome techniques to gain further insight into how adenovirus targets the UPS during infection, and

how adenovirus utilizes the UPS to modulate host cell DDR pathways and host cell chromatin during infection.

6.2. Adenovirus regulation of the ubiquitin-proteasome system

As adenovirus utilizes the UPS for multiple roles during infection it is important that we adopt whole proteome approaches in order to identify novel cellular targets. As such, we used a quantitative mass spectrometric approach that labelled isolated peptides with ‘heavy’ or ‘light’ formaldehyde to distinguish proteins isolated +/- Ad12 E4orf6 expression (section 4.2.7). Whilst we were able to use this technique to identify core histones as a novel target for adenovirus during infection [Fig. 4.10-4.15] our labelling approach and quantitative tandem MS analyses with a Bruker Impact mass spectrometer only identified 256 common cellular proteins from both experiments and an additional 389 proteins that were only identified in one of the two experiments [Fig. 4.10 and 4.11]. Given that the latest generation mass spectrometers typically identify and quantify 5000+ proteins from single experiments it will be important to use these newer mass spectrometers with more efficient protein/peptide labelling techniques in any future analyses to maximise data output. Indeed, one of our collaborators has used Tandem-Mass-Tag (TMT) labelling of peptide N-termini allied with an Orbitrap Fusion Tribridmass spectrometer to quantify the levels of over 5900 proteins during Ad5 infection of A549 cells (Fu, et al. 2017). However, although our collaborators were able to identify over 5900 proteins quantitatively they only identified 20+ proteins that were reduced appreciably in expression after 24h and did not establish fully the role of the early region proteins in the degradation process, which is where our Tet-responsive cell lines have further utility in dissecting the contribution of each of these viral proteins in cellular protein degradation.

As these viral proteins also cooperate to promote cellular protein degradation through the UPS it will be important to generate Ad5/Ad12 E1B-55K/E4orf3, E1B-55K/E4orf6, E4orf3/E4orf6, and E1B-55K/E4orf3/E4orf6 inducible cell lines and perform quantitative tandem mass

spectrometry to identify those proteins that require more than one viral protein for degradation. A current limitation to doing these experiments is the lack of commercially-available TREx plasmids that possess more than one promoter to drive the inducible expression of two or more exogenous proteins in one cell-line. However, as we noted in Chapter 3 (sections 3.2.2.1, 3.2.3.1 and 3.2.4.1), the expression of viral proteins between cell lines was highly variable, suggesting that there might be more than one genomic site for plasmid recombination in the parental U2OS FlpIn cell line, such that we should use these cells to see if we can isolate cell lines that express more than one viral protein at a time. Otherwise, it will be important to construct TREx plasmids that can express multiple exogenous genes in a TET-responsive manner.

As discussed in the Introduction (sections 1.2.2 and 1.2.4.1) and Chapter 3 (sections 3.3.2 and 3.3.3), adenovirus E1B-55K and E4orf3 proteins modulate host cell SUMOylation pathways during infection. In the future the cell lines generated during this project should be used to investigate which cellular proteins are targeted by Ad5 E1B-55K and Ad5/Ad12 E4orf3 for SUMOylation or STUbL-targeted proteasome degradation in response to the expression of these viral proteins. As such we should utilize SUMO1 and SUMO2-specific affimers (Hughes, et al. 2017) coupled to quantitative tandem mass spectrometry to identify cellular proteins that are subject to SUMOylation and/or degradation in response to viral early gene product expression. Moreover, as Ad5 E4orf3 is known to SUMOylate Ad5 E1B-55K (Sohn and Hearing, 2019) it would be interesting to determine the dual effects of Ad5 E1B-55K/E4orf3 expression on host cell protein SUMOylation STUbL-targeted proteasome degradation. Clearly, the identification of cellular proteins that are SUMOylated by Ad5 E1B-55K and/or E4orf3 would only be the first step in characterizing the effects of Ad-induced SUMOylation on cellular protein function.

6.3. Adenovirus regulation of chromatin

We presented data in Chapter 4 to indicate that adenoviruses regulate histone protein levels during infection and that Ad12 E4orf6 targets, selectively, core histones for proteasome-mediated degradation. The effects of adenovirus infection on cellular and viral transcription programmes are well established. It is known, for instance, that 13S E1A utilises TBP, the Mediator complex, CBP/p300 and the 26S proteasome to stimulate viral gene expression during infection (Berk, 2005; Rasti, et al. 2006), whilst 12S E1A regulates cellular transcription programmes through its ability to associate with CBP/p300 and pRB to modulate histone acetylation at the genome level and the selective association/dissociation of coactivator and repressor complexes with cellular and viral chromatin in order to regulate cellular and viral transcription programmes (Horwitz, et al. 2008; Ferrari, et al. 2014). Although not described here, it would be invaluable to generate both Ad5 and Ad12 12S E1A and 13S E1A TET-inducible U2OS FlpIn cell lines to dissect further the contribution of these viral transcriptional regulators in viral and host cell transcription programmes through the modulation of histone readers, writers and erasers. Given our findings with FACT and RBM14 (Chapter 5), ChIP-seq should be used to establish how FACT and RBM14 association with cellular and viral genomes is affected by adenovirus infection and adenovirus early region gene product expression in all of the TET-inducible U2OS FlpIn cell lines. As such, it would be possible to determine the molecular mechanisms regulating FACT and RBM14 function during infection and the contribution of early region proteins in these processes. Indeed, as FACT is known to disassemble H2A-H2B histone dimers, it would be interesting to determine if the FACT complex contributes towards histone loss during infection. Moreover, as RBM14 is implicated in gene splicing it would also be interesting to use direct long read RNA-seq to see whether RBM14 ablation modulates adenovirus early region gene cellular splicing. Interestingly, although E1B-55K, E4orf3 and E4orf6 are all known to modulate p53 transcriptional activity (Yew and Berk, 1992; Dobner, et al. 1996; Soria, et al. 2010), with the exception of E4orf3

(Soria, et al. 2010) the selective recruitment of E1B-55K or E4orf6 to the cellular genome at specific loci during infection has yet to be established. It would be possible to use the TET-inducible U2OS FlpIn cell lines coupled with ChIP-seq and RNA-seq to determine whether these proteins associate more generally with cellular promoters or gene sequences, which would expand our current understanding of the general roles of E1B-55K and E4orf6 in transcription control. Given these few examples it is clear that there is still much to be learnt about the relationship between viral early gene products and the regulation of cellular chromatin. The TET-inducible U2OS FlpIn cell lines generated here will be important in dissecting this complex relationship.

6.4 Adenovirus regulation of DNA damage response pathways

It is well established that many proteins targeted for proteolytic degradation during infection are key players in the cellular DDR and are known to associate with early region gene products during infection (Weitzman and Ornelles, 2005). It would be interesting therefore to perform immunoprecipitation studies with these viral proteins using the TET-inducible U2OS FlpIn E1B-55K, E4orf3 and E4orf6 cell lines to identify novel cellular-interacting proteins that could function in the DDR (or other anti-viral pathways) and/or are targeted for degradation by the UPS during infection. To investigate whether novel E1B-55K, E4orf3 and E4orf6-interacting proteins function in the DDR we could use CRISPR or RNAi to ablate their cellular expression and subject cells to DNA-damaging stimuli (e.g. X-rays for DSBs; UV/HU for SSBs and replication stress) and look at the cellular DDR response (e.g. p53 stabilization, induction of H2AX phosphorylation, Chk1 and/or Chk2 phosphorylation, or the re-localization of 53BP1 or RAD51 to sites of DNA damage). In this context we could also establish how expression of the viral protein modulates the specific DDR pathway engaged by the interacting cellular protein. In support of this approach our laboratory has previously determined that the E1B-55K-interacting protein (E1B-AP5/hnRNPUL1) functions in ATR signalling pathways in both

normal and infected cells (Blackford, et al. 2008). The Weitzman laboratory recently used iPOND to identify cellular proteins that were recruited or excluded from newly made viral DNA during Ad5 DNA replication in infected cells (Charman, et al. 2019). Interestingly, one of the proteins shown to be excluded from viral DNA was the DDR and replication protein, TIMELESS, which our laboratory has shown previously to be targeted for proteasomal degradation by Ad12, but not Ad5 (Patel, PhD thesis, The University of Birmingham, 2013), suggesting that Ad5 also inactivates TIMELESS function during infection. Other cellular proteins such as Claspin were also shown to be excluded from viral DNA during infection (Charman, et al. 2019). It would be interesting to establish whether proteins excluded from viral DNA are targeted for degradation during infection, and moreover, by using the TET-inducible U2OS FlpIn cell lines generated here, establish whether they are targets for Ad5/Ad12 E1B-55K, E4orf3 and/or E4orf6.

The ability of adenovirus to utilise the UPS to modulate chromatin and DDR during infection, and cellular transformation is now well-established. Research presented in this thesis shows that there is still lots to be learnt about adenovirus early gene product function, and their ability to modulate chromatin and DDR during infection through engagement with the UPS. It is clear that adenovirus can still be used as a molecular tool to investigate the DDR and chromatin in both normal and cancer cells and results arising from these studies will not only be important towards understanding the molecular basis of fundamental cellular processes but might be useful towards identifying potential cancer therapeutic targets or the design of oncolytic-selective adenoviruses. Moreover, as most, if not all, viruses modulate UPS, DDR and chromatin function during infection, adenovirus continues to serve as a useful model system for understanding virus-host cell interactions.

7. References

- Ali, F., Dar, J.S., Magray, A.R., Ganai, B.A. and Chishti, M.Z. (2019). "Posttranslational Modifications of Proteins and Their Role in Biological Processes and Associated Diseases." Protein Modificomics, Elsevier: 1-35
- Araujo, F.D., Stracker, T.H., Carson, C.T., Lee, D.V. and Weitzman, M.D. (2005). "Adenovirus type 5 E4orf3 protein targets the Mre11 complex to cytoplasmic aggresomes." Journal of virology, **79**(17): 11382-11391.
- Avvakumov, N., Kajon, A.E., Hoeben, R.C. and Mymryk, J.S. (2004). "Comprehensive sequence analysis of the E1A proteins of human and simian adenoviruses." Virology, **329**(2): 477-492.
- Avvakumov, N., Wheeler, R., D'Halluin, J.C. and Mymryk, J.S. (2002). "Comparative sequence analysis of the largest E1A proteins of human and simian adenoviruses." Journal of virology, **76**(16): 7968-7975.
- Bagdonaite, I. and Wandall, H.H. (2018). "Global aspects of viral glycosylation." Glycobiology, **28**(7): 443-467.
- Baker, A., Rohleder, K.J., Hanakahi, L.A. and Ketner, G. (2007). "Adenovirus E4 34k and E1b 55k oncoproteins target host DNA ligase IV for proteasomal degradation." Journal of virology, **81**(13): 7034-7040.
- Baker, A.T., Aguirre-Hernández, C., Halldén, G. and Parker, A.L. (2018). "Designer oncolytic adenovirus: coming of age." Cancers, **10**(6): 201.
- Barbera, A.J., Chodaparambil, J.V., Kelley-Clarke, B., Joukov, V., Walter, J.C., Luger, K. et al. (2006). "The nucleosomal surface as a docking station for Kaposi's sarcoma herpesvirus LANA." Science, **311**(5762): 856-861.
- Barry, M. and Früh, K. (2006). "Viral modulators of cullin RING ubiquitin ligases: culling the host defense." Science's STKE, **2006**(335): 21-pe21.
- Belotserkovskaya, R. and Reinberg, D. (2004). "Facts about FACT and transcript elongation through chromatin." Current opinion in genetics & development, **14**(2):139-146.
- Benedict, C.A., Norris, P.S., Prigozy, T.I., Bodmer, J.L., Mahr, J.A., Garnett, C.T. et al. (2001). "Three adenovirus E3 proteins cooperate to evade apoptosis by tumor necrosis factor-related apoptosis-inducing ligand receptor-1 and-2." Journal of Biological Chemistry, **276**(5):3270-3278.
- Bergonzini, V., Salata, C., Calistri, A., Parolin, C. and Palù, G. (2010). "View and review on viral oncology research." Infectious agents and cancer, **5**(1):11.
- Berk, A.J.(2005)."Recent lessons in gene expression, cell cycle control, and cell biology from adenovirus." Oncogene, **24**(52):7673-7685.
- Berk, A.J. and Sharp, P.A. (1977). "Sizing and mapping of early adenovirus mRNAs by gel electrophoresis of S1 endonuclease-digested hybrids." Cell, **12**(3):721-732.
- Bernards, R.E.N.E., de Leeuw, M.G., Vaessen, M.J., Houweling, A. and Van der Eb, A.J. (1984). "Oncogenicity by adenovirus is not determined by the transforming region only." Journal of virology, **50**(3):847-853.
- Bernards, R., de Leeuw, M.G., Houweling, A. and van der Eb, A.J. (1986). "Role of the adenovirus early region 1B tumor antigens in transformation and lytic infection." Virology, **150**(1):126-139.
- Bétous, R., Glick, G.G., Zhao, R. and Cortez, D. (2013). "Identification and characterization of SMARCAL1 protein complexes." PloS one, **8**(5): 63149.
- Beylveled, G., Chin, D.J., Del Olmo, E.M., Carter, J., Najera, I., Cillóniz, C. et al. (2018). "Nucleolar Relocalization of RBM14 by Influenza A Virus NS1 Protein." MSphere, **3**(6): 00549-00518
- Blackford, A.N. and Grand, R.J. (2009). "Adenovirus E1B 55-kilodalton protein: multiple roles in viral infection and cell transformation." Journal of virology, **83**(9): 4000-4012.
- Blackford, A.N. and Jackson, S.P. (2017). "ATM, ATR, and DNA-PK: the trinity at the heart of the DNA damage response." Molecular cell, **66**(6): 801-817.

- Blackford, A.N., Bruton, R.K., Dirlik, O., Stewart, G.S., Taylor, A.M.R., Dobner, T. et al. (2008). "A role for E1B-AP5 in ATR signaling pathways during adenovirus infection. " Journal of virology, **82**(15):7640-7652.
- Blackford, A.N., Patel, R.N., Forrester, N.A., Theil, K., Groitl, P., Stewart, G.S. et al. (2010). "Adenovirus 12 E4orf6 inhibits ATR activation by promoting TOPBP1 degradation. " Proceedings of the National Academy of Sciences, **107**(27):12251-12256.
- Blanchette, P., Cheng, C.Y., Yan, Q., Ketner, G., Ornelles, D.A., Dobner, T. et al. (2004). "Both BC-box motifs of adenovirus protein E4orf6 are required to efficiently assemble an E3 ligase complex that degrades p53. " Molecular and cellular biology, **24**(21): 9619-9629.
- Blanchette, P., Kinds Müller, K., Groitl, P., Dallaire, F., Speiseder, T., Branton, P.E. et al. (2008). "Control of mRNA export by adenovirus E4orf6 and E1B55K proteins during productive infection requires E4orf6 ubiquitin ligase activity. " Journal of virology, **82**(6):2642-2651.
- Blanchette, P., Wimmer, P., Dallaire, F., Cheng, C.Y. and Branton, P.E. (2013). "Aggresome formation by the adenoviral protein E1B55K is not conserved among adenovirus species and is not required for efficient degradation of nuclear substrates. " Journal of virology, **87**(9):4872-4881.
- Bos, J.L. (1989). "Ras oncogenes in human cancer: a review. " Cancer research, **49**(17):4682-4689.
- Bos, J.L.(1988). "The ras gene family and human carcinogenesis. " Mutation Research/Reviews in Genetic Toxicology, **195**(3): 255-271.
- Bosu, D.R. and Kipreos, E.T. (2008). "Cullin-RING ubiquitin ligases: global regulation and activation cycles. " Cell division, **3**(1):1-13.
- Boulanger, P.A. and Blair, G.E. (1991). "Expression and interactions of human adenovirus oncoproteins. " Biochemical journal, **275**(2):281-299.
- Boyd, J.M., Subramanian, T., Schaeper, U., La Regina, M., Bayley, S. and Chinnadurai, G. (1993). "A region in the C-terminus of adenovirus 2/5 E1a protein is required for association with a cellular phosphoprotein and important for the negative modulation of T24-ras mediated transformation, tumorigenesis and metastasis. " The EMBO journal, **12**(2):469-478.
- Boyer, J.L. and Ketner, G. (2000). "Genetic analysis of a potential zinc-binding domain of the adenovirus E4 34k protein. " Journal of Biological Chemistry, **275**(20):14969-14978.
- Boyer, J., Rohleder, K. and Ketner, G. (1999). "Adenovirus E4 34k and E4 11k inhibit double strand break repair and are physically associated with the cellular DNA-dependent protein kinase. " Virology, **263**(2):307-312.
- Brackmann, K.H., Green, M., Wold, W.S., Cartas, M., Matsuo, T. and Hashimoto, S. (1980). "Identification and peptide mapping of human adenovirus type 2-induced early polypeptides isolated by two-dimensional gel electrophoresis and immunoprecipitation. " Journal of Biological Chemistry, **255**(14):6772-6779.
- Brestovitsky, A., Nebenzahl-Sharon, K., Kechker, P., Sharf, R. and Kleinberger, T. (2016). "The adenovirus E4orf4 protein provides a novel mechanism for inhibition of the DNA damage response. " PLoS pathogens, **12**(2): e1005420.
- Brenner, S. and Horne, R.W. (1959). "A negative staining method for high resolution electron microscopy of viruses. " Biochimica et biophysica acta, **34**:103-110.
- Bridge, E. and Ketner, G. (1990). "Interaction of adenoviral E4 and E1b products in late gene expression. " Virology, **174**(2):345-353.
- Bridges, R.G., Sohn, S.Y., Wright, J., Leppard, K.N. and Hearing, P. (2016). "The adenovirus E4-ORF3 protein stimulates SUMOylation of general transcription factor TFII-I to direct proteasomal degradation. " MBio, **7**(1): 2184-2115.
- Bristol, M.L., Das, D. and Morgan, I.M. (2017). "Why human papillomaviruses activate the DNA damage response (DDR) and how cellular and viral replication persists in the presence of DDR signaling. " Viruses, **9**(10):268.

- Brownell, J.E., Sintchak, M.D., Gavin, J.M., Liao, H., Bruzzese, F.J., Bump, N.J. et al. (2010). "Substrate-assisted inhibition of ubiquitin-like protein-activating enzymes: the NEDD8 E1 inhibitor MLN4924 forms a NEDD8-AMP mimetic in situ." Molecular cell, **37**(1):102-111.
- Budhiraja, S., Liu, H., Couturier, J., Malovannaya, A., Qin, J., Lewis, D.E. et al. (2015). "Mining the human complexome database identifies RBM14 as an XPO1-associated protein involved in HIV-1 Rev function." Journal of virology, **89**(7):3557-3567.
- Byrd, P., Brown, K.W. and Gallimore, P.H. (1982). "Malignant transformation of human embryo retinoblasts by cloned adenovirus 12 DNA." Nature, **298**(5869):69-71.
- Byrd, P.J., Grand, R.J. and Gallimore, P.H. (1988). "Differential transformation of primary human embryo retinal cells by adenovirus E1 regions and combinations of E1A+ ras." Oncogene, **2**(5):477-484.
- Byun, T.S., Pacek, M., Yee, M.C., Walter, J.C. and Cimprich, K.A. (2005). "Functional uncoupling of MCM helicase and DNA polymerase activities activates the ATR-dependent checkpoint." Genes & development, **19**(9):1040-1052.
- Cai, Q.L., Knight, J.S., Verma, S.C., Zald, P. and Robertson, E.S. (2006). "EC 5 S ubiquitin complex is recruited by KSHV latent antigen LANA for degradation of the VHL and p53 tumor suppressors." PLoS Pathog, **2**(10):116.
- Caporossi, D. and Bacchetti, S. (1990). "Definition of adenovirus type 5 functions involved in the induction of chromosomal aberrations in human cells." Journal of general virology, **71**(4):801-808.
- Carson, C.T., Orazio, N.I., Lee, D.V., Suh, J., Bekker-Jensen, S., Araujo, F.D. et al. (2009). "Mislocalization of the MRN complex prevents ATR signaling during adenovirus infection." The EMBO journal, **28**(6):652-662.
- Cary, R.B., Peterson, S.R., Wang, J., Bear, D.G., Bradbury, E.M. and Chen, D.J. (1997). "DNA looping by Ku and the DNA-dependent protein kinase." Proceedings of the National Academy of Sciences, **94**(9):4267-4272.
- Cathomen, T. and Weitzman, M.D. (2000). "A functional complex of adenovirus proteins E1B-55kDa and E4orf6 is necessary to modulate the expression level of p53 but not its transcriptional activity." Journal of virology, **74**(23):11407-11412.
- Cesarman, E., Damania, B., Krown, S.E., Martin, J., Bower, M. and Whitby, D. (2019). "Kaposi sarcoma." Nature Reviews Disease Primers, **5**(1):1-21.
- Chang, L.S. and Shenk, T.H. (1990). "The adenovirus DNA-binding protein stimulates the rate of transcription directed by adenovirus and adeno-associated virus promoters." Journal of virology, **64**(5):2103-2109.
- Chang, P.C., Izumiya, Y., Wu, C.Y., Fitzgerald, L.D., Campbell, M., Ellison, T.J. et al. (2010). "Kaposi's sarcoma-associated herpesvirus (KSHV) encodes a SUMO E3 ligase that is SIM-dependent and SUMO-2/3-specific." Journal of Biological Chemistry, **285**(8):5266-5273.
- Charman, M., Herrmann, C. and Weitzman, M.D. (2019). "Viral and cellular interactions during adenovirus DNA replication." FEBS letters, **593**(24):3531-3550.
- Chaurushiya, M.S. and Weitzman, M.D. (2009). "Viral manipulation of DNA repair and cell cycle checkpoints." DNA repair, **8**(9):1166-1176.
- Cheng, C.Y., Blanchette, P. and Branton, P.E. (2007). "The adenovirus E4orf6 E3 ubiquitin ligase complex assembles in a novel fashion." Virology, **364**(1):36-44.
- Cheng, C.Y., Gilson, T., Dallaire, F., Ketner, G., Branton, P.E. and Blanchette, P. (2011). "The E4orf6/E1B55K E3 ubiquitin ligase complexes of human adenoviruses exhibit heterogeneity in composition and substrate specificity." Journal of virology, **85**(2):765-775.
- Cheng, C.Y., Gilson, T., Wimmer, P., Schreiner, S., Ketner, G., Dobner, T. et al. (2013). "Role of E1B55K in E4orf6/E1B55K E3 ligase complexes formed by different human adenovirus serotypes." Journal of virology, **87**(11):6232-6245.
- Chow, L.T., Roberts, J.M., Lewis, J.B. and Broker, T.R. (1977). "A map of cytoplasmic RNA transcripts from lytic adenovirus type 2, determined by electron microscopy of RNA: DNA hybrids." Cell, **11**(4):819-836.

- Ciccia, A. and Elledge, S.J. (2010). "The DNA damage response: making it safe to play with knives. " Molecular cell, **40**(2):179-204.
- Cortez, D. (2015). "Preventing replication fork collapse to maintain genome integrity. " DNA repair, **32**:149-157.
- Cory, S., Huang, D.C. and Adams, J.M. (2003). "The Bcl-2 family: roles in cell survival and oncogenesis. " Oncogene, **22**(53):8590-8607.
- Coussens, P.M., Cooper, J.A., Hunter, T. and Shalloway, D. (1985). "Restriction of the in vitro and in vivo tyrosine protein kinase activities of pp60c-src relative to pp60v-src. " Molecular and cellular biology, **5**(10): 2753-2763.
- Cox, J.H., Yewdell, J.W., Eisenlohr, L.C., Johnson, P.R. and Bennink, J.R. (1990). "Antigen presentation requires transport of MHC class I molecules from the endoplasmic reticulum. " Science, **247**(4943):715-718.
- Cuconati, A., Mukherjee, C., Perez, D. and White, E. (2003). "DNA damage response and MCL-1 destruction initiate apoptosis in adenovirus-infected cells. " Genes & development, **17**(23):2922-2932.
- Dallaire, F., Blanchette, P., Groitl, P., Dobner, T. and Branton, P.E. (2009). "Identification of integrin $\alpha 3$ as a new substrate of the adenovirus E4orf6/E1B 55-kilodalton E3 ubiquitin ligase complex. " Journal of virology, **83**(11): 5329-5338.
- Daniell, E., Groff, D.E. and Fedor, M.J. (1981). "Adenovirus chromatin structure at different stages of infection. " Molecular and cellular biology, **1**(12):1094-1105.
- De Jong, R.N. and Van der Vliet, P.C. (1999). "Mechanism of DNA replication in eukaryotic cells: cellular host factors stimulating adenovirus DNA replication. " Gene, **236**(1):1-12.
- De Jong, R.N., van der Vliet, P.C. and Brenkman, A.B. (2003). "Adenovirus DNA replication: protein priming, jumping back and the role of the DNA binding protein DBP. " Curr Top Microbiol Immunol, **272**:187-211.
- Debbas, M. and White, E. (1993). "Wild-type p53 mediates apoptosis by E1A, which is inhibited by E1B. " Genes & development, **7**(4):546-554.
- DeLeo, A.B., Jay, G., Appella, E., Dubois, G.C., Law, L.W. and Old, L.J. (1979). "Detection of a transformation-related antigen in chemically induced sarcomas and other transformed cells of the mouse. " Proceedings of the National Academy of Sciences, **76**(5):2420-2424.
- Deleu, L., Shellard, S., Alevizopoulos, K., Amati, B. and Land, H. (2001). "Recruitment of TRRAP required for oncogenic transformation by E1A. " Oncogene, **20**(57):8270-8275.
- Dobbelstein, M., Roth, J., Kimberly, W.T., Levine, A.J. and Shenk, T. (1997). "Nuclear export of the E1B 55-kDa and E4 34-kDa adenoviral oncoproteins mediated by a rev-like signal sequence. " The EMBO Journal, **16**(14):4276-4284.
- Dobner, T. and Kzhyshkowska, J. (2001). "Nuclear export of adenovirus RNA. " In Nuclear Export of Viral RNAs, **259**: 25-54.
- Dobner, T., Horikoshi, N., Rubenwolf, S. and Shenk, T. (1996). "Blockage by adenovirus E4orf6 of transcriptional activation by the p53 tumor suppressor. " Science, **272**(5267):1470-1473.
- Doucas, V., Ishov, A.M., Romo, A., Juguilon, H., Weitzman, M.D., Evans, R.M. et al. (1996). "Adenovirus replication is coupled with the dynamic properties of the PML nuclear structure. " Genes & development, **10**(2):196-207.
- Downey, J.F., Rowe, D.T., Bacchetti, S., Graham, F.L. and Bayley, S.T. (1983). "Mapping of a 14,000-dalton antigen to early region 4 of the human adenovirus 5 genome. " Journal of Virology, **45**(2):514-523.
- Dunsworth-Browne, M., Schell, R.E. and Berk, A.J. (1980). "Adenovirus terminal protein protects single stranded DNA from digestion by a cellular exonuclease. " Nucleic Acids Research, **8**(3):543-554.
- Dybas, J.M., Herrmann, C. and Weitzman, M.D. (2018). "Ubiquitination at the interface of tumor viruses and DNA damage responses. " Current opinion in virology, **32**:40-47.

- Dye, B.T. and Schulman, B.A. (2007). "Structural mechanisms underlying posttranslational modification by ubiquitin-like proteins." Annu. Rev. Biophys. Biomol. Struct., **36**:131-150.
- Echavarría, M. (2008). "Adenoviruses in immunocompromised hosts." Clinical microbiology reviews, **21**(4): 704-715.
- Eckner, R., Ewen, M.E., Newsome, D., Gerdes, M., DeCaprio, J.A., Lawrence, J.B. et al. (1994). "Molecular cloning and functional analysis of the adenovirus E1A-associated 300-kD protein (p300) reveals a protein with properties of a transcriptional adaptor." Genes & development, **8**(8):869-884.
- Egan, C., Jelsma, T.N., Howe, J.A., Bayley, S.T., Ferguson, B. and Branton, P.E. (1988). "Mapping of cellular protein-binding sites on the products of early-region 1A of human adenovirus type 5." Molecular and cellular biology, **8**(9):3955-3959.
- Endter, C. and Dobner, T. (2004). "Cell transformation by human adenoviruses." Curr Top Microbiol Immunol, **273**:163–214
- Endter, C., Kzhyshkowska, J., Stauber, R. and Dobner, T. (2001). "SUMO-1 modification required for transformation by adenovirus type 5 early region 1B 55-kDa oncoprotein." Proceedings of the National Academy of Sciences, **98**(20):11312-11317.
- Epstein, M.A. (1964). "Virus particles in cultured lymphoblasts from Burkitt's lymphoma." Lancet, **1**:702-703.
- Falgout, B. and Ketner, G. (1987). "Adenovirus early region 4 is required for efficient virus particle assembly." Journal of virology, **61**:3759-3768.
- Feling, R.H., Buchanan, G.O., Mincer, T.J., Kauffman, C.A., Jensen, P.R. and Fenical, W. (2003). "Salinosporamide A: a highly cytotoxic proteasome inhibitor from a novel microbial source, a marine bacterium of the new genus Salinospora." Angewandte Chemie International Edition, **42**(3):355-357.
- Feng, H., Shuda, M., Chang, Y. and Moore, P.S. (2008). "Clonal integration of a polyomavirus in human Merkel cell carcinoma." Science, **319**:1096-1100.
- Fenteany, G., Standaert, R.F., Lane, W.S., Choi, S., Corey, E.J. and Schreiber, S.L. (1995). "Inhibition of proteasome activities and subunit-specific amino-terminal threonine modification by lactacystin." Science, **268**(5211): 726-731.
- Ferrari, R., Gou, D., Jawdekar, G., Johnson, S.A., Nava, M., Su, T. et al. (2014). "Adenovirus small E1A employs the lysine acetylases p300/CBP and tumor suppressor Rb to repress select host genes and promote productive virus infection." Cell host & microbe, **16**(5):663-676.
- Ferrari, R., Pellegrini, M., Horwitz, G.A., Xie, W., Berk, A.J. and Kurdistani, S.K. (2008). "Epigenetic reprogramming by adenovirus e1a." Science, **321**(5892): 1086-1088.
- Flint, S.J. and Sharp, P.A. (1976). "Adenovirus transcription: V. Quantitation of viral RNA sequences in adenovirus 2-infected and transformed cells." Journal of molecular biology, **106**(3):749-771.
- Flint, S.J., Plumb, M.A., Yang, U.C., Stein, G.S. and Stein, J.L. (1984). "Effect of adenovirus infection on expression of human histone genes." Molecular and cellular biology, **4**(7):1363-1371.
- Flint, S.J., Sambrook, J., Williams, J.F. and Sharp, P.A. (1976). "Viral nucleic acid sequences in transformed cells: IV. A study of the sequences of adenovirus 5 DNA and RNA in four lines of adenovirus 5-transformed rodent cells using specific fragments of the viral genome." Virology, **72**(2):456-470.
- Formosa, T. (2012). "The role of FACT in making and breaking nucleosomes." Biochimica Et Biophysica Acta (BBA)-Gene Regulatory Mechanisms, **1819**(3-4):247-255.
- Forrester, N.A., Patel, R.N., Speiseder, T., Groitl, P., Sedgwick, G.G., Shimwell, N.J. et al. (2012). "Adenovirus E4orf3 targets transcriptional intermediary factor 1 γ for proteasome-dependent degradation during infection." Journal of virology, **86**(6):3167-3179.
- Fu, Y.R., Turnell, A.S., Davis, S., Heesom, K.J., Evans, V.C. and Matthews, D.A. (2017). "Comparison of protein expression during wild-type, and E1B-55k-deletion, adenovirus infection using quantitative time-course proteomics." The Journal of general virology, **98**(6):1377.

- Fuchs, M., Gerber, J., Drapkin, R., Sif, S., Ikura, T., Ogryzko, V. et al. (2001). "The p400 complex is an essential E1A transformation target." Cell, **106**(3):297-307.
- Galanty, Y., Belotserkovskaya, R., Coates, J. and Jackson, S.P. (2012). "RNF4, a SUMO-targeted ubiquitin E3 ligase, promotes DNA double-strand break repair." Genes & development, **26**(11): 1179-1195.
- Gallimore, P.H. and Turnell, A.S. (2001). "Adenovirus E1A: remodelling the host cell, a life or death experience." Oncogene, **20**(54): 7824-7835.
- Gallimore, P.H., Byrd, P.J., Whittaker, J.L. and Grand, R.J. (1985). "Properties of rat cells transformed by DNA plasmids containing adenovirus type 12 E1 DNA or specific fragments of the E1 region: comparison of transforming frequencies." Cancer research, **45**(6): 2670-2680.
- Gallimore, P.H., Grand, R.J. and Byrd, P.J. (1986). "Transformation of human embryo retinoblasts with simian virus 40, adenovirus and ras oncogenes." Anticancer Research, **6**(3 Pt B): 499-508.
- Gallimore, P.H., Lecane, P.S., Roberts, S., Rookes, S.M., Grand, R.J. and Parkhill, J. (1997). "Adenovirus type 12 early region 1B 54K protein significantly extends the life span of normal mammalian cells in culture." Journal of virology, **71**(9): 6629-6640.
- Gallimore, P.H., Sharp, P.A. and Sambrook, J. (1974). "Viral DNA in transformed cells: II. A study of the sequences of adenovirus 2 DNA in nine lines of transformed rat cells using specific fragments of the viral genome." Journal of molecular biology, **89**(1): 49-72.
- Garcia, H., Miecznikowski, J.C., Safina, A., Commane, M., Ruusulehto, A., Kilpinen, S. et al. (2013). "Facilitates chromatin transcription complex is an "accelerator" of tumor transformation and potential marker and target of aggressive cancers." Cell reports, **4**(1): 159-173.
- Gell, D. and Jackson, S.P. (1999). "Mapping of protein-protein interactions within the DNA-dependent protein kinase complex." Nucleic acids research, **27**(17): 3494-3502.
- Gilson, T., Blanchette, P., Ballmann, M.Z., Papp, T., Péntzes, J.J., Benkő, M. et al. (2016). "Using the E4orf6-based E3 ubiquitin ligase as a tool to analyze the evolution of adenoviruses." Journal of virology, **90**(16): 7350-7367.
- Gilson, T., Cheng, C.Y., Hur, W.S., Blanchette, P. and Branton, P.E. (2014). "Analysis of the cullin binding sites of the E4orf6 proteins of human adenovirus E3 ubiquitin ligases." Journal of Virology, **88**(7): 3885-3897.
- Giunta, S. and Jackson, S.P. (2011). "Give me a break, but not in mitosis: the mitotic DNA damage response marks DNA double-strand breaks with early signaling events." Cell Cycle, **10**(8): 1215-1221.
- Goldberg, A.L. (2012). "Development of proteasome inhibitors as research tools and cancer drugs." Cell Biology, **199**:583-588.
- Gooding, L.R., Aquino, L., Duerksen-Hughes, P.J., Day, D., Horton, T.M., Yei, S.P. et al. (1991). "The E1B 19,000-molecular-weight protein of group C adenoviruses prevents tumor necrosis factor cytolysis of human cells but not of mouse cells." Journal of Virology, **65**(6): 3083-3094.
- Goodrum, F.D., Shenk, T. and Ornelles, D.A. (1996). "Adenovirus early region 4 34-kilodalton protein directs the nuclear localization of the early region 1B 55-kilodalton protein in primate cells." Journal of Virology, **70**(9): 6323-6335.
- Graham, F.L., Smiley, J., Russell, W.C. and Nairn, R. (1977). "Characteristics of a human cell line transformed by DNA from human adenovirus type 5." Journal of general virology, **36**(1): 59-72.
- Graham, F.L., Van der Eb, A.J. and Heijneker, H.L. (1974). "Size and location of the transforming region in human adenovirus type 5 DNA." Nature, **251**(5477): 687.
- Grand, R.J., Grant, M.L. and Gallimore, P.H. (1994). "Enhanced Expression of p53 in Human Cells Infected with Mutant Adenoviruses." Virology, **203**(2): 229-240.
- Gupta, M., Sueblinvong, V. and Gupta, M.P. (2007). "The single-strand DNA/RNA-binding protein, Pur β , regulates serum response factor (SRF)-mediated cardiac muscle gene expression" Canadian journal of physiology and pharmacology, **85**(3-4).

- Gustafsson, B., Huang, W., Bogdanovic, G., Gauffin, F., Nordgren, A., Talekar, G. et al. (2007). "Adenovirus DNA is detected at increased frequency in Guthrie cards from children who develop acute lymphoblastic leukaemia. " British journal of cancer, **97**(7): 992-994.
- Halbert, D.N., Cutt, J.R. and Shenk, T. (1985). "Adenovirus early region 4 encodes functions required for efficient DNA replication, late gene expression, and host cell shutoff. " Journal of virology, **56**(1): 250-257.
- Hanahan, D. and Weinberg, R.A. (2000). "The hallmarks of cancer." Cell, **100**(1): 57-70.
- Harada, J.N., Shevchenko, A., Shevchenko, A., Pallas, D.C. and Berk, A.J. (2002). "Analysis of the adenovirus E1B-55K-anchored proteome reveals its link to ubiquitination machinery. " Journal of virology, **76**(18): 9194-9206.
- Hartlerode, A.J., Morgan, M.J., Wu, Y., Buis, J. and Ferguson, D.O. (2015). "Recruitment and activation of the ATM kinase in the absence of DNA-damage sensors. " Nature structural & molecular biology, **22**(9): 736.
- Hartmann, T., Xu, X., Kronast, M., Muehlich, S., Meyer, K., Zimmermann, W. et al. (2014). "Inhibition of Cullin-RING E3 ubiquitin ligase 7 by simian virus 40 large T antigen. " Proceedings of the National Academy of Sciences, **111**(9): 3371-3376.
- Hateboer, G., Hijmans, E.M., Nooij, J.B., Schlenker, S., Jentsch, S. and Bernards, R. (1996). "mUBC9, a novel adenovirus E1A-interacting protein that complements a yeast cell cycle defect. " Journal of Biological Chemistry, **271**(42): 25906-25911.
- Hatfield, L. and Hearing, P. (1991). "Redundant elements in the adenovirus type 5 inverted terminal repeat promote bidirectional transcription in Vitro and are important for virus growth in Vivo. " Virology, **184**(1): 265-276.
- Hauer, M.H., Seeber, A., Singh, V., Thierry, R., Sack, R., Amitai, A. et al. (2017). "Histone degradation in response to DNA damage enhances chromatin dynamics and recombination rates. " Nature Structural & Molecular Biology, **24**(2): 99.
- Hidalgo, P., Ip, W.H., Dobner, T. and Gonzalez, R.A. (2019). "The biology of the adenovirus E1B 55K protein. " FEBS letters, **593**(24):3504-3517.
- Ho, T.H., Sitz, J., Shen, Q., Leblanc-Lacroix, A., Campos, E.I., Borozan, I. et al. (2018). "A screen for epstein-barr virus proteins that inhibit the DNA damage response reveals a novel histone binding protein. " Journal of Virology, **92**(14): 00262-00218.
- Hoeben, R.C. and Uil, T.G. (2013). "Adenovirus DNA replication. " Cold Spring Harbor perspectives in biology, **5**(3): a013003.
- Horne, R.W. (1959). "The icosahedral form of an adenovirus. " Jour Mol Biology, **1**: 84.
- Horwitz, G.A., Zhang, K., McBrian, M.A., Grunstein, M., Kurdistani, S.K. and Berk, A.J. (2008). "Adenovirus small e1a alters global patterns of histone modification. " Science, **321**(5892): 1084-1085.
- Howe, J.A., Mymryk, J.S., Egan, C., Branton, P.E. and Bayley, S.T. (1990). "Retinoblastoma growth suppressor and a 300-kDa protein appear to regulate cellular DNA synthesis. " Proceedings of the National Academy of Sciences, **87**(15): 5883-5887.
- Hsu, H.L., Yannone, S.M. and Chen, D.J. (2002). "Defining interactions between DNA-PK and ligase IV/XRCC4. " DNA Repair, **1**(3): 225-235.
- Hu, J., Liu, E. and Renne, R. (2009). "Involvement of SSRP1 in latent replication of Kaposi's sarcoma-associated herpesvirus. " Journal of Virology, **83**(21): 11051-11063.
- Hughes, D.J., Tiede, C., Penswick, N., Ah-San Tang, A., Trinh, C.H., Mandal, U. et al. (2017). "Generation of specific inhibitors of SUMO-1–and SUMO-2/3–mediated protein-protein interactions using Affimer (Adhiron) technology. " Science signalling, **10**(505):2005.
- Hughes, D.J., Wood, J.J., Jackson, B.R., Baquero-Pérez, B. and Whitehouse, A. (2015). "NEDDylation is essential for Kaposi's sarcoma-associated herpesvirus latency and lytic reactivation and represents a novel anti-KSHV target. " PLoS pathogens, **11**(3).

- Huh, K., Zhou, X., Hayakawa, H., Cho, J.Y., Libermann, T.A., Jin, J. et al. (2007). "Human papillomavirus type 16 E7 oncoprotein associates with the cullin 2 ubiquitin ligase complex, which contributes to degradation of the retinoblastoma tumor suppressor." Journal of Virology, **81**(18): 9737-9747.
- Hupp, T.R., Meek, D.W., Midgley, C.A. and Lane, D.P. (1992). "Regulation of the specific DNA binding function of p53." Cell, **71**(5): 875-886.
- Hutton, F.G., Turnell, A.S., Gallimore, P.H. and Grand, R.J. (2000). "Consequences of disruption of the interaction between p53 and the larger adenovirus early region 1B protein in adenovirus E1 transformed human cells." Oncogene, **19**(3): 452.
- Ikeda, F. and Dikic, I. (2008). "Atypical ubiquitin chains: new molecular signals." EMBO reports, **9**(6): 536-542.
- Iwasaki, T., Chin, W.W. and Ko, L. (2001). "Identification and characterization of RRM-containing coactivator activator (CoAA) as TRBP-interacting protein, and its splice variant as a coactivator modulator (CoAM)." Biological Chemistry, **276**(36): 33375-33383.
- Jackson, S.P. and Bartek, J.(2009). "The DNA-damage response in human biology and disease." Nature, **461**(7267): 1071-1078.
- Jang, Y., Elsayed, Z., Eki, R., He, S., Du, K.P., Abbas, T. et al. (2020). "Intrinsically disordered protein RBM14 plays a role in generation of RNA: DNA hybrids at double-strand break sites." Proceedings of the National Academy of Sciences, **117**(10): 5329-5338.
- Javier, R.T. and Butel, J.S. (2008). "The history of tumor virology." Cancer research, **68**(19): 7693-7706.
- Jelsma, T.N., Howe, J.A., Mymryk, J.S., Eveleigh, C.M., Cunniff, N.F. and Bayley, S.T. (1989). "Sequences in E1A proteins of human adenovirus 5 required for cell transformation, repression of a transcriptional enhancer, and induction of proliferating cell nuclear antigen." Virology, **171**(1): 120-130.
- Jochemsen, A.G., Bernards, R., Van Kranen, H.J., Houweling, A., Bos, J.L. and Van der Eb, A.J. (1986). "Different activities of the adenovirus types 5 and 12 E1A regions in transformation with the EJ Ha-ras oncogene." Journal of virology, **59**(3): 684-691.
- Johnson, E.M., Daniel, D.C. and Gordon, J. (2013). "The pur protein family: genetic and structural features in development and disease." Journal of cellular physiology, **228**(5): 930-937.
- Kamitani, T., Kito, K., Nguyen, H.P. and Yeh, E.T. (1997). "Characterization of NEDD8, a developmentally down-regulated ubiquitin-like protein." Journal of Biological Chemistry, **272**(45): 28557-28562.
- Kamura, T., Conrad, M.N., Yan, Q., Conaway, R.C. and Conaway, J.W. (1999). "The Rbx1 subunit of SCF and VHL E3 ubiquitin ligase activates Rub1 modification of cullins Cdc53 and Cul2." Genes & Development, **13**(22): 2928-2933.
- Karve, T.M. and Cheema, A.K. (2011). "Small changes huge impact: the role of protein posttranslational modifications in cellular homeostasis and disease." Journal of amino acid, **2011**: 207691.
- Kindsmüller, K., Grottl, P., Härtl, B., Blanchette, P., Hauber, J. and Dobner, T. (2007). "Intranuclear targeting and nuclear export of the adenovirus E1B-55K protein are regulated by SUMO1 conjugation." Proceedings of the National Academy of Sciences, **104**(16): 6684-6689.
- Kleinberger, T. (2015). "Mechanisms of cancer cell killing by the adenovirus E4orf4 protein." Viruses, **7**(5): 2334-2357.
- Ko, L.J. and Prives, C. (1996). "p53: puzzle and paradigm." Genes & Development, **10**(9): 1054-1072.
- Kobayashi, M., Takaori-Kondo, A., Miyauchi, Y., Iwai, K. and Uchiyama, T. (2005). "Ubiquitination of APOBEC3G by an HIV-1 Vif-Cullin5-Elongin B-Elongin C complex is essential for Vif function." Journal of Biological Chemistry, **280**(19): 18573-18578.
- Kobiyama, K., Takeshita, F., Jounai, N., Sakaue-Sawano, A., Miyawaki, A., Ishii, K.J. et al. (2010). "Extrachromosomal histone H2B mediates innate antiviral immune responses induced by intracellular double-stranded DNA." Journal of virology, **84**(2): 822-832.

- Koç, A., Wheeler, L.J., Mathews, C.K. and Merrill, G.F. (2004). "Hydroxyurea arrests DNA replication by a mechanism that preserves basal dNTP pools. " Journal of Biological Chemistry, **279**(1): 223-230.
- Komatsu, T., Haruki, H. and Nagata, K. (2011). "Cellular and viral chromatin proteins are positive factors in the regulation of adenovirus gene expression. " Nucleic acids research, **39**(3): 889-901.
- Kosulin, K., Haberler, C., Hainfellner, J.A., Amann, G., Lang, S. and Lion, T. (2007). "Investigation of adenovirus occurrence in pediatric tumor entities. " Journal of virology, **81**(14): 7629-7635.
- Krätzer, F., Rosorius, O., Heger, P., Hirschmann, N., Dobner, T., Hauber, J. et al. (2000). "The adenovirus type 5 E1B-55K oncoprotein is a highly active shuttle protein and shuttling is independent of E4orf6, p53 and Mdm2. " Oncogene, **19**(7): 850-857.
- Kress, M., May, E., Cassingena, R. and May, P. (1979). "Simian virus 40-transformed cells express new species of proteins precipitable by anti-simian virus 40 tumor serum. " Journal of virology, **31**(2): 472-483.
- Kulathu, Y. and Komander, D. (2012). "Atypical ubiquitylation the unexplored world of polyubiquitin beyond Lys48 and Lys63 linkages. " Nature reviews Molecular cell biology, **13**(8): 508-523.
- Lam, Y.W., Evans, V.C., Heesom, K.J., Lamond, A.I. and Matthews, D.A. (2010). "Proteomics analysis of the nucleolus in adenovirus-infected cells. " Molecular & Cellular Proteomics, **9**(1): 117-130.
- Landers, J.E., Cassel, S.L. and George, D.L. (1997). "Translational enhancement of mdm2 oncogene expression in human tumor cells containing a stabilized wild-type p53 protein. Cancer research, **57**(16): 3562-3568.
- Lane, D.P. and Crawford, L.V. (1979). "T antigen is bound to a host protein in SY40-transformed cells. " Nature, **278**(5701): 261-263.
- Ledl, A., Schmidt, D. and Müller, S. (2005). "Viral oncoproteins E1A and E7 and cellular LxCxE proteins repress SUMO modification of the retinoblastoma tumor suppressor. " Oncogene, **24**(23): 3810.
- Lee, N., Yario, T.A., Gao, J.S. and Steitz, J.A. (2016). "EBV noncoding RNA EBER2 interacts with host RNA-binding proteins to regulate viral gene expression. " Molecular Cell, **113**(12): 3221-3226.
- Lehman, T.A., Bennett, W.P., Metcalf, R.A., Welsh, J.A., Ecker, J., Modali, R.V. et al. (1991). "p53 mutations, ras mutations, and p53-heat shock 70 protein complexes in human lung carcinoma cell lines. " Cancer research, **51**(15): 4090-4096.
- Leimbacher, P.A., Jones, S.E., Shorrocks, A.M.K., de Marco Zompit, M., Day, M., Blaauwendraad, J. et al. (2019). "MDC1 interacts with TOPBP1 to maintain chromosomal stability during mitosis. " Molecular Cell Biology Research Communications, **74**(3): 571-583. 578.
- Leppard, K.N. and Everett, R.D. (1999). "The adenovirus type 5 E1b 55K and E4 Orf3 proteins associate in infected cells and affect ND10 components. " Journal of General Virology, **80**(4): 997-1008.
- Lethbridge, K.J., Scott, G.E. and Leppard, K.N. (2003). "Nuclear matrix localization and SUMO-1 modification of adenovirus type 5 E1b 55K protein are controlled by E4 Orf6 protein. " Journal of General Virology, **84**(2): 259-268.
- Levine, A.J. (1997). "p53, the cellular gatekeeper for growth and division. " Cell, **88**(3): 323-331.
- Lezon-Geyda, K., Najfeld, V. and Johnson, E.M. (2001). "Deletions of PURA, at 5q31, and PURB, at 7p13, in myelodysplastic syndrome and progression to acute myelogenous leukemia. " Leukemia, **15**(6): 954-962.
- Li, J., Wang, C., Feng, G., Zhang, L., Chen, G., Sun, H. et al. (2020). "Rbm14 maintains the integrity of genomic DNA during early mouse embryogenesis via mediating alternative splicing. " Cell proliferation, **53**(1):12724.
- Li, Q., Zhao, L.Y., Zheng, Z., Yang, H., Santiago, A. and Liao, D. (2011). "Inhibition of p53 by adenovirus type 12 E1B-55K deregulates cell cycle control and sensitizes tumor cells to genotoxic agents. " Journal of virology, **85**(16): 7976-7988.
- Liao, D., Yu, A. and Weiner, A.M. (1999). "Coexpression of the Adenovirus 12 E1B 55 kDa Oncoprotein and Cellular Tumor Suppressor p53 Is Sufficient to Induce Metaphase Fragility of the HumanRNU2Locus. " Virology, **254**(1): 11-23.

- Lichtenstein, D.L., Doronin, K., Toth, K., Kuppuswamy, M., Wold, W.S. and Tollefson, A.E. (2004). "Adenovirus E3-6.7 K protein is required in conjunction with the E3-RID protein complex for the internalization and degradation of TRAIL receptor 2. " Journal of virology, **78**(22): 12297-12307.
- Lin, H.J., Eviner, V., Prendergast, G.C. and White, E. (1995). "Activated H-ras rescues E1A-induced apoptosis and cooperates with E1A to overcome p53-dependent growth arrest. " Molecular and cellular biology, **15**(8): 4536-4544.
- Linzer, D.I. and Levine, A.J. (1979). "Characterization of a 54K dalton cellular SV40 tumor antigen present in SV40-transformed cells and uninfected embryonal carcinoma cells. " Cell, **17**(1): 43-52.
- Liu, H., Naismith, J.H. and Hay, R.T. (2003). "Adenovirus DNA replication. " Curr Top Microbiol Immunol, **272**:131–164.
- Liu, Q., Guntuku, S., Cui, X.S., Matsuoka, S., Cortez, D., Tamai, K. et al. (2000). "Chk1 is an essential kinase that is regulated by Atr and required for the G2/M DNA damage checkpoint. " Genes & development, **14**(12): 1448-1459.
- Liu, Y., Colosimo, A.L., Yang, X.J. and Liao, D. (2000). "Adenovirus E1B 55-kilodalton oncoprotein inhibits p53 acetylation by PCAF. " Molecular and cellular biology, **20**(15): 5540-5553.
- Liu, Y., Shevchenko, A., Shevchenko, A. and Berk, A.J. (2005). "Adenovirus exploits the cellular aggresome response to accelerate inactivation of the MRN complex. " Journal of virology, **79**(22): 14004-14016.
- Lowe, S.W. and Ruley, H.E. (1993). "Stabilization of the p53 tumor suppressor is induced by adenovirus 5 E1A and accompanies apoptosis. " Genes & development, **7**(4): 535-545.
- Lowe, S.W., Ruley, H.E., Jacks, T. and Housman, D.E. (1993). "p53-dependent apoptosis modulates the cytotoxicity of anticancer agents. " Cell, **74**(6): 957-967.
- Luisoni, S. and Greber, U.F. (2016). "Biology of Adenovirus Cell Entry: Receptors, Pathways, Mechanisms. " Adenoviral vectors for gene therapy Elsevier: 27-58.
- Mahon, C., Krogan, N.J., Craik, C.S. and Pick, E. (2014). "Cullin E3 ligases and their rewiring by viral factors. " Biomolecules & Therapeutics, **4**(4): 897-930.
- Maréchal, A. and Zou, L. (2013). "DNA damage sensing by the ATM and ATR kinases. " Cold Spring Harbor Perspectives in Biology, **5**(9): 012716.
- Mathias, P., Galleno, M. and Nemerow, G.R. (1998). "Interactions of soluble recombinant integrin $\alpha v \beta 5$ with human adenoviruses. " Journal of virology, **72**(11): 8669-8675.
- McBride, W.D. and Wiener, A. (1964). "In vitro Transformation of Hamster Kidney Cells by Human Adenovirus Type 12. " Proceedings of the Society for Experimental Biology and Medicine, **115**(4): 870-874.
- McDougall, J.K. (1970). "Effects of adenoviruses on the chromosomes of normal human cells and cells trisomic for an E chromosome. " Nature, **225**(5231): 456-458.
- McDowell, G.S. and Philpott, A. (2013). "Non-canonical ubiquitylation: mechanisms and consequences. " The international journal of biochemistry & cell biology, **45**(8): 1833-1842.
- Miller, M.S., Pelka, P., Fonseca, G.J., Cohen, M.J., Kelly, J.N., Barr, S.D. et al. (2012). "Characterization of the 55-residue protein encoded by the 9S E1A mRNA of species C adenovirus. " Journal of virology, **86**(8): 4222-4233.
- Mirza, M.A. and Weber, J. (1982). "Structure of adenovirus chromatin. " Biochimica et Biophysica Acta (BBA)-Gene Structure and Expression, **696**(1): 76-86.
- Moody, C.A. and Laimins, L.A. (2009). "Human papillomaviruses activate the ATM DNA damage pathway for viral genome amplification upon differentiation. " PLoS Pathogens, **5**(10).
- Moore, M., Horikoshi, N. and Shenk, T. (1996). "Oncogenic potential of the adenovirus E4orf6 protein. " Pr Proceedings of the National Academy of Sciences, **93**(21): 11295-11301.

- Morris, S.J., Scott, G.E. and Leppard, K.N. (2010). "Adenovirus late-phase infection is controlled by a novel L4 promoter. " Journal of virology ,**84**(14): 7096-7104.
- Mücke, K., Paulus, C., Bernhardt, K., Gerrer, K., Schön, K., Fink, A. et al. (2014). "Human cytomegalovirus major immediate early 1 protein targets host chromosomes by docking to the acidic pocket on the nucleosome surface. " Journal of Virology ,**88**(2): 1228-1248.
- Muller, S. and Dobner, T. (2008). "The adenovirus E1B-55K oncoprotein induces SUMO modification of p53. " Cell Cycle ,**7**(6): 754-758.
- Mulnix, R.E., Pitman, R.T., Retzer, A., Bertram, C., Arasi, K., Crees, Z. et al. (2014). "hnRNP C1/C2 and Pur-beta proteins mediate induction of senescence by oligonucleotides homologous to the telomere overhang. " OncoTargets and therapy,**7**: 23.
- Mysiak, M.E., Holthuizen, P.E. and van der Vliet, P.C. (2004). "The adenovirus priming protein pTP contributes to the kinetics of initiation of DNA replication. " Nucleic acids research ,**32**(13): 3913-3920.
- Nagata, K., Guggenheimer, R.A., Enomoto, T., Lichy, J.H. and Hurwitz, J. (1982). "Adenovirus DNA replication in vitro: identification of a host factor that stimulates synthesis of the preterminal protein-dCMP complex. " Proceedings of the National Academy of Sciences ,**79**(21): 6438-6442.
- Nazeer, R., Qashqari, F.S., Albalawi, A.S., Piberger, A.L., Tilotta, M.T., Read, M.L. et al. (2019). "Adenovirus E1B 55-kilodalton protein targets SMARCAL1 for degradation during infection and modulates cellular DNA replication. " Journal of Virology ,**93**(13): 00402-00419.
- Nevels, M., Rubenwolf, S., Spruss, T., Wolf, H. and Dobner, T. (1997). "The adenovirus E4orf6 protein can promote E1A/E1B-induced focus formation by interfering with p53 tumor suppressor function. " Proceedings of the National Academy of Sciences ,**94**(4): 1206-1211.
- Nevels, M., Rubenwolf, S., Spruss, T., Wolf, H. and Dobner, T. (2000). "Two distinct activities contribute to the oncogenic potential of the adenovirus type 5 E4orf6 protein. " Journal of virology ,**74**(11): 5168-5181.
- Nevels, M., Spruss, T., Wolf, H. and Dobner, T. (1999). "The adenovirus E4orf6 protein contributes to malignant transformation by antagonizing E1A-induced accumulation of the tumor suppressor protein p53. " Oncogene ,**18**(1): 9.
- Nevels, M., Täuber, B., Kremmer, E., Spruss, T., Wolf, H. and Dobner, T. (1999). "Transforming potential of the adenovirus type 5 E4orf3 protein. " Journal of virology ,**73**(2): 1591-1600.
- Nevels, M., Täuber, B., Spruss, T., Wolf, H. and Dobner, T. (2001). " "Hit-and-run" transformation by adenovirus oncogenes. " Journal of virology ,**75**(7): 3089-3094.
- Nishiyama, R., Watanabe, Y., Fujita, Y., Le, D.T., Kojima, M., Werner, T. et al. (2011). "Analysis of cytokinin mutants and regulation of cytokinin metabolic genes reveals important regulatory roles of cytokinins in drought, salt and abscisic acid responses, and abscisic acid biosynthesis. " The Plant Cell ,**23**(6): 2169-2183.
- O'Connor, C.M., Nukui, M., Gurova, K.V. and Murphy, E.A. (2016). "Inhibition of the FACT complex reduces transcription from the human cytomegalovirus major immediate early promoter in models of lytic and latent replication. " Journal of virology ,**90**(8): 4249-4253.
- Oh, S.T., Longworth, M.S. and Laimins, L.A. (2004). "Roles of the E6 and E7 proteins in the life cycle of low-risk human papillomavirus type 11. " Journal of Virology ,**78**(5): 2620-2626.
- Orazio, N.I., Naeger, C.M., Karlseder, J. and Weitzman, M.D. (2011). "The adenovirus E1b55K/E4orf6 complex induces degradation of the Bloom helicase during infection. " Journal of virology ,**85**(4): 1887-1892.
- Orlando, J.S. and Ornelles, D.A. (1999). "An arginine-faced amphipathic alpha helix is required for adenovirus type 5 E4orf6 protein function. " Journal of virology ,**73**(6): 4600-4610.
- Ornelles, D.A. and Shenk, T. (1991). " Localization of the adenovirus early region 1B 55-kilodalton protein during lytic infection: association with nuclear viral inclusions requires the early region 4 34-kilodalton protein. " Journal of virology ,**65**(1): 424-429.

- Ortiz-Meoz, R.F., Jiang, J., Lazarus, M.B., Orman, M., Janetzko, J., Fan, C. et al. (2015). "A small molecule that inhibits OGT activity in cells. " *ACS chemical biology*, **10**(6): 1392-1397.
- Ou, H.D., Kwiatkowski, W., Deerinck, T.J., Noske, A., Blain, K.Y., Land, H.S. et al. (2012). "A structural basis for the assembly and functions of a viral polymer that inactivates multiple tumor suppressors. " *Cell*, **151**(2): 304-319.
- Pääbo, S., Weber, F., Kämpe, O., Schaffner, W. and Peterson, P.A. (1983). "Association between transplantation antigens and a viral membrane protein synthesized from a mammalian expression vector. " *Cell*, **33**(2): 445-453.
- Pancholi, N.J., Price, A.M. and Weitzman, M.D. (2017). "Take your PIKK: tumour viruses and DNA damage response pathways. " *Philosophical Transactions of the Royal Society B: Biological Sciences*, **372**(1732): 20160269.
- Parkin, D.M. (2006). "The global health burden of infection-associated cancers in the year 2002. " *International journal of cancer*, **118**(12): 3030-3044.
- Pasquini, L.A., Paez, P.M., Moreno, M.A.B., Pasquini, J.M. and Soto, E.F. (2003). "Inhibition of the proteasome by lactacystin enhances oligodendroglial cell differentiation. " *Journal of Neuroscience*, **23**(11): 4635-4644.
- Peeper, D.S., Dannenberg, J.H., Douma, S., te Riele, H. and Bernards, R. (2001). "Escape from premature senescence is not sufficient for oncogenic transformation by Ras. " *Nature cell biology*, **3**(2): 198.
- Pennella, M.A., Liu, Y., Woo, J.L., Kim, C.A. and Berk, A.J. (2010). "Adenovirus E1B 55-kilodalton protein is a p53-SUMO1 E3 ligase that represses p53 and stimulates its nuclear export through interactions with promyelocytic leukemia nuclear bodies. " *Journal of virology*, **84**(23): 12210-12225.
- Petroski, M.D. and Deshaies, R.J. (2005). "Function and regulation of cullin-RING ubiquitin ligases. " *Nature reviews Molecular cell biology*, **6**(1): 9-20.
- Pleguezuelos-Manzano, C., Puschhof, J., Huber, A.R., van Hoeck, A., Wood, H.M., Nomburg, J. et al. (2020). "Mutational signature in colorectal cancer caused by genotoxic pks+ E. coli. " *Nature*, 1-8.
- Plummer, M., de Martel, C., Vignat, J., Ferlay, J., Bray, F. and Franceschi, S. (2016). "Global burden of cancers attributable to infections in 2012: a synthetic analysis. " *The Lancet Global Health*, **4**(9): e609-e616.
- Pombo, A., Ferreira, J., Bridge, E. and Carmo-Fonseca, M. (1994). "Adenovirus replication and transcription sites are spatially separated in the nucleus of infected cells. " *The EMBO journal*, **13**(21): 5075-5085.
- Pruijn, G.J., van Driel, W. and van der Vliet, P.C. (1986). "Nuclear factor III, a novel sequence-specific DNA-binding protein from HeLa cells stimulating adenovirus DNA replication. " *Nature*, **322**(6080): 656.
- Querido, E., Blanchette, P., Yan, Q., Kamura, T., Morrison, M., Boivin, D. et al. (2001). "Degradation of p53 by adenovirus E4orf6 and E1B55K proteins occurs via a novel mechanism involving a Cullin-containing complex. " *Genes & Development*, **15**(23): 3104-3117.
- Querido, E., Marcellus, R.C., Lai, A., Charbonneau, R., Teodoro, J.G., Ketner, G. et al. (1997). "Regulation of p53 levels by the E1B 55-kilodalton protein and E4orf6 in adenovirus-infected cells. " *Journal of virology*, **71**(5): 3788-3798.
- Rasti, M., Grand, R.J., Mymryk, J.S., Gallimore, P.H. and Turnell, A.S. (2005). "Recruitment of CBP/p300, TATA-binding protein, and S8 to distinct regions at the N terminus of adenovirus E1A. " *Journal of virology*, **79**(9): 5594-5605.
- Rasti, M., Grand, R.J., Yousef, A.F., Shuen, M., Mymryk, J.S., Gallimore, P.H. et al. (2006). "Roles for APIS and the 20S proteasome in adenovirus E1A-dependent transcription. " *The EMBO journal*, **25**(12): 2710-2722.
- Rauschhuber, C. (2011). "Analysis of Adenovirus-Host Interactions to Improve Recombinant Adenoviral Vectors for Gene Therapy" (Doctoral dissertation, lmu).
- Reyes, E.D., Kulej, K., Pancholi, N.J., Akhtar, L.N., Avgousti, D.C., Kim, E.T. et al. (2017). "Identifying host factors associated with DNA replicated during virus infection. " *Molecular & Cellular Proteomics*, **16**(12): 2079-2097.

- Rieder, C.L. and Cole, R.W. (1998). "Entry into mitosis in vertebrate somatic cells is guarded by a chromosome damage checkpoint that reverses the cell cycle when triggered during early but not late prophase. " The Journal of cell biology, **142**(4): 1013-1022.
- Rodriguez, M.S., Dargemont, C. and Hay, R.T. (2001). "SUMO-1 conjugation in vivo requires both a consensus modification motif and nuclear targeting. " Journal of Biological Chemistry, **276**(16): 12654-12659.
- Ross, P.J., Kennedy, M.A., Christou, C., Quiroz, M.R., Poulin, K.L. and Parks, R.J. (2011). "Assembly of helper-dependent adenovirus DNA into chromatin promotes efficient gene expression. " Journal of virology, **85**(8): 3950-3958.
- Rous, P. (1911). "A sarcoma of the fowl transmissible by an agent separable from the tumor cells. " The Journal of experimental medicine, **13**(4): 397.
- Rowe, W.P., Huebner, R.J., Gilmore, L.K., Parrott, R.H. and Ward, T.G. (1953). "Isolation of a cytopathogenic agent from human adenoids undergoing spontaneous degeneration in tissue culture. " Proceedings of the Society for Experimental Biology and Medicine, **84**(3): 570-573.
- Ruley, H.E. (1983). "Adenovirus early region 1A enables viral and cellular transforming genes to transform primary cells in culture. " Nature, **304**(5927): 602-606.
- Russell, W.C. (2000). "Update on adenovirus and its vectors. " Journal of general virology, **81**(11):2573-2604.
- Russell, W.C. (2009). "Adenoviruses: update on structure and function." Journal of General Virology, **90**(1):1-20.
- Saban, S.D., Silvestry, M., Nemerow, G.R. and Stewart, P.L. (2006). "Visualization of α -helices in a 6-Ångstrom resolution cryoelectron microscopy structure of adenovirus allows refinement of capsid protein assignments. " Journal of virology, **80**(24): 12049-12059.
- Sabbatini, P., Lin, J., Levine, A.J. and White, E. (1995). "Essential role for p53-mediated transcription in E1A-induced apoptosis. " Genes & development, **9**(17): 2184-2192.
- Saha, B., Wong, C.M. and Parks, R.J. (2014). "The adenovirus genome contributes to the structural stability of the virion. " Viruses, **6**(9): 3563-3583.
- Salahuddin, S., Fath, E.K., Biel, N., Ray, A., Moss, C.R., Patel, A. et al. (2019). "Epstein-Barr virus latent membrane protein-1 induces the expression of SUMO-1 and SUMO-2/3 in LMP1-positive lymphomas and cells. " Scientific reports of cetacean research, **9**(1): 1-13.
- Sancar, A., Lindsey-Boltz, L.A., Ünsal-Kaçmaz, K. and Linn, S. (2004). "Molecular mechanisms of mammalian DNA repair and the DNA damage checkpoints. " Annual review of biochemistry, **73**(1): 39-85.
- Sarangi, P. and Zhao, X. (2015). "SUMO-mediated regulation of DNA damage repair and responses. " Trends in biochemical sciences, **40**(4): 233-242.
- Sarikas, A., Hartmann, T. and Pan, Z.Q. (2011). " The cullin protein family. " Genome biology, **12**(4): 220.
- Sarnow, P., Hearing, P., Anderson, C.W., Halbert, D.N., Shenk, T. and Levine, A.J. (1984). "Adenovirus early region 1B 58,000-dalton tumor antigen is physically associated with an early region 4 25,000-dalton protein in productively infected cells. " Journal of virology, **49**(3): 692-700.
- Sarnow, P., Ho, Y.S., Williams, J. and Levine, A.J. (1982). "Adenovirus E1b-58kd tumor antigen and SV40 large tumor antigen are physically associated with the same 54 kd cellular protein in transformed cells. " Cell, **28**(2): 387-394.
- Schaack, J., Ho, W.Y., Freimuth, P. and Shenk, T. (1990). "Adenovirus terminal protein mediates both nuclear matrix association and efficient transcription of adenovirus DNA. " Genes & development, **4**(7): 1197-1208.
- Schaeper, U., Boyd, J.M., Verma, S., Uhlmann, E., Subramanian, T. and Chinnadurai, G. (1995). "Molecular cloning and characterization of a cellular phosphoprotein that interacts with a conserved C-terminal domain of adenovirus E1A involved in negative modulation of oncogenic transformation. " Proceedings of the National Academy of Sciences, **92**(23): 10467-10471.

- Schmid, M., Kindsmüller, K., Wimmer, P., Groitl, P., Gonzalez, R.A. and Dobner, T. (2011). "The E3 Ubiquitin Ligase Activity Associated with the Adenoviral E1B-55K–E4orf6 Complex Does Not Require CRM1-Dependent Export. " Journal of Virology, **85**(14): 7081-7094.
- Schreiner, S., Bürck, C., Glass, M., Groitl, P., Wimmer, P., Kinkley, S. et al. (2013). "Control of human adenovirus type 5 gene expression by cellular Daxx/ATRAX chromatin-associated complexes. " Nucleic acids research, **41**(6): 3532-3550.
- Schreiner, S., Wimmer, P. and Dobner, T. (2012). "Adenovirus degradation of cellular proteins. " Future microbiology, **7**(2): 211-225.
- Schreiner, S., Wimmer, P., Sirma, H., Everett, R.D., Blanchette, P., Groitl, P. et al. (2010). "Proteasome-dependent degradation of Daxx by the viral E1B-55K protein in human adenovirus-infected cells. " Journal of virolog, **84**(14): 7029-7038.
- Serrano, M., Lin, A.W., McCurrach, M.E., Beach, D. and Lowe, S.W. (1997). "Oncogenic ras provokes premature cell senescence associated with accumulation of p53 and p16INK4a. " Cell, **88**(5): 593-602.
- Sesta, A., Cassarino, M.F., Terreni, M., Ambrogio, A.G., Libera, L., Bardelli, D. et al. (2020). "Ubiquitin-specific protease 8 mutant corticotrope adenomas present unique secretory and molecular features and shed light on the role of ubiquitylation on ACTH processing. " Neuroendocrinology, **110**(1-2): 119.
- Shenk, T.E. (2001). "Adenoviridae: the viruses and their replication. " Fundamental virology: 1053-1088.
- Shiroki, K., Hashimoto, S., Saito, I., Fukui, Y., Kato, H. and Shimojo, H. (1984). "Expression of the E4 gene is required for establishment of soft-agar colony-forming rat cell lines transformed by the adenovirus 12 E1 gene. " Journal of virology, **50**(3): 854-863.
- Shope, R.E. and Hurst, E.W. (1933). "Infectious papillomatosis of rabbits: with a note on the histopathology. " The Journal of experimental medicine, **58**(5): 607-624.
- Shvarts, A., Brummelkamp, T.R., Scheeren, F., Koh, E., Daley, G.Q., Spits, H. et al. (2002). "A senescence rescue screen identifies BCL6 as an inhibitor of anti-proliferative p19ARF–p53 signaling. " Genes & development, **16**(6): 681-686.
- Sieber, T. and Dobner, T. (2007). "Adenovirus type 5 early region 1B 156R protein promotes cell transformation independently of repression of p53-stimulated transcription. " Journal of virology, **81**(1): 95-105.
- Singh, S., Kumar, R. and Agrawal, B. (2018). "Adenoviral vector-based vaccines and gene therapies: Current status and future prospects. " Adenoviruses, IntechOpen.
- Skinner, G.R. (1976). "Transformation of primary hamster embryo fibroblasts by type 2 simplex virus: evidence for a "hit and run" mechanism. " British journal of experimental pathology, **57**(4): 361.
- Smith, G.C. and Jackson, S.P. (1999). "The DNA-dependent protein kinase. " Genes & Development, **13**(8): 916-934.
- So, S., Davis, A.J. and Chen, D.J. (2009). "Autophosphorylation at serine 1981 stabilizes ATM at DNA damage sites. " Journal of Cell Biology, **187**(7): 977-990.
- Sohn, S.Y. and Hearing, P. (2012). "Adenovirus regulates sumoylation of Mre11-Rad50-Nbs1 components through a paralogue-specific mechanism. " Journal of Virology, **86**(18): 9656-9665.
- Sohn, S.Y. and Hearing, P. (2016). "Adenovirus early proteins and host SUMOylation. " MBio, **7**(5): e01154-01116.
- Sohn, S.Y. and Hearing, P. (2016). "The adenovirus E4-ORF3 protein functions as a SUMO E3 ligase for TIF-1 γ sumoylation and poly-SUMO chain elongation. " Proceedings of the National Academy of Sciences, **113**(24): 6725-6730.
- Sohn, S.Y. and Hearing, P. (2019). "Mechanism of Adenovirus E4-ORF3-Mediated SUMO Modifications. " MBio, **10**(1): e00022-00019.
- Sohn, S.Y., Bridges, R.G. and Hearing, P. (2015). "Proteomic analysis of ubiquitin-like posttranslational modifications induced by the adenovirus E4-ORF3 protein. " Journal of virology, **89**(3): 1744-1755.
- Soria, C., Estermann, F.E., Espantman, K.C. and O'Shea, C.C. (2010). "Heterochromatin silencing of p53 target genes by a small viral protein. " Nature, **466**(7310): 1076-1081.

- Soucy, T.A., Smith, P.G., Milhollen, M.A., Berger, A.J., Gavin, J.M., Adhikari, S. et al. (2009). "An inhibitor of NEDD8-activating enzyme as a new approach to treat cancer. " Nature ,**458**(7239): 732-736.
- Spyridopoulos, I., Isner, J.M. and Losordo, D.W. (2002). "Oncogenic ras induces premature senescence in endothelial cells: role of p21 Cip1/Waf1. " Basic research in cardiology ,**97**(2): 117-124.
- Steegenga, W.T., Riteco, N., Jochemsen, A.G., Fallaux, F.J. and Bos, J.L. (1998). "The large E1B protein together with the E4orf6 protein target p53 for active degradation in adenovirus infected cells. " Oncogene ,**16**(3): 349.
- Stehelin, D., Varmus, H.E., Bishop, J.M. and Vogt, P.K. (1976). "DNA related to the transforming gene (s) of avian sarcoma viruses is present in normal avian DNA. " Nature ,**260**(5547): 170-173.
- Stencel-Baerenwald, J.E., Reiss, K., Reiter, D.M., Stehle, T. and Dermody, T.S. (2014). "The sweet spot: defining virus–sialic acid interactions. " Nature Reviews Microbiology ,**12**(11): 739-749.
- Sterner, D.E. and Berger, S.L. (2000). "Acetylation of histones and transcription-related factors. " Microbiol. Mol. Biol. Rev ,**64**(2): 435-459.
- Stillman, B.W., Lewis, J.B., Chow, L.T., Mathews, M.B. and Smart, J.E. (1981). "Identification of the gene and mRNA for the adenovirus terminal protein precursor. " Cell **23**(2): 497-508.
- Stracker, T.H., Carson, C.T. and Weitzman, M.D. (2002). "Adenovirus oncoproteins inactivate the Mre11–Rad50–NBS1 DNA repair complex. " Nature ,**418**(6895): 348.
- Subramanian, T., Zhao, L.J. and Chinnadurai, G. (2013). "Interaction of CtBP with adenovirus E1A suppresses immortalization of primary epithelial cells and enhances virus replication during productive infection. " Virology ,**443**(2): 313-320
- Sundararajan, R., Cuconati, A., Nelson, D. and White, E. (2001). "Tumor necrosis factor- α induces Bax-Bak interaction and apoptosis, which is inhibited by adenovirus E1B 19K. " Journal of Biological Chemistry ,**276**(48): 45120-45127.
- Surget, S., Khoury, M.P. and Bourdon, J.C. (2014). "Uncovering the role of p53 splice variants in human malignancy: a clinical perspective. " OncoTargets and therapy,**7**: 57.
- Täuber, B. and Dobner, T. (2001). "Adenovirus early E4 genes in viral oncogenesis. " Oncogene ,**20**(54): 7847.
- Tammsalu, T., Matic, I., Jaffray, E.G., Ibrahim, A.F., Tatham, M.H. and Hay, R.T. (2015). "Proteome-wide identification of SUMO modification sites by mass spectrometry. " Nature protocols ,**10**(9): 1374.
- Tejera, B., López, R.E., Hidalgo, P., Cárdenas, R., Ballesteros, G., Rivillas, L. et al. (2019). "The human adenovirus type 5 E1B 55kDa protein interacts with RNA promoting timely DNA replication and viral late mRNA metabolism. " PloS one ,**14**(4): e0214882.
- Thomas, D.L., Schaack, J., Vogel, H. and Javier, R. (2000). "Several E4 region functions influence mammary tumorigenesis by human adenovirus type 9. " Journal of virology ,**75**(2): 557-568.
- Tremblay, M.L., McGlade, C.J., Gerber, G.E. and Branton, P.E. (1988). "Identification of the phosphorylation sites in early region 1A proteins of adenovirus type 5 by amino acid sequencing of peptide fragments. " Journal of Biological Chemistry ,**263**(13): 6375-6383.
- Trentin, J.J., Van Hoosier Jr, G.L. and Samper, L. (1968). "The oncogenicity of human adenoviruses in hamsters. " Proceedings of the Society for Experimental Biology and Medicine ,**127**(3): 683-689.
- Trentin, J.J., Yabe, Y. and Taylor, G. (1962). "The Quest for Human Cancer Viruses: A new approach to an old problem reveals cancer induction in hamsters by human adenovirus. " Science ,**137**(3533): 835-841.
- Trotman, L.C., Mosberger, N., Fornerod, M., Stidwill, R.P. and Greber, U.F. (2000). "Import of adenovirus DNA involves the nuclear pore complex receptor CAN/Nup214 and histone H1. " Nature cell biology ,**3**(12): 1092-1100.
- Turnell, A.S. and Grand, R.J. (2012). "DNA viruses and the cellular DNA-damage response. " Journal of General Virology ,**93**(10): 2076-2097.

- Turnell, A.S., Grand, R.J., Gorbea, C., Zhang, X., Wang, W., Mymryk, J.S. et al. (2000). "Regulation of the 26S proteasome by adenovirus E1A. " The EMBO journal ,**19**(17): 4759-4773.
- Valentine, R.C. and Pereira, H.G. (1965). "Antigens and structure of the adenovirus. " Journal of molecular biology ,**13**(1): 13-1N13.
- Van Damme, E., Laukens, K., Dang, T.H. and Van Ostade, X. (2010). "A manually curated network of the PML nuclear body interactome reveals an important role for PML-NBs in SUMOylation dynamics. " International journal of biological sciences ,**6**(1): 51.
- Vink, E.I., Zheng, Y., Yeasmin, R., Stamminger, T., Krug, L.T. and Hearing, P. (2015). "Impact of adenovirus E4-ORF3 oligomerization and protein localization on cellular gene expression. " Viruses ,**7**(5): 2428-2449.
- Vogelstein, B., Lane, D. and Levine, A.J. (2000). "Surfing the p53 network. " Nature, **408**(6810): 307.
- Walden, H., Podgorski, M.S., Huang, D.T., Miller, D.W., Howard, R.J., Minor Jr, D.L. et al. (2003). "The structure of the APPBP1-UBA3-NEDD8-ATP complex reveals the basis for selective ubiquitin-like protein activation by an E1. " Molecular cell Biology,**12**(6): 1427-1437.
- Wang, T., Liu, Y., Edwards, G., Krzizike, D., Scherman, H. and Luger, K. (2018). "The histone chaperone FACT modulates nucleosome structure by tethering its components. " Life science alliance ,**1**(4).
- Watanabe, Y., Bowden, T.A., Wilson, I.A. and Crispin, M. (2019). "Exploitation of glycosylation in enveloped virus pathobiology. " Biochimica et Biophysica Acta (BBA)-General Subjects.
- Waye, M.M.Y. and Sing, C.W. (2010). "Anti-viral drugs for human adenoviruses. " Pharmaceuticals ,**3**(10): 3343-3354.
- Webster, L.C. and Ricciardi, R.P. (1991). "Trans-dominant mutants of E1A provide genetic evidence that the zinc finger of the trans-activating domain binds a transcription factor. " Molecular and cellular biology ,**11**(9): 4287-4296.
- Wei, H. and Zhou, M.M. (2010). "Viral-encoded enzymes that target host chromatin functions. " Biochimica et Biophysica Acta (BBA)-Gene Regulatory Mechanisms ,**1799**(3-4): 296-301.
- Weiden, M.D. and Ginsberg, H.S. (1994). "Deletion of the E4 region of the genome produces adenovirus DNA concatemers. " Proceedings of the National Academy of Sciences ,**91**(1): 153-157.
- Weigel, S. and Dobbelstein, M. (2000). "The nuclear export signal within the E4orf6 protein of adenovirus type 5 supports virus replication and cytoplasmic accumulation of viral mRNA. " Journal of Virology ,**74**(2): 764-772.
- Weiss, R.S. and Javier, R.T. (1997). "A carboxy-terminal region required by the adenovirus type 9 E4 ORF1 oncoprotein for transformation mediates direct binding to cellular polypeptides. " Journal of virology ,**71**(10): 7873-7880.
- Weitzman, M.D. (2005). "Functions of the adenovirus E4 proteins and their impact on viral vectors. " Front Biosci ,**10**(1106): e17.
- Weitzman, M.D. and Ornelles, D.A. (2005). "Inactivating intracellular antiviral responses during adenovirus infection. " Oncogene ,**24**(52): 7686-7696.
- White, E. (1993). "Regulation of apoptosis by the transforming genes of the DNA tumor virus adenovirus. " Proceedings of the Society for Experimental Biology and Medicine ,**204**(1): 30-39.
- White, E. (1996). "Life, death, and the pursuit of apoptosis. " Genes & development ,**10**(1): 1-15.
- White, E. (2001). "Regulation of the cell cycle and apoptosis by the oncogenes of adenovirus. " Oncogene ,**20**(54): 7836.
- Whittaker, J.L., Byrd, P.J., Grand, R.J. and Gallimore, P.H. (1984). "Isolation and characterization of four adenovirus type 12-transformed human embryo kidney cell lines. " Molecular and cellular biology ,**4**(1): 110-116.
- Whyte, P., Buchkovich, K.J., Horowitz, J.M., Friend, S.H., Raybuck, M., Weinberg, R.A. et al. (1988). "Association between an oncogene and an anti-oncogene: the adenovirus E1A proteins bind to the retinoblastoma gene product." Nature,**334**(6178): 124-129.

- Wilkinson, K.A. and Henley, J.M. (2010). "Mechanisms, regulation and consequences of protein SUMOylation." Biochemical Journal ,**428**(2): 133-145.
- Williams, G.T. (1991). "Programmed cell death: apoptosis and oncogenesis." Cell ,**65**: 1097-1098.
- Wimmer, P., Blanchette, P., Schreiner, S., Ching, W., Groitl, P., Berscheminski, J. et al. (2013). "Cross-talk between phosphorylation and SUMOylation regulates transforming activities of an adenoviral oncoprotein." Oncogene ,**32**(13): 1626.
- Winkler, D.D. and Luger, K. (2011). "The histone chaperone FACT: structural insights and mechanisms for nucleosome reorganization." Journal of Biological Chemistry ,**286**(21): 18369-18374.
- Woo, J.L. and Berk, A.J. (2007). "Adenovirus ubiquitin-protein ligase stimulates viral late mRNA nuclear export." Journal of virology,**81**(2): 575-587.
- Wright, J. and Leppard, K.N. (2013). "The human adenovirus 5 L4 promoter is activated by cellular stress response protein p53." Journal of virology ,**87**(21): 11617-11625.
- Wu, E. and Nemerow, G.R. (2004). "Virus yoga: the role of flexibility in virus host cell recognition." Trends Microbiol ,**12**(4): 162-169.
- Yau, R. and Rape, M. (2016). "The increasing complexity of the ubiquitin code." Nature Cell Biology ,**18**(6): 579-586.
- Yew, P.R. and Berk, A.J. (1992). "Inhibition of p53 transactivation required for transformation by adenovirus early 1B protein." Nature ,**357**(6373): 82-85.
- Yew, P.R., Liu, X. and Berk, A.J. (1994). "Adenovirus E1B oncoprotein tethers a transcriptional repression domain to p53." Genes & development ,**8**(2): 190-202.
- Yondola, M.A. and Hearing, P. (2007). "The adenovirus E4 ORF3 protein binds and reorganizes the TRIM family member transcriptional intermediary factor 1 alpha." Journal of virology ,**81**(8): 4264-4271.
- Yoshiyama, K.O., Sakaguchi, K. and Kimura, S. (2013). "DNA damage response in plants: conserved and variable response compared to animals." Biology ,**2**(4): 1338-1356.
- Young, L.S., Yap, L.F. and Murray, P.G. (2016). "Epstein–Barr virus: more than 50 years old and still providing surprises." Nature Reviews Cancer ,**16**(12): 789.
- Yousef, A.F., Fonseca, G.J., Pelka, P., Ablack, J.N.G., Walsh, C., Dick, F.A. et al. (2010). "Identification of a molecular recognition feature in the E1A oncoprotein that binds the SUMO conjugase UBC9 and likely interferes with polySUMOylation." Oncogene ,**29**(33): 4693.
- Zalmanzon, E. (1987). "Transforming and oncogenic properties of the adenovirus genome." Ekspiermental'naia onkologija ,**9**(3): 3-8.
- Zantema, A., Schrier, P.I., Davis-Olivier, A.R.J.A., van Laar, T.H.E.O. and Vaessen, R.T. (1985). "Adenovirus serotype determines association and localization of the large E1B tumor antigen with cellular tumor antigen p53 in transformed cells." Molecular and cellular biology ,**5**(11): 3084-3091.
- Zhao, H.U.I. and Piwnica-Worms, H. (2001). "ATR-mediated checkpoint pathways regulate phosphorylation and activation of human Chk1." Molecular and cellular biology ,**21**(13): 4129-4139.
- Zhao, L.Y. and Liao, D. (2003). "Sequestration of p53 in the cytoplasm by adenovirus type 12 E1B 55-kilodalton oncoprotein is required for inhibition of p53-mediated apoptosis." Journal of virology ,**77**(24): 13171-13181.
- Zhao, L.Y., Santiago, A., Liu, J. and Liao, D. (2007). "Repression of p53-mediated transcription by adenovirus E1B 55-kDa does not require corepressor mSin3A and histone deacetylases." Journal of Biological Chemistry ,**282**(10): 7001-7010.
- Zhao, Y., Morgan, M.A. and Sun, Y. (2014). "Targeting Neddylaton pathways to inactivate cullin-RING ligases for anticancer therapy." Antioxidants & redox signaling ,**21**(17): 2383-2400.

Zheng, N., Schulman, B.A., Song, L., Miller, J.J., Jeffrey, P.D., Wang, P. et al. (2002). "Structure of the Cul1–Rbx1–Skp1–F box Skp2 SCF ubiquitin ligase complex. " Nature ,**416**(6882): 703-709.

Zheng, Z.-M. (2010). "Viral oncogenes, noncoding RNAs, and RNA splicing in human tumor viruses." International journal of biological sciences ,**6**(7): 730.

Zhou, L., Zhang, W., Sun, Y. and Jia, L. (2018). "Protein neddylation and its alterations in human cancers for targeted therapy. " Cellular Signalling ,**44**: 92-102.

Zou, L., Liu, D. and Elledge, S.J. (2003). "Replication protein A-mediated recruitment and activation of Rad17 complexes. " Proceedings of the National Academy of Sciences ,**100**(24): 13827-13832.

Zur Hausen, H. (1976). "Condylomata acuminata and human genital cancer." Cancer res. **36**(2 pt 2): 794.

Zur Hausen, H. (1967). "Induction of specific chromosomal aberrations by adenovirus type 12 in human embryonic kidney cells." Journal of virology,**1**(6): 1174-1185.

Zur Hausen, H. (2009). "The search for infectious causes of human cancers: where and why." Virology ,**392**(1): 1-10.